Differential G protein activation by fusion proteins between the human δ-opioid receptor and $G_{i1}\alpha/G_{o1}\alpha$ proteins

A THESIS PRESENTED FOR

THE DEGREE OF

DOCTOR OF PHILOSOPHY

BY

HYO-EUN MOON

DIVISION OF BIOCHEMISTRY AND MOLECULAR BIOLOGY

INSTITUTE OF BIOMEDICAL AND LIFE SCIENCES

UNIVERSITY OF GLASGOW

JANUARY 2001

ProQuest LLC.
789 East Eisenhower Parkway
P.O. Box 1346
Ann Arbor, MI 48106 – 1346

ABSTRACT

Assessment of the functional activities of agonists acting on the human δ-opioid receptor (hDOR) which couples to G proteins of the $G_i/G_o\alpha$ class usually involves the measurement of adenylyl cyclase (AC) activity. To assess the relative capacitiy of the hDOR to activate closely related G proteins, fusion proteins were constructed in which the α subunits of either G_{i1} or G_{o1}, containing point mutations to render them insensitive to the actions of pertussis toxin (PTx), were linked in frame with the C-terminus of the receptor. Following transient and stable expression in HEK293 cells both constructs bound the antagonist [^{3}H] naltrindole with high affinity. D-ala^2, D-leu^5 enkephalin [DADLE] effectively inhibited forskolin-stimulated AC activity in intact cells in a concentration-dependent but PTx-insensitive manner. The high affinity GTPase activity of both constructs was also stimulated by DADLE with similar potency. However, enzyme kinetic analysis of agonist stimulation of GTPase activity demonstrated that the GTP turnover number produced in response to DADLE was more than 3 times greater for $G_{i1}\alpha$ than for $G_{o1}\alpha$. As the effect of agonist in both cases was to increase V_{max} without increasing the observed K_m for GTP this is consistent with receptor promoting greater guanine nucleotide exchange on, and thus activation of, $G_{i1}\alpha$ compared to $G_{o1}\alpha$. An equivalent fusion protein between the human μ-opioid receptor –1 and $G_{i1}\alpha$ produced a similar DADLE-induced GTP turnover number as the hDOR-$G_{i1}\alpha$ fusion construct, consistent with agonist occupation of these two opioid receptor subtypes being equally efficiently coupled to activation of $G_{i1}\alpha$.

In addition, I have investigated the characteristics of the ternary complex of agonist-GPCR-G protein using high affinity agonist binding studies with the fusion proteins. GDP reduced the binding of the agonist [^{3}H] DADLE but not the antagonist [^{3}H] naltrindole to both the receptor alone and all the hDOR-$G_{i1}\alpha$ (Xaa^{351}) fusion proteins. For the fusion proteins the pEC_{50} for GDP was strongly correlated with the n-octanol/H_20 partition co-efficient of G protein residue^{351}. Fusion proteins in which this residue was either isoleucine or glycine displayed similar association kinetics for [^{3}H] DADLE. However, the rate of dissociation of [^{3}H] DADLE was substantially greater for the glycine-containing fusion protein than that containing isoleucine, indicating the more hydrophobic residue imbued greater stability to the agonist-receptor-G protein ternary complex. This resulted in a higher affinity of binding of [^{3}H] DADLE to the fusion protein containing isoleucine^{351}. In expectation with the binding data, maximal DADLE-stimulated GTP hydrolysis was 2 fold greater with the isoleucine^{351} containing fusion protein and the potency of DADLE was 7 fold greater with the isoleucine^{351} fusion protein than for the version containing glycine. These results demonstrate that the stability of the ternary complex between hDOR, $G_{i1}\alpha$ and an agonist (but not antagonist) ligand is dependent upon the nature of residue^{351} of the G protein and that this determines the effectiveness of information flow from receptor to G protein.

CONTENTS

LIST OF FIGURES

LIST OF TABLES

ABBREVIATIONS

α α subunit of G proteins

A adenosine

ADP adenosine-5'-diphosphate

ATP adenosine-5'-triphosphate

APS ammonium persulphate

aa amino acid

A_{1A} receptor Adenosine$_{1A}$ receptor

α_{2A}AR α_{2A} adrenergic receptor

AC adenylyl cyclase

bps base pairs

BNTX 7-benzylidenenaltrexone

B_{max} maximum receptor level

BSA bovine serum albumin

β_2AR β_2-adrenergic receptor

β/γ beta and gamma subunits of G proteins

BW373U86 (+/-)-4-[(a-R*)-a-[(2S*,5R*)-4-allyl-2,5-di-methyl-1-piperazinyl]-3-hydroxybenzyl]-N,N-diethylbenzamide

cAMP 3', 5'-cyclic adenosine mono-phosphate

CAM constitutive active mutants

cDNA complementary DNA

CTx cholera toxin

CHO cells chinese hamster ovary cells

CPM counts per minute

DADLE [D-Ala^2, D-Leu^5]-enkephalin

DPDPE [D-Pen^2, D-Pen^5]-enkephalin

DAMGO [D-Ala^2, N-MePhe^4, Gly-ol]-enkephalin

DALCE [D-Ala^2, Leu^5, Cys^6]-enkephalin

DSLET [D-Ser^2, Leu^5]-enkephalyl-Thr

DMEM Dulbecco's Modified of Eagle's Medium

DTLET Tyr-D-Thr-Gly-Phe-Leu-Thr

Del-II deltorphine II

DPM disintergrations per minute

DTT dithiothreitol

E. coli. *Escherichia coli*

EC_{50} concentration that gives half-maximal stimulation of ligand

E_{max} maximum level of agonist stimulation

EDTA ethylenediaminetetra acetic acid

Egl-10 *Caenorhabditis elegans*

5′-NTII naltrindole-5'-isothiocyanate

5-HT_{1A} R 5-Hydroxytryptamine$_{1A}$ receptor

$GABA_BR1$ $GABA_B$ receptor 1

$GABA_BR2$ $GABA_B$ receptor 2

GAP GTPase activating protein

GPCRs G-protein coupled receptors

GRKs G protein receptor kinases

G protein guanine nucleotide binding protein

$G_{i1}\alpha$ inhibitory α subunit of trimeric G protein

$Gs\alpha$ stimulatory α subunit of trimeric G protein

GDP guanine di-phosphate

GTP guanine tri-phosphate

Gpp[NHp] guanylyl 5′ -[βγ imido] diphosphate

[^{35}S] GTPγS [^{35}S] Guanosine 5′-[3-o-thio] triphosphate

[γ-^{32}P] GTP [γ-^{32}P] Guanosine tri-phosphate

h hour

HEK293 human embryonic kidney 293

HEK293T human embryonic kidney 293 T

HEPES 4-[2-Hydroxyethyl]-1-piperazine-N′-2-ethane-Sulphonic acid

IC_{50} concentration of the unlabeled drug that blocks 50 % of the specific binding of the radioligand

LPA lysophosphatidic acid

MAPK mitogen activated protein kinase

MBP maltose-binding protein

MEM minimum essential medium

mRNA messenger ribonucleic acid

Mr relative molecular marker

min minute

NBCS new born calf serum

NTB naltriben

NG108-15 cells neuroblastoma X glioma hybrid cells

ORF open reading frame

PAGE polyacrylamide gel electrophoresis

PBS phosphate buffered saline

PCR polymerase chain reaction

pEC_{50} negative log conversion of EC_{50}

pIC_{50} negative log conversion of IC_{50}

pK_i negative log conversion of K_i

PKC protein kinase C

PKA protein kinase A

PLC phospholipase C

PLD phospholipase D

PTx *pertussis toxin*

PCR polymerase chain reaction

R receptor

R. T. room temperature

RGS regulator of G protein signalling

SNPs single-nucleotide polymorphisms

SAP shrimp alkaline phosphatase

Sf9 *Spodoptera frugiperda*

S.E.M. standard error of the mean

Sec second

S.D. standard deviation

SDS sodium dodecyl sulphate

SDS-PAGE sodium dodecyl sulphate-polyacrylamide gel electrophoresis

Sst2p *Saccharomyces cerevisiae*

TCA trichloroacetic acid

TEMED N, N, N′, N′ tetramethyethylenediamine

TM transmembrane helix

Tris Tris(hydroxymethyl) aminomethane

$t_{1/2}$ half life dissociation (min)

kb kilobase

$K_{H/L}$ = affinity constant of the agonist-detected high (H) or low (L) affinity sites or the single site detected

K_d dissociation constant, affinity of the radioligand for the receptor

K_m Michaelis Menten Constant

K_i inhibition constant

K_{off} dissociation (off-rate) binding

K_{ob} observed rate constant (min^{-1})

K_{on} association (on-rate) binding

kDa kilodaltons

V_{max} maximum velocity of maximally effective concentration of agonist

WT wild type

OPIOID RECEPTOR ABBREVIATIONS

rDOR rat δ-opioid receptor

mDOR mouse δ-opioid receptor

hDOR human δ-opioid receptor

hMOR-1 human μ opioid receptor-1

MOR μ opioid receptor

KOR κ opioid receptor

FUSION PROTEINS ABBREVIATIONS

1. Human δ–opioid receptor $G_{i1}\alpha/G_{o1}\alpha$ fusion proteins

hDOR-$G_{i1}\alpha$ (wild type);

Fusion protein of the human δ-opioid receptor and a $G_{i1}\alpha$ (wild type)

hDOR-$G_{i1}\alpha$ (Ile^{351});

Fusion protein of the human δ-opioid receptor and a isoleucine^{351} mutant of $G_{i1}\alpha$

hDOR-$G_{i1}\alpha$ (Gly^{351});

Fusion protein of the human δ-opioid receptor and a glycine^{351} mutant of $G_{i1}\alpha$

hDOR-$G_{i1}\alpha$ (Xaa^{351});

Fusion protein mutants of the human δ-opioid receptor and a Xaa^{351} mutants of $G_{i1}\alpha$

hDOR-$G_{o1}\alpha$ (wild type);

Fusion protein of the human δ-opioid receptor and a $G_{o1}\alpha$ (wild type)

hDOR-$G_{o1}\alpha$ (Ile^{351});

Fusion protein of the human δ-opioid receptor and a isoleucine^{351} mutant of $G_{o1}\alpha$

hDOR-$G_{o1}\alpha$ (Gly^{351});

Fusion protein of the human δ-opioid receptor and a glycine^{351} mutant of $G_{o1}\alpha$

hDOR-$G_{o1}\alpha$ (Xaa^{351});

Fusion protein mutants of the human δ-opioid receptor and a Xaa^{351} mutants $G_{o1}\alpha$

2. Human A_1-adenosine receptor $G_{i1}\alpha$ fusion proteins

A_1-$G_{i1}\alpha$ (wild type);

Fusion protein of the A_1 adenosine receptor and a $G_{i1}\alpha$ (wild type)

A_1-$G_{i1}\alpha$ (Ile^{351});

Fusion protein of the A_1 adenosine receptor and a isoleucine^{351} mutant of $G_{i1}\alpha$

A_1-$G_{i1}\alpha$ (Gly^{351});

Fusion protein of the A_1 adenosine receptor and a glycine^{351} mutant of $G_{i1}\alpha$

3. Human β_2–adrenoreceptor $G_s\alpha$ fusion proteins

β_2AR-$G_s\alpha$S;

Short splice variant of the α-subunit of the stimulatory G protein of AC

β_2AR-$G_s\alpha$L;

Long splice variant long splice variant of the α-subunit of the stimulatory G protein of AC

β_2AR(Δ26) $G_s\alpha_L$;

26 amino acids deletions of the C-terminal tail of the β_2AR in β_2AR-Gsα fusion proteins

β_2AR(Δ70) $G_s\alpha_L$;

70 amino acids deletions of the C-terminal tail of the β_2AR in β_2AR-Gsα fusion proteins

4. α_{2A} adrenergic receptor $G_{i1}\alpha$ fusion proteins

α_{2A} -$G_{i1}\alpha$ (wild type);

Fusion protein of the α_{2A} adrenoceptor and $G_{i1}\alpha$ (wild type)

α_{2A} -$G_{i1}\alpha$ (Ile^{351});

Fusion protein of the α_{2A} adrenoceptor and a isoleucine^{351} mutant of $G_{i1}\alpha$

α_{2A} -$G_{i1}\alpha$ (Gly^{351});

Fusion protein of the α_{2A} adrenoceptor and a glycine^{351} mutant of $G_{i1}\alpha$

ACKNOWLEDGEMENTS

First of all I really would like to thank my Ph.D supervisor, Professor. Graeme Milligan for his everlasting vision, guidance, consideration, tolerance and warm advice towards me. I also thank my assessor, Dr. Leslie. Fixer, my uncle, Dr. Byung-Seok Lee, my teachers, Professor. Kyu-Won Kim and Associate Professor. Ho-Sung Kang for their continuous support and advice. My deep gratitude also goes to everyone in the laboratory: Antonella Cavalli, Alison Mclean, Alex Groake, Craig Carr, Chee-wai Fong, Daljit Bahia, Douglas Ramsay, Elaine Barclay, Elaine Kellet, Gui-jie Feng, Hannah Murdoch, Martine Sautel, Marcel Hoffmann, Mary Mcvey, Moira Wilson, Patricia Stevens, Philip Wesley, Richard Ward, Sandra Milasta, Sandosh Padmanabhan, Tomas Drmota, Vicky Jackson, for their technical assistance, professional co-operation and friendship.

I thank the Institute of Biomedical and Life Sciences, University of Glasgow Postgraduate Scholarship & the ORS Award (Overseas Research Students Awards). Without this financial assistance, I would not carry on my study here abroad.

I greatly appreciate my loving parents, two brothers, Hyuck-po and Jong-ha for their unconditional forever love, support, patience and understanding towards me for my time away from home. My forever friend, Dr. Graham Edward Fagg in Tennessee, USA and his parents, Mary and Graham in Dover, England are also deserved to mention, for their warm encouragement and trust in me. Good Christian friends, Gill and Niall, sincere Korean minister, Rev. Sung-Do Han, warm teacher, Dr. Petr

Svobodap in Prague, Czech Republic and good catholic friend, Agnieszka in Warsaw, Polland have filled my joyful moments with good friendships.

My LORD, peace, love and wisdom of GOD have been always leading my life.

Psalm 23:1-2,

The Lord is my shepherd, I shall not be in want.

He makes me lie down in green pastures, he leads me beside quiet waters.

Finally, I will miss the coffee in Little Italy.

CHAPTER I

Introduction

1.1. Cellular signalling in the central nervous system

A large number of G-protein coupled receptors (GPCRs) allow a wide range of ligands to initiate signal transduction across the plasma membranes of eukaryotic cells. Ligand binding to many different mammalian cell-surface receptors activates *signal-transducing G proteins,* and then the *effector enzyme* adenylyl cyclase (AC) to generate the intracellular second messenger, cAMP. The identification of G proteins and their role in activating AC to synthesise cAMP in response to hormonal stimulation in the mid-1970s was a great step forward in understanding transmembrane signal transduction (Gilman, 1987).

Most neurotransmitter act through cell-surface GPCRs (Martens, 1992), which are synthesised in the endoplasmic reticulum, undergo post-translational modifications in the Golgi complex and are delivered to the plasma membrane of neurones in cell bodies, dendrites and axon terminals (Yung *et al.*, 1995). There is growing evidence that, *in vivo*, in the nervous system, the intracellular trafficking and subcellular localisation of these receptors undergo complex and physiologically relevant regulation by the neurotransmitter environment.

Opioid receptors are cell surface glycoproteins that provide specific binding sites for a variety of opioid alkaloids and peptides. These are used in the treatment of pain. The recent cloning of opioid receptors has established that the products of three genes form the known subtypes, the δ (DOR), μ (MOR) and k opioid (KOR) receptors which

have distinct pharmacological profiles and discrete but overlapping distributions in brain. However there are many aspects of opioid receptors that still remain poorly understood. The benefits of using a GPCR-G protein fusion protein strategy have been widely described (Seifert *et al.*, 1999: Milligan, 2000). Using this fusion protein strategy, I planned to understand the signalling pathways of δ opioid receptor (DOR).

1.2. G protein-coupled receptors (GPCRs)

Nearly 2000 GPCRs (Ji *et al.*, 1998) have been reported since bovine opsin was cloned in 1983 (Nathans and Hogness, 1983) and the β_2AR in 1986 (Dixon *et al.*, 1986). The GPCR superfamily can be subdivided into three major subfamilies: the rhodopsin/β-adrenergic, vasoactive intestinal polypeptide (VIP)/secretin, and the metabotropic glutamate receptor families. They are classified into over 100 subfamilies according to their sequence homology, ligand structure, and function. A substantial degree of amino acid homology is found among members of a particular subfamily, but comparisons between subfamilies show significantly less or no similarity. Although the majority of GPCRs mediate signal transduction via G proteins, emerging evidence indicates that some of these receptor are also capable of sending signals via alternative signal molecules, e.g., Jak2 kinase, phospholipase Cγ, or protein kinase C. These alternative pathways are an indication of the overall diversity occurring in the GPCR superfamily.

I. Structural features

Glycosylation, palmitoylation, the formation of disulfide bridges between cysteines and the phosphorylation of serine and threonine residues are known types of post-translational modifications of GPCRs.

a) General structure: N-terminal segment, Seven TMs, Three exoloops, Three/four cytoloops, and C-terminal segment

As shown in **Figure 1.1**, all GPCRs have an extracellular N-terminal segment, seven transmembranes (TMs), which form the TM core, three exoloops, three cytoloops, and a C-terminal segment. A fourth cytoplasmic loop is formed when the C-terminal segment is palmitoylated at specific Cys residues. Each of the seven TMs is generally composed of 20-27 amino acids. On the other hand, N-terminal segments (7-595 amino acids), loops (5-230 amino acids), and C-terminal segments (12-359 amino acids) vary in size, indicative of their diverse structures and functions. Interestingly, there is a weak positive correlation between N-terminal segment length and ligand size (Ji *et al.*, 1995), suggesting a role in ligand binding, in particular for large polypeptides and glycoprotein hormones. The ubiquitous seven TM structures allow glycosylation and ligand binding at the N-terminal segment and palmitoylation at the C-terminal. Phosphorylation also occurs at the C-terminal segments and leads to desensitisation. (Lefkowitz *et al.*, 1998).

Figure 1.1. Structural features of a G protein coupled receptor

Amino acid sequence of the wild type δ opioid receptor in the proposed transmembrane topology is shown in the picture.

Figure 1.1

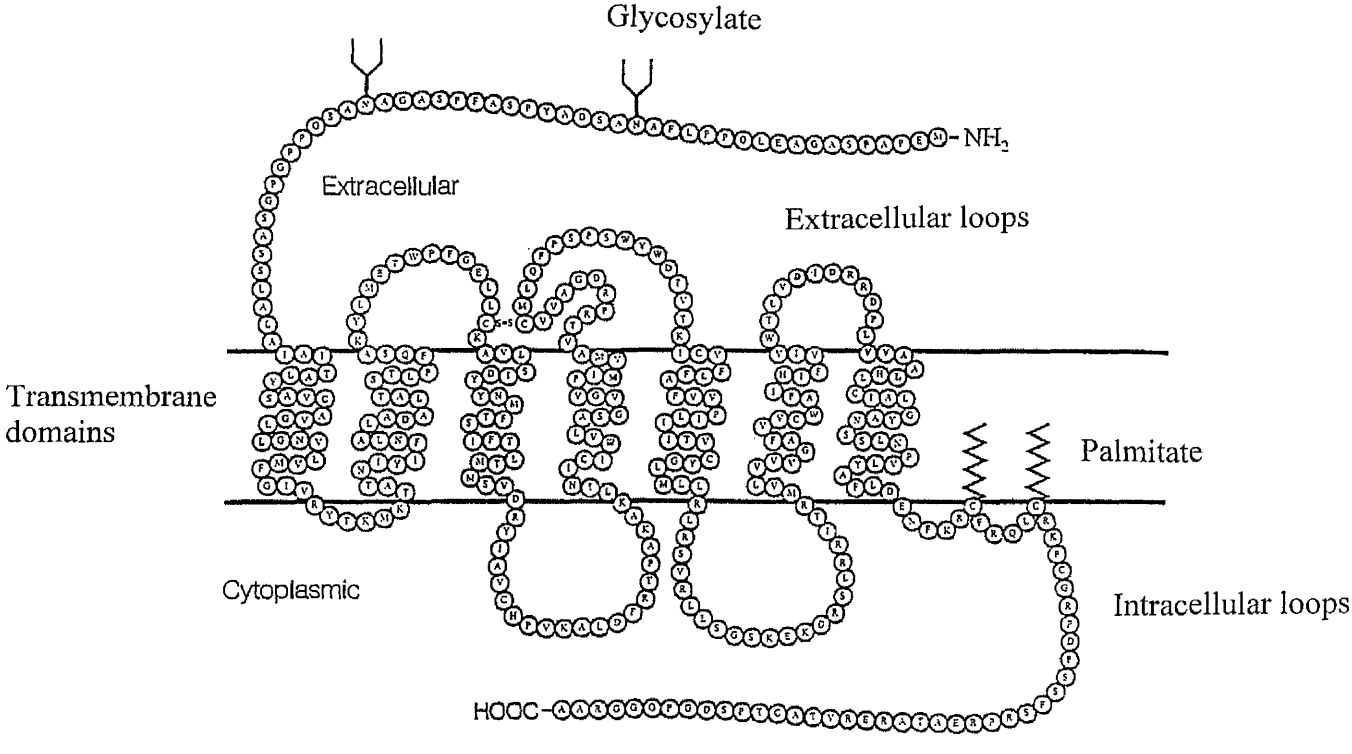
Glycosylate
Extracellular
Extracellular loops
Transmembrane domains
Palmitate
Cytoplasmic
Intracellular loops

b) Glycosylation

Glycosylation of plasma membrane proteins is a common post-translational modification that is thought to be important for protein folding in internal organelles and in some cases for membrane targeting and function. The two common classes of glycosylation are those containing N-glycosidically linked oligosaccharide chains attached to asparagine residues and O-glycosidically linked oligosaccharide chains linked to serine or threonine residues in the polypeptide (Lennarz, 1983).

c) Palmitoylation

Palmitoylation of specific cysteine residues has been demonstrated for several GPCRs. Post-translational acylation anchors the N-terminal portion of the cytoplasmic tail to the plasma membrane, creating a fourth intracellular loop. The acyl group is attached by a labile thioester bond to the cysteine residue, which allows the process to be reversed and gives cells the potential to control this modification. For receptors, abolition of palmitoylation by site-directed mutagenesis has been shown to either decrease coupling to G proteins (Hayashi *et al.*, 1997: Jensen *et al.*, 1995: Okamoto *et al.*, 1997), affect receptor internalisation (Kawate and Menon, 1994: Eason *et al.*, 1994), or modulate receptor phosphorylation by regulatory kinases (Moffett *et al.*, 1996). Agonist stimulation of the β_2 adrenergic receptor (β_2AR) has also been shown to increase the amount of covalently attached [^{3}H] palmitate (Mouillac *et al.*, 1992) as a result of an increased turnover rate of the receptor-bound palmitate (Loisel *et al.*, 1996).

A similar agonist-promoted increase in the turnover rate of receptor-bound palmitate has been observed for the α_{2A} adrenergic receptor (α_{2A}AR) (Kennedy and Limbird, 1994), the D_2-dopamine receptor (Ng *et al.*, 1994), and the m_2-muscarinic receptor (Hayashi and Haga, 1997).

d) Dimerisation

The GPCR family is probably the largest in the human genome. It has been demonstrated that members of this family can pair up with their own kind (homodimerisation). For example, using differentially (Flag and c-Myc) epitope-tagged receptors, Cvejic and Devi, (1997) examined the ability of mouse δ-opioid receptor (mDOR) to dimerise and the role of receptor dimerisation in agonist-induced internalisation. Agonists at the DOR increased the formation of receptor monomer, potentially a necessary step in the process of agonist-induced receptor internalisation. It has also been shown, however, that β-adrenoceptor agonists stabilise dimer formation and enhance receptor activation (Hebert *et al.*, 1996). Moreover Jordan and Devi, (1999) examined the ability of κ-opioid receptor (KOR) to heterodimerise with δ-opioid receptor (DOR) or μ-opioid receptor (MOR). They compared the ligand-binding properties of KOR-DOR heterodimers with those of KOR or DOR. The KOR-DOR heterodimer synergistically binds highly selective agonists and potentates signal transduction, which demonstrated that KOR-DOR heterodimers have been shown to have a pharmacology distinct from either DOR or KORs. Thus heterodimerisation of these GPCRs represents a novel mechanism that modulates their function. Data from the

opioid receptor study (Jordan and Devi, 1999) it might be interesting to find heterodimer-selective compounds.

In addition, several recent studies have provided evidence that GPCRs can pair up with even rather distantly related relatives to form larger oligomers (heterodimerisation) with distinct properties (Jones *et al.*, 1998: White *et al.*, 1998: Kaupmann *et al.*, 1998: Kuner *et al.*, 1999: Ng *et al.*, 1999: Martin *et al.*, 1999). These investigators described the identification of a second $GABA_B$ receptor, $GABA_BR_2$, which must be co-expressed with $GABA_BR_1$ to provide membrane delivery of the receptor and this was the first clear evidence for the existence of heterodimers. Rocheville and co-workers, (2000) showed that the dopamine D_2 receptor and the somatostatin SST_5 receptor can form heterodimers.

e) Phosphorylation

Many GPCRs come to be phosphorylated after agonist binding. One of the most intensively studied modification mechanisms involves phosphorylation by a family of G protein-coupled receptor kinases (GRKs), which are a family of serine/threonine protein kinases that specifically recognise agonist-occupied GPCR proteins as substrates. Phosphorylation of an activated GPCR leads to attenuation of receptor-G protein coupling. This reflects that binding of an arrestin to a GRK-phosphorylated receptor prevents coupling of that receptor to its cognate G protein.

Six distinct mammalian GRKs are known. These differ in tissue distribution and in regulatory properties (Premont *et al.*, 1995). The intracellular localisation of GRKs to membrane-bound receptor substrates is the most important known regulatory feature of these enzymes. The β adrenergic receptor kinases (GRK2 and GRK3) were named as activities that phosphorylated the agonist-occupied β_2 adrenergic receptor. They are targeted to the membrane by associating with heterotrimeric G protein βγ subunits released upon receptor activation of G proteins, however, their substrate specificity is not limited to adrenergic receptors (Benovic *et al.*, 1989). Within the past few years, a novel subfamily of the GRKs has emerged from molecular cloning studies. This subfamily includes the mammalian GRK4, GRK5, and GRK6, as well as the Drosophila GPRK2 sequence. GRK5 is the most extensively characterised of these new kinases and has been shown to phosphorylate rhodopsin, α_2 and β_2 adrenergic receptors, and m2-muscarinic receptors. All GRKs appear to play the same general cellular role of desensitising activated GPCRs, but utilise distinctly individual means to the same end.

II. Functional regulations

a) Desensitisation

Receptor desensitisation is a rapid and reversible loss of agonist affinity and receptor function, which is produced by uncoupling of the receptor from its G protein. This process is believed to be dependent upon the phosphorylation of serine/threonine

residues by GRKs (Pei *et al.*, 1995) and the binding of cytosolic proteins known as β-arrestins (Gurevich *et al.*, 1995). Two types of desensitisation can be distinguished on the basis of the underlying mechanism. Homologous desensitisation is mediated by agonist-dependent activation of the same receptor, whereas heterologous desensitisation is caused by activation of a different receptor. An important component of desensitisation, which occurs within seconds to minutes of receptor activation, is uncoupling of the activated receptor from its G proteins by receptor phosphorylation. Two classes of protein kinases mediate this phosphorylation. A unique class of serine/threonine protein kinases, namely G protein receptor kinases (GRKs), mediate agonist-dependent phosphorylation of GPCRs and initiate homologous desensitisation, which depends on their functional co-factors, the arrestins. Second messenger-dependent kinases [protein kinase C (PKC)] and [protein kinase A (PKA)] mediate phosphorylation of receptors in response to second messenger production and initiate heterologous desensitisation. Associated with desensitisation, many GPCRs becomes internalised into intracellular endosomes via the clathrin-coated vesicular pathway in a process dependent upon the GTPase dynamin (Chu *et al.*, 1997). Pei *et al.*, (1995) investigated the role of mDOR phosphorylation in receptor desensitisation. When expressed in HEK293 cells and exposed to agonist, the DOR underwent receptor-specific desensitisation within 10 min. These investigators concluded that short term desensitisation of the DOR involves phosphorylation of the receptor by one or more GPCR kinases but not PKC.

b) Internalisation and sequestration

In recent years, the phosphorylation of serines and threonines has become widely accepted as being important for agonist-dependent GPCR internalisation (Lefkowitz *et al.*, 1998). Several GPCRs, including β_2AR and neurotensin receptors, and ion channel receptors such as the N-methyl-D-aspartate receptor, have been shown to undergo agonist-induced tyrosine phosphorylation (Lu *et al.*, 1999). Kramer *et al.*, (2000) demonstrated that the DOR is phosphorylated at tyrosine residues in response to its stimulation by an agonist. The phosphorylation of one or more tyrosine residues appears to be important for opioid receptor signalling (MAPK activation) and agonist-dependent receptor regulation (internalisation).

c) Down-regulation

Receptor down-regulation is a loss of receptors from a cell that results from long-term (hours to days) continuous exposure of cells to agonists. Here there is an irreversible loss from the plasma membrane due to both internalisation and degradation, and after also a reduction in mRNA levels (Hausdorff *et al.*, 1990). Down-regulation may occur under pathological circumstances such as when there is continuous secretion of hormones and neurotransmitters from tumours. Down-regulation is also important during long-term administration of receptor agonists for therapeutic reasons, when it may be responsible for tolerance or tachyphylaxis (Lefkowitz, 1993). The requirement for downregulation are still not very clear, although there seems to be a requirement for

functional coupling with Gα, as S49 lymphoma cyc$^-$ cells lacking endogenous $G_s\alpha$ exhibit very little agonist-induced downregulation of the β_2AR (Mahan *et al.*, 1985).

III. Receptor activation models (Figure 1.2)

a) Two state receptor theory

In the two-state model of agonist action (Leff, 1995: Bond *et al.*, 1995), receptors are proposed to exist in equilibrium between two conformations, an active form (R*) and an inactive form (R). It is known that receptors exist in two states, R (receptor alone) and RG (receptor coupled to the G protein). The former has a low affinity for agonists, while the latter has a high affinity. Agonists act by preferentially binding to and enriching the active conformation, thereby increasing effector activity, whereas inverse agonists bind preferentially to the inactive (R) conformational state, leading to a reduction in ' basal ' effector activity. Neutral antagonists bind equally well to both R and R*, thus do not alter either the equilibrium between the two states and do not alter effector activity.

b) Ternary complex model and extended ternary complex model

Perhaps the most widely accepted model used to describe agonist activation of GPCRs is the ternary complex model, which accounts for the co-operative interactions

among receptor, G protein and agonist. These models generalised the classical model by allowing receptors to interact with ligands as well as G proteins. In its full version the ternary complex model assumes that four receptor species, R, AR, RG, and ARG, exist at equilibrium.

Work by Cotecchia *et al.*, (1990) and Kjelsberg *et al.*, (1992) on the α_{1B}-adrenoceptor suggests that this receptor may exist in active R_a and inactive R_i forms. Additional evidence for receptor activation has come from Parma *et al.*, (1993) who found CAM forms of thyrotropin and LH receptors, respectively. Based on such experimental results, Samama *et al.*, (1993) extended the ternary complex model to include the possibility of receptor activation. In their model, six receptor species are considered to exist at equilibrium, R_i, R_a, AR_i, AR_a, R_aG, and AR_aG. In the extended ternary complex model, receptor activation is a necessary precondition for G protein coupling.

c) Cubic ternary complex (CTC) model

A new equilibrium model of the interactions between receptors, ligands, and G proteins - the cubic ternary complex (CTC) model - has been proposed. The CTC model is a generalisation of the extended ternary complex model of Samama *et al.,* (1993) by permitting G proteins to interact with receptors in both their active and inactive states. Thus, in the CTC model eight receptor species exist at equilibrium, four native receptor

species and their four ligand-bound couterparts, R_i, R_a, AR_i, AR_a, R_iG, R_aG, AR_iG, and AR_aG. **[R_i: inactive receptor, R_a: active receptor, A: ligand, G: G protein]**

Figure 1.2. Receptor activation models

a) The ternary complex model

This model takes into account the role of the coupling G protein in receptor activation as the presence of guanine nucleotide appears to convert the receptor from a high to low affinity state. The scheme shows M as the affinity of R (receptor) for G (G protein), α as the efficacy of the ligand and K the receptor affinity of the ligand. K = [HR]/[H][R], M = [RG]/[R][G], α = [HRG][R]/[HR][RG].

b) The extended ternary complex model

This shows the revised or allosteric ternary complex model. This model introduces an explicit isomerisation step regulating the formation of the state of the receptor from R to R*, which is capable of binding to the G protein. J represents an equilibrium constant in receptor isomerisation. J = [R*]/[R], K = [HR]/[H][R], M = [R*G]/[R*][G], α = [HR*G][R*]/[HR*][R*G], β = [HR*][R]/[HR][R*].

c) The cubic ternary complex (CTC) model

A single receptor can form two distinct activated conformations that selectively interact with different G proteins. A = agonist, R = receptor and G = G protein

Figure 1.2

a)

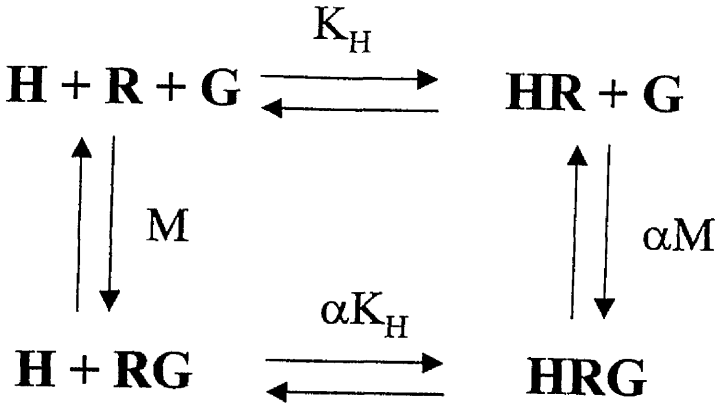

b)

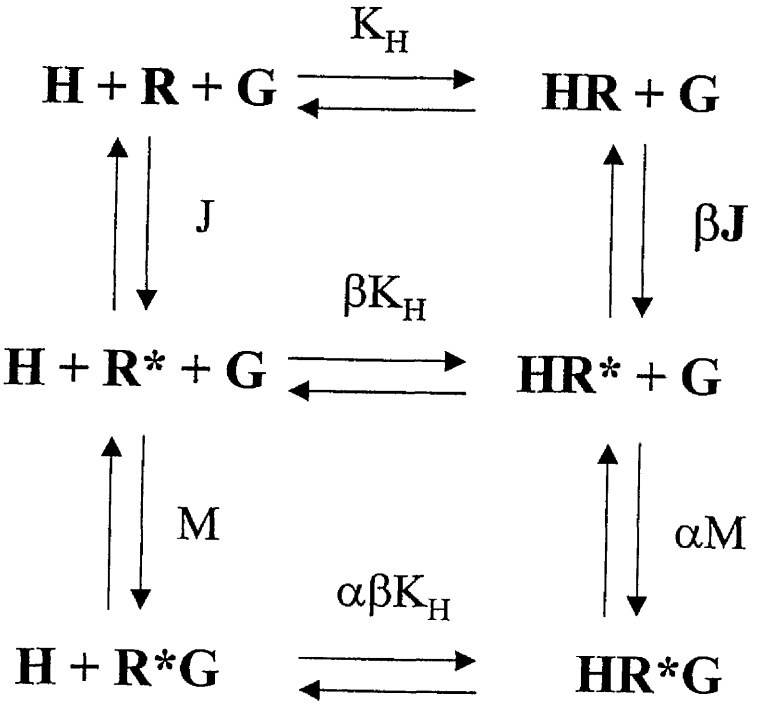

c)

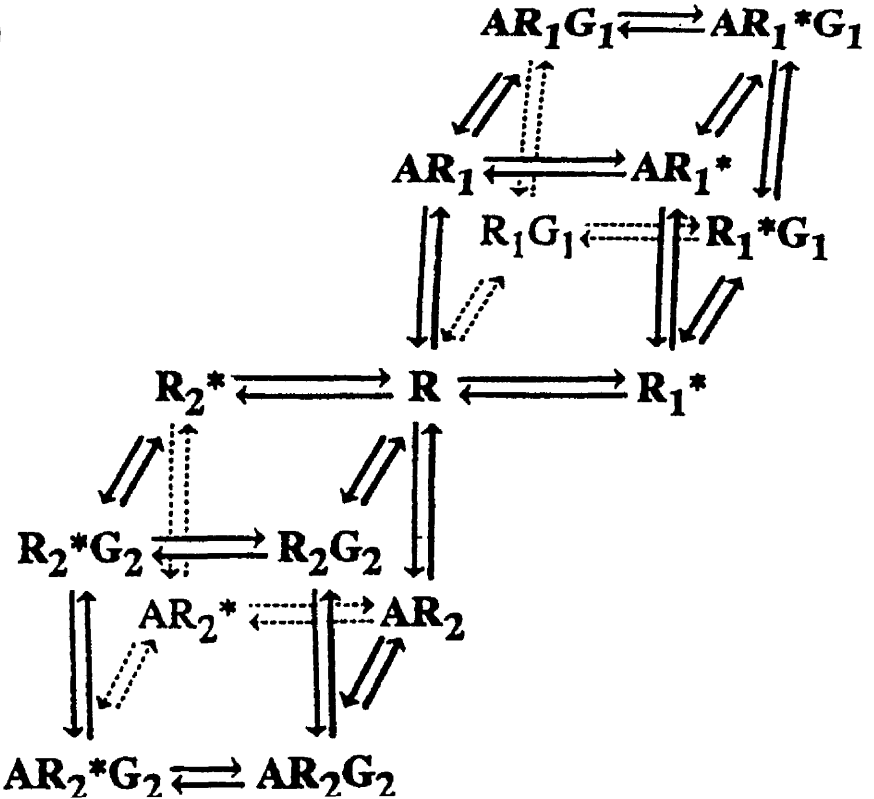

d) Inverse agonism of Constitutive Active Mutants (CAM)

Inverse agonists are ligands that preferentially stabilise inactive conformations of GPCRs. In a range of systems, sustained treatment with inverse agonist can produce substantially greater upregulation of receptor levels than antagonists (Milligan and Bond, 1997). The use of constitutively active mutant (CAM) GPCRs allows to display enhanced agonist-independent signal transduction compared to the equivalent wild-type GPCR when expressed at similar level (Samama *et al.,* 1993). Inverse agonists cause upregulation of a CAM α_{1B} receptor, CAM β_2AR and wild type β_2 and H_2 receptor. (Pei *et al.*, 1994: MacEwan and Milligan, 1996: Lee *et al.*, 1997: Smit *et al.*, 1996). Pei *et al.*, (1994) first examined that sustained treatment of CHO cells expressing a CAM form of the human β_2AR with betaxolol resulted in an approximate doubling of its levels. Also MacEwan and Milligan, (1996) demonstrated that following stable transfection of the CAM β_2AR in NG108-15 cells both sotalol and betaxolol produced strong upregulation. Wild type rat H_2 receptor in transfected CHO cells was also reported that the inverse agonist cimetidine, but not the neutral antagonist burimamide, causes an increase in the number of constitutively active H_2 receptors (Smit *et al.*, 1996). A rather different scenario could be proposed from studies on a Leu^{124} to Ala mutation of the H_2 receptor. This mutation limits both basal and histamine-stimulated cAMP productions, and cimetidine failed to cause significant upregulation of this form of the receptor. In another study, after upregulation of a CAM α_{1B} receptor produced by treatment with phentolamine, basal phospholipase D (PLD), basal PLD activity was increased and the

agonist phenylephrine was then able to stimulate PLD activity to greater levels (Lee *et al.*, 1997).

1.3. The human δ-opioid receptor (hDOR)

I. Opioids for medical use

Opium has been extracted from poppy seeds (*Papaver somniferum*) for several thousand years to treat cough and diarrhoea, to relieve pain, and also because it evokes euphoria. The active ingredients of opium are alkaloid compounds, the so-called opioids. These molecules display strong analgesic and addictive properties and have been the subject of intense investigations. Morphine is the most active component of opium and was the first opioid to be isolated. Today, morphine remains the most potent pain-killer used clinically, despite a considerable number of adverse side-effects. Although the 1980s and 1990s led to the development of many novel potent opioids by the pharmaceutical industry, the ideal analgesic is still awaited eagerly. The illegal abuse of heroin, a diacetylated morphine derivative, represents a major public health problem, but mechanisms underlying opioid addiction are still poorly understood.

II. Cloning

The DOR was the first opioid receptor to be cloned. Two groups independently cloned the mouse DOR (mDOR) by preparing an expression library from mouse neuroblastoma x rat glioma hybrid NG 108-15 cells and transfecting the library into monkey fibroblast (COS) cells (Evans *et al.*, 1992: Kieffer *et al.*, 1992, 1994). The use

of the NG108-15 cell line was a critical step because these cells express DOR at a greater density than is normally found in brain tissue (Knapp *et al.*, 1995b). Both groups used radioligand binding assays to detect mDOR but used different expression screening procedures. A cDNA sequence encoding a 372-amino acid protein was identified. The rat DOR (rDOR) was cloned by Fukuda *et al.,* (1993) from a rat cerebellum cDNA library by a hybridisation screening method using an mDOR DNA as probe. The rDOR also had 372 amino acids with 97% homology to the mDOR. Finally, the human DOR (hDOR) was cloned using hybridisation-screening methods (Knapp *et al.*, 1994). cDNA fragments obtained from human striatum and temporal cortex libraries showed a highly homologous nucleotide sequence to the mDOR. The open reading frame (ORF) encoded a 372 residue protein with 93% homology to both the mDOR and rDOR. Later hDOR was also cloned by Simonin *et al.* (1994) from the SH-SY5Y human neuroblastoma cell line.

III. Structural features

The DOR, which belongs to the seven transmembrane GPCR superfamily, possesses a common three-dimensional structure that spans the cell membrane seven times, forming three extracellular loops and three intracellular loops. This has consensus glycosylation sites at Asn^{18} and Asn^{32} in the N-terminal and there is likely to be a disulfide bond between Cys^{121} and Cys^{198}. In the C-terminal of the receptor, there are sites for palmitoylation at Cys^{328} and Cys^{333}.

IV. Main functions and regulations

The δ-opioid receptor (DOR) is discretely distributed in the central nervous system and the highest densities are found in olfactory bulb, neocortex, caudate putamen and nucleus accumbens. The thalamus, hypothalamus and brain stem have a moderate density of the DOR. The DOR appears to have a role in analgesia, gastrointestinal motility, mood and behaviour as well as in cardiovascular regulation. It is well established that most DOR-mediated events are dependent on the activity of *Pertussis toxin* (PTx)-sensitive G proteins. It is also well established that DOR-selective ligands inhibit intracellular cAMP levels via $G_i/_o\alpha$ proteins and modulate the activity of voltage-gated calcium and potassium channels. The $G_i\alpha$ subunit interacts with AC, leading to its acute inhibition and subsequently to a reduction in cAMP levels in the cell. However, chronic activation of inhibitory receptors has been shown to lead to an increase in cAMP accumulation upon withdrawal of the inhibitory agonist, in other words, " AC superactivation " is observed (Avidor-Reiss *et al.*, 1995). AC superactivation is believed to play a role in the development of tolerance and withdrawal following prolonged opiate exposure (Avidor-Reiss *et al.*, 1995).

Cvejic and Devi, (1997) examined the ability of mDOR to dimerise and the role of receptor dimerisation in agonist-induced internalisation. Using differentially (Flag and c-Myc) epitope-tagged receptors, these investigators showed that the DOR exist as dimers and that agonist treatment modulates the level of dimers. Also Jordan and Devi, (1999) examined the ability of the κ opioid receptor (KOR) to heterodimerise with DOR

or μ-opioid receptor (MOR) by co-expressing myc-tagged KORs with either Flag-tagged DORs or Flag-tagged MORs. They compared the ligand-binding properties of highly selective agonists and antagonists to KOR-DOR heterodimers with those of KOR or DOR in membranes from cells expressing either KOR or DOR or both KOR and DOR. The KOR-DOR heterodimer synergistically bound highly selective agonists and potentiated signal transduction. Thus heterodimerisation of these GPCRs may represent a novel mechanism to modulate their function.

Knockout strategies involve generating transgenic mice possessing a discrete gene deletion that results in failure to express a particular gene product. The absence of a particular gene product may **1)** disrupt an intricate system of homeostasis and development resulting in severe pathology or the death of the mutant or **2)** result in a deregulated system where alternative systems compensate for the loss of the deleted gene product. Recently, mice lacking MORs (MOR-deficient mice) or opioid peptides have been produced by gene targeting, providing molecular tools to study opioid function *in vivo* (Sora *et al.*, 1997: Matthes *et al.*, 1996). Sora *et al.,* (1997) generated a transgenic MOR knockout mouse by homologous recombination technology and used this to study interactions between DOR and MOR in the central nervous system. Although the heterozygous knockout mice exhibit about 54% of wild-type levels of MOR expression, the homozygous knockout mice displayed 0% receptor expression. These investigators used hot-plate and tail-flick tests and found that DOR-selective agonist [D-Pen^2, D-Pen^5]-enkephalin (DPDPE) induced a weaker than expected antinociceptive effect in μ-knockout mice compared with control animals. These results

indicate that the DOR is functional and mediates antinociception in the absence of the MOR. Matthes *et al.*, (1996) showed that an analgesic dose of morphine decreased respiratory frequency and increased respiration time in wild-type mice. However, no change in respiratory parameters could be measured in similarly treated MOR-deficient mice. Respiratory depression is the primary factor in the lethal toxicity of morphine. Zhu *et al.,* (1999) used gene targeting to delete exon 2 of mDOR-1, which encodes the DOR. These investigators demonstrated that DOR-1 mutant mice do not develop analgesic tolerance to morphine, genetically demonstrating a central role for DOR-1 in this process. The use of opioid-receptor-deficient mice in animal models for the study of chronic pain, stress and reward mechanisms should provide substantial insights of DOR, MOR or KORs.

Human opioid receptors of the DOR, MOR and KOR subtypes have been successfully expressed in *Escherichia coli (E. coli.)* as fusions to the C-terminus of the periplasmic maltose-binding protein (MBP) product of the malE gene, a soluble periplasmic protein that is part of the maltose import chain in *E. coli.* (Stanasila *et al.*, 1999). Binding of [^{3}H] diprenorphine to intact cells or membrane preparations was saturable, with a K_d of 2.5 nM, 0.66 nM and 0.75 nM for hDOR, hMOR and hKORs respectively. Receptor high-affinity state for agonists was reconstituted in the presence of heterotrimeric G proteins. This study demonstrated that opioid receptors can be expressed in a functional form in bacteria and pointed out the advantage of *E. coli.* as an expression system for pharmacological studies.

Constitutively active mutant (CAM) GPCRs display enhanced agonist-independent signal transduction compared to the equivalent wild-type GPCR when expressed at similar levels (Samama *et al.*, 1993). Ligands which display inverse agonism at GPCRs decrease this intrinsic activity. Expression of the DOR in Rat-1 fibroblasts resulted in the inverse agonist ICI174864 being able to cause inhibition of basal high affinity GTPase activity and of the binding of [^{35}S] GTPγS in a membranes of a clone of these cells which expresses high levels of the receptor (Mullaney *et al.*, 1996). These effects were blocked by co-addition of the neutral antagonist TIPP[ψ], demonstrating a requirement for the DOR. The inverse agonist properties of ICI174864 could also be demonstrated in whole cells, where stimulation of forskolin-amplified adenylyl cyclase (AC) activity was produced by ICI174864.

V. Identification of DOR domains mediating receptor function

The DOR regions involved in mediating receptor function have been identified by the construction of chimeric receptors containing sequences from KOR and MOR, site-directed mutagenesis of specific amino acid residues within the receptor and by the construction of truncation or deletion mutants.

- **Identification of ligand-binding domains**

Using the idea that opioid ligands are bivalent molecules in which one portion of the ligand mediates signal transduction while another ligand site determines selectivity toward DOR, KOR or MOR. Metzger and Ferguson, (1995) explained the selectivity of drug binding to opioid receptors. When the sixth transmembrane helix (TM) and third extracellular loop of the DOR were replaced by the analogous MOR-sequence, the chimeric receptor bounds DOR-selective drugs with affinities similar to control MORs. These data were interpreted to mean that the third extracellular loop sequence in the chimeric receptor adopts a conformation that blocks DOR-selective agonist binding to sites in the highly conserved TMs of the receptor.

a). The third extracellular of the DOR is critical for ligand binding.

Ligand selectivity for DOR depends on recognition sites spanning the fifth through seventh TMs. Meng *et al.*, (1995) constructed chimeric receptors from cloned rat δ-opioid receptor (rDOR) and KOR. DOR-selective peptides showed moderate affinity for κ(1-141)/δ(132-372) and κ(1-227)/δ(215-372) constructs, which retain the native fifth through seventh TMs of the DOR. However these drugs had no affinity for κ(1-141) /δ(132-214)/κ(228-380) and δ(1-214)/κ(228-380) constructs, which contain the fifth through seventh TMs of the KOR. Also, antagonist ligands bound with high affinity to an KOR/DOR-chimeric receptor containing DOR sequence carboxyl to the second extracellular loop (amino acids 215-372).

In addition, Wang *et al.*, (1994) constructed chimaeric receptors in which mDOR sequence from the N terminus and mMOR sequence from the C-terminus were ligated at each of the seven TMs. Chimeric receptors exhibited a loss of D-Ala^2, N-MePhe^4, Gly-ol]-enkephalin [DAMGO, MOR agonist]-binding affinity whenever the first extracellular loop of the MOR was lacking and a loss of [D-Ser^2, Leu^5]-enkephalyl-Thr [DSLET, DOR agonist]-binding whenever the third extracellular loop of the DOR was missing from the chimeric receptor. Also, these investigators found that point mutations in the third extracellular loop of the DOR that replaced both Arg^{291} and Arg^{292} with Gln selectively reduced the binding of DSLET but not of nonselective opioid agonists. Binding of the DOR selective antagonist, naltrindole was also unaffected by this double-point mutation. These results indicates that **1)** the third extracellular loop of the DOR play an important role in the high-affinity binding of the DOR-selective agonist DSLET and **2)** the first extracellular loop of the MOR play an important role in high-affinity DAMGO binding.

Other work was performed on chimeric receptors combining DOR/KOR or DOR/MOR sequences (Meng *et al.*, 1996). They also introduced a number of point mutations in the third extracellular loop of the DOR. Some of these mutations reduced the affinity of some DOR-selective ligands, whereas none of the mutations were sufficient to ablate the binding of DOR-selective ligands. These results also indicated that a region composed of the sixth TM and the third extracellular loop is essential in determining selectivity of drugs for DORs.

In another study, with cells expressing wild type DOR or MOR or one of two DOR/MOR-chimeric receptors in transfected HEK293 cells, the binding of three DOR agonists (SNC80, DPDPE, Del-II) and DOR-selective antagonist naltrindole were measured (Valiquette *et al.*, 1996). The third extracellular loop sequence of DOR was replaced by that from the MOR. In both chimeric constructs, the binding of all four DOR-selective ligands was significantly reduced. Specific key residues in the third extracellular loop region was substituted by Ala or Gly for the wild type amino acid at 20 different positions between 275 and 312 (sixth TM-seventh TM of the DOR). In particular, replacement of Ala for Trp^{284}, Val^{296}, and Val^{297} consistently reduced the binding of the DOR ligands tested, suggesting that these three residues are involved in the selectivity of these drugs.

Furthermore, a hDOR mutant in which Trp^{284} was replaced by Leu ($W^{284}L$) caused a 42-fold shift toward higher drug concentrations in the K_i for binding of SNC121 but not other DOR ligands (Li *et al.*, 1996). This suggests that SNC121 interacts with Trp^{284} in a unique manner that is not shared by other DOR-selective ligands.

b). First extracellular loop

A chimeric DOR/MOR/DOR receptor was constructed by replacing the first extracellular loop of the cloned rat DOR for the same region in the cloned rat MOR. This substitution conferred high affinity for [^{3}H] DAMGO to the chimeric receptor (Onogi *et al.*, 1995). Because of seven amino acids difference in the first extracellular

loops of the MOR and DOR, site-directed mutagenesis was used individually to replace those seven residues in the DOR with the corresponding amino acids of MOR (Minami *et al.*, 1996). Only upon replacement of Lys^{108} was high affinity binding of the MOR-selective agonist DAMGO produced. To further characterise the structural requirement for the residue at position 108, Lys^{108} was replaced by 19 other amino acids. These revealed that it was not so much substitution by Asn at position 108 as it was elimination of the more obstructive Lys at position 108 that allowed high-affinity DAMGO binding.

c) Second extracellular loop

Chimeric receptors constructed by Meng *et al.*, (1996) from cloned rat opioid receptors which substituted the second extracellular loop of the DOR for that of either the KOR or MOR were shown to be insufficient to confer selective binding of DOR-selective ligands. Also using a chimera of the δ(1-186)/μ(208-234)/δ(213-372), DOR-selective ligands bound to the second loop with affinity similar to the wild type DOR (Li *et al.*, 1996). This precludes a role for the second extracellular loop in determining DOR ligand recognition.

d) TM domains

The role of residues in the TMs of the DOR in ligand binding is under investigation. A study conducted soon after the cloning of opioid receptors showed that

the Asp^{95} residue in TM2 of the mDOR was responsible for high affinity agonist binding, but not involved in the binding of antagonists and nonselective agonists (Kong *et al.*, 1993). When Asp^{95} was replaced with Asn, the mutant receptor exhibited a selective reduction in the binding of DOR-selective agonist ligands without any alteration in the binding of DOR-selective antagonists.

The third putative TM domain of DOR contains a conserved Asp^{128} residue that is typically found in biogenic amine binding GPCRs [for example, human β_2AR, human α_{2A}AR, human m_1 muscarinic, rat $5HT_A$ serotonin, rat D_2 dopamine, human H_2 histamine] and is generally believed to form an ion pair with the cationic neurotransmitters. When this residue was mutated to Ala it did not modify the binding affinity of a representative set of opioid compounds, including bremazocine, diprenorphine, naloxone, Tyr-D-Thr-Gly-Phe-Leu-Thr [DTLET], $D\text{-}Ala^2$, $D\text{-}Leu^5$-enkephalin [DADLE], $D\text{-}Pen^2$, $D\text{-}Pen^5$-enkephalin [DPDPE], deltorphine II [Del-II], +/--4-(a-R*)-a-(2S*,5R*)-4-allyl-2,5-di-methyl-1-piperazinyl-3-hydroxybenzyl-N,N-diethylbenzamide [BW373U86], and naltrindole. It nevertheless decreased receptor expression level and affected the binding of three agonists, DADLE, DTLET and BW373U86. However, Asp^{128} to Asn mutation strongly impaired the binding of all of the above ligands and highlighted differential modes of interaction for alkaloids and peptides. These results indicate that Asp^{128} is situated in a region of the receptor that is important for ligand binding as the Asp to Asn mutation shifted the affinity of all opioid ligands tested.

Three-dimensional computer modelling of the receptor has identified the role of TM aromatic residues in ligand recognition of the DOR, which span TMs III to VII and consist of tyrosine, phenylalanine, and tryptophan residues (Befort *et al.*, 1996). Based on this model, these investigators mutated residues Tyr^{129}(TM III), Trp^{173} (TM IV), Phe^{218} (TM V), Phe^{222} (TM V), Trp^{274} (TM VI), and Tyr^{308} (TM VII) of the DOR. They found that mutations of Tyr^{129} caused the greatest shifts in drug affinity toward higher concentrations. Mutations at Phe^{218}, Phe^{222}, and Tyr^{308} had modest effects on the affinity of all agonists tested. Mutation of Trp^{173} and Trp^{274} caused 40-fold affinity shifts for some ligands and had no effect on others. Taken together, these data demonstrate the importance of the TMs in ligand binding and suggest that DOR-selective ligands interact at different amino acid residues to mediate binding.

e) N-terminus domain

A subsequent study revealed that both DPDPE and naltrindole bind to the N-terminus chimeric κ(1-78)/δ(70-372) receptor but not to the reverse chimeric δ(1-69)/κ(79-380) receptor; this finding suggests that the N-terminal domain of the DOR is not critical for binding of DOR-selective ligands (Kong *et al.*, 1994).

• DOR domains mediating down-regulation.

In 1996, Cvejic *et al.,* investigated the down-regulation of the mDOR using truncation mutants. When the C-terminal 37 amino acids in the intracellular tail of the

receptor were deleted, receptor down regulation in response to chronic (2-48h) DOR-selective agonist, DADLE treatment was blocked. By contrast when the mDOR was truncated by 15 amino acids, the receptor did down-regulate on chronic DADLE treatment. When the cytoplasmic tail residue Thr^{353} was mutated to an Ala in the mDOR, receptor down-regulation was blocked. Even though Cvejic *et al.*, (1996) demonstrated that Thr^{353} of the mDOR played an important role in down-regulation, this mechanism must be different for the human receptor, because Thr^{353} is already an Ala in the hDOR sequence (Knapp *et al.*, 1994) and the human receptor down-regulates on chronic agonist exposure (Malatynska *et al.*, 1996).

- **DOR domains mediating signal transduction cascades.**

Recently, there were two reports about the creation of constitutively active DOR through mutagenesis. One study demonstrated that the replacement of an Asp residue in TM3 with Ala, His, or Lys would endow the mutated receptors with constitutive activity. Although naltrindole still functioned an antagonist at an Asp to Ala mutant, it became an agonist at the receptor with the Ala to Lys mutation (Cavalli *et al.*, 1999). Another study mutated the same Asp residue (Asp^{128}) in TM3, the Tyr residue immediately below Asp in TM3 (Tyr^{129}), and a Tyr residue in TM7 (Tyr^{308}) (Befort *et al.*, 1999). All these receptor mutants exhibited constitutive activity, suggesting that the wild type DOR use these residues to maintain an inactive state in the absence of agonists.

Classical opioid antagonists (i.e., naloxone, naltrexone, naltriben, and TIPPψ) were found to behave as agonists on the MOR and DOR with mutations at a conserved Ser residue in TM4 (DORS177L and MORS196L). The mutated receptors were not constitutively active, suggesting that Ser plays a specific role in the ligand-induced receptor process (Claude *et al.*, 1996). A partial agonist to antagonist conversion was also observed in the DOR with a TM2 Asp mutation (Bot *et al.*, 1998). These results suggest that ligand interactions with residues of TM helices can alter the conformation of the DOR to permit signalling of the receptor to second messenger systems.

Merkouris *et al.*, (1996) examined which regions of DOR mediate interactions with G proteins through the use of synthetic peptides. They found that peptides homologous to the third intracellular loop inhibited both GTPase activity and [^{35}S] GTPγS binding activity. In addition, these investigators also examined the effect of the peptides on binding of the agonist [^{3}H] DSLET. Peptides homologous to the third intracellular loop reduced [^{3}H] DSLET binding, whereas peptides homologous to the second intracellular loop did not. Unexpectedly, a peptide homologous to residues 322 through 333 of the C-terminus also reduced [^{3}H] DSLET binding. These findings suggest that the C-terminal tail may interact with receptor-associated G proteins but, it is not vital because neither GTPase activity or [^{35}S] GTPγS binding activity was blocked in the presence of this peptide.

1.4. Guanine nucleotide binding proteins (G proteins)

I. Structures, functions and mechanisms

GPCRs transduce a large variety of signals across the cell membrane via heterotrimeric G proteins. G proteins transduce ligand binding to these receptors into intracellular responses that underlie physiological responses of tissues and organisms. G protein heterotrimers consist of three subunits named α, β and γ. So far some 20α, 6β and 12γ polypeptides have been identified. All α-subunits share biochemical and structural properties and these are summarised in **Table 1.1**. Four main classes of G proteins are known: G_s, $G_{i/o/t}$, G_q and $G_{12/13}$. They can be classified into the following structurally and functionally related groups:

1) α_s **– group**: the members of this group stimulate the isoforms of AC
2) $\alpha_{i/o/t}$ **– group**: this can be divided into $\alpha_{i/o/z}$ and $\alpha_{t/g}$ subunits. The $\alpha_{i/o/z}$ subunits inhibit some isoforms of AC; they also inhibit and stimulate neuronal Ca^{2+} and K^+ channels, respectively (an effect that is due to the release of free βγ-dimers). The $\alpha_{t/g}$ subunits are transducins and gustducin, which stimulate the retinal cGMP-phosphodiesterases and presumably a related gustatory effector, respectively.
3) α_q **– group**: these subunits activate the β-isoenzymes of PLC and non-receptor tyrosine kinases of the *btk*-family.
4) $\alpha_{12/13}$ **– group**: regulate low-molecular-weight G proteins of the Rho-family (which affect the cytoskeleton) and Na^+-H^+-exchange.

The cycle of G protein activation can be summarised into a four-step reaction **(Figure 1.3).**

1) The basal state, in which the G protein is a αβγ-heterotrimer with GDP, bound to the α–subunit: In the absence of activation by a receptor, the rate of GDP release ($K_{off} \leq 0.1$ min $^{-1}$) is much lower than the rate of GTP hydrolysis ($K_{cat} \geq 0.1$ min $^{-1}$); this kinetic feature clamps the system in the 'off' position.

2) Receptor-mediated GDP release: The agonist-liganded, activated receptor interacts with the cognate G protein(s) and dramatically accelerates the rate of GDP release from the α-subunit. In the absence of added GTP (or of its hydrolysis-resistant analogues), agonist (A), receptor (R) and G protein (G) form a ternary complex (ARG), in which the agonist is bound with considerably higher affinity than if bound to the receptor alone. This high affinity state is typically seen in binding experiments that use membrane preparations. However, in intact cells, GTP concentrations are high and GTP binds instantaneously to the empty guanine-nucleotide-binding pocket.

3) Subunit dissociation and effector regulation: upon binding of GTP in the presence of Mg^{2+}, the α-subunit undergoes a change in conformation; the activated α-subunit ($\alpha* - GTP - Mg^{2+}$) dissociates from the βγ-dimer; both the GTP-bound α-subunit and the free βγ-dimer can then interact with appropriate effector proteins and modulate their activity.

4) Deactivation and return to the basal state: the intrinsic GTPase activity of the α-subunit cleaves the terminal phosphate group of GTP; the GDP-liganded α-subunit re-associates with βγ which results in the deactivation of both components. The system then relaxes to the basal state.

Figure 1.3. The GTPase cycle of trimeric G proteins

The **'turn-on'** step begins when the activated receptor (R*) associates with the trimer of (α•GDP•$\beta\gamma$), causing dissociation of GDP. Then GTP binds to the complex of R* with the trimer in its 'empty' state (α_e•$\beta\gamma$), and the resulting GTP-induced conformational change causes α•GTP to dissociate from R* and from $\beta\gamma$. After the **'turn-off'** step (hydrolysis of bound GTP to GDP and inorganic phosphate, Pi), α•GDP reassociates with $\beta\gamma$.

Figure 1.3

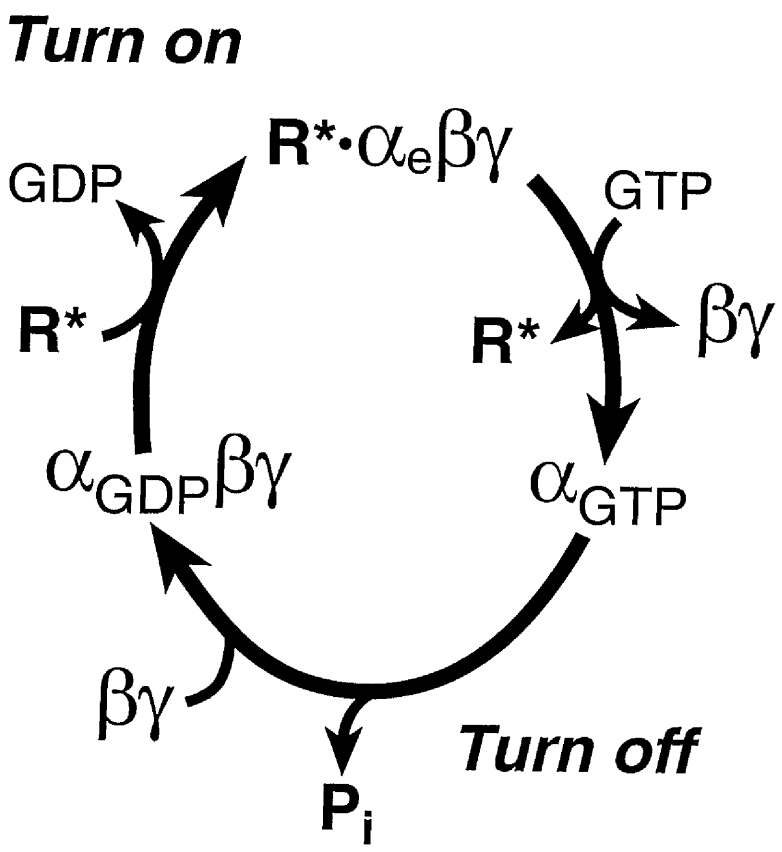

Table 1.1. Biochemical properties of G protein α-subunits

Feature	Property of α-subunits
Structure	40-46 kDa: RAS-like (~20 kDa) and helical domain (~20 kDa)
Guanine nucleotide binding	GDP/GTP-bound in cleft between the two domains; inactive in the GDP-bound form; active in the GTP-Mg^{2+}-bound form and when joined to GDP-Mg^{2+}.
Conformational switch	Accommodated by changes in three discontiguous regions (switch I-III)
Membrane anchoring	Via co-translational (aminoterminal myristoylation, e.g. $G_i\alpha$) and post-translational modification (palmitoylation on Cys close to the N-terminus)
Receptor binding and Activation	To C-terminus of Gα: strand β6/helix α5 and last ~10 amino acids. GDP/GTP-exchange reaction catalysed by the appropriate receptor in a manner dependent on βγ-dimers
Effector regulation	Group-specific for α-subunits. Effector binding to three discontiguous regions (switch II; the region adjacent to switch III; helix α4 and the loop connecting α4 and α6)
Deactivation	By intrinsic GTPase and by reassociation with βγ-dimers (which bind to the amnioterminus and to switch II of Gα)
Regulation	GTPase accelerated and effector regulation blocked by RGS proteins through binding to switch regions I-III
Bacterial exotoxin	Catalyse NAD-dependent ADP-ribosylation of:
Cholera toxin	Arg187/188, Arg201/202 in splice variants of $G_s\alpha$, ($G_t\alpha$) → persistent activation due to impaired GTP-hydrolysis;
Pertussis toxin	A Cys close to C-terminus in $G_o\alpha$, $G_i\alpha$, $G_t\alpha$ → Blocks receptor binding

II. G protein α subunits

There are 20 different mammalian Gα subunits to date, classified into 4 subfamilies according to the similarity of their amino acids (56% to 95%). As seen in Table 1.2, there are 17 gene products, with splice variants of $G_s\alpha$ and $G_o\alpha$, and their size ranges from 39 to 52 kDa (Iismaa *et al.*, 1994). Members of the same subfamily may activate the same effector (e.g., AC or PLC) although this is not absolute.

a) $G_s\alpha$ subfamily

The $G_s\alpha$ subfamily is so named due to the ability of these G proteins to stimulate the enzyme AC upon binding of GTP (Cassel and Selinger, 1978: Ross and Gilman, 1977). G_s is ubiquitously expressed in all cells, and thus, in principle, could be purified from any source. The initial purification was from rabbit liver. Ross *et al.*, (1979) found two protein components, either of which by itself catalyses the formation of cyclic AMP with Mg-ATP as substrate, which were found plasma membranes of wild type S49 cells, rat or rabbit liver, or avian erythrocytes and also found in an AC-deficient hepatoma cell line. Mixture of the two reconstitutes Mg-ATP-dependent, fluoride-and Guanylyl 5′-βγ imido-diphosphate [Gpp[NH]p]-stimulable activity. Also mixture of AC-S49 membranes with a crude detergent-solubilised preparation of the regulatory protein reconstitutes hormone-stimulable AC activity. The latter findings permitted the purification of G_s by Northup *et al.*, (1980). $G_s\alpha$ has 4 splice variants, known as $G_s\alpha1$, $G_s\alpha2$, $G_s\alpha3$, and $G_s\alpha4$ (Bray *et al.*, 1986). $G_s\alpha1$ and $G_s\alpha3$ are identical except that

$G_s\alpha 3$ lacks a single stretch of 15 amino acids (from exon 3). $G_s\alpha 2$ and $G_s\alpha 4$ are identical to $G_s\alpha 1$ and $G_s\alpha 3$ respectively but have 3 additional nucleotides at the 5′ end of exon 4. The longer forms ($G_s\alpha 1$ and $G_s\alpha 2$) are known as $G_s\alpha$ long ($G_s\alpha(L)$) while the shorter forms ($G_s\alpha 3$ and $G_s\alpha 4$) are known as $G_s\alpha$ short ($G_s\alpha(S)$). $G_s\alpha$ can activate all 9 mammalian ACs.

$G_{olf}\alpha$ is grouped under the $G_s\alpha$ subfamily due to high homology with $G_s\alpha$. It is selectively expressed in the cilia cells of the olfactory bulb and thus *in vivo* only couples to the very large class of olfactory receptors. It has an ability to activate the olfactory specific AC type III.

Members of the $G_s\alpha$ subfamily are ADP-ribosylated by cholera toxin (CTx) from *Vibrio cholerae* at a crucial arginine residue [arginine 201 in $G_s\alpha(L)$] in the GTPase domain. ADP-ribosylation induced by CTx interferes with receptor-stimulated GTP hydrolysis.

b) $G_i\alpha$ subfamily

First visualised as a 41-kDa substrate for ADP-ribosylation by PTx, oligomeric Gi was purified from rabbit liver and human erythrocytes by techniques nearly identical to those developed for Gs. Nukada *et al.*, (1986) purified $G_i\alpha$ from bovine brain and the cDNA encodes a protein with 354 amino acid residues and a calculated molecular weight of 40, 400. Itoh *et al.*, (1986) screened a rat C6 glioma cDNA library with an

oligonucleotide probe based on amino acid sequence data obtained with purified rat brain $G_i\alpha$ and $G_o\alpha$.

$G_{i1}\alpha$ is one of the largest members of the Gi family with a *Mr* of 41 kDa and is a substrate for ADP-ribosylation by PTx **(Figure 1.4)**. $G_{i2}\alpha$ is the smallest of the three Gi proteins, is also substrate for ADP-ribosylation by PTx and shares around 88% amino acid identity with $G_{i1}\alpha$. $G_{i3}\alpha$ is the third of the Gi family and is thought to stimulate various ion channels in the plasma membrane. An amiloride-sensitive Na^+ channel was identified in renal epithelial cell line A6 which could be activated via $G_{i3}\alpha$ (Cantiello *et al.*, 1989), apparently via stimulation of phospholipase A_2 (Cantiello *et al.*, 1990). Members of the $G_{i1}\alpha$ family have been shown to cause inhibition of cAMP via AC, an effect that is blocked by treatment with PTx.

$G_o\alpha$ is named for G ' other ', first identified as a 39 kDa PTx substrate purified from bovine brain (Neer *et al.*, 1984: Milligan and Klee, 1985) and is distributed mainly in neuronal and electrically excitable cells. It was demonstrated that this α subunit could inhibit the opening of a voltage sensitive N-type Ca^{2+} channel as well as K^+ channel (Heschler *et al.*, 1988). The expression of G_o proteins is restricted to neuronal and endocrine systems and the heart and it is highly abundant in mammalian brain. $G_o\alpha$ splice variants display differential tissue distribution. Three distinct subforms, i.e., $G_{o1}\alpha$, G_{o2} α and G_{o3} α have been identified, with G_{o1} and G_{o2}, representing splice variants whereas G_{o3} represents a recently characterised post-translational modification of $G_{o1}\alpha$ which represents about 30% of the total G_o in brain (Exner *et al.*, 1999).

$G_t\alpha$ (or transducin), which was purified at about the same time as G_s is a major component of the disks of the retinal rod outer segment. It was first identified as the transducing entity between activated rhodopsin and the phosphodiesterase responsible for lowering levels of cGMP and thus causing influx of Na^+ from the outside of the cell, depolarisation and initiation of nerve impulses to the brain. Two $G_t\alpha$ subunits, $G_{t1}\alpha$ and $G_{t2}\alpha$, have been cloned (Yatsunami and Khorana, 1985: Medinski *et al.*, 1985).

Figure 1.4. Structure of $G_{i1}\alpha$ subunit

The structures of $G_{i1}\alpha$ with $GTP\gamma S \bullet Mg^{2+}$ complex (top) or GDP (bottom). In the top figure, the α helical domain (left) and G domain (right) of $G_{i1}\alpha$ are shown together with the switch segments (switch II) (adapted from Sprang 1997).

A. Structure of $G_{i1}\alpha$ with $GTP\gamma S \bullet Mg^{2+}$ complex

B. Structure of $G_{i1}\alpha$ with GDP

Figure 1.4

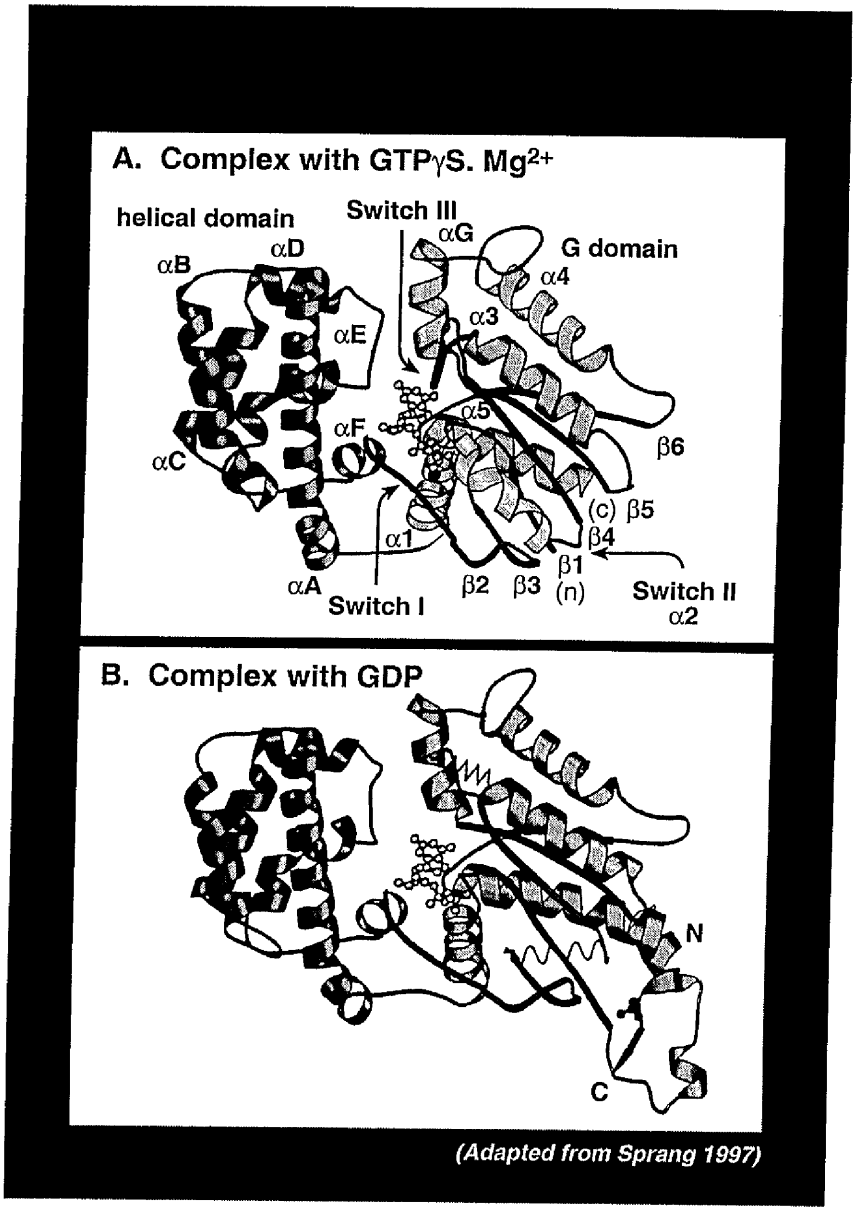
A. Complex with GTPγS. Mg2+
helical domain
Switch III
αG
G domain
αD
αB
α4
α3
αE
α5
αF
β6
αC
(c) β5
β4
α1
β1
αA
β2
β3
(n)
Switch II
α2
Switch I
B. Complex with GDP
N
C
(Adapted from Sprang 1997)

c) $G_q\alpha$ subfamily

The $G_q\alpha$ superfamily consists of five members whose α–subunits show different expression patterns. $G_q\alpha$ and $G_{11}\alpha$, which are 88 % identical, seem to be almost ubiquitously expressed. By contrast, the expression of $G_{14}\alpha$, which is 81 % identical with $G_q\alpha$, is more restricted. The human $G_{16}\alpha$ and its murine counterpart $G_{15}\alpha$ are only expressed in a subset of hematopoietic cells (Wilkie *et al.*, 1991). $G_{15}\alpha$ and $G_{16}\alpha$, which are 85 % identical, have been placed into the G_q family since their sequences show the highest similarity toward $G_q\alpha$ (57%). All five members of the $G_q\alpha$ family share functional properties, i.e., they allow communication between Ca^{2+}-mobilizing GPCRs and phosphoinositidases of the phospholipase Cβ (PLCβ) class in a PTx-insensitive manner (Simon *et al.*, 1991). It was demonstrated that receptors for interleukin 8 and C5a interact selectively with G_{16} but not with G_q and G_{11} (Wu *et al.*, 1993). Offermanns and Simon, (1995) have showed that a wide variety of structurally and functionally different GPCRs can couple to G_{15} and G_{16}, indicating that G_{15} and G_{16} are unique, i.e., they possess the ability to nonselectively couple a large variety of receptors to PLC.

d) $G_{12}\alpha$ subfamily

$G_{12}\alpha$ and $G_{13}\alpha$ proteins are ubiquitously expressed but their functions are only recently beginning to be understood. There is evidence implicating their involvement in regulating a range of signalling pathways. For example, both subunits stimulate the

Na^+/H^+ exchanger (NHE), via PKC dependent ($G_{12}\alpha$), and independent pathways ($G_{13}\alpha$). The thrombin receptor has been shown to activate both subunits in platelet membranes (Offermanns *et al.*, 1994). As thromboxane A_2, lysophosphatidic acid (LPA), and endothelin receptor induce serum response factor via these G proteins in a C3 exotoxin-dependent manner (Mao *et al.*, 1998) a direct role for the Rho GTPase is implicated in these events.

Recently $G_{12}\alpha$ was found to stimulate Brutons tyrosine kinase (Btk) and $Gap1^m$, a RasGAP, *in vitro* and *in vivo* (Jiang *et al.*, 1998). $G_{12}\alpha$ interacts with a conserved domain composed of the pleckstrin-homology domain and the adjacent Btk and $Gap1^m$. The Rho guanine nucleotide exchange factor p115 RhoGEF was found to be a direct effector of $G_{13}\alpha$ (Hart *et al.*, 1998). Activated $G_{13}\alpha$ stimulated its capacity to catalyse nucleotide exchange on Rho. By comparison, activated $G_{12}\alpha$ inhibited stimulation of p115 RhoGEF by $G_{13}\alpha$. Thus $Gap1^m$ and p115 RhoGEF appeared to provide a link between signalling by heterotrimeric and monomeric G proteins.

Table 1.2. Classification of Gα subunits, their distribution and effectors

Subtype	Expression	Effectors
$G_s\alpha$ Subfamily		
$G_s\alpha$ (4 splice variants)	Ubiquitous	↑ Adenylyl Cyclase
		↑ Ca^{2+} Channels, Na^+ Channels
$G_{olf}\alpha$	Olfactory	↑ Adenylyl Cyclase
$G_i\alpha$ Subfamily		
$G_{i1}\alpha$	Widespread	↓ Adenylyl Cyclase, etc
$G_{i2}\alpha$	Ubiquitous	↓ Adenylyl Cyclase, etc
$G_{i3}\alpha$	Widespread	↓ Adenylyl Cyclase, etc
$G_o\alpha$	Neuroendocrine	↑ K^+ Channels, Ca^{2+} Channels
		↓ Adenylyl Cyclase
$G_{gust}\alpha$	Taste Buds	↑ cGMP Phosphodiesterase
$G_{t1}\alpha$	Retinal Rods	↑ cGMP Phosphodiesterase
$G_{t2}\alpha$	Retinal Cones	↑ cGMP Phosphodiesterase
$G_z\alpha$	Neuroendocrine	↓ Adenylyl Cyclase, etc
$G_q\alpha$ Subfamily		
$G_q\alpha$	Widespread	↑ Phospholipase C
$G_{11}\alpha$	Widespread	↑ Phospholipase C
$G_{14}\alpha$	Widespread	↑ Phospholipase C
$G_{15}\alpha$	Circulatory	↑ Phospholipase C
$G_{16}\alpha$	Circulatory	↑ Phospholipase C
$G_{12}\alpha$ Subfamily		
$G_{12}\alpha$	Ubiquitous	RhoGEF & others
$G_{13}\alpha$	Ubiquitous	RhoGEF & others

III. G βγ subunits

The β and γ subunits of heterotrimeric G proteins form a tightly associated dimer complexes in the plasma membrane. So far 6 different Gβ and 12 different Gγ subunits have been identified (Clapham *et al.*, 1997). Gβ and Gγ subunits are very widely expressed with the exception of γ1, present only in the photoreceptor cells, and γ2 and γ3 which are restricted to the brain.

Structurally the Gβγ complex has been described as a " propeller " based on crystallography studies (Sondek *et al.*, 1996). Gβ subunit is made up of 2 structurally distinct regions, an amino terminal segment and a repeating sequence. This results in a 7-membered β-propeller structure based on 7 WD-40 repeats (Lambright *et al.*, 1996) and Gγ subunits interact with β through a N-terminal coiled-coil and via extensive contacts all along the base of β.

The Gα•GDP complex released from the effector molecule is bound with βγ to form a βγ•Gα•GDP complex that has high affinity towards GPCRs. Equally, the GPCR has a higher affinity for agonist when coupled with βγ•Gα•GDP. The interaction of agonist with the (R) (βγ•Gα•GDP) complex induces the release of GDP bound to Gα such that exchange of GDP with external GTP is facilitated. The resulting (A)(R)(βγ•Gα•GDP) complex dissociates to form Gα•GTP, Gβγ, agonist and receptor. The Gα•GTP complex can now activate the effector molecules. From this scheme, a

major function of the βγ subunit is to recognise the GDP bound form of Gα and to promote its binding to receptor and agonist, thus facilitating the recycling of Gα•GDP to Gα•GTP.

Gβγ subunits inhibit GDP release from Gα following Gα-catalysed GTP hydrolysis thus rendering reactivation dependent upon the interaction of Gα with ligand-activated GPCRs (Sprang, 1997). The Gβγ subunits themselves can play active roles in signal transduction. For example, through regulation of K^+ channels, PLC β and certain isoforms of AC in animal cells, and activation of the pheromone response pathway in budding yeast. Clearly, Gβγ subunits enhance receptor interaction with Gα subunits.

Table 1.3. Biochemical properties of G protein βγ-dimers

Feature	Property of βγ-dimers
Structure	Tightly associated, rigid dimer – no conformational change upon activation
β (35 kDa)	Seven WD40 repeats (1 repeat = 4 antiparallel β-strands) form a 7-bladed propeller core
γ (7-10 kDa)	Extended α-helix forms coiled-coil with Gβ
Membrane anchoring	Via carboxyterminal isoprenoid lipid modification on Gγ
Receptor recognition	βγ-dimers required for receptor mediated activation of Gα-subunits
Effector regulation	Conditional: type II-like AC isoforms; βγ-dependent stimulation requires presence of active $G_s\alpha$. Unconditional (direct regulation): PLC-β2; GIRK K^+ and neuronal Ca^{2+} channels; type I-like AC; dynamin I; non-receptor protein tyrosine kinases (BTK and TSK)
Deactivation	By GDP-liganded α-subunits
Regulation	By phosducin (a 33 kDa protein that binds and scavenges free βγ-dimers) and phosducin-like proteins. βγ-dimers provide docking sites for some GPCR kinases, which phosphorylate the agonist-bound receptor

IV. Covalent modifications of G proteins

a) ADP-ribosylation

Modulation by PTx has been used as a useful tool to characterise certain G protein-dependent signalling pathways. PTx is also called Islet activating protein (IAP). It is produced by *Bordetella pertussis* and causes ADP-ribosylation of a cysteine side chain four amino acids from the C-terminus of the α-subunits of G_i, G_o, and G_t. This prevents activation of the G protein trimer by its receptor (Katada *et al.*, 1982: West, 1985). Efficient ADP-ribosylation by PTx requires the complete αβγ trimer and isolated α-subunits are reported to be poor substrates (Casey *et al.*, 1989). The βγ-subunits may act by promoting favourable contacts of the α-subunits with PTx or by relieving unfavourable contacts between the G protein and the toxin (Scheuring *et al.*, 1998).

Formation of the complex between PTx, NAD^+ and $G_{i1}\alpha$ is of interest in charactersing the ADP-ribosylation of a G protein. The crystal structures of both $G_{i1}\alpha$ (Mixon *et al.*, 1995) and PTx (Stein *et al.*, 1994) have been solved. The structures permit interpretation of the transition state chemistry in the context of known protein structures. Scheuring *et al.*, (1998) has described the steady-state kinetics, substrate commitment factor, kinetic isotope effects, and the transition-state structure for the ADP-ribosylation of recombinant α–subunit of the G protein $G_{i1}\alpha$ catalysed by PTx.

b) Phosphorylation

Phosphorylation of G proteins is the least well characterised of the covalent modifications. The first evidence that G proteins may be regulated by phosphorylation derived from observations that treatment of platelet membranes with partially purified PKC resulted in phosphorylation of a 41 kDa protein (Katada *et al.*, 1985). Kozasa *et al.*, (1996) have shown that $G_{12}\alpha$ serves as a substrate for phosphorylation by various isoforms of PKC *in vitro* suggesting PKC regulates α_{12}-mediated signalling pathway by preventing their association with $\beta\gamma$. The α_{12} was shown to be phosphorylated by PKC and the phosphorylated α_{12} provided a tighter interaction of $\beta\gamma_{12}$ with $G_o\alpha$ and $G_{i2}\alpha$ (Morishita *et al.*, 1995).

c) Palmitoylation

Palmitoylation is a post-translational modification that is limited to a subset of cellular proteins among which proteins involved in signal transduction are prevalent (Casey, 1995). This thioesterification of cysteine residues by palmitate distinguishes itself from other lipid modifications such as prenylation and myristoylation by its reversibility. Indeed, in contrast to myristoyl and prenyl moieties that are added co-translationally and generally remain attached to the proteins until the protein gets degraded, the protein-bound palmitate is added post-translationally and turns over more rapidly than the protein itself (Omary *et al.*, 1981: Bonatti *et al.*, 1989). Biologically regulated changes in the palmitoylation state of either receptors or G proteins may have

important functional consequences. For example, it has been found that mutations to prevent palmitoylation of the $G_o\alpha$ subunit inhibit their association with the plasma membrane and thus their signalling function (Grassie *et al.,* 1994). McCallum *et al.*, (1995) have shown that the palmitoylation status of the cysteine residues at positions 9 and 10 in murine $G_{11}\alpha$ played a central role in defining membrane association of this G protein and indicated that much of the particulate fraction of the expressed palmitoylation-resistant mutants represented non-functional rather than correctly folded protein. Palmitoylation of $G_s\alpha$ has also been reported to increase its affinity for $G\beta\gamma$ (Iiri *et al.*, 1996). For example, activation of $G_s\alpha$ through receptor stimulation, following direct activation with aluminum fluoride and cholera toxin or as a result of site-directed mutagenesis has been shown to lead to increased incorporation of [^{3}H] palmitate into $G_s\alpha$ during pulse labelling experiments. Because pulse-chase-labelling experiments clearly indicated that stimulation increased the depalmitoylation rate, the enhanced incorporation was attributed to an accelerated turnover rate of the $G_s\alpha$ -bound palmitate (Degtyarev *et al.*, 1993: Wedegaertner *et al.*, 1994).

Wise and Milligan, (1997) demonstrated the general utility of generating chimeric GPCR-G protein fusion proteins to examine receptor regulation of G protein activation and that agonist-induced signal transduction to acylation-deficient mutants of $G_{i1}\alpha$ can be rescued by expressing these polypeptides as fusion constructs with the receptor. Moreover these studies indicated that effective agonist-induced signal transduction is unaffected by the palmitoylation potential of the receptor. Loisel *et al.*, (1999) also examined the acylation/deacylation cycle of the proteins in relation to their activity

status, using the advantage of a fusion protein composed of the stimulatory α subunit of G_s covalently attached to the β_2AR. When expressed in Sf9 cells, both the receptor and the $G_s\alpha$ moieties of the fusion protein were found to be palmitoylated via thioester linkage. These investigators have reported that stimulation of the β_2AR-Gsα fusion protein with β-adrenergic agonists promotes rapid depalmitoylation of both the receptor and the Gα subunit and inhibited their repalmitoylation.

d) Myristoylation

Co-translational myristoylation has been ascribed as one of the key means of targeting of specific G protein α subunits to the plasma membrane. (Casey, 1995: Milligan *et al.*, 1995). Both myristoylation and palmitoylation may also contribute to protein-protein interactions between the G protein α subunit and both receptors and the G protein βγ complex. Addition of myristate occurs only on the α subunits of the Gi-family of G proteins because they contain the consensus sequence (MGXXXS) for the enzyme *N*-myristoyl-CoA transferase. The glycine that is found at codon 2 acts as the acceptor when it is exposed following removal of the initiator methionine. The $G_s\alpha$ subunit is not myristoylated (Buss *et al.,* 1987). It has an N-terminal glycine but no serine at position 6.

V. Regulators of G protein signalling (RGS proteins); GTPase Activating Proteins (GAPs) for heterotrimeric G proteins

The slow intrinsic rate of GTP hydrolysis by Gα proteins is regulated by interactions with so-called GTPase activating proteins or GAPs. GAPs were first recognised as regulators of protein synthesis factors and low molecular weight GTPases such as Ras. It is now clear that certain effectors of G protein-regulated pathways can act as GAPs on cognate Gα proteins (Berstein *et al.*, 1992). Furthermore, there exists a large, recently discovered family of GAPs for Gα proteins known as regulators of G protein signalling or RGS proteins. These were discovered functionally as negative regulators of G protein signalling in *Saccharomyces cerevisiae* (Sst2p) (Dohlman and Thorner, 1997) and *Caenorhabditis elegans* egg-laying behaviour (Egl-10) (Koelle and Horvitz, 1996). Sst2p and Egl-10 both contain a conserved RGS domain of 120 amino acids. These accelerate the GTPase reaction of the G protein α subunit. In addition, RGS proteins inhibit effector regulation. A mammalian RGS protein, GAIP, was independently cloned in a two-hybrid screen for $G_{i3}\alpha$-interacting proteins (DeVries *et al.*, 1995). Subsequently, over 15 mammalian genes have been identified that contain the conserved RGS domain. *In vitro* biochemical studies have shown that RGS proteins have GAP activity for purified $G_i\alpha$ and $G_q\alpha$ and can enhance GTP hydrolysis rates as much as 100-fold (Koelle, 1997). RGS4 is capable of accelerating GTP hydrolysis of Gi-proteins by constraining the residues involved in catalysis (Tesmer *et al.*, 1997).

Effects of purified GAIP and RGS4 on purified $G_{i1}\alpha$, $G_{i2}\alpha$, $G_{i3}\alpha$, $G_o\alpha$, and $G_s\alpha$ have been examined *in vitro* (Berman *et al.*, 1996). These investigators have found that

two RGS family members, GAIP and RGS4, are GTPase-activating proteins (GAPs), accelerating the rate of GTP hydrolysis by $G_{i1}\alpha$ at least 40-fold. All G_i subfamily members assayed were substrates for these GAPs; $G_s\alpha$ was not. The GAP activity of RGS proteins is consistent with their proposed role as negative regulators of G protein-mediated signalling.

VI. Receptor-G protein coupling interactions

The coupling of GPCRs with heterotrimeric G proteins has long been a topic of great interest, as this directly affects the activation of secondary downstream effectors, and ultimately the final physiological response.

a) G protein domains essential for coupling with receptor

There are at least 3 regions of Gα postulated to contact the receptor, with the strongest evidence pointing to the C-terminus.

On the α subunit, the best-characterised receptor contact region is at the C terminus (Bourne, 1997: Sprang, 1997). Data in support of this model include that the *unc* mutation of $G_s\alpha$, which results from an Arg-Pro alteration 6 amino acids from the C-terminus, prevents productive interactions with GPCRs (Sullivan *et al.*, 1987). The last 7 amino acids of the α subunit are disordered in the heterotrimer crystal structures, and

analysis of receptor-binding peptides selected from a combinatorial peptide library shows that these 7 residues are the most critical (Martin *et al.*, 1996). Also, studies using chimeric Gα subunits confirmed that the last 5 residues play an important role in specifying receptor-G protein interaction. Conklin *et al.*, (1993) replaced C-terminal amino acids of $G\alpha_q$ with the corresponding residues of $G\alpha_{i2}$ to create $G\alpha_q/\alpha_{i2}$ chimeras that can mediate stimulation of PLC by receptors, otherwise coupled exclusively to G_i. A minimum of three $G\alpha_{i2}$ amino acids, including the glycine three residues from the C-terminus, sufficed to switch the receptor specificity of the $G\alpha_q/\alpha_{i2}$ chimeras. These investigators proposed that a C-terminal turn, centred on this glycine, plays an important part in specifying receptor interactions with G proteins in the $G_i/G_o/G_z$ family.

Evidence that the N-terminus of Gα was involved in GPCR coupling was shown by a study in which a photo-affinity peptide corresponding to the IC3 region of the α_{2A}-adrenergic receptor can be cross-linked to the amino terminus of $G_o\alpha$ (Taylor *et al.*, 1994). This confirmed previous work by Hamm *et al.*, (1988) on the inhibition of interaction of $G_t\alpha$ with rhodopsin using a synthetic N-terminal peptide of $G_t\alpha$.

Finally, a third region of Gα that may contact the receptor surface was mapped to residues 311 to 328 of $G_t\alpha$ (Hamm *et al.*, 1989: Hamm, 1991). This peptide behaved like the last 11 residues of $G_t\alpha$ in inhibiting $G_t\alpha$ activation by photorhodopsin and at the same time induced spectral changes in photorhodopsin. The analogous region in Ras was postulated to be the G5 region where the guanine ring interacts with the side chains in this region (Conklin *et al.*, 1993b).

VII. Suramin: a nonpeptide G protein antagonist

Suramin, a symmetric polysulphonated naphtylamine-benzamide-derivative, has been used for more than 70 years in the treatment of African sleeping sickness and river blindness. As well as being effective against various *Trypanosoma* species and the adult filariae of *Onchocerca volvulus,* suramin also exerts inhibitory effects on an array of mammalian targets such as P_2 purinergic receptors, DNA polymerase and growth-factor receptors (Voogd *et al.*, 1993). Moreover, among its targets are G protein α-subunits, Suramin acts as a G protein inhibitor because it limits the rate-limiting step in activation of the Gα subunits, i.e., the exchange of GDP for GTP. In the submicromolar to micromolar concentration range, suramin and suramin analogues suppress the rate of spontaneous GDP-release from purified G protein α-subunits (Hohenegger *et al.*, 1998). The effect of suramin on GDP release can be reversed upon addition of an effector, indicating that binding of an effector and of suramin are mutually excusive (Freissmuth *et al.*, 1996).

I.5. Adenylyl cyclase (AC)

I. General overview

In the late 1950s Sutherland and co-workers discovered 3', 5'-cyclic adenosine monophosphate (cAMP), which was the pivotal event that led to the current paradigm of hormone signalling via second messengers. The ACs are the family of enzymes that synthesise cAMP (Krupinski *et al.*, 1989). The synthesis of cAMP by AC is modulated by hormones and neurotransmitters acting via receptors that activate G proteins. To date, mRNAs encoding nine distinct isoenzymes of AC have been identified (Houslay and Milligan, 1997: Avidor-Reiss *et al.*, 1997). Sequence and functional similarities allow the categorisation of these ACs into six classes.

a) AC type I (AC-I);

Stimulated by Ca^{2+}/calmodulin, possibly independently of $G_s\alpha$ stimulation.

Inhibited by $G\beta\gamma$ subunits.

b) AC-VIII;

Stimulated by Ca^{2+}/calmodulin.

c) AC-V and AC-VI;

Inhibited by low levels of Ca^{2+}.

Unaffected by $G\beta\gamma$ subunits.

d) AC-II, AC-IV, and AC-VII;

AC-II, AC-IV are highly activated by Gβγ subunits in the presence of activated $G_s\alpha$.

AC-II, AC-VII are stimulated by activation of PKC.

e) AC-III;

Stimulated by a high concentration of Ca^{2+}/calmodulin in the presence of $G_s\alpha$.

Unaffected by Gβγ subunits.

f) AC-IX;

Activated by $G_s\alpha$ only.

II. Structure

Cloning studies have identified multiple types of AC which are all stimulated by $G_s\alpha$. All ACs are associated with the plasma membrane and hydropathy analyses suggest that they span the membrane 12 times. The nine cloned isoforms of mammalian AC share a primary structure consisting of two TM regions, M_1 and M_2, and two cytoplasmic regions, C_1 and C_2 (Krupinski *et al.*, 1989). The TM regions each contain six predicted membrane-spanning helices. The function of M_1 and M_2, aside from membrane localisation, is unknown despite their topological analogy to transporters. The C_1 and C_2 regions are subdivided into C_{1a} and C_{1b} and C_{2a} and C_{2b}. The C_{1a} and C_{2a}

domains heterodimerise with each other in solution (Yan *et al.*, 1996). These domains can also form homodimers. The C_{1b} region is large (~15 kDa), variable, and contains several regulatory sites. The C_{2b} is very short in some isoforms and lacks identified functions; hence C_2 and C_{2a} are sometimes referred to interchangeably.

The structure of the type II AC C_2 region revealed a homodimer with two C_2 monomers in a wreath-like arrangement. Two forskolin molecules bind to this groove in the homodimer. The type C C1a region and type II C_2 region arrange themselves in a heterodimeric wreath that is nearly identical in overall structure to the C_2 homodimer, with some critical differences in detail (Tesmer *et al.*, 1997). The activity of mammalian AC depends on the heterologous association of C_{1a} and C_2. This is not the case for many other related cyclases.

III. Regulatory mechanisms of AC

a) G protein α subunits and βγ subunits

Transmission of signals through G proteins can be achieved by the use of either α or βγ subunits. It had been generally believed that α subunits were the prime signal transmitters. Only a few systems such as certain types of K^+ channels and the effector in the yeast pheromone pathway (Dietzel and Kurgan, 1987) were thought to be regulated by βγ subunits. However, it has been shown that βγ subunits can by themselves regulate

the activity of a number of mammalian effectors such as certain types of AC and PLC.Thus it has become increasingly obvious that βγ subunits will play a central role in many signalling pathways.

Activation by the GTP-bound G protein α subunit $G_s\alpha$ is synergistic, not competitive, with respect to forskolin. GTP-$G_s\alpha$ binds to a crevice on the outside of the wreath formed by α2′ and α3′ of C_2 and by the N-terminal portion of C_1 (Tesmer *et al.*, 1997). $G_i\alpha$ selectively inhibits AC types V and VI and binds to the AC catalytic core on a groove pseudosymmetrically related to the $G_s\alpha$ binding groove (Tesmer *et al.*, 1997).

Gβγ subunits conditionally regulate several AC. Type II AC is activated by Gβγ when $G_s\alpha$ is bound. The Gβγ site is adjacent to, but does not overlap, the $G_s\alpha$ site, consistent with conditional activation. The α4-β6 region of $G_s\alpha$ was predicted to interact with AC based on mutagenic analysis, but no such contact with the catalytic domain was seen in the crystal structure. Gβγ regulation of the soluble AC model has not been established, even though the known binding site is located within the type II C_2 domain. C_{1b}, M_1, or M_2 might be involved in either of these processes. Tang and Gilman, (1991) have shown that βγ subunits have been found to have regulatory effects on certain types of AC. In the presence of G_s alpha, the α subunit of the G protein that activates AC, one form of AC was inhibited by βγ, some forms were activated by βγ, and some forms were not affected by βγ. Moreover, Gao and Gilman, (1991) have cloned and expressed a cDNA that encodes a widely distributed form of mammalian AC (EC 4.6.1.1).

b) Free metal ions (Mn^{2+})

Mn^{2+} activates mammalian AC strongly and millimolar concentrations of free Ca^{2+} inhibit. These effects are unlikely to have any physiological meaning or to reflect distinct binding sites for these ions.

c) P-site inhibitors

P-site inhibitors are a class of nucleoside inhibitors of AC. P-site inhibition is potentiated when AC is activated and is hypersensitive to certain mutations that slightly reduce enzyme activity.

d) Forskolin

Forskolin is a hydrophobic activator of all the mammalian AC except type IX. It is an extremely powerful activator, increasing activity by up to 1000 fold. The forskolin binding pocket is a narrow hydrophobic crevice that almost completely buries the forskolin molecule once bound.

e) Ca^{2+}/calmodulin

Ca^{2+}/calmodulin activates type I AC by binding to a putative helical region on the C_{1b} (Wu *et al.*, 1993). The precise activation mechanism is unknown. If other

Ca^{2+}/calmodulin activated enzymes are precedents, it is likely that Ca^{2+}/calmodulin binding will disrupt an autoinhibitory interaction between the C_{1a}/C_2 catalytic core and sequences within the C_{1b}.

f) Protein phosphorylation

PKC activates type II AC by phosphorylating it on Thr-1057 (Bol *et al.*, 1997). This site is within a region known to be required for PKC activation (Levin and Reed, 1995). CAM kinase II inhibits type III AC by phosphorylating it at Ser-1076 (Wei *et al.*, 1996). This Ser is at the outer lip of the active site, hence its phosphorylation could directly interface with catalysis. PKC phosphorylates Ser-674 in the C_{1b} of type VI (Chen *et al.*, 1997) and appears to regulate a low affinity secondary binding site for $G_s\alpha$. CAM kinase IV phosphorylates type I AC in its C_{1b} domain and disables Ca^{2+}/ calmodulin activation by interfering with the calmodulin binding site (Wayman *et al.*, 1996).

CHAPTER II

Materials and Methods

MATERIALS AND METHODS (CHAPTER 2)

2.1. Materials

2.1.1. General Reagents

ALEXIS CORPORATION LTD., Bingham, Nottingham, U.K.

Dithiothreitol (DTT)

AMERSHAM INTERNATIONAL PLC., Buckinghamshire, U.K

Enhanced chemiluminescence reagent, ECL detection film

BDH

Ammonium persulphate ($AmpSO_4$), glucose, glycine, Na_2HPO_4

BECTON DICKINSON

Plastipak® sterile syringes

CALBIOCHEM-NOVABIOCHEM LTD., Beeston, Nottingham, U.K.

Geneticin (G-418)

CAMBIO LTD., Cambridge, U.K.

Fast-link™ DNA ligation and screening kit

CRUACHEM LIMITED., Glasgow, U.K.

Oligonucleotides

FISHER., Scientific Equipment, Loughborough, U.K.

Acetic acid, Ethylenediaminetetra acetic acid (EDTA), NaCl, $MgCl_2$, 4-[2-Hydroxyethyl]-1-piperazine-N'-2-ethane-Sulphonic acid (HEPES)

FUJI PHOTO FILM LTD., Tokyo, Japan

X-ray film

GIBCO BRL LIFE TECHNOLOGIES INC., Paisley, U.K.

Lipofectamine™, Tris

INVITROGEN., San Diego, CA, U.S.A.

pcDNA3, pcDNA(3.1)

ICN

Mycoplasma removal agent (MRA)

MERCK LTD., Poole, Dorset, U.K.

Agar, NaOH

OXOID LTD., Hampshire, U.K.

Tryptone, yeast extract

PACKARD INSTRUMENTS., BV, Netherlands

Ultima Gold XR liquid scintilation cocktail

PREMIER BEVERAGES., Stafford, U.K.

Marvel

PIERCE., Rockford, IL.

Enhanced chemiluminescence reagent

PHARMACIA., Piscataway, NJ

dNTP's (dATP, dCTP, dGTP, dTTp)

PROMEGA LTD., Southampton, U.K.

Restriction enzymes, Wizard^{TM} Miniprep kit, Wizard^{TM} DNA clean-up kit,

Geneticin (G-418)

QIAGEN LTD., Southampton, U.K.

Qiagen® plasmid maxiprep kit

ROCHE MOLECULAR BIOCHEMICALS LTD., Lewes, East Sussex, U.K.

App[NH]p*, Aprotinin, creatine phosphate, creatine kinase, GTP, GTPγS, Tris, N-

Glycosidase F (NGF), restriction enzymes, Bovine serum albumin faction V,

Shrimp alkaline phosphatase (SAP)/alkaline phosphatase, DNA Molecular Weight

Marker X (0.07-12.2 kbp), DOTAP Liposomal Transfection Reagent, T4 DNA ligase

*App[NH]p: AMP-PNP (Adenylyl imidodiphosphate)

SCOTTISH ANTIBODY PRODUCTION UNIT., Lanarkshire, U.K.

Horseradish peroxidase conjugated donkey anti-rabbit IgG

SIGMA CHEMICAL COMPANY., Poole, Dorset, U.K.

Alumina, ATP, ampicillin, cholera toxin, DOWEX AG50 W-X4 (200-400 mesh), forskolin, imidazole, mineral oil, Ouabain, Pertussis toxin (PTx), N, N, N′, N′ tetramethyethylenediamine (TEMED), thimerosal, TRICINE Acetic acid, DMSO, hydrochloric acid, KCl, KH_2PO_4, K_2HPO_4, NaCl, Na_2CO_3, $NaHCO_3$, NaH_2PO_4, sucrose, sodium dodecyl sulphate (SDS), trichloroacetic acid (TCA), Coomassie Blue R-250, Ponseau S, Trypsin

STRATEGENE LTD., Cambridge, U.K.

Pfu DNA Polymerase

WHATMAN INTERNATIONAL LTD., Maidstone, U.K.

Brandell GF/C Glassfibre filters

2.1.2. Radiochemicals

AMERSHAM PHARMACIA BIOTECH PLC., Buckinghamshire, U.K.

[^{3}H] Adenine (specific activity: 23.0 Ci/mmol)

NEN™ LIFE SCIENCE PRODUCTS LNC., Stevenge, Hertfordshire, U.K.

[^{3}H] naltrindole (specific activity: 33.0 Ci/mmol)

[^{3}H] DADLE (specific activity: 55.3 Ci/mmol)

[^{3}H] diprenorphine (specific activity: 58.0 Ci/mmol)

[γ-^{32}P] GTP (specific activity: 30.0 Ci/mmol)

2.1.3. Antisera

Anti-Gα antisera

These antisera were generated against synthetic peptides described in Goldsmith *et al.*, (1988). Conjugates of these peptides with keyhole-limpet haemocyanin were injected subcutaneously into New Zealand White rabbits. Bleeds were obtained from the ear artery. Amino acid sequence of the synthetic peptides derived from the various Gα are listed below:

Antiserum	Peptide Sequence	Amino acid Sequence	Identification	Reference
I1C	LDRIAQPNYI	159-168 aa of $G_{i1}\alpha$	$G_{i1}\alpha$	Green *et al* (1990)
ON1	GCTLSAEERAA LERSK	1–16 aa of $G_{o1}\alpha$ and $G_{o2}\alpha$	$G_{o1}\alpha$, $G_{o2}\alpha$	Georgoussi *et al* (1993)

Anti-rabbit IgG

Donkey polyclonal antibody conjugated with horseradish peroxidase, produced by the Scottish Antibody production unit, Lankarshire, U.K.

2.1.4. Tissue culture

AMERICAN TISSUE CULTURE COLLECTION., Rockville, U.S.A.

Human embryonic kidney (HEK293) cells

GIBCO BRL LIFE TECHNOLOGIES INC., Paisley, Strathclyde, Scotland, U.K.

Glutamine (2000 mM), Newborn calf serum (NBCS), Optimem-1 medium, $NaHCO_3$ (7.5 % $^{W}/_{V}$)

SIGMA CHEMICAL COMPANY., Poole, Dorset, U.K.

Dulbecco's Modified of Eagle's Medium (DMEM), Minimum Essential Medium (MEM), Trypsin-EDTA solution

IWAKI SCITECH DIV, Asahi Techno Glass.,

Dishes 10 cm diameter, Flasks 25 cm^2 and 75 cm^2, Plates 6, 12 and 24 wells,

Disposable cell scraper

STERILIN BIBBY LTD., Stone, Staffordshire, U.K.

Pipettes 5 ml, 10 ml and 25 ml, centrifuge tube 50 ml

2.1.5. Standard buffers

a) Tris-EDTA-$MgCl_2$ Buffer (TEM)

Tris	75 mM
EDTA	5 mM
$MgCl_2$	12.5 mM

pH adjusted to 7.5 at 25 °C

This was made up for [^{3}H] naltrindole/diprenorphine binding and [^{3}H] DADLE binding assays.

b) Tris-EDTA Buffer (TE)

Tris	75 mM
EDTA	5 mM

pH adjusted to 7.5 at 4 °C

This was made up for washing of binding experiments and was usually made up as a 5X stock solution and diluted when required.

c) Tris-EDTA Buffer (TE)

Tris	10 mM
EDTA	0.1 mM

pH adjusted to 7.5 at 4 °C

This was made up for membrane preparation and protein measurement.

d) Phosphate-buffered Saline (PBS)

KCl	2.7 mM
KH_2PO_4	1.5 mM
NaCl	140 mM
Na_2HPO_4	8 mM

pH adjusted to 7.5

This was made up as a 10X stock solution and diluted when required.

Usually for 1 litre in PBS (1X) buffer, NaCl (10 g), KCl (0.25 g), Na_2HPO_4 (1.8 g) and KH_2PO_4 (0.3 g). (sterilised PBS – autoclaved)

e) Tris Buffered Saline (TBS)

NaCl	150 mM
Tris/HCl	20 mM

pH adjusted to 7.5

This was usually made up from 30 ml of 1M Tris (pH 7.5) and 20 ml of 5M NaCl for a 1 litre solution and used for SDS-PAGE.

f) Tris Buffered Saline with Tween (TBST)

NaCl	150 mM
Tris/HCl	20 mM

Tween 20(0.1%)

pH adjusted to 7.5

This was made up by adding Tween 20 (0.1% $^{v}/_{v}$) to TBS buffer for SDS-PAGE.

g) Laemmli Buffer (2x)

DTT	0.4 M
SDS	0.17 M
Tris/HCl (pH 8.0)	50 mM
Urea	5 M
Bromophenol Blue	0.01% $^{W}/_{V}$

This was stored in aliquots at –20 °C until required.

h) Gel Running Buffer

Glycine	36 g
Tris	7.5 g
10% SDS	25 ml

Total volume **dissolved in 2.5 litre H_20**

This was made up for SDS-PAGE gel running buffer.

i) Western transfer buffer

Glycine	72 g
Tris	15 g

Total volume **dissolved in 4 litre H_20 and 1 litre methanol**

This was made up for western transfer buffer and usually kept in 4 ° C without methanol.

2.2. Molecular biology for subcloning

Molecular biological works were performed in an environment where contamination of DNA and DNAse were kept to a minimum. I autoclaved all materials (e.g., pipette tips (yellow/blue), eppendorfs, buffers, water, PCR tubes, *etc*), cleaned up the bench and pipetters with 70% alcohol, and wore gloves for every experiments.

2.2.1. Reagents for Molecular biology

a) Tris-acetate-EDTA Buffer (TAE)

Tris-acetate	40 mM
EDTA	1 mM

pH adjusted to 8.0

This was made up for DNA agarose gel analysis.

Usually for 300 ml in TAE buffer, 72.6g Tris base, 17.13ml glacial acetic acid and 30ml 0.5M EDTA (pH 8.0)

b) Luria Bertani (LB) medium

For 1 litre:

Bacto-tryptone	10 g
Bacto-yeast extract	5 g
NaCl	10 g

These were dissolved in deionised water and autoclaved at 126 ° C for 11 min.

c) Gel Loading Buffer (6X)

for 10 ml:

Bromophenol Blue (2%)	1.25 ml
Sucrose	4 g

These were dissolved in autoclaved water to a final volume of 10 ml. The buffer was stored in aliquots at –20 ° C.

d) LB Ampicillin Agar Plates

This was made up of the same components as LB and bacto-agar (1.5 % $^{w}/_{v}$) added. After autoclaving, bottle was left to be cool and ampicillin (100µl/100ml) added to a final concentration of 50 µg/ml. The liquid LB agar was poured into 100 mm diameter Petri dishes, allowed to be solid and stored at 4 ° C.

2.2.2. Transformations and DNA purifications/preparation from bacteria

Transformation, the transfer of DNA into *E.coli*, produces multiple copies of the DNA from the bacteria replicates, such as DH5α.

a) Preparation of competent bacteria (DH5α)

Solution 1 (for 100 ml)

Potassium acetate (1 M)	3 ml
$RbCl_2$ (1 M)	10 ml

$CaCl_2$ (1 M)	1 ml
$MnCl_2$ (1 M)	5 ml
Glycerol (80% $^{v}/_{v}$)	18.75 ml

The final volume was made up to 100 ml with deionised water and pH adjusted to 5.8 with 100 mM acetic acid. The solution was filter-sterilised and stored at 4 ° C.

Solution 2 (for 40 ml)

MOPS (100 mM: pH 6.5)	4 ml
$CaCl_2$ (1 M)	3 ml
$RbCl_2$ (1 M)	0.4 ml
Glycerol (80% $^{v}/_{v}$)	7.5 ml

The final volume was made up to 40 ml with deionised water and pH adjusted to 6.5 with HCl. The solution was filter-sterilised and stored at 4 ° C.

A conical flask with 250 ml of LB was inoculated with 5 ml of culture of DH5α *E. coli* overnight, allowed to incubate at 37 ° C with shaking for 4-5 h until the optical density (at 550 nm) of the culture reached 0.48. Then the culture was chilled on ice for 5 min, and the bacteria collected by spinning in a chilled centrifuge at low speed (~3000 rpm). The pellet was resuspended in 100 ml of solution 1 for 5 min on ice. The bacteria cells were pelleted as before, and then resuspended in 5 ml of solution 2 for 15 min on ice. The DH5α bacteria are ready for transformation or can be stored at –80 ° C in aliquots until required.

b) Preparation of " Ultra-Competent " *E.coli* (Inoue Method)

SOB Medium

Bacto tryptone (2 % $^{w}/_{v}$)

Yeast extract (0.5 % $^{w}/_{v}$)

NaCl (10 mM)

KCl (2.5 mM)

$MgCl_2$ (10 mM)

$MgSO_4$ (10 mM)

---

pH was adjusted to 6.7-7.0.

TB (Transformation Buffer)

Pipes (10 mM)

$MnCl_2$ (55 mM)

$CaCl_2$ (15 mM)

KCl (250 mM)

---

pH was adjusted to 6.7 with 5 N KOH prior to adding the $MnCl_2$.

Inoue *et al.*, (1990) introduced " High efficiency transformation of *E.coli* with plasmids ". The *E.coli* was inoculated in LB overnight, grown in 250 ml " SOB "at 18C until the optical density (at 600 nm) of the culture reached 0.6. Then the culture was chilled on ice for 10 min, and the bacteria collected by spinning in a chilled centrifuge at low speed (~2500 g) for 10 min at 4 ° C. The pellet was resuspended gently in 80 ml of ice cold " TB ", left for 10 min and the bacteria collected by spinning in a chilled centrifuge at low speed (~2500 g) for 10 min at 4 ° C. The

bacteria cells were then added DMSO to a final concentration of 7 %, placed on ice for 10 min. " Ultra-competent " bacteria are ready for transformation or can be stored at liquid nitrogen until required.

c) Transformation of DNA

Each plasmid DNA (5 µl/ 10-50 ng) was incubated with 50 µl of competent bacteria in a sterile 13 ml white top tube for 15 min on ice. Then the DNA/ bacteria mixture was heated at 42 ° C for 60-90 sec, and straightly back into ice for 2 min. 450 µl of LB or SOB was added and the bacteria cells containing LB incubated in a 37 ° C for 45 min. LB ampicillin agar plates were pre-warmed at 37 ° C. For normal transformation of whole plasmid DNA, ~50 µl of this mix was plated out on LB ampicillin agar plate with ethanol-washed plater, left at 37 ° C incubator to absorb the liquid, and finally incubated at 37 ° C overnight. On next day, colonies was picked from the plate and cultured in LB for the further purification of DNA. Moreover, for ligation of enzyme-digested DNAs, ~100 µl of the mixture was used for plating. Cells can be kept as glycerol stocks for up to 2 years.

d) DNA Purification/preparation

The DNA from the inoculated cultures in LB was purified the Promega Wizard™ Miniprep/Maxiprep kits, Qiagen Maxiprep kit according to the manufacture's intructions, to obtain large copies of DNA.

2.2.3. Polymerase Chain Reaction (PCR)

Polymerase chain reaction (PCR) was performed by accurate pipetter and all the materials (PCR tubes, tips, pipette box, eppendorf tubes etc) were autoclaved and sterilised before the use.

A DOR cDNA was obtained from Glaxo-Wellcome Research and Development (Stevenage, UK).

a) Construction of the hDOR-$G_{i1}\alpha$ (wild type) fusion protein

- The last 157 bps fragment of the human DOR was amplified by PCR using the following oligonucleotides primers:

PCR reaction:

Primer 25 pmole/each

5′ sense primer 1 =1.1 µl

5′ antisense primer 2 =2.3 µl

DNA (template) 10-100 ng (0.1 µg/µl) = 0.7 µl

Deoxynucleotides tri-phosphate (dNTP's)

0.2-0.25 mM (0.2 mM each dATP, dCTP, dGTP, dTTP)

= 2 µl from 5 mM stock

Pfu polymerase (1 unit) = 1 µl

Pfu polymerase buffer (10X) = 5 µl

H_20 (sterilised) = 37.99 µl

Total V = 50 µl

PCR cycles:

The reaction conditions were as follows;

Preheating	95 ° C	5 min	**1 cycle**
Adding *Pfu* polymerase			
Denaturation	95 ° C	50 sec	
Annealing	37 ° C	50 sec	**30 cycles**
Extension	72 ° C	25 sec	

All reactions were performed on a Hybaid OmniGene temperature cycler.

Primer:

Sense 5′–GACGAGAACTTCAAG– 3′

Antisense 5′–AGTGTGCAGCC**GGATCC**CGCGGCAGCGCCA– 3′

BamHI

- The ORF of a PTx-sensitive rat $G_{i1}\alpha$ was amplified by PCR using the following primers:

PCR reaction:

Primer 25 pmole/each

5′ sense primer 1 = 1 µl

5′ antisense primer 2 = 1 µl

DNA (template) 10-100 ng (0.1 µg/µl) = 2 µl

dNTP's 0.2-0.25 mM (0.2 mM each dATP, dCTP, dGTP, dTTP)

= 2 µl from 5 mM stock

Pfu polymerase (1 unit) = 1 µl

Buffer (X 10) = 5 µl

H_20 (sterilised) = 38 µl

Total V = 50 µl

PCR cycles:

The reaction conditions were as follows:

Preheating	95 ° C	5 min	**1 cycle**
Adding *Pfu* polymerase			
Denaturation	95 ° C	1 min	
Annealing	55 ° C	1 min	**30 cycles**
Extension	72 ° C	3 min	

95° for 1 min

55° for 1 min **1 cycle**

72° for 10 min

All reactions were performed on a Hybaid OmniGene temperature cycler.

Primer:

Sense 5′ – CTG**GGATCC**GGCTGCACACTGAGCGCTGAG – 3′

BamHI

Antisense 5′ – GA**GAATTC**TTAGAAGAGACCACAGTC – 3′

EcoRI

b) Construction of the hDOR-$G_{o1}\alpha$ (wild type) fusion protein

A fragment of 1065 bps from the cDNA encoding $G_{o1}\alpha$ was modified by introducing the flanking restriction sites 5′ *BglII* and 3′ *XbaI* by PCR amplification.

Primer:

Sense 5′ –GCCTT**AGATCT**ATGGGATGTACTCTGAGCGC– 3′

BglII

Antisense 5′ – GC**TCTAGA**TCAGTACAAGCCACAGCCCCG– 3′

XbaI

2.2.4. Agarose DNA gel electrophoresis and purification from agarose gel

First the DNA required for agarose gel electrophoresis was diluted to the appropriate concentration (1 μg) with sterilised water. Gel loading buffer (6X) was added in the ratio 1:5 with the diluted DNA. Agarose gel was prepared in 35 ml TAE buffer **(2.2.1a)** to a final concentration of 0.8-2 % $^{w}/_{v}$ agarose, which is dependent upon the size of the DNA fragments to be separated. For example, 35 ml TAE buffer at 1 % agarose was made up of 700 μl 50 X TAE buffer, 0.35 g agarose and 35 ml water. This mixture was heated in the microwave oven for about 1-2 min. 2 μl of ethidium bromide (EtBr, 10 mg/ml) were added, mixed well with the liquid agarose and poured into the chamber of the electrophoresis kit (Life technologies, Gibco Horizon 58 with Model 200 power pack). The appropriate combs were inserted to form wells in the gel. The gel was left to be set and 1 X TAE buffer (200 ml) was added to cover it. Then the prepared DNA and DNA molecular marker were loaded into the wells and the electrophoresis started (75 → 100 V) for about 30-60 min. Finally the gel examined under UV light and an electronic image printed. Used gel should carefully dispose in a separate waste to avoid contamination.

Purification of DNA fragments from agarose gel was performed using the QIAquick Gel Extraction kit (Qiagen, West Sussex, U.K). First the desired DNA fragment on the gel was excised with a clean, sharp scalpel and transferred into a 1.5 ml eppendorf tube. The gel slice was weighed and 3 volumes of Buffer QG to 1 volume of gel (100mg/100μl) were added. The tube was incubated at 50-55 ° C for 10

min until the gel slice has completely dissolved (the color of the mixture is yellow). 0.7 volume of isopropanol was added to the sample and mixed by inverting. Then the sample was transferred to a QIAquick column fitted on tope of a 2 ml collection tube. The whole assembly was centrifuged for 1 min at about 13,000 rpm in a micro-centrifuge and the flow-through discarded. 0.5 ml of Buffer QG was added to the QIAquick column, and centrifuged as before to remove all traces of agarose from the column. The column was washed with 0.75 ml of Buffer PE by repeating the centrifugation and discarding the waste. The column was further centrifuged for an additional 1 min, discarding the waste from Buffer PE and placed into a clean and sterile 1.5 ml eppendorf tube. 50 μl of sterilised water or Buffer EB was added to the centre of the QIAquick column, stand for 1 min, and centrifuged for 1 min at 13,000 rpm. The eluted DNA fragment can be kept in –20 ° C or used immediately (i.e., restriction enzyme digestion *etc*).

2.2.5. Restriction enzyme treatment and measurement DNA concentration

Restriction enzyme treatment was used in order to subclone cDNAs to vectors (pcDNA 3). In order, sterilised H_20, DNA, Buffer and restriction enzyme were added step by step and incubated at the suitable temperatures according to different enzyme for at least 2 h or overnight.

Normally, the concentration of DNA was measured using absorption observation of UV spectrophotometer (UV-1201, Shimadzu). 1 A_{260} unit of double-stranded DNA is corresponding to 50 μg/ml.

2.2.6. DNA Sequencing

Sequencing of constructed DNAs was done by the Molecular Biology Support Unit located at the Anderson College, Institute of Virology, University of Glasgow. All fusion constructs were fully sequenced to identify hDOR cDNA and the correct amino acid Cys^{351}Xaa of $G_{i1}\alpha$ before the use.

2.2.7. Construction of hDOR-$G_{i1}\alpha$ (wild type) and PTx–resistant hDOR-$G_{i1}\alpha$ (Xaa^{351}) fusion protein mutants

A DOR cDNA was obtained from Glaxo-Wellcome Research and Development (Stevenage, UK). The last 157 bps fragment of the human DOR was amplified by PCR using the oligonucleotides primers **[see 2.2.3(a)].** Also the ORF of a PTx-sensitive rat $G_{i1}\alpha$ was amplified by PCR using the primers **[see 2.2.3(a)].**

The PCR amplified fragments were digested with appropriate enzymes [157 bps fragment of hDOR and $G_{i1}\alpha$(wild type)]. All three different fragments were ligated to pcDNA3.1 (Invitrogen, Netherlands) through these restriction sites **(see Figures 3.1A, 3.2A)**

$Cys^{351}Xaa$ PTx-resistant form of rat $G_{i1}\alpha$ had been generated previously (Bahia *et al.*, 1998). PTx-resistant hDOR-$G_{i1}\alpha$ (Xaa^{351}) fusion proteins were constructed by recovering the unique restriction sites *EcoNI* and *EcoRI* fragment from $G_{i1}\alpha$ $Cys^{351}Xaa$ mutants (Ile, Leu,Phe,Val, Ser, Arg, Ala or Gly) and replacing the equivalent section of hDOR-$G_{i1}\alpha$ (wild type) fusion proteins **(see Figures 3.1B, 3.2B).** All fusion constructs were fully sequenced to identify hDOR cDNA and the correct amino acid $Cys^{351}Xaa$ of $G_{i1}\alpha$.

2.2.8. Construction of hDOR-$G_{o1}\alpha$ (wild type) and PTx-resistant hDOR-$G_{o1}\alpha$ (Xaa^{351}) fusion protein mutants

5′ 120bps of hDOR cDNA was digested with *KpnI* and *BssHI* and the remaining 1020bps fragment from the hDOR-$G_{i1}\alpha$ (wild type) was digested with *BssHI* and *BamHI.*

A fragment of 1065bps from the cDNA encoding $G_{o1}\alpha$ was modified by introducing the flanking restriction sites 5′ *BglII* and 3′ *XbaI* by PCR amplification **[see 2.2.3(b)].** Three different fragments were ligated into pcDNA 3.1 using the compatibility of *BamHI* and *BglII* **(see Figures 3.3A, 3.4A).**

Using the same approach as for the hDOR-$G_{i1}\alpha$(Xaa^{351}) mutants, $Cys^{351}Xaa$ PTx resistant forms of $G_{o1}\alpha$ had been generated previously (Bahia *et al.*, unpublished). The PTx resistant hDOR-$G_{o1}\alpha$ (Xaa^{351}) fusion proteins were constructed by recovering the *ClaI* and *ApaI* fragment from $G_{o1}\alpha$ (Xaa^{351}) mutants (Ile/Leu/Gly) and

replacing the equivalent segment of the hDOR-$G_{o1}\alpha$(wild type) fusion protein **(see Figures 3.3B, 3.4B)**. All fusion proteins were fully sequenced prior to use.

2.3. Assays for functional experiments

2.3.1. Radioligand Binding

Membranes of all the hDOR receptor and the PTx-resistant hDOR-$G_{i1}\alpha$ (Xaa^{351}) fusion proteins were prepared for all the radioligand binding experiments.

a) Antagonist [^{3}H] naltrindole binding studies

Binding to membranes expressing the hDOR receptor and the PTx-resistant hDOR-$G_{i1}\alpha$ (Xaa^{351}) fusion proteins were carried out as follows:
Binding assays were initiated by the addition of 5-10 μg of protein to assay buffer (75 mM Tris, 5 mM EDTA, 12.5 mM $MgCl_2$, pH 7.4) containing the antagonist radioligand [^{3}H] naltrindole (NEN life sciences products) to membranes expressing the hDOR receptor and the PTx-resistant hDOR-$G_{i1}\alpha$ (Xaa^{351}) fusion proteins. Non specific binding was determined in the presence of 100 μM unlabeled naloxone. Reaction was incubated for 60 min at 25° C, and bound ligand was separated from free ligand by vacuum filtration through GF/C filters. The filters were washed three times with ice-cold wash buffer (75 mM Tris, 5 mM EDTA, pH 7.4), and bound ligand was determined by liquid scintillation counting. Saturation binding experiments were done using radioligand concentrations covering the range of 0.1 – 10 nM ([^{3}H] naltrindole). GDP and suramin competition binding experiments were carried out using 2 - 2.5 nM of [^{3}H] naltrindole.

b) Antagonist [^{3}H] diprenorphine binding studies

Binding to membranes expressing the PTx-resistant hMOR-$G_{i1}\alpha$ (Ile^{351}) fusion proteins were carried out as the same as [^{3}H] naltrindole binding experiments: Binding assays were initiated by the addition of 5-10 μg of protein to assay buffer (75 mM Tris, 5 mM EDTA, 12.5 mM $MgCl_2$, pH 7.4) containing the antagonist radioligand [^{3}H] diprenorphine (NEN life sciences products). Non specific binding was determined in the presence of 100 μM unlabeled naloxone. Reaction was incubated for 60 min at 25 ° C, and bound ligand was separated from free ligand by vacuum filtration through GF/C filters. The filters were washed three times with ice-cold wash buffer (75 mM Tris, 5 mM EDTA, pH 7.4), and bound ligand was determined by liquid scintillation counting. Saturation binding experiments were done using radioligand concentrations covering the range of 0.1 – 10 nM ([^{3}H] diprenorphine).

c) Agonist [^{3}H] DADLE binding studies

Agonist [^{3}H] DADLE binding to membranes expressing the hDOR and the hDOR-$G_{i1}\alpha$ (Xaa^{351})/-$G_{o1}\alpha$ (Xaa^{351}) fusion proteins were carried out as same as the antagonist binding assays. Binding assays were initiated by the addition of 5-10 μg of protein to assay buffer (75 mM Tris, 5 mM EDTA, 12.5 mM $MgCl_2$, pH 7.4) containing the radioligand [^{3}H] DADLE (NEN life sciences products). Non specific binding was determined in the presence of 10 μM unlabeled DADLE. Reaction was incubated for 60 min at 25° C, and bound ligand was separated from free ligand by vacuum filtration through GF/C filters. The filters were washed three times with ice-

cold wash buffer (75 mM Tris, 5 mM EDTA, pH 7.4), and bound ligand was determined by liquid scintillation counting. Saturation binding experiments were done using radioligand concentrations covering the range of 0.1 – 20 nM ([^{3}H] DADLE). GDP and suramin competition binding experiments were carried out using 1 - 1.5 nM of [^{3}H] DADLE. The association and dissociation binding experiments was carried out using 1-2 nM of [^{3}H] DADLE on different time scales at 25° C. After 50-60 min incubation of dissociation experiments, 10 μM unlabeled naloxone was added to initiate the dissociation of bound [^{3}H] DADLE.

2.3.2. High Affinity GTPase

High affinity GTPase assay was performed as described in Gierschik *et al.*, (1994). Assay mix (for 100 tubes) was prepared as follows:

COMPONENTS	VOLUME (μl)	Final concentration
Creatine phosphate (0.4 M)	250	20 mM
Creatine kinase (2.5 U/μl)	200	0.1 U/μl
App[NH]p (0.04 M)	25	0.2 mM
ATP (0.04 M; pH 7.5)	250	2 mM
Ouabain (0.01 M)	1000	2 mM
NaCl (4 M)	250	200 mM
$MgCl_2$ (1 M)	50	10 mM
DTT (0.1 M)	200	4 mM
EDTA (0.02 M; pH 7.5)	50	0.2 mM

Tris/HCl (2 M; pH 7.5)	200	80 mM
GTP (10^{-4} M; pH 7.5)	50	1 μM
Deionised H_20 to final volume	5000	

[γ-^{32}P] GTP (50, 000 CPM/Assay) was used for individual experiments and added to the above mix.

The assay was carried out at 1.5 ml eppendorf tubes:

Membrane protein (10μg/assay: 0.5 μg/μl)	20 μl
*Agonist or water or GTP	10 μl
Water	20 μl
Assay mix	50 μl
	Total volume: 100 μl

*Assay was set up under 3 different conditions: basal (water), agonist added, and non-specific activities (GTP), with a final concentrations of agonist (at various concentrations), water, or GTP (10^{-4} M) respectively.

To measure the potency for DADLE (pEC_{50} values) to activate the fusion proteins was monitored in high affinity GTPase activity assays with a range of concentrations of DADLE ($10^{-13} \sim 10^{-4}$ M). Also, when DADLE (100 μM)-stimulated GTPase activity was monitored at a wide range of GTP concentrations on membranes, the effect of the agonist was predominantly to increase V_{max} of the GTPase activity

with only a minor effect on the estimated K_m for GTP.

The assay was carried in triplicate and incubated at 37 ° C for 30-40 min. 900 µl of ice-cold charcoal slurry (5% activated charcoal in 10 mM H_3PO_4) was added to every tube to stop the reaction. Every tubes containing charcoal was spun down at 13,000 rpm for 20 min in a chilled (4 ° C) centrifuge. 500 µl of the supernant was taken out and transferred into vials Cerenkov radiation counting in a Beckman radioisotope counter. Radiowastes should be carefully thrown away.

2.3.3. Adenylyl cyclase catalytic activity

Whole intact cell adenylyl cyclase (AC) assays were performed essentially as described by Wong, (1994) and Merkouris *et al.,* (1997). This whole cell AC assay is based on the use of [^{3}H] adenine which labels the intracellular adenine nucleotide pool and measurement of subsequent conversion of [^{3}H] ATP to [^{3}H] cAMP on AC stimulation.

The [^{3}H] cAMP thus produced is separated from [^{3}H] adenine and [^{3}H] ATP by a two-step column method (Salomon *et al.,* 1979: Taussig *et al.*, 1994). Cells of the two clones were split into 12 well plates and grow in geneticin containing medium (700 µg/ml G418 sulphate in DMEM) until about 80% confluence. One day before the assay, plates were incubated overnight with [^{3}H] adenine at 1 µCi per well and PTx (25ng/ml) was added at the same time. On the day of assay, plates were left at 37 °C, removed medium, washed with 2 ml of HEPES buffered DMEM. HEPES buffered

DMEM medium [1X DMEM, 2 mM L-glutamine, 20 mM HEPES (pH 7.4), 1 mM 3-isobutyl-1-methylxanthine, and 1 % penicillin/streptomycine] containing increasing concentrations of DADLE was then added and the cells incubated for 30 min at 37 °C. Forskolin (50 μM) was also used as a control. The reaction was terminated on ice by addition of 1ml of stop solution (5 % $^{w}/_{v}$ TCA, 1 mM ATP, 1 mM cAMP: 2.5 g TCA, 17.6 mg cAMP, 27.5 g ATP per total 50 ml of solution) to extract [^{3}H] adenine nucleotides. The TCA-added plates were left for 30 min on ice, scraped into eppendorf tubes and spun down for 3-5 min at 13,000 rpm at 4 ° C. The plates can be stored at –20 ° C or at 4 ° C for a short time if the columns to separate the nucleotides were ready.

Separation of cAMP from the other adenine nucleotides is based essentially on the method of Salomon *et al.*, (1974). The Dowex and alumina columns were set up in accordance to Farndale *et al.*, (1991). First, a rack of Dowex columns and a rack of alumina columns with precise alignment of the column positions were used. Columns were made from 5 ml syringes fitted with glass wool at the base to form a retaining mesh for the resins. Dowex resins were washed extensively in deionised water, followed by 3 washes in 1 M HCl, and again with water. It was finally resuspended 1:1 with deionised water in a beaker and kept in uniform suspension using a magentic stirrer. 2 ml of this suspension was pipetted into the columns, giving a 1 ml bed volume. Alumina resins were washed once in water and once in 0.1 M Imidazole (pH 7.3). It was similarly resuspended in deionised water and pipetted into the columns. The columns were plugged to prevent the resins from drying when not in use. Before using the columns, the Dowex columns were pre-washed through 3 washes of 2 ml of

1 M HCl, followed by 5 washes of 2 ml of deionised water; the alumina columns were washed 4 times with 2 ml of 0.1 M Imidazole (pH 7.3) and 3 time washes with deionised water.

The separation of [^{3}H] cAMP from the rest of the labelled components (e.g., [^{3}H] ATP, [^{3}H] ADP, [^{3}H] AMP, [^{3}H] adenine *etc*) starts with the Dowex columns. Dowex 50 resins are negatively charged and hence are not expected to bind any of the components. However, the passage of cAMP is preferentially retarded in the column, probably by a non-specific interaction with the Dowex resin, and allows other labelled components to be washed away (Farndale *et al.,* 1991). The alumina resin instead binds cAMP less avidly than other adenine nucleotides as the cyclisation leads to the loss of vicinal hydroxyls on the ribose ring. Imidazole, which competes for the purine binding site, can therefore displace cAMP from alumina columns.

Harvested cell extract was loaded to separate cAMP from other radiolabelled nucleotides (adenosine, AMP, ADP etc) by Dowex and then Alumina chromatography. Firstly the samples (supernants) were added by pipetting into the Dowex column placed over scintillation vials and washed by 3 ml of deionised water. The eluant was collected in vials containing 5 ml of liquid scintillant. This mixture contained [^{3}H] labelled adenine nucleotides except [^{3}H] cAMP. Next the rack of Dowex columns was placed on top of the alumina columns, making sure that the eluant from the upper Dowex columns go straight into the alumina columns. Then the Dowex columns were washed with 5 times of 2 ml of deionised water into the alumina columns and removed. This step displaces cAMP from the Dowex to the alumina columns. 3 times of 2 ml of 0.1 M Imidazole (pH 7.3) were added to the

directly alumina columns and the eluant was collected in vials containing 9 ml of liquid scintillant, which contained only [^{3}H] cAMP. Finally, [^{3}H] cAMP was eluted from the alumina with 0.1 M imidazole (pH 7.3) and quantified. Both sets of vials were counted in Beckman scintillation counter. Data was analysed as the ratio of [^{3}H] cAMP to total [^{3}H] adenine nucleotides (X100).

2.4. Tissue Culture

2.4.1. Routine Tissue culture:

growth, maintenance and harvesting of cells

The cell lines used for the present study are Human embryonic kidney (HEK293) cells for stable transfections and Human embryonic kidney T (HEK293T) cells for transient transfections. The HEK293T cell line is derivative of HEK293 that gives higher levels of expression with transient transfections. Flasks of cells were incubated in cell culture incubators (Jencons Nuaire) in an atmosphere of 95% air / 5% CO_2 at 37 °C. Cells were grown in continuous monolayer culture in 75 cm^2 /25 cm^2 sterile tissue culture flasks in growth medium [Dulbecco's Modified of Eagle's Medium (DMEM) supplemented with 2 mM L-glutamine and 10% NewBorn Calf Serum (NBCS)]. Every passages of confluent monolayer cells in the flasks were splited by the addition of 1.0 ml trypsin solution (0.1 % $^{W}/_{V}$ trypsin, 0.025% $^{W}/_{V}$ EDTA, and 10 mM glucose, pH 7.4) after washing sterilised 1 X PBS (phosphate buffered saline). When all the cells were detached, trypsinisation was terminated by the addition of 10-20 mls of growth medium (DMEM) containing 5 – 10 % NBCS. Harvested cells were centrifuged at about 1000 rpm for about 5 min at room temperature. Finally, supernant was taken off and the cell pellet was resuspended in growth medium and plated out as 1:10 to 1:15 for routine maintenance of cell line.

When cells in 75 cm^2 flasks or dishes reached confluency or the particular treatment time had elapsed they were harvested by scraping the monolayer into the

medium and the cells were collected in a 50ml centrifuge tube or 13 ml polypropylene tube on ice. The tubes were centrifuged at 1500-2000 rpm for 5 min at 4 ° C in a Beckman TJ-6 benchtop centrifuge. The supernant was discarded and the cell pellet was resuspended in a 50 ml of ice-cold PBS [NaCl (10 g), KCl (0.25 g), Na_2HPO_4 (1.8 g) and KH_2PO_4 (0.3 g), pH 7.4] and centrifuged as before. Again the supernant was discarded and the pellet was resuspended in 1 X PBS and recentrifuged. The supernant was again discarded and the pellet was stored at –80 ° C until required.

2.4.2. Transient transfections

Transient transfection of DNA into HEK293T cells was optimised in 10 cm^2 dishes using Lipofectamine™ as transfection reagent (Gibco Life Technologies) according to the manufacturer's instructions.

First, confluent HEK293T cells of a 75cm^2 flask was split into 100mm diameter tissue culture dishes the day before transfection. On the day of transfection, the confluency of cells should be between 60 to 80%. For each dish, about 10-15 μg of DNA was used, diluted in 0.8 ml of serum-free Optimem-1 medium (Gibco Life Technologies). Also Lipofectamine™ (25-30 μl) diluted in Optimem-1 medium to give a 0.1 mg/ml solution in 0.8 ml of mixture (Lipofectamine™/Optimem-1 medium). Then both equal volumes of the diluted DNA and Lipofectamine™ were mixed together by dropping Lipofectamine™ containing Optimem medium to DNA suspension mixture (0.8 ml of DNA suspension and 0.8 ml of Lipofectamine™ suspension) and incubated at room temperature for 30-40 min. In the meantime, cells,

which are ready for transfection on the dish, were rinsed twice with 37 ° C pre-warmed Optimem-1. Finally, 6.4 ml of Optimem-1 medium was added to the DNA/ Lipofectamine™ mixture and mixed well (total volume: 8 ml), and then added to the cells on the dish.

2.4.3. Generation and Maintenance of Stable cell lines

Appropriately HEK293 cells were grown to 60 - 70% confluency in 100 mm diameter tissue culture dishes for transient transfections. cDNAs (10-15 μg) encoding either hDOR-$G_{i1}\alpha$ (Ile^{351})/-$G_{o1}\alpha$ (Ile^{351}) fusion proteins were diluted with 0.1 μg/μl upto 100-150 μl in sterilised H_20. These two fusion proteins were added to a sterile 13 ml polypropylene tube containing serum-free Optimem-1 medium to a final volume of 800 μl. Lipofectamine™ (25-30 μl per one tube) was added to another sterile tube containing serum-free medium to a final volume of 800 μl DNA. Mediums containing Lipofectamine™ were dropped into medium containing DNAs. DNA/liposome complexes (1.6 ml) were incubated to form for 30-40 min during which time the cell monolayers ready for transfections were washed twice with serum-free medium. Then 6.4 ml of serum-free medium was added to the DNA/liposome complexes to a final volume of 8 ml and the whole mixtures added to one 100mm dish of cells. One 100 mm dish was for hDOR-$G_{i1}\alpha$ (Ile^{351}), another for hDOR-$G_{o1}\alpha$ (Ile^{351}), the third for normal HEK293 cells as a control.

After 6-7 h incubation at 37 ° C, medium was replaced with normal DMEM containing 5% NBCS. 48 h after DNA transfection, two transfected dishes and one

untransfected dish were trypsinised and split 1:3 into new 100 mm tissue culture dishes. Untransfected cells were also split into 1:3 (as a control) and one was maintained with normal medium and the other with medium containing geneticin sulphate. Antibiotic (Geneticin G-418 in the case of pcDNA 3 vector) was added to all dishes. A very high concentration of G-418 (1 mg/ml) was used initially to select for resistant clones, and the medium changed every 2-3 days to maintain a good selection environment. After 7 to 10 days, when the untransfected cells (control dish) in the medium containing geneticin sulphate were dead and another transfected cells confluent, isolated clones of cells in the transfected dishes were picked. The picked clones (about 24 for each type of DNA transfected) were detached from the dish by scraping with sterile blue tips and at the same time transferring into 24 well plate with 0.5 ml of medium. The clones were grown in 24 well plate in 1 ml of G-418 (800 μg/ml) per well and medium changed every 4-5 days until the confluent.

After 7-10 days, each confluent clone was split 1:2 into 25 cm^2 flasks and grown until about 80 % of confluency. When individual clones in one of the 25 cm^2 flask were confluent, cells were harvested for assaying their receptor levels. Once the best clones were obtained for both fusion proteins, cells growing in the another 25 cm^2 flask were expanded to 75 cm^2 flask in medium containing G-418 (800 μg/ml). The rest of clones were harvested and preserved at –200 ° C in liquid nitrogen tanks. Routine cultures of stable cell lines were in DMEM medium containing 700 μg/ml of G-418.

2.4.4. Preservation of cell lines: storage and recovery

Stable cell lines were preserved in the earliest passage possible (passage 1-5). Both best clones for the fusion proteins in 75 cm^2 flasks were grown to confluency before trypsinisation. After centrifugation, the cell pellet was suspended in 1 ml of NBCS with 10 % DMSO (as a cryo-protectant). The cell suspension was transformed into sterile 1.5ml cryovials, and labelled clearly according to the early passages. These followed to a slow freezing process; the first 3 to 6 h in a –20 ° C freezer, then overnight in a –80 ° C freezer, and finally long term storage in –200 ° C liquid nitrogen tanks. Also the rest of clones were preserved in the same way into 1.5ml cryovials and kept in liquid nitrogen tanks.

Preserved cell line can be rescued by thawing the cryovial in 37 ° C water bath and resuspended in 10 ml of pre-warmed medium. Then the cell suspension was centrifuged at 1000 rpm for about 5 min at R. T. to remove all traces of DMSO. Finally the cell pellet was resuspended in about 10-15 ml of normal medium or medium containing G-418 (700 μg/ml) and grown in 75 cm^2 flask.

2.4.5. Treatment of cells with Pertussis toxins

Pertussis toxin (PTx), Islet activating protein; IAP from *Bordetella pertussis* : sterile filtered solution of 50 μg/ml in 50 % (v/v) glycerol containing 50 mM Tris, pH 7.5, 10 mM glycine, and 0.5 M sodium chloride (Sigma). PTx was kept in –20 ° C. A buffer containing 25 mM sodium phosphate, pH 9.0, 0.5 M sodium chloride and 4 %

($^{v}/_{v}$) glycerol is recommended for dilution. Preincubate the PTx in the presence of 1-5 mM adenosine triphosphate (ATP) and 1-5 mM dithiothreitol (DTT) for *in vitro* use with cell membranes. Preincubation with ATP and DTT is not recommended for use with intact cells or *in-vivo* use (Moss *et al.*, 1983).

Stable or transiently expressing cells were treated with PTx *in vivo*. PTx stock was diluted to a final concentration of 200 μg/ml. It was added directly into the dishes or the flasks under aseptic environment, followed by incubation for the appropriate amount of time. PTx was added to a final concentration of 25 ng/ml to the medium before 16h harvesting the transfected cells.

2.4.6. Labelling of cells with [^{3}H] adenine for AC assays

One day before the assay, cells stably expressing hDOR-$G_{i1}\alpha$ (Ile^{351})/-$G_{o1}\alpha$ (Ile^{351}) fusion proteins were labelled and incubated with [^{3}H] adenine (Amersham pharmacia biotech, 1.0 μCi/ml per well in 12 well plates, 0.5 μCi/ml per well in 24 well plates) in DMEM containing 700 μg/ml of G-418 overnight.

2.5. Other protocols

2.5.1. Preparation of plasma membrane fractions

Membranes were prepared according to the method of Koski and Klee, (1981). Frozen cell pastes were thawed on ice and resuspended in 2 ml of ice-cold T/E buffer (10 mM Tris-HCl, 0.1 mM EDTA, pH 7.5) and transferred to a pre-chilled glass homogenizer. Then the harvested cells were homogenized, on ice, with 40-50 strokes of a hand-held teflon-on-glass homogenizer. Again the resulting homogenates were passed through orange needles with 8-10 strokes, transferred to the eppendorf tubes and spinned down at 1000 rpm for 10 min at 4 ° C. The supernant (0.5-1 ml) was taken and transferred to ultracentrifuge tubes (Beckman Instruments, Inc). Centrifuge tubes were placed in a type TLA-100.2 (Beckman Instruments, Inc) and centrifuged at very high speed 50,000-75,000 rpm for 30 min at 4 ° C. Before the centrifugation, all the tubes were balanced and rotor was pre-chilled at 4 ° C. The supernant was discarded and pellet resuspended in 2-5 ml of T/E buffer, to make the aliquots of small volume and to give an approximate protein concentration of 1-3 μg/μl. The samples were then frozen at –80 ° C in 100-200 μl fractions until required.

2.5.2. Determination of protein concentration

Protein concentrations were determined by the method of Lowry *et al* (1951), using Bovine Serum Albumin (BSA, 0-2.0 mg/ml) as standard. The samples were read at 492 nM on **SLT. SPECTRA**.

2.5.3. Deglycosylation of glycosylated forms of hDOR-$G_{o1}\alpha$ (Ile^{351}) fusion protein

For the deglycosylation reaction, membranes from HEK293 cells stably expressing hDOR-$G_{o1}\alpha$ (Ile^{351}) fusion protein containing N-Glycosidase F (Roche Molecular Biochemicals) (membranes 5μl, denaturation buffer 5μl, reaction buffer 10 μl, NGF 2.4 units/10μl) were incubated overnight at R.T. Both samples of untreated and N-Glycosidase F-treated resolved in 10% SDS-PAGE at the same time. Following transfer to nitrocellulose, both samples were immunoblotted with antiserum ON1 (specific for the N-terminal hexapeptide of $G_{o1}\alpha$).

Reaction principle:

Protein—asn—GlcNAc—Glycan → Protein—asp + NH_3 + GlcNAc—Glycan

2.5.4. Western blotting

A) Preparation of SDS-PAGE gel

SDS-PAGE (sodium dodecyl sulphate-polyacrylamide gel electrophoresis) was normally performed with 10% acrylamide resolving gels. It was prepared as follows:

10% Resolving Gel

Water (deionised)	8.3 ml	**(2)**
Acrylamide (30 % $^{W}/_{V}$), bis-acrylamide (0.8 % $^{W}/_{V}$)	6 ml	**(1)**
Tris/HCl (1.5M, pH 8.8), SDS (0.4% $^{W}/_{V}$)	8 ml	**(3)**
Glycerol (50 % $^{W}/_{V}$)	1.6 ml	
Ammonium persulphate ($AmpSO_4$) (10% $^{W}/_{V}$)	90 µl	**(5)**
TEMED	8 µl	**(4)**
Total volume	**23.9 ml**	

30 % acrylamide/0.8 % bis-acrylamide solution was made up of H_20 and kept in 4°C freeze (light-sensitive). $AmpSO_4$ was diluted in water.

The above resolving gel is sufficient for a single gel cast in a Hoefer Gel Caster with two 180 X 160 mm glass plates and 1.5 mm spacers. After setting up the gel following the numbering of the right side, the gel was layered with 0.1 % $^{w}/_{v}$ SDS and polymerised at R.T for about 60-90 min.

After the gel had polymerised, the layer was washed off and the stacking gel prepared:

Stacking Gel

Water (deionised)	9.75 ml	**(2)**
Acrylamide (30 % $^{W}/_{V}$), bis-acrylamide (0.8 % $^{W}/_{V}$)	1.5 ml	**(1)**
Tris/HCl (0.5M, pH 6.8), SDS (0.4% $^{W}/_{V}$)	3.75 ml	**(3)**
Ammonium persulphate (APS) (10% $^{W}/_{V}$)	150 µl	**(5)**

TEMED	8 µl	(4)
Total volume	**15.1 ml**	

The gel was set up according to the numbering of the right side, a 15 well teflon comb was layered on top of the stacking gel, polymerised for about 60 min. Made up gels can be kept at 4 ° C for 2-3 days until required.

B) Electrophoresis of SDS-PAGE

Gel running buffer was made upto 2.5 litre for electrophoresis tank. Protein samples (30-50 µg per lane) were diluted 1:1 ratio in Laemli buffer (2X), heated for 5 min at 95 ° C on a heating block. A Hamilton syringe was used to load samples into the wells of the gel. Prestained protein markers was also loaded into the front line of gel. Then, electrophoresis of 10 % SDS-PAGE gel was usually at 30 mA constant current overnight (about 14-16 h) and the voltage set at least 90 V, and the power at least 10 W.

C) Protein transfer onto nitrocellulose membranes (Western blotting)

After electrophoresis, the glass plates with the gel were taken out from the kit. 5 litre of western transfer buffer was prepared, nitrocellulose membranes and Whatman filter papers cut to the right size of the gel and pre-wetted in buffer. The nitrocellulose membranes and gel combined together, then sandwiched between two pieces of Whatman filter paper and assembled into a LKB Transphor apparatus. The

nitrocellulose membrane was positioned nearer to the positive end, which protein transfer on the gel could be performed to the nitrocellulose membranes from the negative to the positive at 1.5 mA for 90 to 120 min. After that, the protein transferred to the nitrocellulose membranes can be detected by temporarily staining with a solution consisting of 0.1 % $^{w}/_{v}$ Ponceau S and 3 % $^{w}/_{v}$ TCA, followed by wash buffer.

D) Incubation with antibodies

Protein transferred to the nitrocellulose membranes were covered with 5 % non-fat milk (Marvel) in PBS or TBS overnight at 4 ° C or 2-3 h at R.T with shaking at slow speed. All antibodies were diluted in 1-3 % Marvel in PBS or TBS. Membranes containing antibodies were incubated for 1-2 h at R.T. with shaking. After primary antibody treatment, the membranes were washed at least 3-4 times with PBST or TBST before the secondary antibody was added. Used antibodies can be stored with a trace of thimerosal for no more than 5 times or 3 months.

Dilutions of the used antibodies as follows:

Primary antibody	Dilution	Secondary antibody	Dilution
I1C	1:1000	Anti-rabbit IgG	1:2000
ON1	1:6000	Anti-rabbit IgG	1:10000

E) Enhanced chemiluminescence

Visualisation and detection of horse-radish-peroxidase conjugated antibodies on the nitrocellulose membrane was performed by enhanced chemiluminescence (ECL) (Amersham, U.K) or SuperSignal® enhanced chemiluminescence reagent (Pierce, U.S.A) according to the manufacturer's instructions. Membranes were washed with wash buffer several times before incubation with the ECL reagent (1:1 ratio of solution A and B). After 2-3 min incubation, the membranes were covered by tow pieces of clear plastic sheet and removed air bubbles carefully. Finally, the nitrocellulose membranes were put into a film cassette, carried to the darkroom and a light sensitive X-ray film (Fuji photo film Ltd) put on top of the membranes. The film was developed in an automatic film developer (Kodak Xomat) after an exposure time (10 sec-5 min).

f) Staining of gels with Coomassie Blue

Following electrophoresis, gels were soaked, with gentle shaking on a rotary shaker, for 1 h in 45 % ($^{v}/_{v}$) methanol, 10 % ($^{v}/_{v}$) acetic acid containing 0.25 % ($^{w}/_{v}$) Coomassie Blue R-250. Destaining was achieved by washing gels in several changes of 45 % ($^{v}/_{v}$) methanol, 10 % ($^{v}/_{v}$) acetic acid.

2.6. Data analysis and statistical method

All the data were analysed using **GraphPad Prism (3.0)** version. All the statistics (P values) were compared with t test (unpaired).

CHAPTER III

Comparisons of the activation of $G_{i1}\alpha$ and $G_{o1}\alpha$ using fusion proteins between the human δ-opioid receptor and these G proteins

INTRODUCTION (Chapter 3)

The superfamily of regulatory GTP hydrolases (G proteins) includes Ras and its close homologues, translation elongation factor, and heterotrimeric G proteins. Here, the heterotrimeric G proteins will be discussed. GPCRs transduce a large variety of signals across the cell membrane via heterotrimeric G proteins. G proteins transduce ligand binding to these receptors into intracellular responses which underlie physiological responses of tissues and organisms. G protein heterotrimers consist of three subunits named α, β and γ. So far some 20α, 6β and 12γ polypeptides have been identified. Four main classes of G proteins are known: Gs, which stimulates adenylyl cyclases; Gi, which inhibits adenylyl cyclases; Gq, which activates phospholipase C; and G_{12} which regulate cytoskeletal structure. G proteins are inactive with GDP tightly bound to the α-subunit. When the activated receptor interacts with a heterotrimeric G protein it induces GDP release and this is followed by association of GTP with the empty nucleotide-binding site (Birnbaumer *et al.*, 1990; Hamm, 1998). GTP binding induces a conformational change that results in dissociation of the heterotrimer into α and βγ subunits and activation of downstream effectors by both Gα·GTP and free Gβγ subunits. G protein deactivation is required to turn-off the cellular response and occurs when the Gα subunit hydrolyses GTP to GDP and inorganic phosphate. The α subunit/ GDP complex can then reassociate with the βγ subunits to form the heterotrimeric G protein. The Gα subunit contains two domains; a domain involved in binding and hydrolysing GTP (the G domain) that is structurally similar to the superfamily of GTPases and a unique helical domain that buries the GTP in the core of the protein. The β subunit has a 7-membered β-propeller structure

based on 7 WD-40 repeats (Lambright *et al.*, 1996) and γ subunits interact with β through a N-terminal coiled-coil and via extensive contacts all along the base of β. The βγ subunits themselves can play active roles in signal transduction, for example, through regulation of K^+ channels, PLC β and certain isoforms of AC in animal cells, and activation of the pheromone response pathway in budding yeast. βγ subunits inhibit GDP release from Gα in Gα-catalysed GTP hydrolysis thus rendering reactivation dependent upon the interaction of Gα with ligand-activated receptors (Sprang, 1997). Clearly, βγ subunits enhance receptor interaction with α subunits. Single Ala mutations in residues of the β subunit that contact the α subunit block receptor-mediated GTP/GDP exchange. A number of effector enzymes have been shown to display GTPase activating protein (GAP) activity towards their partner G proteins and Regulators of G protein Signalling (RGS) proteins play key roles in accelerating the GTP hydrolysis rates of at least the Gi and Gq families of G proteins (Koelle, 1997).

The relatively recent cloning of opioid receptors has established that the products of three distinct genes form the known subtypes, namely, the δ (DOR), μ (MOR), and κ (KOR)- opioid receptors. These are highly homologous with overlapping distributions but these opioid receptors have distinct pharmacological profiles. The endogenous opioid peptide-receptor systems mediate important physiologic functions related to pain perception, locomotion, motivation, reward, autonomic function, immunomodulation and hormone secretion. The DOR has been associated with several physiological functions, including analgesia (Heyman *et al.*, 1988), tolerance (Abdelhamid *et al.*, 1991; Kest *et al.*, 1996) and reproduction (Zhu and Pintar, 1998).

The DOR is expressed in multiple regions of the adult nervous system, with high levels in the olfactory bulb, striatum, cortex, hippocampal formation, pons, spinal cord and dorsal root ganglion (Zhu *et al.*, 1998). DOR selective drugs may have potential clinical benefits which include greater relief of neuropathic pain (Dickenson, 1997), reduced respiratory depression (Cheng *et al.*, 1993) and constipation (Sheldon *et al.*, 1990), as well as a minimal potential for the development of physical dependence (Cowan *et al.*, 1998). A major signalling mechanism of the DOR is to inhibit cAMP production through Gi/Go family G proteins, an effect which is blocked by treatment with pertussis toxin (Law *et al.*, 1985b). The DOR also stimulates potassium channel conductance through Gi/Go proteins and inhibits calcium channel conductance through Go proteins. The expression of Go proteins is restricted to neuronal and endocrine systems and the heart and it is highly abundant in mammalian brain. Three distinct subforms, i.e., $G_{o1}\alpha$, G_{o2} α and G_{o3} α have been identified, with G_{o1} and G_{o2}, representing splice variants whereas G_{o3} represents a recently characterised post-translational modification of $G_{o1}\alpha$ and represents about 30% of the total Go in brain (Exner *et al.*, 1999). The cDNA for DOR was first cloned using hybridization screening methods (Knapp *et al.*, 1994; Simonin *et al.*, 1994). Pharmacological studies have suggested at least two DOR subtypes. In general, the δ_1 receptor subtype is preferentially activated by the agonists [D-Pen^2, D-Pen^5]-enkephalin/[D-Ala^2, D-Leu^5]-enkephalin and antagonised by 7-benzylidenenaltrexone/[D-Ala^2, Leu^5, Cys^6]-enkephalin while the δ_2 receptor is activated by [D-Ala^2, D-Glu^4] deltorphin (Mattia *et al.*, 1991, 1992; Hiller *et al.*, 1996) /[D-Ser^2, Leu^5]-enkephalyl-Thr and antagonised by naltriben/ naltrindole-5'-isothiocyanate. A transgenic μ-opioid knockout mouse has been used to study possible interactions between DOR and MOR in the central

nervous system (Sora *et al.*, 1997 a,b). They found that the antinociceptive effect of DPDPE, a classic δ-selective receptor agonist, appeared to be dependent on intact MOR. Wang *et al.*, (1994) constructed chimeric receptors from the second extracellular loop sequences of hMOR which was replaced with that of KOR. This result suggests that this region contributes substantially to the KOR's selectivity in dynorphin ligand recognition. Meng *et al.*, (1995) also constructed four different chimeric receptors from KOR and DOR. The results show that the DOR and KOR bind the same opioid core differently and achieve their selectivity through different mechanisms. These chimeric receptors were capable of binding opioid ligands and following introduction of a number of point mutations into the second extracellular loop and the top half of TM domain IV of the DOR helix. It was concluded that a region composed of the second extracellular loop and the top half of TM domain IV of the DOR helix was particularly important in the binding of prodynorphin products.

GPCRs interact with G proteins to regulate the downstream activity of effector systems. To understand these signalling pathways, transient transfection has provided a convenient method of overexpressing the components. The efficiency of GPCR and G protein coupling depends on the ratio and the absolute concentrations of each (Kenakin, 1997). However, in co-transfection studies with GPCRs and G proteins, it has been an unresolved pharmacological problem to achieve precisely defined GPCR: G protein ratios. Also, the efficacy and potency of agonist ligands depends on which specific G protein activation-deactivation cycle step is assessed (Seifert *et al.*, 1999). For some G proteins (Gs and Gq), it is difficult to analysis GPCR-Gα coupling at the G protein level by measuring GTPγS binding and GTP hydrolysis. A method to control ratio of the receptor and G proteins has been to employ purified G protein α

subunits in reconstitution assays (Hartman *et al.*, 1996; Hellmich *et al.*, 1997; Glass *et al.*, 1999; Jian *et al.*, 1999). This has been a useful methodology for precise kinetic analysis of receptor-G protein coupling and allowed definition of the identity and concentration of each component.

In 1994, Bertin *et al.* introduced a new and rather unusual strategy, the construction of a fusion protein between the human β_2-adrenoceptor and the α subunit of its cognate G protein Gs. This construct was shown to be more efficient than non-fused β_2AR at stabilising high affinity agonist binding and resulted in agonist activation of AC when expressed in Gsα-deficient S49 cyc $^-$ lymphoma cells. In 1997, Bertin *et al* reported that use of the β_2AR-Gsα fusion protein in tumour cells prevented tumour proliferation in cell culture and in syngeneic mice. Subsequently several groups have concluded that the basic properties of fusion proteins, including the defined 1:1 stoichiometry of the signalling partners and the close physical proximity of the signalling partners following expression are attractive for analysis. The fusion protein strategy has now been applied successfully to a number of GPCRs and G proteins. Fusions are produced by linking the ORF of the two proteins using DNA restriction enzyme, PCR - based techniques, or both. Expression levels of fusion proteins can be determined by [^{3}H] antagonist saturation binding and these provide direct measures of expression level of the associated G proteins (Wise *et al.*, 1997). Furthermore, they can be detected with antibodies if the receptor is epitope-tagged (Seifert *et al.*, 1998; Fong *et al.*, 1999). Moreover, the unique properties of fusion proteins have allowed measurements of GPCR-regulated GTP turnover number and Km values for GTP hydrolysis by the fused G protein (Wise *et al.*, 1997; Seifert *et al.*, 1998; Carr *et al.*, 1998; Kellet *et al.*, 1999; Fong *et al.*, 1999). Kobilka and co-workers

studied the β_2AR/Gsα interaction using variant receptor and G protein fusion proteins expressed in insect Sf9 cells using baculovirus expression systems (Seifert *et al.*, 1998; Wenzel-Seifert *et al.*, 1998; Seifert *et al.*, 1999), which allow effective measurement of the effects of ligands due to low basal high-affinity GTPase activity. For example, it has been shown that marked coupling differences exist between β_2AR-GsαS (the short splice variant of the α-subunit of the stimulatory G protein of AC) and β_2AR-GsαL (the long splice variant). Specifically, the β_2AR in β_2AR-GsαL showed hallmarks of constitutive activity, whereas β_2AR in β_2AR-GsαS did not. This difference may be due to the lower GDP affinity of GsαL than GsαS (Seifert *et al.*, 1998). To overcome the difficulty in measuring agonist stimulation of high-affinity GTPase activity following co-transfection of the human IP protanoid receptor and Gs α, Fong and colleagues constructed a human IP prostanoid receptor-Gsα fusion protein to allow significant agonist output (Fong *et al.*, 1998; Fong and Milligan, 1999). Comparisons between co-transfection of receptor and non-fused G protein and the receptor-G protein fusion protein have been demonstrated. β_2AR-Gsα fusion proteins reconstituted greater high-affinity agonist binding and induced significantly higher AC activation than β_2AR expressed in combination with the α-subunit of Gs (Seifert *et al.*, 1998). Importantly however, a comparative analysis of ligand efficacy at fusion proteins between the human adenosine A_1 receptor and PTx-resistant forms of the α-subunits of each G_{i1}, G_{i2}, G_{i3} and G_{o1} indicated the difference between fused and non-fused systems was much less than for β_2AR-Gsα coupling (Wise *et al.*, 1999).

It has been reported that the extreme C-terminal region of G protein α-subunits is a key element for GPCR activation (Conklin *et al.*, 1993; Liu *et al.*, 1995; Bourne *et al.,* 1997; Medici *et al.*, 1997) and modification of three amino acids from the C-terminus of α subunits of the PLC-linked G protein Gq has been shown to cause alteration in the GPCRs which can activate the G protein (Conklin *et al.*, 1993). Following co-expression of the IP prostanoid receptor with a chimeric G protein, G_{i1}/Gs(6) which had the backbone of $G_{i1}\alpha$ with only the six amino acids of the C-terminus derived from Gsα, agonist stimulation of GTPase activity was more effective, thus indicating a key role of the extreme C-terminal region of G-protein α-subunits (Fong *et al.,* 1998; Fong and Milligan, 1999).

Modulation by pertussis toxin has been used as a useful tool to characterise certain G protein-dependent signalling pathways. Pertussis toxin is also called Islet activating protein (IAP). It is produced by *Bordetella pertussis* and causes ADP-ribosylation of a cysteine side chain four amino acids from the C-terminus of the α-subunits of Gi, Go, and Gt. This prevents activation of the G protein trimer by its receptor (Katada and Ui, 1982;West, 1985). Efficient ADP-ribosylation by PTX requires the αβγ trimer and isolated α-subunits are reported to be poor substrates (Casey *et al.*, 1989). The βγ-subunits may act by promoting favorable contacts of the α-subunits with PTx or by relieving unfavorable contacts between the G protein and the toxin (Scheuring *et al.*, 1998).

To understand the signalling pathways of $G_{i1}\alpha$ following activation by α_{2A}AR, A_1R and $5HT_{1A}$AR, fused PTx-resistant mutants of G_{i1} have been expressed in

mammalian cell lines (COS-7, Rat1 fibroblast, HEK293). This has allowed the interactions of GPCRs with the endogenous Gi proteins to be abolished by PTx treatment with the interactions between GPCRs and the fixed and mutated G proteins being preserved. The α_{2A}AR- $G_{i1}\alpha$(Gly ^{351}) fusion protein has been shown to have the capacity to activate both endogenously expressed Gi and PTx-resistant fused Gi protein in Rat1-fibroblasts stably expressing this construct (Burt *et al.*, 1998). Agonist-regulated GTPase activity between fused and endogenous G proteins was measured in membranes of PTx-untreated and treated cells. The α_{2A}AR-$G_{i1}\alpha$ (Gly^{351}) fusion protein was able to inhibit forskolin-amplified AC activity. However, following PTx treatments, α_{2A}AR agonists could no longer regulate this activity. The same was true for p44 MAP kinase and p70 S6 kinase. These observations demonstrate the effects to be due to activation of the endogenous $G_{i1}\alpha$ proteins, not the fused Gi protein. Other, unexpected differences between the isolated receptor and fusion proteins have been observed (Sautel and Milligan, 1998). The α_{2A}AR-$G_{i1}\alpha$ (Gly ^{351}) fusion protein coupled to endogenous Gi proteins to inhibit AC activity with a lower effectiveness than the isolated receptor. However, unlike non-fused α_{2A}AR, the fused receptor was unable to couple to endogenous Gs proteins. Two possibilities, which could explain these observations, can be considered. First, this fusion protein attached some physical constraint to the receptor such that its interaction with endogenous $G_s\alpha$ was covered whereas interactions with endogenous $G_i\alpha$ may be less effected. Secondly, differences in the distribution of the isolated receptor and the fusion proteins in the plasma membrane may limit availability and access to the endogenous G proteins. Unlike the above, high affinity GTPase activity and AC regulation by $5HT_{1A}$R-$G_{i1}\alpha$ (Ile ^{351}) and $5HT_{1A}$R- $G_{i1}\alpha$ (Gly ^{351}) fusion protein stably expressed in

HEK293 cells is unaffected by PTx treatment, indicating both the functionality of the agonist-activated fusion protein and a lack of interaction with endogenously expressed $G_i\alpha$ proteins (Kellet *et al.*, 1999). Moreover, spiperone functioned as an inverse agonist in membranes expressing $5HT_{1A}R\text{-}G_{i1}\alpha$ (wild type) and $5HT_{1A}R\text{-}G_{i1}\alpha$ (Ile^{351}) fusion proteins but not the $5HT_{1A}R\text{-}G_{i1}\alpha$ (Gly^{351}) fusion protein. This demonstrates that alteration of a single amino acid in the C-terminal region of $G_{i1}\alpha$ can regulate agonist-independent constitutive activity of GPCRs. Dupuis *et al.,* (1999) have also used PTx-resistant $5HT_{1A}R\text{-}G_{o1}\alpha$ fusion proteins to measure agonist efficacy and Wenzel-Seifert *et al.*, (1999) have demonstrated highly efficient coupling of the human formyl peptide receptor to fused $G_{i1}\alpha$, $G_{i2}\alpha$ and $G_{i3}\alpha$.

GPCR-Gi/Go fusion proteins have provided useful tools to determine the kinetics of GTP hydrolysis, the efficacies of agonists and measurement of downstream effector signalling (Kellet *et al.*, 1999; Burt *et al.*, 1998). The aim of this present study was to understand the signalling of the hDOR coupling to the closely related G_{i1} and G_{o1} proteins using the fusion protein strategy.

RESULTS (Chapter 3)

Construction of the PTx–resistant hDOR-$G_{i1}\alpha$ (Xaa^{351})/ $G_{o1}\alpha$ (Xaa^{351}) fusion protein mutants

The hDOR-$G_{i1}\alpha$(wild type) and the hDOR-$G_{i1}\alpha$ (Xaa^{351}) mutants (Ile/Leu/Phe/Val/Ser/Ala/Gly/Arg) were constructed in pcDNA3.1 (Invitrogen, The Netherlands). The cDNA encoding the hDOR, originally cloned in pCDNA4, was obtained from Dr. C. Scorer (Glaxo Wellcome R. and D, Stevenage, U.K.). The last 157 bps of the hDOR was amplified by PCR in which the stop codon was deleted and a 3′*BamHI* site added. The open reading frame (ORF) of wild type rat $G_{i1}\alpha$ was used as a template in order to synthesise a PCR fragment, characterised by the deletion of the ATG start codon and by the addition of 5′*BamHI* and 3′*EcoRI* restriction sites. The hDOR cDNA was digested with *BamHI* and *NotI* to generate a 5′-1012bp fragment. The PCR amplified fragments (157bps fragment of hDOR and $G_{i1}\alpha$) and the remaining segment of the hDOR was ligated to pcDNA3.1 through these restriction sites **(Figures 3.1A, 3.2A).** Cys ^{351} Xaa PTx resistant forms of rat $G_{i1}\alpha$ were generated previously (Bahia *et al.*, 1998). The PTx resistant hDOR-$G_{i1}\alpha$ (Xaa^{351}) fusion proteins were constructed by recovering the unique *EcoNI* and *EcoRI* fragments from $G_{i1}\alpha$ (Xaa^{351}) mutants (Ile/Leu/Phe/Val/Ser/Ala/ Gly/Arg) and replacing the equivalent section of the hDOR-$G_{i1}\alpha$ (wild type) fusion protein **(Figures 3.1B, 3.2B).**

Secondly, the 5′120bps of hDOR cDNA was digested with *KpnI* and *BssHI* and the remaining 1020bps fragment from the hDOR-$G_{i1}\alpha$ (wild type) was digested with *BssHI* and *BamHI*. A fragment of 1065bps from the cDNA encoding $G_{o1}\alpha$ was

modified by introducing the flanking restriction sites *5′BglII* and *3′XbaI* by PCR amplification. Three different fragments were ligated into pcDNA3.1 using the compatibility of *BamHI* and *BglII* **(Figures 3.3A, 3.4A)**. Using the same approach as for the hDOR-$G_{i1}\alpha$(Xaa^{351}) mutants, Cys ^{351} Xaa PTx resistant forms of $G_{o1}\alpha$ had been generated previously (Bahia et al., unpublished). The PTx resistant hDOR-$G_{o1}\alpha$ (Xaa^{351}) fusion proteins were constructed by recovering the *ClaI* and *ApaI* fragment from $G_{o1}\alpha$ (Xaa^{351}) mutants (Ile/Leu/Gly) and replacing the equivalent segment of the hDOR-$G_{o1}\alpha$(wild type) fusion protein **(Figures 3.3B, 3.4B)**. All fusion proteins were fully sequenced prior to use **(Figures 3.1C, 3.3C).**

Characterisation of the hDOR-G_{i1}/G_{o1} fusion proteins following transient expression in HEK293T cells

I. Analysis of expression using [^{3}H] naltrindole binding studies

All of the constructs could be transiently expressed in HEK293T cells. Transient transfection of these constructs (8, 10, 12, 15, 18μg of DNA) into HEK293T cells was optimised in 10cm^2 dishes using Lipofectamine™ as transfection reagent- (data not shown). This gave a reasonable expression level (1-6 pmol/mg of protein), monitored by the appearance of specific binding sites for [^{3}H] naltrindole, which is a neutral antagonist for the hDOR **(Figures 3.5A, 3.5B).** Although levels of expression of the constructs varied between individual transfections, there was no specific pattern of expression associated with the identity of the G protein mutant. Saturation binding studies using [^{3}H] naltrindole indicated this ligand was bound with high affinity (K_d: 0.1-0.8 nM) by all the constructs. This is similar to the results obtained by Meng *et al*, (2000) for the isolated receptor K_d= 0.3 ± 0.1 nM. **Figure 3.6A and Figure 3.7A** are representative [^{3}H] naltrindole saturation binding experiments for the hDOR-$G_{i1}\alpha$ (Ile ^{351}) and -$G_{i1}\alpha$ (Gly ^{351}) fusion proteins respectively. Membranes expressing these fusion proteins were prepared and their level of expression (B_{max}) and dissociation constant (K_d) for [^{3}H] naltrindole measured. Scatchard plots (bound/free versus bound) were produced **(Figures 3.6B, 3.7B).** The K_d for [^{3}H] naltrindole at hDOR-$G_{i1}\alpha$ (Ile ^{351}) after PTx treatment (25ng/ml, 16h) of cells was 0.77 ± 0.12 nM (mean ± S.E.M, n=3) and that of hDOR-$G_{i1}\alpha$ (Gly ^{351}) was 0.13 ± 0.02 nM (mean ± S.E.M, n=3). Surprisingly, the K_d of [^{3}H] naltrindole for the hDOR-$G_{i1}\alpha$ (Ile^{351}) was about 6 times higher than that of the hDOR-$G_{i1}\alpha$ (Gly^{351}) ($P < 0.001$). Chapter 4 will examine

this in greater detail.

Table 3.1. Comparison of the K_d for [^{3}H] naltrindole to bind transiently expressed hDOR-$G_{i1}\alpha$ (Ile^{351}) and hDOR-$G_{i1}\alpha$ (Gly^{351}) fusion proteins.

Constructs	K_d for [^{3}H] naltrindole (nM)
hDOR-$G_{i1}\alpha$ (Ile^{351})	0.77 ± 0.12
hDOR-$G_{i1}\alpha$ (Gly^{351})	0.13 ± 0.02***

This data represent means ± S.E.M from three independent experiments.

*** Significantly different from hDOR-$G_{i1}\alpha$ (Ile^{351}), $P < 0.001$.

II. Immunological detection

All the fusion proteins were transiently transfected into HEK293T cells and cell membranes were prepared and loaded in 10% SDS-PAGE followed by immunoblotting. Antiserum I1C, specific for an internal domain (159-168 aa) of $G_{i1}\alpha$ (Green *et al.*, 1990), was used to detect the expression of the hDOR-G_{i1} fusion proteins **(Figures 3.8A, 3.8B).** In Figure 3.8A, western blotting was performed in four different conditions – 1st; boiling/reducing, 2nd; boiling/non-reducing, 3rd; non-boiling/reducing, 4th; non-boiling/non-reducing -. The conditions of 1st (lanes 2, 3) and 2nd (lanes 5, 6) seemed to be successful in detecting strong bands corresponding to hDOR-G_{i1} fusion proteins, but not in mock (pcDNA 3.1) loaded lanes (lanes 1, 4, 7, 10) as a negative control. All the hDOR-G_{i1} fusion proteins were detected with antiserum I1C, as shown in Figure 3.8B. The fusion proteins were detected as multiple bands which may reflect differential glycosylation A deglycosylation experiment using N-glycosidase F was successful in reducing the mobility and complexity of bands corresponding to the stably expressed hDOR-$G_{o1}\alpha$ (Ile^{351}) fusion protein **(Figure 3.17B).** There are a range of examples of detecting the expression of fusion proteins, including

5-HT_{1A}-$G_{i1}\alpha$ fusion protein with antiserum I1C (Kellet *et al.*, 1999),

FPR-$G_i\alpha$ fusion protein (Wenzel-Seifert *et al.*, 1999),

β_2AR-Gsα fusion protein (Seifert *et al.*, 1999).

III. Agonist-regulated high affinity GTPase activity

G proteins are enzymes which function to bind and hydrolysis GTP, producing GDP and inorganic phosphate. To monitor G protein mediated enzymatic activity (GTP hydrolysis), breakdown of $\gamma[^{32}P]$ GTP with the production of $[^{32}Pi]$ can be measured and $[^{32}Pi]$ is then separated from remaining $\gamma[^{32}P]$ GTP and the rate of GTP hydrolysis measured (Gierschik *et al.*, 1994). Each assay tube contained 50pmol of GTP (0.5 μM) in addition to approximately 50000cpm. The specific activity of the GTP is thus approx. 1000 cpm per pmol.

The rate of hydrolysis of GTP is calculated as

$$\frac{C}{S.A.} \times 2 \times \frac{1000}{P} \times \frac{1}{T}$$

Where: C = the counts in a 500μl sample
S.A = the specific activity of the GTP
P = the amount of protein present (μg)
T = the time of assay (min)

This gives the rate of hydrolysis of GTP in pmol/min/mg of membrane protein. The GTPase assay is suitable for determination of ligand efficacies and potencies because it monitors receptor-G protein coupling at steady state.

Following transient expression and prior PTx treatment (25ng/ml, 16h) of cells expressing the hDOR-$G_{i1}\alpha$ (Ile^{351}) fusion protein, membranes were prepared and PTx-insensitive high affinity GTPase activity and the effect of varying concentrations of

DADLE was monitored using 0.5 μM GTP as substrate. Stimulation of GTPase activity was produced in a concentration-dependent manner with $pEC_{50} = 7.1 \pm 0.1$ (mean ± S.E.M, n=3) for DADLE **(Figure 3.9A).** Equivalent experiments on membranes expressing the hDOR-$G_{i1}\alpha$ (Gly^{351}) showed a significantly lower potency for DADLE with $pEC_{50} = 6.2 \pm 0.1$ (mean ± S.E.M, n=3) **(Figure 3.9B).** This value was significantly different from hDOR-$G_{i1}\alpha$ (Ile^{351}) ($P < 0.005$). Equivalent experiments on membranes expressing the hDOR-$G_{o1}\alpha$ (Ile^{351}) fusion protein demonstrated a similar potency for DADLE of for the hDOR-$G_{i1}\alpha$ (Ile^{351}) with pEC_{50} = 7.2 ± 0.3 (mean ± S.E.M, n=3) **(Figure 3.9C)**. This value was not significantly different ($P = 0.61$). As expected, naltrindole was not able to stimulate the GTPase activity of these fusion proteins (data not shown).

Table 3.2. Comparison of the potency of DADLE to stimulate high affinity GTPase activity of the hDOR-fusion proteins

Constructs	pEC_{50}
hDOR-$G_{i1}\alpha$ (Ile^{351})	7.1 ± 0.1
hDOR-$G_{i1}\alpha$ (Gly^{351})	6.2 ± 0.1**
hDOR-$G_{o1}\alpha$ (Ile^{351})	7.2 ± 0.3

The data represent means ± S.E.M from three independent experiments.

** Significantly different from hDOR-$G_{i1}\alpha$ (Ile^{351}), $P < 0.005$.

IV. Kinetics of agonist-stimulated GTP hydrolysis and measurement of GTP turnover number

As GTP hydrolysis is an enzymatic reaction it is possible to determine the velocity of a maximally effective concentration of agonist and thus measure V_{max} and K_m of this process by using a wide range of substrate (GTP) concentrations. The defined 1:1 stoichiometry of GPCR and Gα in the fusion proteins allows determination of ligand-regulated GTP turnover number in a membrane system (i.e. mol GTP hydrolysed per unit time per mol fusion protein) (Seifert *et al.*, 1998; Wise *et al.*, 1997). Membranes prepared from cells expressing the hDOR fusion proteins [hDOR-$G_{i1}\alpha$ (Ile^{351}), -$G_{i1}\alpha$ (Gly^{351}), -$G_{o1}\alpha$(Ile^{351})] and pretreated with PTx (25ng/ml, 16h) were assayed for basal and 100 μM DADLE-stimulated GTPase activity at GTP concentrations from 20 nM to 2 μM. The effect of the agonist was predominantly to increase V_{max} of the GTPase activity with only a minor effect on the estimated K_m. Direct plots of the GTPase activity versus GTP concentrations were obtained for cells expressing hDOR-$G_{i1}\alpha$ (Ile^{351}), -$G_{i1}\alpha$ (Gly^{351}), -$G_{o1}\alpha$ (Ile^{351}) **(Figures 3.10A, 3.11A, 3.12A).** Eadie-Hofstee plots (velocity versus velocity/substrate) are commonly used to estimate V_{max} and K_m for substrate. B_{max} values of receptor antagonist, ([^{3}H] naltrindole) saturation binding was assessed on the same membranes and thus the GTPase activities (V_{max} for DADLE –V_{max} for basal) were divided by expression level (B_{max}) to calculate DADLE-induced turnover number for GTP. Eadie-Hofstee plots of cells expressing hDOR-$G_{i1}\alpha$ (Ile^{351}), -$G_{i1}\alpha$ (Gly^{351}), -$G_{o1}\alpha$ (Ile^{351}) are shown. **(Figures 3.10B, 3.11B, 3.12B)**, K_m, V_{max} and turnover number were obtained and shown in **Table 3.3.**

Table 3.3. DADLE (100 μM) -stimulated GTP hydrolysis is greatest for hDOR when activating $G_{i1}\alpha(Ile^{351})$.

	hDOR-$G_{i1}\alpha$ (Ile^{351})	hDOR-$G_{i1}\alpha$ (Gly^{351})	hDOR-$G_{o1}\alpha$ (Ile^{351})
GTP turnover number (+DADLE) (min^{-1})	9.5 ± 0.1	4.9 ± 1.1*	3.0 ± 0.1***
K_m GTP (basal) (μM)	0.41 ± 0.05	0.70 ± 0.11	0.68 ± 0.09
K_m GTP (+DADLE) (μM)	0.54 ± 0.06	0.73 ± 0.07	0.62 ± 0.10

The data represent means ± S.E.M from three independent experiments.

* Significantly different from hDOR-$G_{i1}\alpha$ (Ile^{351}), $P < 0.05$.

*** Significantly different from hDOR-$G_{i1}\alpha$ (Ile^{351}), $P < 0.0001$.

The turnover number for DADLE-stimulated GTP hydrolysis and K_m for GTP of basal and maximal DADLE (100 μM) stimulation are compared for the hDOR-$G_{i1}\alpha$ (Ile^{351}), -$G_{i1}\alpha$ (Gly^{351}) and -$G_{o1}\alpha$ (Ile^{351}) fusion proteins in Table 3.3. The rank order of GTP hydrolysis is the highest in the hDOR-$G_{i1}\alpha$ (Ile^{351}) and the lowest in -$G_{o1}\alpha$ (Ile^{351}) fusion proteins, which demonstrates that GTP hydrolysis for $G_{i1}\alpha$ by hDOR is faster than that for $G_{o1}\alpha$. The K_m for GTP of basal and DADLE-stimulation was not different but minor differences were seen with the different fusion protein mutants. As previously noted for the α_{2A}-adrenoceptor substitution of Ile^{351} by Gly substantially reduced the agonist-induced turnover number (Jackson *et al.*, 1999).

Characterisation of the hDOR-Gi/Go fuslon proteins stably expressed in HEK293 cells

I. Setting up of stable cell lines

Stable cell lines of hDOR-$G_{i1}\alpha$ (Ile^{351}) and hDOR-$G_{o1}\alpha$ (Ile^{351}) fusion proteins were set up using antibiotic (geneticin sulphate, 1mg/ml) as selection. A number of the selected clones expressing hDOR-$G_{i1}\alpha$ (Ile^{351}) and -$G_{o1}\alpha$ (Ile^{351}) fusion proteins are shown in **Figures 3.13A and 3.13B.** The specific binding of a single, near saturating, concentration of [^{3}H] naltrindole and the DADLE stimulated high affinity GTPase activity of the same membranes of a number of clones of these stable cell lines were correlated. **(Figures 3.14A, 3.14B).** In general, clones expressing higher levels of hDOR-$G_{o1}\alpha$ (Ile^{351}) were identified but these gave lower DADLE stimulated GTPase activity per mol of fusion protein that those expressing hDOR-$G_{i1}\alpha$ (Ile^{351}).

II. Analysis using [^{3}H] naltrindole binding studies

Similar experiments to these reported earlier on transient transfections were repeated on cell lines stably expressing the fusion proteins. Clone no.6 of the hDOR-$G_{i1}\alpha$ (Ile^{351}) fusion protein and no.9 of the hDOR-$G_{o1}\alpha$ (Ile^{351}) fusion protein were selected and expanded with maintenance of antibiotic selection (geneticin sulphate, 700 μg/ml). The K_d and B_{max} of both clones were assessed by [^{3}H] naltrindole binding experiments with nonspecific binding defined in the presence of 100 μM naloxone. The level of expression in clones no.6 and no.9 slightly increased with passage. It was thus difficult to estimate the exact B_{max} of the clones. The B_{max} of clone no.6 was between 3-6 pmol/mg of protein and that of clone no.9 between 5-10 pmol/mg of protein. The K_d of clone no.6 for [^{3}H] naltrindole was 0.47 ± 0.04 nM (mean ± S.E.M, n=3) and that of clone no.9 was 0.89 ± 0.35 nM (mean ± S.E.M, n=3, P = 0.11). These values were not significantly different. **Figures 3.15A and 3.16A** are typical examples of saturation experiments for the clones. Scatchard plots were generated **(Figures 3.15B, 3.16B)** to estimate K_d and B_{max}.

III. Glycosylation and deglycosylation of the hDOR-$G_{o1}\alpha$ (Ile^{351}) fusion protein

Glycosylation of plasma membrane proteins is a common post-translational modification that is thought to be important for protein folding in internal organelles and in some cases for membrane targeting and function. The two common classes of glycosylation are those containing N-glycosidically linked oligosaccharide chains attached to asparagine residues and O-glycosidically linked oligosaccharide chains linked to serine or threonine residues in the polypeptide (Lennarz, 1983). Cell membranes from stable cell lines expressing the hDOR-$G_{o1}\alpha$ (Ile^{351}) fusion protein (5-10 pmol/mg of protein) were prepared and their protein resolved by SDS-PAGE followed by immunoblotting. Antiserum ON1, specific for the N-terminal hexadecapeptide of isoforms of $G_{o1}\alpha$ and $G_{o2}\alpha$ was used. It detected three strong bands but not in mock (pcDNA3.1) transfected cells (Lane1) **(Figure 3.17A),** which may represent differential glycosylation (Mr 75-95 kDa). During optimisation of this reaction, rat brain cortex Go, (a 39kDa polypeptide) was used as a positive control (data not shown). NGF (N-Glycosidase F) was used for structural analysis of the presence of N-linked carbohydrate. After the deglycosylation reaction, the protein was analysed on 10% SDS-PAGE, where a shift to a lower apparent molecular mass (~75kDa) was observed, consistant with the removal of aspargine-linked glycan chains **(Figure 3.17B).**

IV. Functional analysis of agonist regulated high affinity GTPase activity

Prior PTx treated (25ng/ml, 16h) cell membranes were prepared and the potency for DADLE to activate the fusion proteins was monitored in high affinity GTPase activity assays with a range of concentrations of DADLE. The comparison of pEC_{50} values between hDOR-$G_{i1}\alpha$ (Ile^{351}) and -$G_{o1}\alpha$ (Ile^{351}) fusion proteins is shown **(Figures 3.18A, 3.18B).** The pEC_{50} for clone no.6 was 7.50 ± 0.18 (mean ± S.E.M, n=3) and that of clone no.9 was 7.32 ± 0.23 (mean ± S.E.M, n=3). These values were not significantly different (P= 0.35). Previously, the pEC_{50} values following transient expression of both constructs were shown to be similar **(Table 3.1).**

Table 3.4. Comparison of high affinity GTPase activity by the hDOR-$G_{i1}\alpha$ (Ile^{351}) and hDOR-$G_{o1}\alpha$ (Ile^{351}) fusion proteins.

High affinity GTPase activity (pmol/mg/min)	**hDOR-$G_{i1}\alpha$ (Ile^{351})**	**hDOR-$G_{o1}\alpha$ (Ile^{351})**
Basal (+PTx)	20.34 ± 1.05	16.24 ± 2.67
DADLE (10^{-4} M) (+PTx)	62.10 ± 6.12	28.99 ± 3.92

All the data represent means ± S.E.M from three independent experiments.

V. Kinetics of DADLE-stimulated high affinity GTPase activities and measurement of GTP turnover number

When DADLE (100 μM)-stimulated GTPase activity was monitored at a wide range of GTP concentrations on membranes prepared from prior PTx treated clones (no.6 and no.9), the effect of the agonist was predominantly to increase V_{max} of the GTPase activity with only a minor effect on the estimated K_m for GTP **(Figures 3.19A, 3.20A)**. Eadie-Hofstee plots were generated to measure V_{max}, K_m and turnover number (min^{-1}) from direct GTP saturation graphs **(Figures 3.19B, 3.20B).** The K_m values of basal and DADLE (100 μM)-stimulated GTPase for the hDOR-$G_{i1}\alpha$ (Ile^{351}) fusion protein were 0.53 ± 0.07 μM (mean ± S.E.M, n=3) and 0.50 ± 0.07 μM (mean ± S.E.M, n=3) respectively. In comparison, the K_m values of basal and DADLE (100 μ M)-stimulated GTPase for the hDOR-$G_{o1}\alpha$ (Ile^{351}) fusion protein were 0.66 ± 0.09 μM (mean ± S.E.M, n=3) and 0.47 ± 0.12 μM (mean ± S.E.M, n=3) respectively. Parallel saturation binding experiments with [^{3}H] naltrindole on the same membranes measured expression levels of the fusion proteins in both clones and thus allowed calculation of the DADLE-induced turnover number for GTP by the hDOR-$G_{i1}\alpha$ (Ile^{351}) construct as 8.07 ± 0.35 min^{-1} (mean ± S.E.M, n=3). In comparison, the hDOR-$G_{o1}\alpha$ (Ile^{351}) fusion protein produced a DADLE-stimulated GTPase turnover number of only 2.07 ± 0.72 min^{-1} (mean ± S.E.M, n=3). These values were significantly different ($P < 0.01$).

V. Sensitivity to pertussis toxin

In cells stably expressing the hDOR-$G_{i1}\alpha$ (Ile^{351}) fusion protein (clone no.6), PTx treatment (25ng/ml, 16h) was performed to see if PTx affected the signalling of DADLE **(Figure 3.21)**. The calculated pEC_{50} values for untreated and treated membranes were similar, which demonstrated that PTx treatment does not affect the signalling of the hDOR-$G_{i1}\alpha$ (Ile^{351}) fusion protein. In other words, the GTPase activity following PTx treatment of these membranes is due entirely to activation of the linked $G_{i1}\alpha$ and there appears to be little or no activation of endogenous Gi-like proteins.

VI. Measuring downstream effects: adenylyl cyclase activity

To compare the regulation of a downstream effect of receptor occupancy on both stably expressed hDOR-$G_{i1}\alpha$ (Ile^{351}) (clone no.6) and -$G_{o1}\alpha$ (Ile^{351}) (clone no.9) fusion proteins, AC activity and its regulation by DADLE was measured. Intact cell AC assays were performed essentially as described by Wong, (1994) and Merkouris *et al.*, (1997). This whole cell AC assay is based on the use of [^{3}H] adenine which labels the intracellular adenine nucleotide pool and measurement of subsequent conversion of [^{3}H] ATP to [^{3}H] cAMP on AC stimulation. The [^{3}H] cAMP thus produced is separated from [^{3}H] adenine and [^{3}H] ATP by a two-step column method (Salomon *et al.,* 1979). Cells of the two clones were split into 12 well plates and grow in geneticin containing medium until about 80% confluence. One day before the assay, plates were incubated overnight with [^{3}H] adenine at 1 μCi per well and PTx (25ng/ml) was added at the same time. HEPES buffered DMEM medium containing increasing concentrations of DADLE was then added and the cells incubated for 30 min at 37 °C. The reaction was terminated on ice by addition of 1ml of stop solution to extract [^{3}H] adenine nucleotides. Harvested cell extract was loaded to separate cAMP from other radiolabelled nucleotides (adenosine, AMP, ADP etc) by Dowex and then Alumina chromatography. Finally, [^{3}H] cAMP was eluted from the alumina with 0.1M imidazole (pH 7.3) and quantified.

Initially, forskolin (50μM)-stimulated AC activity of cells stably expressing the isolated hDOR was assessed to pre-check the inhibition of AC activity upon addition of increasing concentrations of DADLE. With PTx treatment, the effect of DADLE on AC activity was fully attenuated. This confirms that the hDOR signals inhibition of

AC via Gi-like G proteins (data not shown). Using the two fusion protein expressing clones, the pEC_{50} value for DADLE to inhibit forskolin stimulated AC activity was 10.06 ± 0.38 in untreated cells (mean ± S.E.M, n=3) and 9.58 ± 0.14 (mean ± S.E.M, n=3) in PTx treated cells of the hDOR-$G_{i1}\alpha$ (Ile^{351}) fusion protein (clone no.6). The maximal inhibition of forskolin stimulation was 75-85%. These values were not significantly different (P = 0.11). By comparison, the pEC_{50} for DADLE inhibition of forskolin stimulated AC activity for the hDOR-$G_{o1}\alpha$ (Ile^{351}) fusion protein = 9.84 ± 0.36 in untreated (mean ± S.E.M, n=3) and = 9.32 ± 0.08 for PTx treated cells (mean ± S.E.M, n=3) was monitored for -$G_{o1}\alpha$ (Ile^{351}) 65-75% of inhibition was obtained. These values were not significantly different (P = 0.08). **Figures 3.22A and 3.22B** are typical examples of experiments on each clone. First of all, these results demonstrate that forskolin stimulated AC activity could be inhibited through both $G_{i1}\alpha$ and $G_{o1}\alpha$ linked to the agonist-occupied hDOR. Secondly, PTx treatment did not affect the regulation of AC by either of the two constructs. In other words, this is due to activation of the linked $G_{i1}\alpha/G_{o1}\alpha$ rather than via activation of endogenous Gi-like proteins.

Table 3.5. Comparison of signalling by the hDOR-$G_{i1}\alpha$ (Ile^{351}) and hDOR-$G_{o1}\alpha$ (Ile^{351}) fusion proteins.

	hDOR-$G_{i1}\alpha$ (Ile^{351})	hDOR-$G_{o1}\alpha$ (Ile^{351})
K_d for [^{3}H] naltrindole (nM)	0.47 ± 0.04	0.88 ± 0.35
pEC_{50} for DADLE (high affinity GTPase activity)	7.50 ± 0.18	7.32 ± 0.23
GTP turnover number (min^{-1}) (+DADLE)	8.07 ± 0.35	2.07 ± 0.72**
K_m GTP (basal) (μM)	0.53 ± 0.07	0.66 ± 0.09
K_m GTP (+DADLE) (μM)	0.50 ± 0.08	0.47 ± 0.12
pEC_{50} for DADLE (nM) (-PTx: AC activity)	10.06 ± 0.38	9.84 ± 0.36
pEC_{50} for DADLE (nM) (+PTx: AC activity)	9.58 ± 0.14	9.32 ± 0.08

All the data represent means ± S.E.M from three independent experiments.

** Significantly different from hDOR-$G_{i1}\alpha$ (Ile^{351}), $P < 0.01$.

VII. Characterisation of transiently expressed hMOR-$G_{i1}\alpha$ (Ile^{351}) fusion protein

To compare the signalling of the hDOR and hMOR, which are highly homologous (Knapp *et al.*, 1995: Law *et al.*, 2000), a similar strategy as for hDOR was used to a generate hMOR-1-$G_{i1}\alpha$ (Ile^{351}) fusion protein. This was used to explore the relative capacity of hMOR-1 and hDOR to activate $G_{i1}\alpha$. I was given the hMOR-1-$G_{i1}\alpha$ (Ile^{351}) fusion protein which was constructed by Dr. Dominique Massotte, (Departement des recepteurs et proteines membranaires, (CNRS UPR 9050), Ecole Superieure de Biotechnologie de Strasbourg, Illkirch-Graffenstaden, France). The hMOR-1 isoform (Pan *et al.*, 1999) of the hMOR (Wang *et al.*, 1994) was used in these studies. The cDNA of hMOR-1 was amplified by PCR in order to shorten the 5′ end by introducing a *KpnI* site. At the same time, the stop codon was removed and another *KpnI* site was introduced. The sequence amplified by PCR was digested with *KpnI* and purified on an agarose gel. This was ligated into the *KpnI* site of pcDNA3 containing $G_{i1}\alpha$ (Ile^{351}) **(Figure 3.23).** This fusion protein was fully sequenced prior to use.

Transient transfection of the construct into HEK293T cells was carried using Lipofectamine™ as transfection reagent for the hDOR fusion proteins. This gave a reasonable expression level (0.8-2 pmol/mg of protein), monitored by the appearance of specific binding sites for [^{3}H] diprenorphine, which is a general antagonist for all the opioid receptors. Saturation binding studies using [^{3}H] diprenorphine indicated this ligand was bound with high affinity. Membranes expressing this fusion protein

were prepared and its level of expression (B_{max}) and K_d for [^{3}H] diprenorphine measured. **(Figures 3.24A, 3.24B).** The K_d for [^{3}H] diprenorphine at hMOR-$G_{i1}\alpha$ (Ile ^{351}) after PTx treatment (25ng/ml, 16h) of cells was 0.44 ± 0.18 nM (mean ± S.E.M, n=3).

Following transient expression and prior PTx treatment (25ng/ml, 16h) of cells expressing the hMOR-$G_{i1}\alpha$ (Ile^{351}) fusion protein, membranes were prepared and the effect of varying concentrations of DADLE was monitored. Stimulation of GTPase activity was produced in a concentration-dependent manner with pEC_{50} = 6.6 ± 0.2 (mean ± S.E.M, n=3) **(Figure 3.25).** This value was significantly different ($P < 0.05$) from these of hDOR-$G_{i1}\alpha$ (Ile^{351}) and hDOR-$G_{o1}\alpha$ (Ile^{351}) **(Table 3.2).**

Basal and 100 μM DADLE-stimulated GTPase activity was then measured at various GTP concentrations. The effect of the agonist was predominantly to increase V_{max} of the GTPase activity with only a minor effect on the estimated K_m **(Figures 3.26A, 3.26B).** B_{max} values for receptor was assessed on the same membranes and thus the GTPase activities were divided by expression level to calculate DADLE-induced turnover number for GTP as 10.1 ± 1.0 min^{-1} **(Table 3.5),** equivalent to that produced by the hDOR-$G_{i1}\alpha$ (Ile^{351}) fusion protein. Therefore, these two opioid receptor subtypes were equally effective in activating $G_{i1}\alpha$.

Table 3.6. Characterisation of the hMOR-$G_{i1}\alpha$ (Ile^{351}) fusion protein

	hMOR-$G_{i1}\alpha$ (Ile^{351})
K_d for [^{3}H] diprenorphine (nM)	0.44 ± 0.18
pEC_{50} for DADLE	6.6 ± 0.2*
(high affinity GTPase activity)	
GTP turnover number (min^{-1})	10.1 ± 1.0
(+DADLE)	
K_m GTP	0.69 ± 0.08
(basal) (μM)	
K_m GTP	0.75 ± 0.08
(+DADLE) (μM)	

All the data represent means ± S.E.M from three independent experiments.

***Significantly different from hDOR-$G_{i1}\alpha$ (Ile^{351}) and hDOR-$G_{o1}\alpha$ (Ile^{351}), $P < 0.05$.**

Discussion (Chapter3)

I. Using the fusion protein strategy to understand the regulation of G protein activation by the human δ-opioid receptor

In this current study I have examined the regulation of activation of the G proteins $G_{i1}\alpha$ and $G_{o1}\alpha$ by the hDOR using a fusion protein strategy. Since the cloning of opioid receptors, the individual pharmacological and biochemical profiles of the μ, δ and κ-opioid receptors have been better defined. However, there are many aspects of opioid receptor biology that still remain poorly understood. A major signalling pathway of the hDOR is to inhibit cAMP production. This is transduced by Gi-Go family G proteins as PTx blocks opioid effects (Law *et al.*, 1985b) The specific G proteins that mediate δ-selective effects on cAMP production have been characterised through the use of IgG fractions specific for individual G protein α subunits (McKenzie and Milligan, 1990). It was found that DADLE-mediated inhibition of forskolin-stimulated cAMP production was $G_{i2}\alpha$-dependent in NG-108-15 cells. Using a similar approach, antipeptide anti-G protein antisera against $G_i\alpha$ and $G_o\alpha$ were used to examine the interaction of rat brain cortical opioid receptors with the G protein, Go (Georgoussi *et al.*, 1993; Georgoussi *et al.*, 1995). Fusion proteins derive from a single open reading frame (ORF), which allow expression of a single polypeptide containing the sequences of both a GPCR and G protein. The benefits of these strategies have recently been extensively reviewed (Seifert *et al.*, 1999; Milligan, 2000). However, because the fusion of a receptor C-terminus to

the Gα N–terminus is artificial, it may be a concern that the fusion substantially alters the properties of receptor and G protein coupling. For example, in Rat1 fibroblasts, an α_{2A}-adrenoreceptor-$G_{i1}\alpha$ fusion protein does not only activate the fused $G_{i1}\alpha$ partner but also endogenous G proteins (Burt *et al.*, 1998) and this also results in loss of Gs coupling of the α_{2A}-adrenoreceptor (Sautel and Milligan, 1998). However, comparison of the coupling of human formyl peptide receptor to $G_{i2}\alpha$ in the fused and non-fused state by visualising activated G proteins by photoaffinity labelling showed that there were only minor differences in FPR-$G_{i2}\alpha$ coupling between the fused and non-fused states (Wenzel-Seifert *et al.*, 1999). The strongest properties of these fusion proteins are first to have defined 1:1 stoichiometry of the partners, which can provide highly efficient receptor-G protein coupling (Wenzel-Seifert *et al.*, 1999). Secondly, it has been shown that this strategy provides a useful tool for pharmacological examination of the mechanism of activation of G proteins by an agonist-occupied receptor, particularly, agonist-receptor efficacy. This can be quantified with high affinity GTPase studies and [^{35}S] GTPγS binding studies. In addition, investigation of receptor-PTx-resistant $G_i\alpha$ and $G_o\alpha$ fusion proteins has shown agonist-stimulated GTP hydrolysis, which was unaffected by prior PTx treatment; thus demonstrating the effect to occur via the G protein linked to the receptor (Wise *et al.*, 1997b; Jackson *et al.*, 1999). The extreme C-terminus of G protein α subunits is known to be an important contact site for GPCRs and ADP-ribosylation by PTx of the Cys (C^{351}) located four amino acids from the C-terminus abolishes interaction with GPCRs. In early studies, a single alteration introduced by mutating this PTx-sensitive Cys of G_{i1} resulted in a method to measure interaction efficiency between GPCRs and G proteins in terms of GTP hydrolysis (Bahia

et al., 1998). Based on the above previous studies, the construction of cDNAs encoding fusion proteins between the hDOR and its cognate G proteins, $G_{i1}\alpha/G_{o1}\alpha$ was performed and successfully used in the current study. This construction provided problems. Thus, the subcloning strategy was approached in a stepwise fashion. The last 157bps of a hDOR cDNA was first amplified by PCR to generate a 5′*NotI* and a new 3′*BamHI* restriction site by removing the stop codon. The remaining segment of hDORs was digested with 5′*BamHI* and 3′*NotI*. 5′*BamHI* and 3′*EcoRI* restriction site were added to $G_{i1}\alpha$ (wild type) by PCR followed removing of the ATG start codon. Finally, the three different fragments were ligated into pcDNA3.1 in a single four-fragment ligation reaction **(Figures 3.1A, 3.2A).** However, because the hDOR now had *BamHI* sites at both 5′ and 3′ ends, the orientation for ligation is unsure. Figure 3.2A (first clone) shows an example of a product ligated incorrectly. Initially a combination of *SacII* and *EcoRI* was tried to recover $G_{i1}\alpha$. This caused a problem because of the new generation of a *SacII* site in the region joining the C-terminal of the receptor and N-terminal of the Gi protein. Another unique restriction pairing - *EcoNI* and *EcoRI* - allowed recovery of a segment of $G_{i1}\alpha$ (Xaa^{351}) mutants (Ile/Leu/Phe/Val/Ser/Ala/Arg/Gly) and their replacement for the equivalent section of the hDOR-$G_{i1}\alpha$ (wild type) fusion protein **(Figures 3.1B, 3.2B).** A PTx-resistant hDOR-$G_{i1}\alpha$ (Pro^{351}) was also constructed in the same manner, but it was not used further because of the unique aliphatic-like structure of the cyclic imino amino acid. A proline residue at this position in G_{i1} might be expected to disrupt interaction with the hDOR. The *unc* mutation of Gsα, which results from an Arg-Pro alteration 6 amino acid from the C-terminus, is known to prevent productive interactions with GPCRs (Sullivan *et al.*, 1987). In a similar way, a hDOR-

$G_{o1}\alpha$ (wild type) fusion protein was also constructed. Here the initial 120bps from the original hDOR in pcDNA4 was digested with *KpnI* and *BssHII* and the remaining segment of 1020bps from hDOR-$G_{i1}\alpha$ (wild type) was digested with *BssHII* and *BamHI* separately. The ORF of $G_{o1}\alpha$ (1065bps) had 5′*BglII* and 3′*XbaI* sites introduced by PCR. The three different fragments were then ligated into pcDNA3.1 by using the compatibility of *BamHI* and *BglII* **(Figures 3.3A, 3.4A).** PTx-resistant hDOR-$G_{o1}\alpha$ (Xaa^{351}) mutants (Ile/Leu/Gly) were generated by using the unique restriction sites- *ClaI* and the second last polylinker in pcDNA3.1, *ApaI* (due to several *XbaI* sites in $G_{o1}\alpha$) from previously constructed $G_{o1}\alpha$ (Xaa^{351}) mutants (Ile/Leu/Gly) and replacing the equivalent segment of hDOR-$G_{o1}\alpha$ (wild type) **(Figures 3.3B, 3.4B).**

II. Successful transient and stable transfections

All the fusion proteins could be expressed successfully in transient transfection using HEK293 cells and Lipofectamine^{TM} transfection reagent as assessed by [^{3}H] naltrindole binding studies **(Figures 3.5A, 3.5B).** Also, immunological detection demonstrated the expression of all the fusion proteins, which showed bands of appropriate size, which were not in mock (pcDNA 3.1) transfected cells **(Figures 3.6A, 3.6B).** One of the benefits of fusion proteins, is they have a 1:1 stoichiometry of expression of GPCR and G protein. For this reason direct saturation ligand binding studies using [^{3}H] antagonist allowed measurement of the level of expression of the G protein as well as the GPCR. This is difficult to quantify with independently co-expressed GPCRs and G proteins. Initially, all the fusion proteins (hDOR-Gi/Go fusion proteins) were transiently transfected and receptor expression measured by single-concentration [^{3}H] naltrindole-binding assay. With the same membranes, high affinity GTPase activity was measured in response to a maximal concentration (100 μM) of DADLE. Three different fusion protein mutants -hDOR-$G_{i1}\alpha$ (Ile^{351}), -$G_{i1}\alpha$ (Gly^{351}), -$G_{o1}\alpha$ (Ile^{351}) were selected to compare the effect of point mutation and G protein identification on signal initiation. It was previously demonstrated that the hydrophobicity of $residue^{351}$ of the G protein determines the extent of activation by the α_{2A}-adrenoceptor (Bahia *et al.*, 1998). Conversion of binding data to Scatchard plots showed the ligand affinity for [^{3}H] naltrindole for the transiently expressed hDOR-$G_{i1}\alpha$ (Ile^{351}) and -$G_{i1}\alpha$ (Gly^{351}) fusion proteins **(Figures 3.7A, 3.7B, 3.8A, 3.8B).** According to my results, the K_d for [^{3}H] naltrindole for the hDOR-$G_{i1}\alpha$ (Ile^{351}) fusion protein (0.77

± 0.12 nM, mean ± S.E.M, n=3) was about 6 times higher than for the hDOR-$G_{i1}\alpha$ (Gly^{351}) fusion protein (0.13 ± 0.02 nM, mean ± S.E.M, n=3) (P< 0.001). It has been considered that naltrindole is a neutral δ-antagonist and it can prevent the activity of an inverse agonist (Neilan *et al.*, 1999). One possibility to explain these different K_d values for the same receptor is that naltrindole behaves as an inverse agonist on the hDOR-$G_{i1}\alpha$ (Ile^{351}) fusion protein, which may have greater constitutive activity due to the mutation to the strong hydrophobic, aliphatic amino acid, Ile, but not on the Gly^{351} residue containing fusion protein. Previously spiperone was shown to act as an inverse agonist for $5HT_{1A}$-$G_{i1}\alpha$ (Ile^{351}) but not for $5HT_{1A}$-$G_{i1}\alpha$ (Gly^{351}) (Kellet *et al.*, 1999). In other experiments which chapter 4 will introduce the effect of GDP on the binding of the agonist [^{3}H] DADLE was dependent upon the identity of $residue^{351}$ of the G protein and GDP increased the binding of [^{3}H] naltrindole to hDOR-$G_{i1}\alpha$ (Ile^{351}). In chapter 4, more explanation will introduce the stability of ternary complexes of two different mutant fusion proteins regarding association and dissociation kinetics of agonist binding. Following stable transfection, comparisons of the K_d for [^{3}H] naltrindole between hDOR-$G_{i1}\alpha$ (Ile^{351}) and -$G_{o1}\alpha$ (Ile^{351}) was obtained **(Table 3.4, Figures 3.15A, 3.15B, 3.16A, 3.16B).** The K_d was not different by 0.47 ± 0.04 nM (mean ± S.E.M, n=3) for the hDOR-$G_{i1}\alpha$ (Ile^{351}) and by 0.88 ± 0.35 nM (mean ± S.E.M, n=3) for -$G_{o1}\alpha$ (Ile^{351}) fusion proteins after PTx treatment (P = 0.11).

III. Comparison of agonist potency to activate $G_{i1}\alpha$ and $G_{o1}\alpha$

GPCR-G protein fusion proteins have been useful tools for pharmacological analysis of agonist efficacy (Wise *et al.,* 1997). Because they have a clear 1:1 stoichiometry of expression of the two protein partners, these fusion proteins have overcome the problem of how estimates of ligand efficacy alter with varying ratios of co-expression of GPCRs and G proteins. Ligand regulation of guanine nucleotide exchange on the fused G protein provides the most appropriate means to utilise the unique features of GPCR-G protein fusion proteins (Milligan *et al.*, 2000). 'Agonist efficacy' is defined as a measure of the ability of an agonist bound receptor to stimulate a measurable response in a cell or tissue (Quock *et al.*, 1999). Previously, PTx-resistant fusion protein mutants have been constructed with the Gi-family of PTx sensitive G proteins containing mutation of the cysteine side chain four amino acids (Cys^{351}) from the C-terminus of the α-subunits of Gi and Go (Jackson *et al.*, 1999; Wise *et al.*, 1999; Dupuis *et al.,* 1999). With the same approach, PTx-resistant hDOR-$G_{i1}\alpha$ (Xaa^{351})/$G_{o1}\alpha$ (Xaa^{351}) fusion proteins mutants were constructed to monitor the differential capacities of ligands to activate Gi and Go. The agonist DADLE was used to compare potency for two selective hDOR-fusion proteins -hDOR-$G_{i1}\alpha$ (Ile^{351}) and -$G_{o1}\alpha$ (Ile^{351})- following transient expression. DADLE had $pEC_{50} = 7.1 \pm 0.1$ for -$G_{i1}\alpha$ (Ile^{351}) and $pEC_{50} = 7.2 \pm 0.3$ for -$G_{o1}\alpha$ (Ile^{351}) respectively (means ± S.E.M, n=3). Equivalent experiments were performed on two stably expressing clones of hDOR-$G_{i1}\alpha$ (Ile^{351}) and -$G_{o1}\alpha$ (Ile^{351}) with $pEC_{50} = 7.5 \pm 0.18$ for -$G_{i1}\alpha$ (Ile^{351}) and $pEC_{50} = 7.32 \pm 0.23$ for -$G_{o1}\alpha$ (Ile^{351}) (means ±

S.E.M, n=3). Summarising the above results, the potency for DADLE was similar for both transient and stable expression and for $-G_{i1}$ and $-G_{o1}$ as well **(Figures 3.9A, 3.9C, 3.18A, 3.18B).** The maximum level of DADLE-stimulation of the GTPase activity, E_{max}, varied with levels of fusion protein expression. It was calculated that stimulation of Gi is much higher than that for Go of the hDOR. This will be further explained later related to the rate of GTP hydrolysis (Kcat). It is clear that GPCR-Gα fusion proteins can interact with βγ-subunits (Seifert *et al.*, 1998; Wise *et al.*, 1997). Regarding this, there still remains question about the role of βγ-subunits. In the earliest studies on the β_2AR-Gsα fusion protein constructed by Bertin *et al*, (1994) ADP-ribosylation of Gsα by cholera toxin (CTx) was dependent on the presence of βγ-subunits. However, in Sf9 insect membranes expressing β_2AR-GsαL, mammalian $\beta_1\gamma_2$-complex was without effect (Seifert *et al.*, 1998), whereas in COS cell membranes expressing α_{2A}AR-G_{i1}α (Gly ^{351}), the GTPase activity was increased by co-expression of the $\beta_1\gamma_2$ complex (Wise *et al.*, 1997). For this reason, the effect of βγ-complex remains to be further investigated for the hDOR fusion proteins. Secondly, only DADLE was used to examine the possible differential agonist activation of Gi and Go of the hDOR. Thus the effects of other ligands requires to be analysed.

IV. Comparison GTP turnover of $G_{i1}\alpha$ and $G_{o1}\alpha$ by the human δ-opioid receptor

One attraction of the fusion protein strategy which encodes the functions of both proteins in the same polypeptide has been the ability to activate guanine nucleotide exchange (i.e. GTPγS binding) and hydrolysis (GTPase activity) by the G protein element of the fusion (Wise *et al.*, 1997; Carr *et al.*, 1998; Kellet *et al.*, 1999). For example, at a maximally effective concentration of 5-HT, each of the 5-HT_{1A} receptor $G_{i1}\alpha$ fusion proteins studied caused a large stimulation of membrane GTPase activity (Kellet *et al.*, 1999). In studies of a α_{2A}AR-$G_{i1}\alpha$ (Gly^{351}) fusion protein transiently expressed in COS cells, the agonist UK14304 increased V_{max} of the fusion protein as a GTPase with a GTP turnover number of 3 min^{-1} (Wise *et al.*, 1997). Although Gs-coupled GPCRs often have been mentioned as being difficult to record agonist-stimulated GTPase activity, a FLAG-tagged human IP prostanoid (FhIPR)-Gsα fusion protein, stably expressed in HEK293 cells could produce a robust iloprost-mediated GTPase activity. Cell membranes expressing the hDOR fusion proteins [hDOR-$G_{i1}\alpha$ (Ile^{351}) and -$G_{o1}\alpha$ (Ile^{351})] both transiently and stably were assayed for basal and 100 μM DADLE-stimulated GTPase activity with increasing concentrations of GTP. The effect of DADLE was to significantly increase V_{max} of GTPase activity with only a minor effect on the estimated K_m for GTP. The direct plots of Michaelis Menten kinetics and Eadie-Hofstee transformation were produced to obtain V_{max} for basal and agonist stimulation, K_m for GTP and turnover number for cells expressing hDOR-$G_{i1}\alpha$ (Ile^{351}) and -$G_{o1}\alpha$ (Ile^{351}) **(Figures 3.10A, 3.10B, 3.12A, 3.12B, 3.19A, 3.19B, 3.20A, 3.20B,**

Tables 3.3, 3.4). Summarising the two different expression systems and constructs, it was shown that K_m for hDOR-$G_{i1}\alpha$ (Ile^{351}) was lower than that for -$G_{o1}\alpha$ (Ile^{351}) and the turnover number for DADLE of the hDOR-$G_{i1}\alpha$ (Ile^{351}) was 3-4 times higher than that of -$G_{o1}\alpha$ (Ile^{351}). As GDP release is the rate limiting step of agonist-induced G protein activation and deactivation (Gilman, 1987), the greater hydrolysis rate shows that the receptor was more efficient at activating G_{i1} than G_{o1}.

V. Comparison of agonist potency to regulate AC activity via the hDOR fusion proteins

Fusion proteins have been shown to activate AC more efficiently than the isolated GPCR and G protein expressed as separate proteins. The β_2AR-Gsα fusion protein constructed by Bertin *et al,* (1994) demonstrated the importance of physical proximity of GPCR and Gα for their efficient coupling compared with the non-fused state (Bertin *et al.*, 1994). The hDOR inhibits intracellular cAMP levels via Gi-Go proteins. In cells expressing the isolated hDOR, DADLE mediated inhibition of forskolin-amplified AC activity, which was obliterated after PTx treatment of the cells (data not shown).

AC inhibition by two stable expressed fusion constructs (clone no.6 and 9 of each) was shown to give a robust inhibition of forskolin stimulated cAMP production, in presence of DADLE **(80-85% for -$G_{i1}\alpha$: 65-75% for -$G_{o1}\alpha$),** which was stronger than for the isolated receptor. The pEC_{50} values for DADLE on both stably expressing the hDOR-$G_{i1}\alpha$ (Ile^{351}) and -$G_{o1}\alpha$ (Ile^{351}) fusion proteins were measured and PTx treatment did not affect the potency of DADLE or level of inhibition of AC activity **(Tables 3.4, Figures 3.22A, 3.22B).** Moreover, the level of inhibition for hDOR-$G_{i1}\alpha$ (Ile^{351}) fusion proteins was much stronger than that for -$G_{o1}\alpha$ (Ile^{351}), even though the expression level of hDOR-$G_{i1}\alpha$ (Ile^{351}) was always lower than that of -$G_{o1}\alpha$ (Ile^{351}). This demonstrated that hDOR-$G_{i1}\alpha$ (Ile^{351}) and -$G_{o1}\alpha$ (Ile^{351}) fusion proteins could directly regulate AC activity and fused $G_{o1}\alpha$ was able to inhibit AC activity as the same way as fused $G_{i1}\alpha$.

The α_{2A}AR-$G_{i1}\alpha$ (Gly^{351}) fusion protein has the capacity to activate both endogenously expressed Gi and PTx-resistant fused Gi protein in stably expressing Rat1-fibroblasts (Burt *et al.,* 1998). However the α_{2A}AR-$G_{i1}\alpha$ (Gly^{351}) fusion protein was unable to regulate secondary messengers. A possible reason is that the C-tail of α_{2A}AR (20 a.a) is significantly shorter than that of the β_2AR(84 a.a): the difference in function between the two fusions could be due to the differential length of the C-terminal tail. In cells expressing 5-HT_{1A}-$G_{i1}\alpha$ fusion proteins, 5-HT is able to produce robust AC inhibition (Kellet *et al.*, 1999). Wenzel-Seifert *et al*, (1998) reported how deletions of the C-terminal tail of the β_2AR in β_2AR-Gsα fusion proteins [β_2ARGsα_L, β_2AR(Δ26) Gsα_L, β_2AR(Δ70) Gsα_L] affected the coupling of the β_2AR to Gsα by studying GTPγS binding, GTPase activity and AC activity. Restricting the mobility of Gsα relative to the β_2AR results in a decrease of GTP hydrolysis, prolonged G protein activation and thus enhanced AC stimulation.

Opioid receptor is known to mediate MAP kinase phosphorylation. It could be very interesting to investigate and compare the regulation of MAP kinase pathways by hDOR-Gi and hDOR-Go fusion proteins. In fact, it was shown that DOR expressed in Rat1 fibroblasts was able to initiate activation of the MAP kinase cascade in a Gi-dependent manner (Burt *et al.*, 1996). M_1 muscarinic acetylcholine receptor is able to couple to Go to activate a novel PKC-dependent mitogenic signalling pathway independent activation (Biesen *et al.,* 1996). The regulation of MAP kinase by Go activated opioid receptors still remains to be investigated.

VI. Alteration of a single amino acid (Cys^{351}) in $G_{i1}\alpha$ modulates the stimulation by DADLE

It has been shown that the physiochemical properties of residue 351 in the C-tail of G protein modulate the agonist efficacy of PTx-resistant GPCR-G proteins. PTx-treatment in cells expressing these constructs prevents the cross-talk of GPCRs to endogenous Gi-proteins and made possible measurements of the comparative activity of fused C^{351} modified G proteins. The hDOR-$G_{i1}\alpha$ (Ile^{351}) and -$G_{i1}\alpha$ (Gly^{351}) fusion proteins transiently expressed have different activation of GTPase activity by agonist. The potency for DADLE at hDOR-$G_{i1}\alpha$ (Ile^{351}) (pEC_{50} = 7.1 ± 0.1, mean ± S.E.M, n=3) was shown to be a significantly higher than for –$G_{i1}\alpha$ (Gly^{351}) (pEC_{50} = 6.2 ± 0.1, mean ± S.E.M, n=3) ($P<0.005$) **(Figures 3.9A, 3.9B, Table 3.2).** DADLE-stimulated GTPase activity with increasing concentration of GTP allowed me to calculate the rate of GTP hydrolysis between different DOR constructs: the turnover number for DADLE-stimulated GTP hydrolysis on hDOR-$G_{i1}\alpha$ (Ile^{351}) was 9.5 ± 0.1 min^{-1} (mean ± S.E.M, n=3) and –$G_{i1}\alpha$ (Gly^{351}) was 4.9 ± 1.1 min^{-1} (mean ± S.E.M, n=3). The K_m (μM) for GTP respectively for basal and DADLE-stimulated GTPase activity was 0.41 ± 0.05 and 0.54 ± 0.06 respectively for hDOR-$G_{i1}\alpha$ (Ile^{351}) and 0.70 ± 0.11 and 0.73 ± 0.07 respectively for –$G_{i1}\alpha$ (Gly^{351}). **(Figures 3.10A, 3.10B, 3.11A, and 3.11B, Table 3.3).** Jackson *et al.*, (1999) demonstrated the relative intrinsic activity of agonists for PTx-resistant α_{2A} AR-$G_{i1}\alpha$ (Ile^{351})/wild type/(Gly^{351}) fusion proteins could be regulated by structural alteration in fused G proteins by mutating $residue^{351}$. This was the first demonstration that the relative intrinsic activity of a range of agonists can be modified

by a point mutation on the G protein rather than on the receptor.

VII. Pertussis toxin treatment did not affect the signalling of the hDOR fusion proteins.

In my current studies, I have examined the cross-talk of GPCR-Giα/Goα fusion proteins with endogenous G proteins by treatment with or without PTx. On cells stably expressing the hDOR-$G_{i1}\alpha$ (Ile^{351}) fusion protein, DADLE stimulated high affinity GTPase activity was monitored in presence or absence of PTx, and no difference was observed: calculated pEC_{50} value were identical **(Figure 3.21)**. Again, in cell lines stably expressing hDOR-$G_{i1}\alpha$ (Ile^{351}) and -$G_{o1}\alpha$ (Ile^{351}) fusion proteins, DADLE regulated AC activity in a concentration dependent manner. PTx treatment did not affect this either **(Table 3.4)** The same results were shown in cells stably expressing PTx-resistant 5-HT_{1A}-$G_{i1}\alpha$ fusion proteins, essentially no effect on agonist stimulated GTPase activity or AC activity was observed after PTx (Kellet *et al.*, 1999). Lack of functional access to the endogenous Gi for the receptor moiety could explain the preferential coupling with fused G protein versus endogenous. In marked contrast, the α_{2A}AR-$G_{i1}\alpha$ (Gly^{351}) fusion protein expressed in Rat1-fibroblasts interacted very efficiently with endogenous Gi-proteins as monitored by high affinity GTPase activity and by AC activity (Burt *et al.*, 1998). In conclusion, the hDOR fusion proteins signal through the G protein moiety and all measurements reflect the activation of the engineered G protein mutants.

VIII. The hMOR-1 activates $G_{i1}\alpha$ as efficiently as the hDOR

The hMOR is also coupled to its effectors predominantly via members of the Gi-family of PTx sensitive G proteins (Connor and Christie, 1999: Law *et al.*, 2000). To assess the relative capacity of the hMOR-1 and hDOR to activate $G_{i1}\alpha$, the hMOR-1 -$G_{i1}\alpha$ (Ile^{351}) fusion protein was constructed and expressed transiently in HEK293T cells **(Figure 3.23).** This construct was compared with the hDOR-$G_{i1}\alpha$ (Ile^{351}). This bound [^{3}H] diprenorphine with high affinity (K_d = 0.44 ± 0.18 nM, mean ± S.E.M, n=3) **(Figures 3.24A, 3.24B)** and high affinity GTPase activity was stimulated in the presence of varying concentrations of DADLE. The pEC_{50} value was 6.6 ± 0.2 (mean ± S.E.M, n=3) **(Figure 3.25).** However, a maximally effective concentration of DADLE stimulated hydrolysis of GTP with a turnover number as 10.1 ± 1.0 min^{-1} (mean ± S.E.M, n=3) **(Figures 3.26A, 3.26B, Table 3.5).** The results were clear-cut in that the GTP turnover number of $G_{i1}\alpha$ (Ile^{351}) following maximal occupation of the hMOR-1 by DADLE was not different from that produced by the hDOR. These results indicate that the hMOR-1 activates $G_{i1}\alpha$ as efficiently as the hDOR, at least when DADLE is employed as the common agonist ligand.

Figure 3.1. Graphic representation of construction of hDOR-$G_{i1}\alpha$ fusion proteins

A. Construction of a hDOR-$G_{i1}\alpha$ (wild type) fusion protein

A cDNA encoding hDOR and the ORF of rat $G_{i1}\alpha$ (wild type) was constructed into pcDNA (3.1), by digesting *BamHI* and *NotI* from hDOR and by removing the stop codon from hDOR and the start codon of $G_{i1}\alpha$ and adding *BamHI* sites to both to allow ligation.

B. Construction of PTx-resistant hDOR-$G_{i1}\alpha$ (Xaa^{351}) fusion proteins mutants

cDNAs encoding PTx-resistant hDOR-$G_{i1}\alpha$ (Xaa^{351}) fusion protein (I/L/F/V/S/R/A/G) mutants were constructed by recovering unique restriction fragments (*EcoNI* and *EcoRI* fragment) from modified forms of $G_{i1}\alpha$ (Bahia *et al.*, 1998). These were used to replace the equivalent fragment from hDOR-$G_{i1}\alpha$ (wild type).

C. Genetic code for mutations

All of the (Xaa^{351}) residues in hDOR-$G_{i1}\alpha$ fusion proteins were sequenced prior to use.

A

Subcloning Strategy

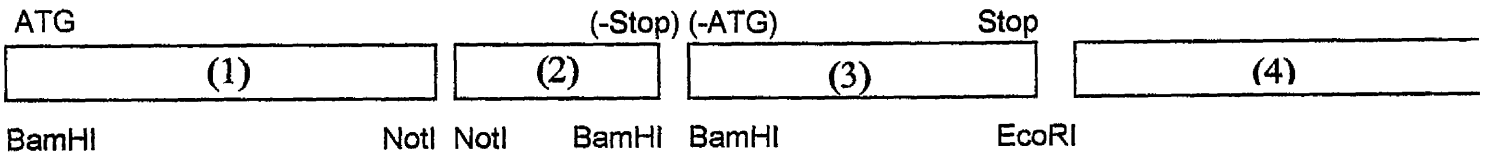

Graphic Representation :

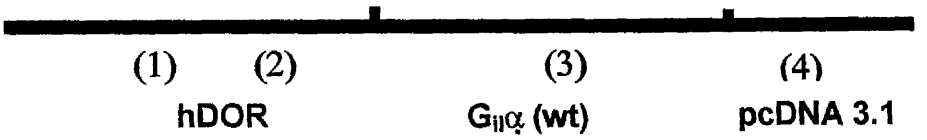

B

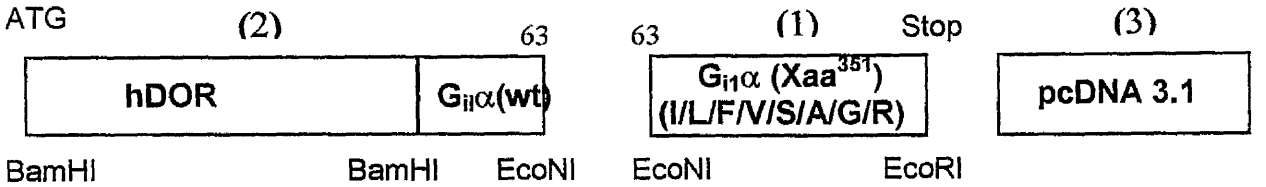

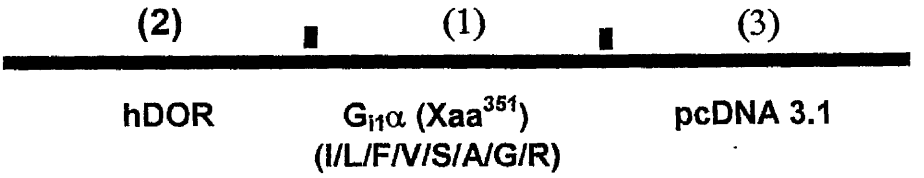

C

A.A.	Genetic code	A.A.	Genetic code
Ile	ATC	Ser	AGC
Leu	CTC	Ala	GCG
Phe	TTC	Arg	CGG
Val	GTG	Gly	GGT

Figure 3.2. DNA agarose gel analysis of hDOR-$G_{i1}\alpha$ fusion proteins

A. DNA agarose gel analysis of hDOR-$G_{i1}\alpha$ (wild type) fusion protein

DNAs from *E.coli* clones (selected clones of transformed ligated hDOR/ $G_{i1}\alpha$ mix) were digested with *BglII* and resolved in a 1% agarose gel. Clones in lane 2,3 and 4 contain digested fragments close to the approximate length of 4.6kb, 1.6kb and 1.1kb expected for the hDOR-$G_{i1}\alpha$ (wild type) fusion protein. The clone in lane1 contains a digested fragment of the wrong orientation.

B. DNA agarose gel analysis of PTx-resistant hDOR-$G_{i1}\alpha$ (Xaa^{351}) fusion protein mutants

DNAs from *E.coli* clones (selected clones of transformed ligated hDOR/ $G_{i1}\alpha$ (Xaa^{351}) fusion protein mix) were digested with *BglII* and resolved in a 1% agarose gel. This is a typical example of digested hDOR-$G_{i1}\alpha$ (Val^{351}) (lanes 1, 2, 3, 4) and -$G_{i1}\alpha$ (Ala^{351}) (lanes 5, 6, 7) fusion proteins. All the clones contain digested fragments close to the approximate lengths of 4.6 kb, 1.6 kb and 1.1 kb expected for hDOR-$G_{i1}\alpha$ (Xaa^{351}) fusion proteins.

A

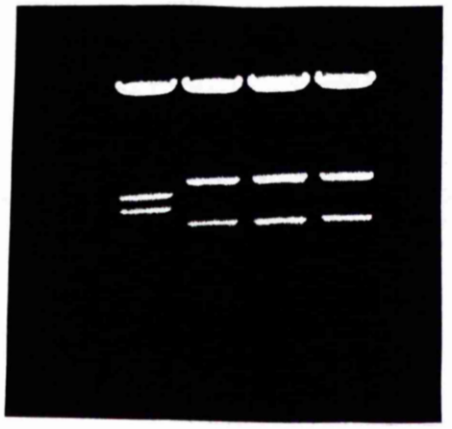

B

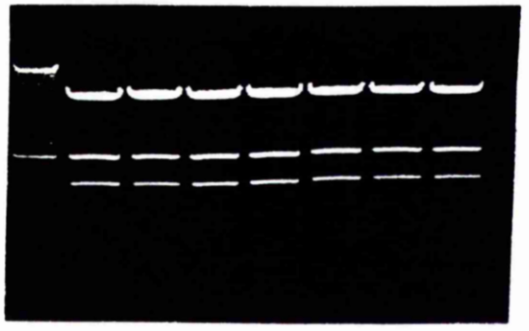

Figure 3.3. Graphic representation of construction of hDOR-$G_{o1}\alpha$ fusion proteins

A. Construction of a hDOR-$G_{o1}\alpha$ (wild type) fusion protein

A cDNA encoding hDOR and the ORF of $G_{o1}\alpha$ (wild type) was constructed into pcDNA (3.1), by digesting with *KpnI* and *BssHII* sites from hDOR in pcDNA4 and by digesting with *BssHII* and *BamHI* sites from the hDOR-$G_{i1}\alpha$ (wild type) and adding a *BglII* sites for the N-terminus of $G_{o1}\alpha$ to ligate both ends using compatibility.

B. Construction of PTx-resistant hDOR-$G_{o1}\alpha$ (Xaa^{351}) fusion protein mutants

PTx-resistant hDOR-$G_{o1}\alpha$ (Xaa^{351}) fusion protein mutants were constructed by recovering the unique *ClaI* and *ApaI* restriction fragment for mutant $Cys^{351}Xaa$ forms of $G_{o1}\alpha$. These were used to replace the equivalent fragment from hDOR-$G_{o1}\alpha$ (wild type).

C. Genetic code for mutations

All of the (Xaa^{351}) residues in hDOR-$G_{o1}\alpha$ fusion proteins were sequenced prior to use.

A

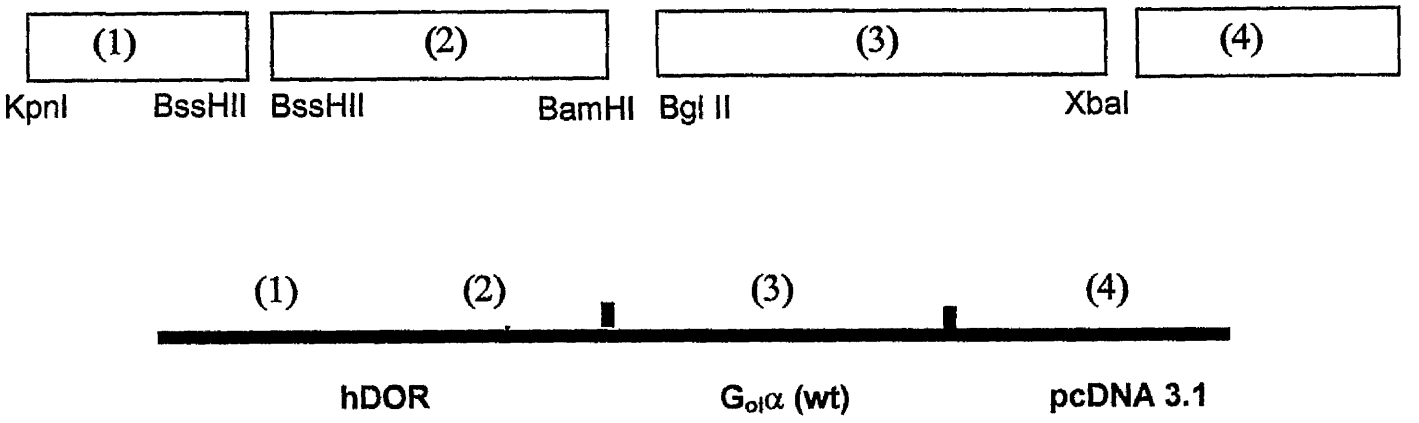

B

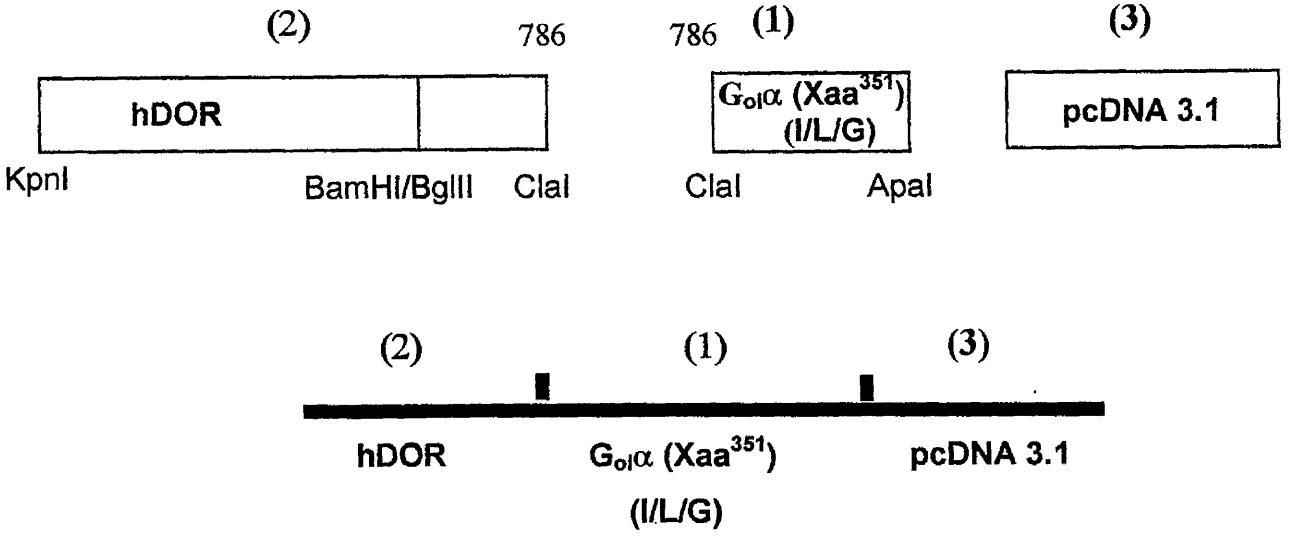

C

A.A.	Genetic code
Ile	ATC
Leu	CTC
Gly	GGG

Figure 3.4. DNA agarose gel analysis of hDOR-$G_{o1}\alpha$ fusion proteins

A. DNA agarose gel analysis of hDOR-$G_{o1}\alpha$ (wild type) fusion protein

DNAs from *E.coli* clones (selected clones of transformed ligated hDOR/ $G_{o1}\alpha$ mix) were digested with *BglII* and resolved in a 1% agarose gel. Clones in lanes 2, 3 and 6 contain digested fragments close to the approximate length of 6.0 kb and 1.6 kb expected for the hDOR–$G_{o1}\alpha$ (wild type) fusion protein. The clones in lanes 1, 4, 5, 7 contain a digested fragment of the wrong ligation products.

B. DNA agarose gel analysis of PTx resistant hDOR-$G_{o1}\alpha$ (Xaa^{351}) fusion protein mutants

DNAs from *E.coli* clones (selected clones of transformed ligated hDOR/ $G_{o1}\alpha$ (Xaa^{351}) fusion protein mutants) were digested with *BglII* and resolved in a 1% agarose gel. Clones in lanes 1, 2 [-$G_{o1}\alpha$ (Ile^{351})], 3, 4 [-$G_{o1}\alpha$ (Leu^{351})] and 5, 6 [-$G_{o1}\alpha$ (Gly^{351})], contain digested fragments close to the approximate lengths of 6.0 kb, 1.6 kb expected for the hDOR–$G_{o1}\alpha$ (Xaa^{351}) fusion protein mutants.

A

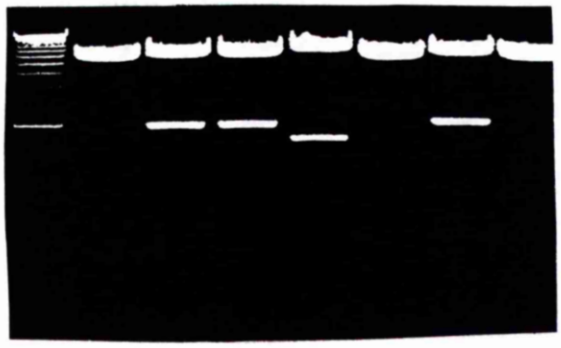

B

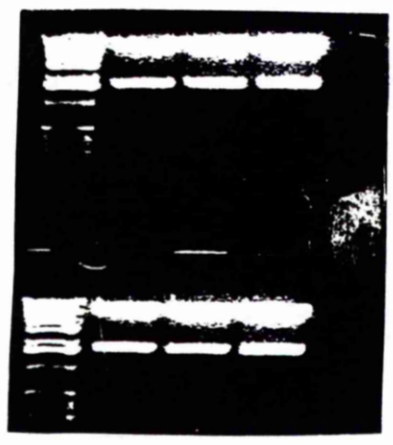

Figure 3.5. [^{3}H] naltrindole binding studies on transiently expressed hDOR-$G_{i1}\alpha$/$G_{o1}\alpha$ fusion proteins

A. [^{3}H] naltrindole-binding assay on transiently expressed hDOR-$G_{i1}\alpha$ (wild type) and hDOR-$G_{i1}\alpha$ (Xaa^{351}) fusion protein mutants

Following transient transfection of hDOR-$G_{i1}\alpha$ (wild type) and hDOR-$G_{i1}\alpha$ (Xaa^{351}) fusion protein mutants into HEK293T cells using Lipofectamine™ membranes were prepared and expression assessed by [^{3}H] naltrindole binding (~5 nM). Non specific binding was assessed in parallel in the presence of 100 μM unlabelled naloxone. Specific binding of [^{3}H] naltrindole was obtained by substrating non-specific binding counts from total binding counts. This is a representative example of one experiment performed in triplicate (mean ± S.D). Xaa^{351} amino acids are represented by the standard one-letter code.

B. [^{3}H] naltrindole-binding assay on transiently expressed hDOR-$G_{o1}\alpha$ (wild type) and hDOR-$G_{o1}\alpha$ (Xaa^{351}) fusion protein mutants

Following transient transfection of hDOR-$G_{o1}\alpha$ (wild type) and hDOR-$G_{o1}\alpha$ (Xaa^{351}) fusion protein mutants into HEK293T cells using Lipofectamine™, a binding experiment with prepared membranes was performed as in Figure 3.5A. This is a representative example of one experiment performed in triplicate (mean ± S.D).

A

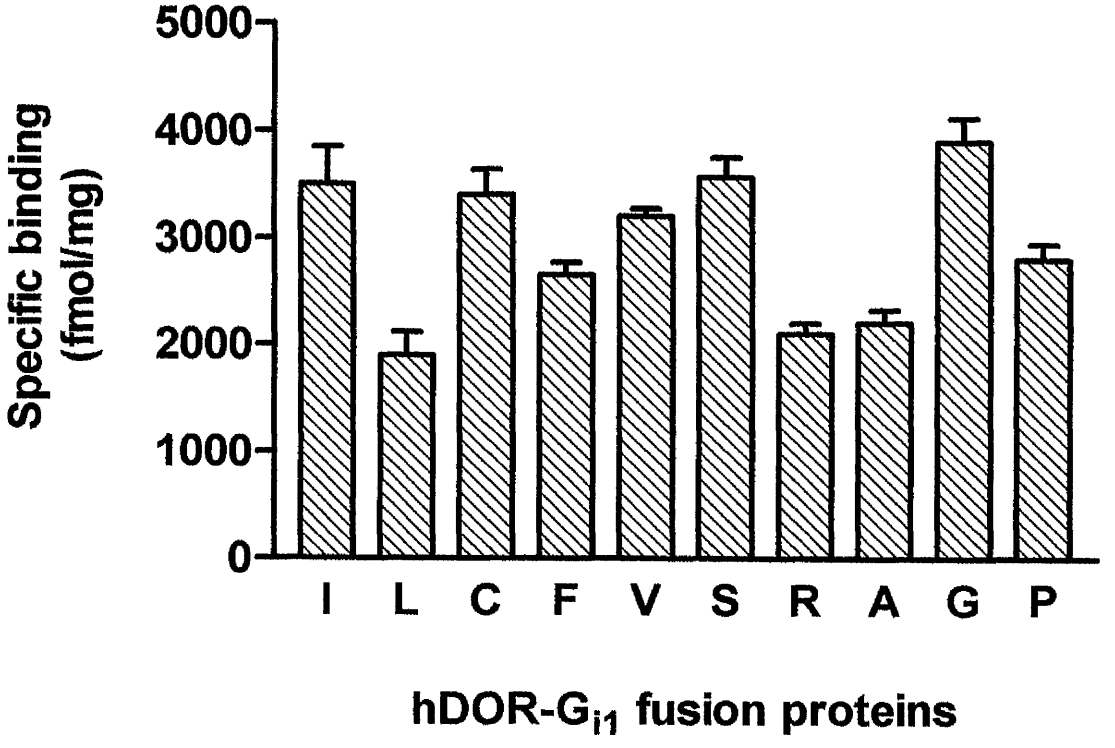
Specific binding (fmol/mg)
5000
4000
3000
2000
1000
0
I L C F V S R A G P
hDOR-G_{i1} fusion proteins

B

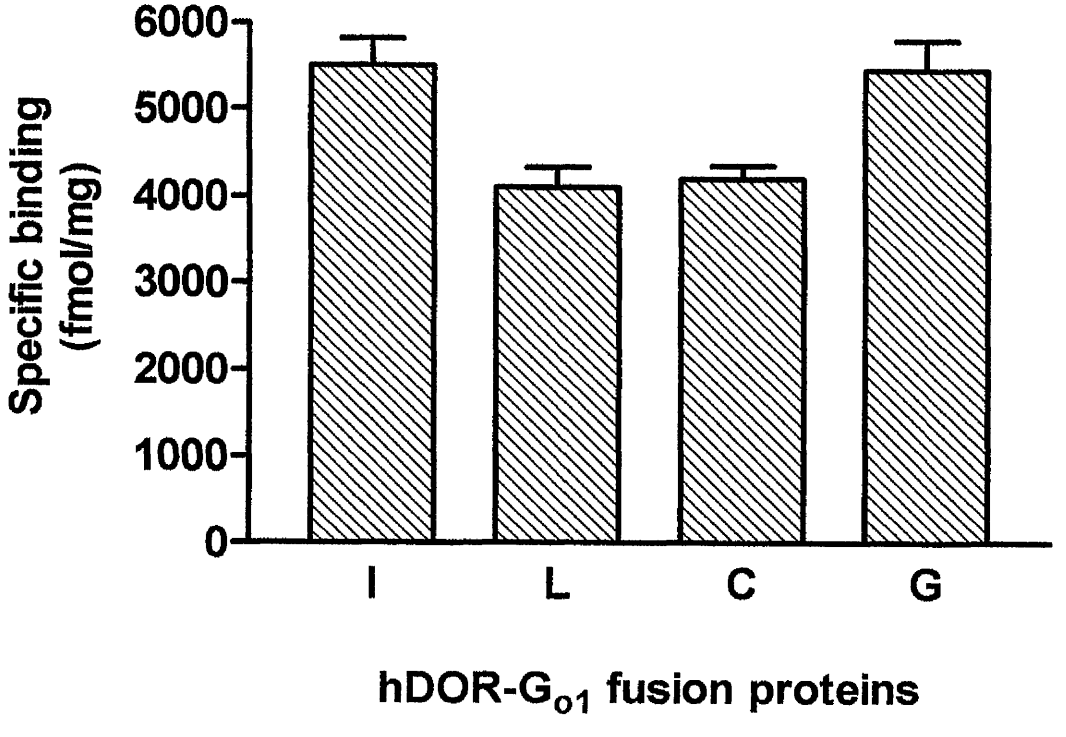
Specific binding (fmol/mg)
6000
5000
4000
3000
2000
1000
0
I L C G
hDOR-G_{o1} fusion proteins

Figure 3.6. Analysis of [^{3}H] naltrindole saturation binding to transiently expressed hDOR-$G_{i1}\alpha$ (Ile^{351}) fusion proteins

A. [^{3}H] naltrindole saturation-binding studies to membranes of cells transiently expressing the hDOR-$G_{i1}\alpha$ (Ile^{351}) fusion protein

Following transient expression of the hDOR-$G_{i1}\alpha$ (Ile^{351}) fusion protein and prior PTx treatment (25ng/ml, 16h), saturation binding studies using [^{3}H] naltrindole were performed on membranes of HEK293T cells. B_{max} of hDOR-$G_{i1}\alpha$ (Ile^{351}) varied in individual experiments (1~6 pmol/mg). The K_d of [^{3}H] naltrindole for hDOR-$G_{i1}\alpha$ (Ile^{351}) was estimated as 0.77 ± 0.12 nM (means ± S.E.M, n=3). This is a representative example of three experiments performed.

B. Scatchard analysis

Scatchard plot was generated from the data of Figure 3.6A. The slope of the graph provides the negative inverse of K_d ($-1/K_d$), while the X-intercept is the B_{max}. This is a typical example of three experiments performed.

A

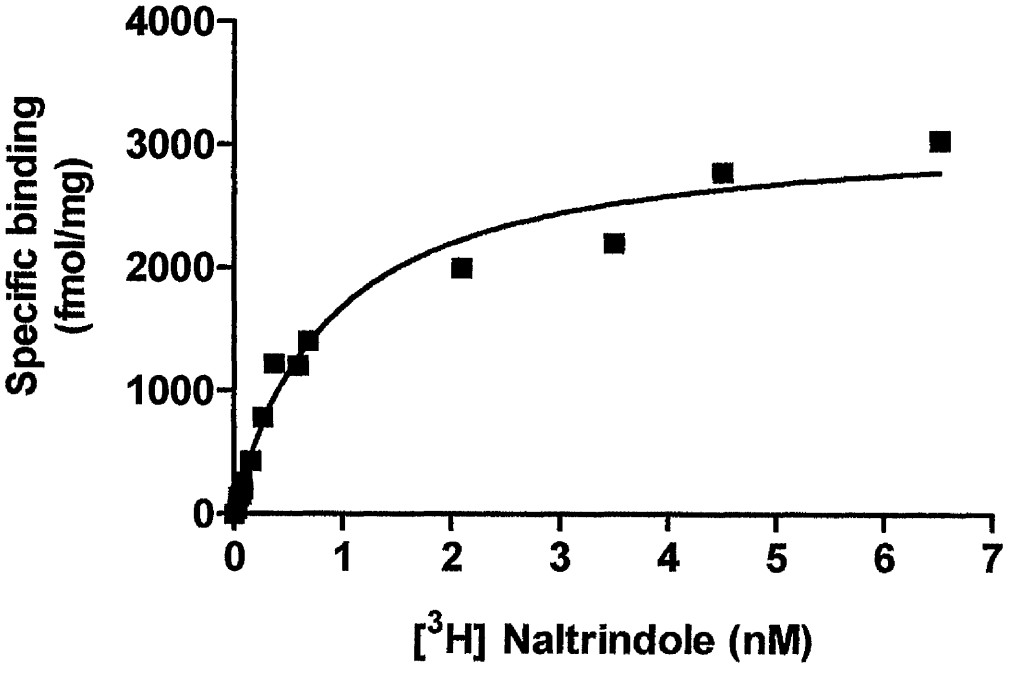
Specific binding (fmol/mg)
4000
3000
2000
1000
0
0
1
2
3
4
5
6
7
[3H] Naltrindole (nM)

B

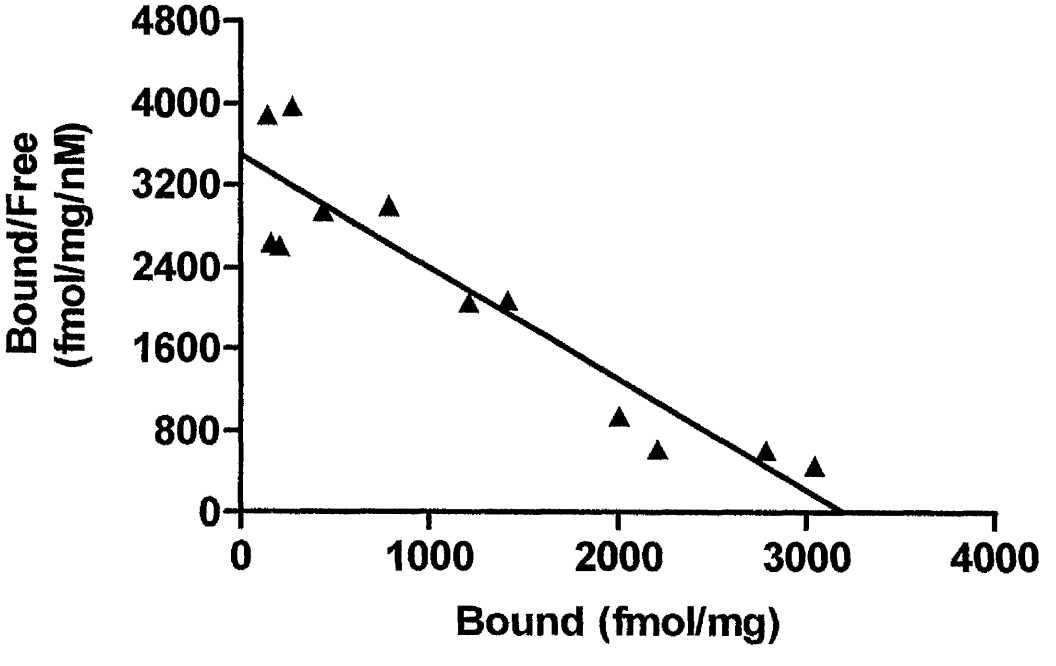
Bound/Free (fmol/mg/nM)
4800
4000
3200
2400
1600
800
0
0
1000
2000
3000
4000
Bound (fmol/mg)

Figure 3.7. Analysis of [^{3}H] naltrindole saturation binding to transiently expressed hDOR-$G_{i1}\alpha$ (Gly^{351}) fusion proteins

A. [^{3}H] naltrindole saturation-binding studies to membranes transiently expressing hDOR-$G_{i1}\alpha$ (Gly^{351}) fusion protein

Following transient expression of the hDOR-$G_{i1}\alpha$ (Gly^{351}) fusion protein and prior PTx treatment (25ng/ml, 16h), saturation binding studies using [^{3}H] naltrindole were performed on membranes of HEK293T cells. B_{max} of the hDOR-$G_{i1}\alpha$ (Gly^{351}) varied in individual experiments (1-6 pmol/mg). The K_d of [^{3}H] naltrindole for hDOR-$G_{i1}\alpha$ (Gly^{351}) was estimated as 0.13 ± 0.02 nM (means ± S.E.M, n=3). This is a representative example of three experiments performed.

B. Scatchard analysis

Scatchard plot was generated from the data of the Figure 3.7A. The slope of the graph provides the negative inverse of K_d ($-1/K_d$), while the X-intercept is the B_{max}. This is a typical example of three experiments performed in triplicate.

A

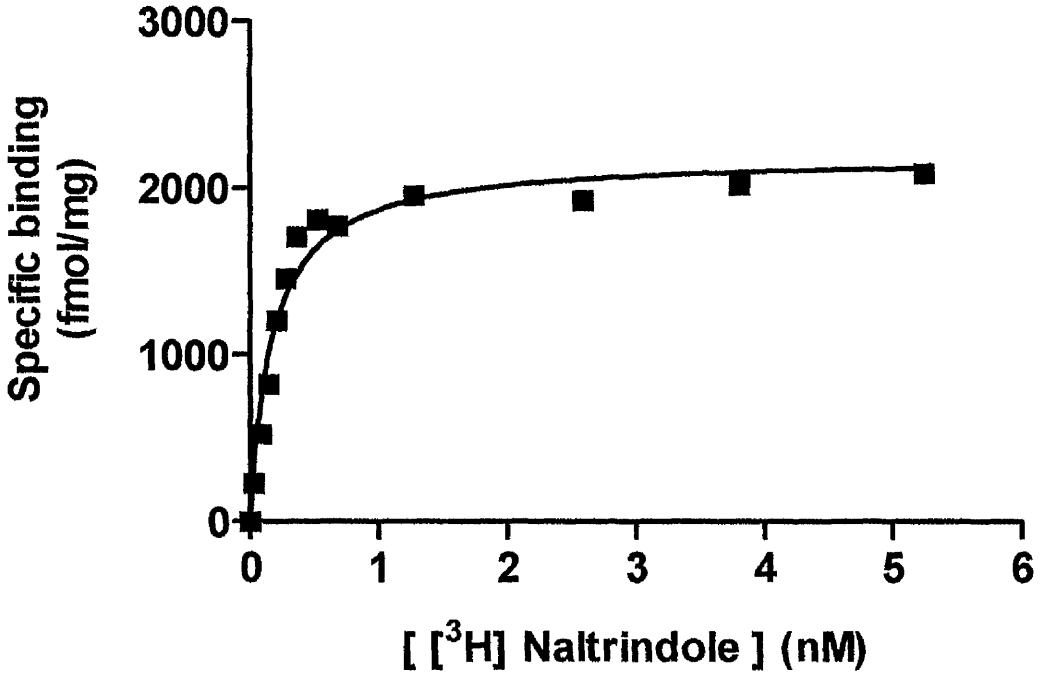
Specific binding
(fmol/mg)
3000
2000
1000
0
0
1
2
3
4
5
6
[[3H] Naltrindole] (nM)

B

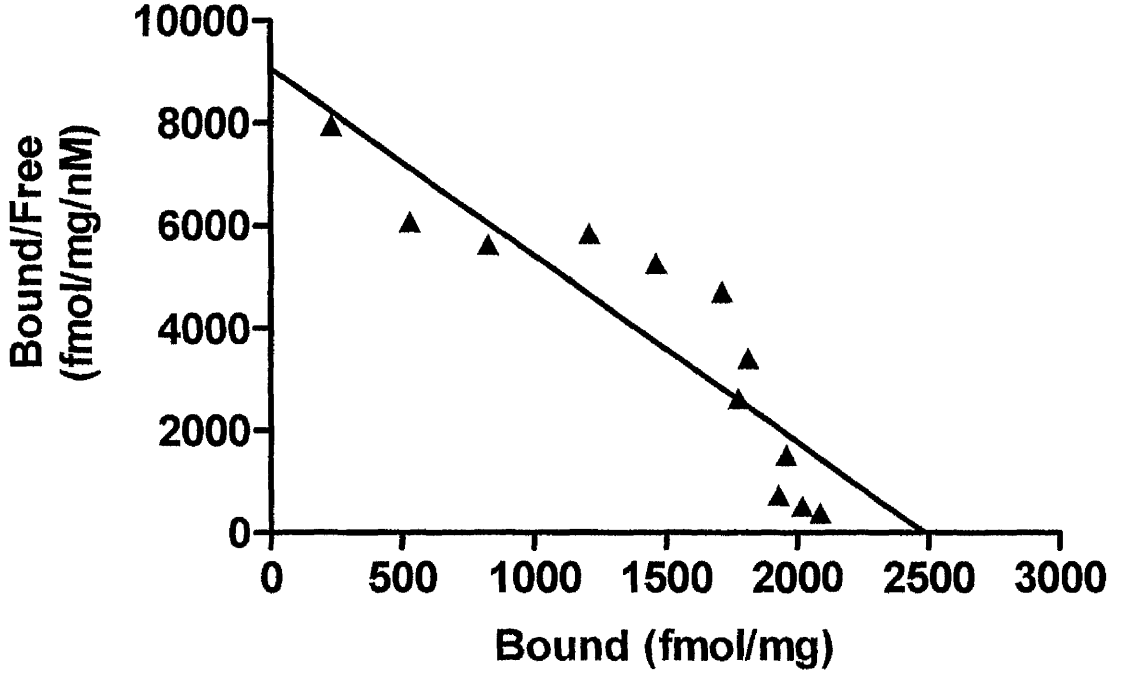
Bound/Free
(fmol/mg/nM)
10000
8000
6000
4000
2000
0
0
500
1000
1500
2000
2500
3000
Bound (fmol/mg)

Figure 3.8. Immunodetection of hDOR-$G_{i1}\alpha$ fusion proteins

A. Optimisation of immunological detection of hDOR-$G_{i1}\alpha$ (Xaa^{351}) fusion protein mutants

Immunoblotting with antiserum I1C to detect hDOR-$G_{i1}\alpha$ fusion protein mutants was optimised under four different conditions - 1^{st}; boiling/reducing, 2^{nd}; boiling/non-reducing, 3^{rd}; non-boiling/reducing, 4^{th}; non-boiling/non-reducing -. Two fusion proteins hDOR-$G_{i1}\alpha$ (Ile^{351}) (lanes 2, 5, 8, 11) and -$G_{i1}\alpha$ (Ser^{351}) (lanes 3, 6, 9, 12) were used as were mock-transfected cells (lanes 1, 4, 7, 10). The conditions of 1^{st} (lanes 2, 3) and 2^{nd} (lanes 5, 6) seemed to be successful in detecting strong signals in the positive but not in mock (pcDNA3.1) loaded lanes. Possible degradation products from the fusion proteins (lanes 3, 4, 6, 7, 10) were detected around ~27kDa, but not in mock loaded lane (lanes 1, 4, 7, 10).

B. Immunological detection of hDOR-$G_{i1}\alpha$ (Xaa^{351}) fusion protein mutants

Immunoblotting with I1C antiserum, which is specific against an internal domain (159-168 aa) of $G_{i1}\alpha$ indicated multiple immunoreactive proteins corresponding to the fusion protein (Green *et al*, 1990).

A

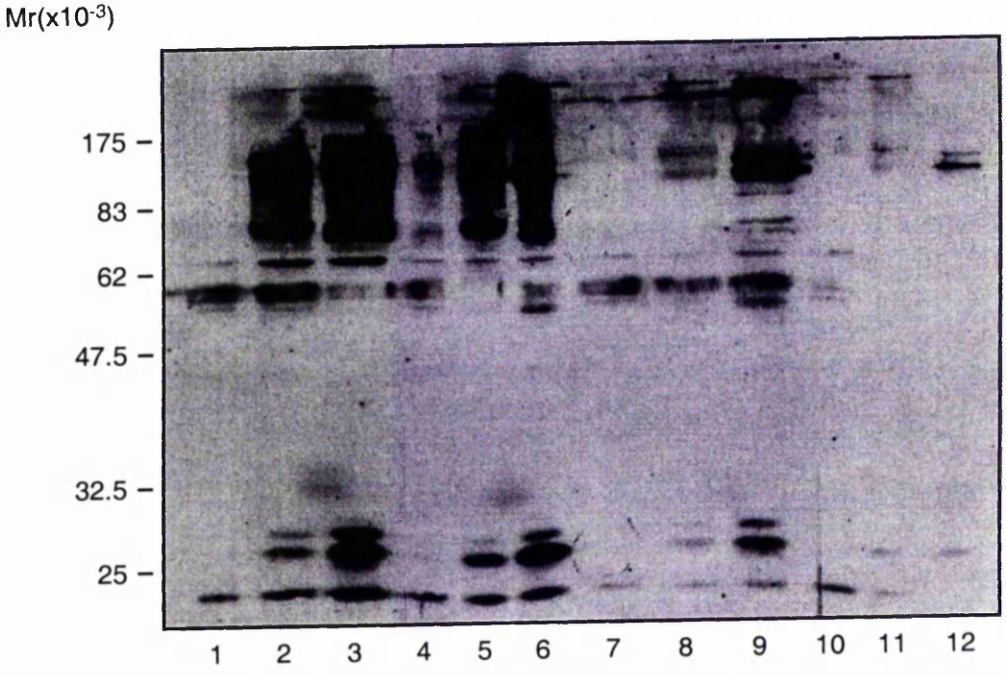

B

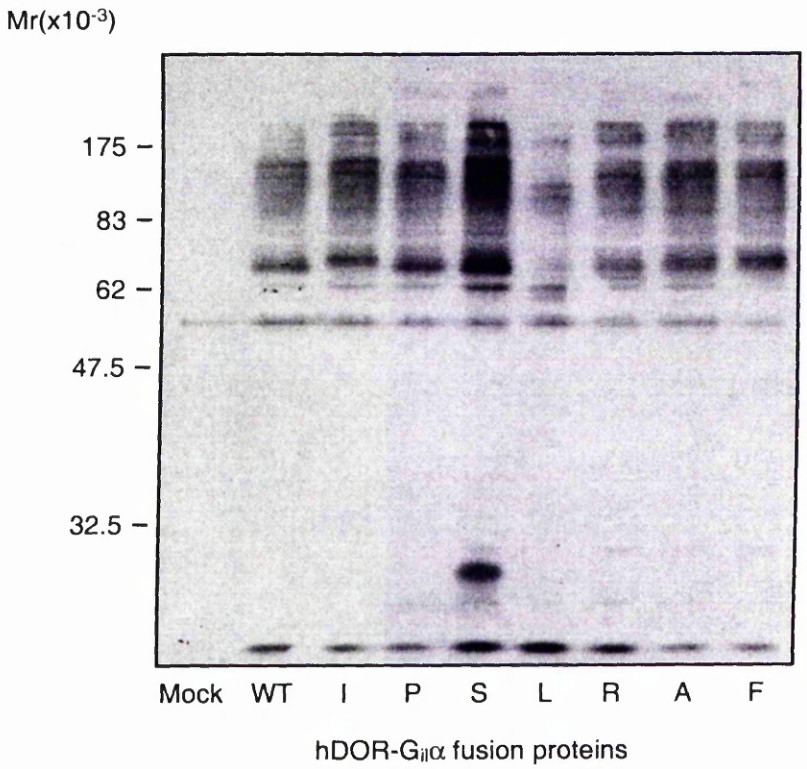
Mr(x10-3)
175
83
62
47.5
32.5
Mock
WT
I
P
S
L
R
A
F
hDOR-Gilα fusion proteins

Figure 3.9. Comparison of the potency of DADLE to stimulate the high affinity GTPase activity of transiently expressed hDOR-$G_{i1}\alpha/G_{o1}\alpha$ fusion proteins

A. DADLE stimulation of the high affinity GTPase activity of transiently expressed hDOR-$G_{i1}\alpha$ (Ile^{351}).

Following transient expression of the hDOR-$G_{i1}\alpha$ (Ile^{351}) fusion protein and prior PTx treatment (25ng/ml, 16h), high affinity GTPase activity was measured in the presence of varying concentrations of DADLE. The pEC_{50} value was 7.1 ± 0.1 (mean ± S.E.M, n=3).

B. DADLE stimulation of the high affinity GTPase activity of transiently expressed hDOR-$G_{i1}\alpha$ (Gly^{351}).

Following transient expression of hDOR-$G_{i1}\alpha$ (Gly^{351}) and prior PTx treatment (25ng/ml, 16h), high affinity GTPase activity was measured in the presence of varying concentrations of DADLE. The pEC_{50} value was 6.2 ± 0.1 (mean ± S.E.M, n=3).

C. DADLE stimulation of the high affinity GTPase activity of transiently expressed hDOR-$G_{o1}\alpha$ (Ile^{351}).

Following transient expression of hDOR-$G_{o1}\alpha$ (Ile^{351}) and prior PTx treatment (25ng/ml, 16h), high affinity GTPase activity was measured in the presence of varying concentrations of DADLE. The pEC_{50} value was 7.2 ± 0.3 (mean ± S.E.M, n=3).

A

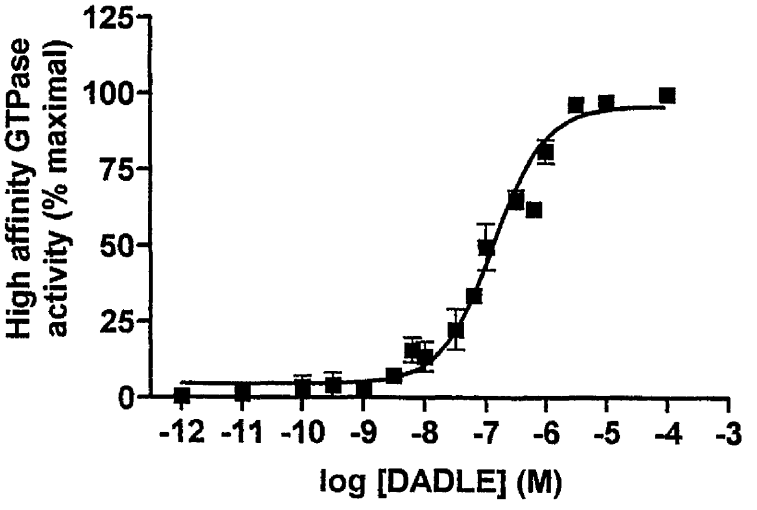
High affinity GTPase activity (% maximal)
125
100
75
50
25
0
-12 -11 -10 -9 -8 -7 -6 -5 -4 -3
log [DADLE] (M)

B

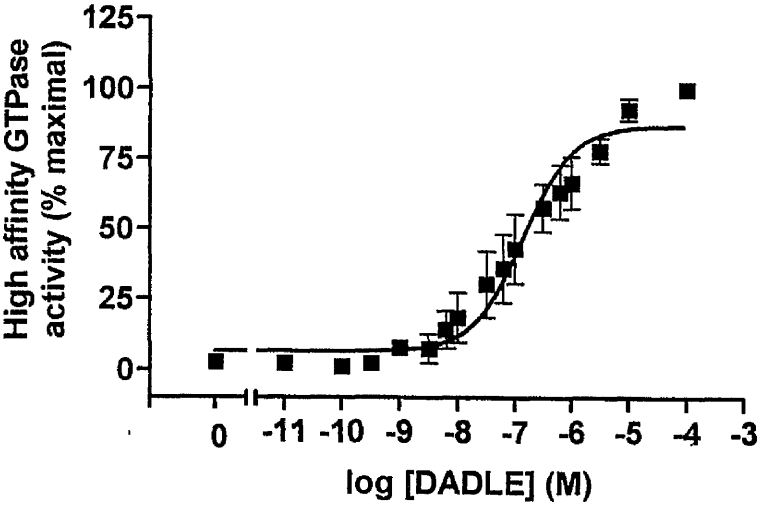
High affinity GTPase activity (% maximal)
125
100
75
50
25
0
0 -11 -10 -9 -8 -7 -6 -5 -4 -3
log [DADLE] (M)

C

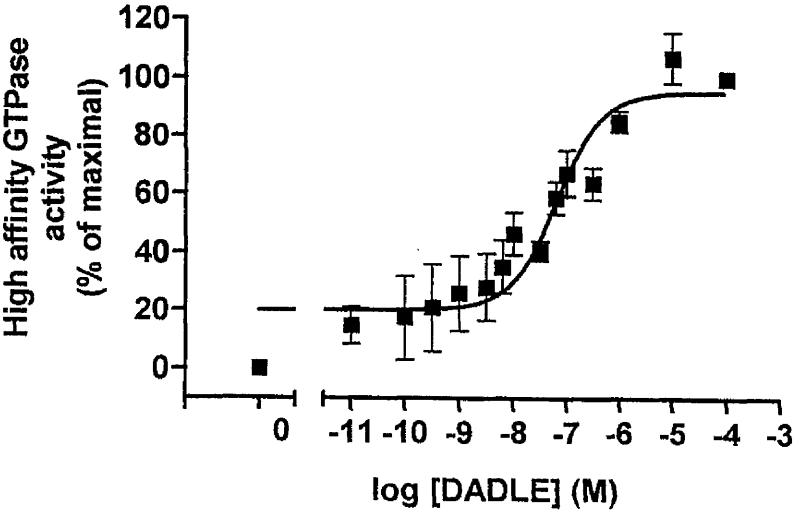
High affinity GTPase activity (% of maximal)
120
100
80
60
40
20
0
0 -11 -10 -9 -8 -7 -6 -5 -4 -3
log [DADLE] (M)

Figure 3.10. The kinetics of DADLE-stimulated GTP hydrolysis of transiently expressed hDOR-$G_{i1}\alpha$ (Ile^{351}).

A. DADLE-stimulated high affinity GTP activity at various GTP concentrations

Following transient expression of hDOR-$G_{i1}\alpha$ (Ile^{351}) and prior PTx treatment (25ng/ml, 16h), basal (▲) and DADLE (100μM)-stimulated (□) high affinity GTPase activity was measured at increasing concentrations of GTP. This is a representative example of three experiments performed.

B. Eadie-Hofstee analysis

An Eadie-Hofstee plot was produced from the data of Figure 3.10A. The maximum velocity (Vmax) was obtained by the difference in y-intercept between the basal (▲) and DADLE-stimulated (□) activity and the Michaelis-Menten constant (K_m) for GTP was determined by the negative value of the slope of the graph. K_m GTP (basal) was 0.41 ± 0.05 nM and K_m GTP (DADLE) was 0.54 ± 0.06 nM (means ± S.E.M, n=3). GTP turnover number was calculated as 9.5 ± 0.1 min^{-1} (mean ± S.E.M, n=3); V_{max} (DADLE)-V_{max} (basal)/B_{max} of expression level in the same membrane preparation. This is typical of three experiments performed.

A

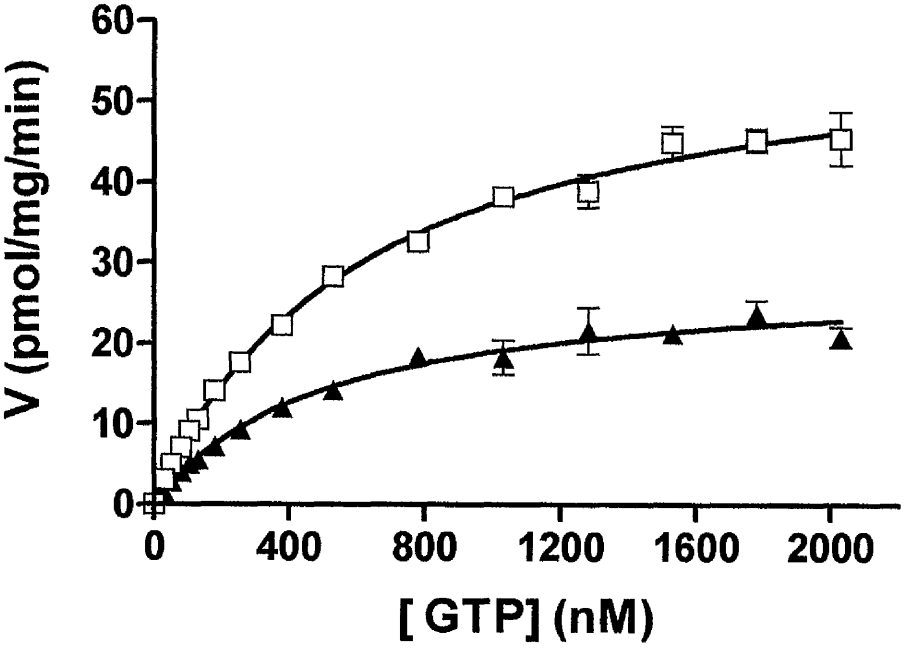
60
50
40
30
20
10
0
V (pmol/mg/min)
0
400
800
1200
1600
2000
[GTP] (nM)

B

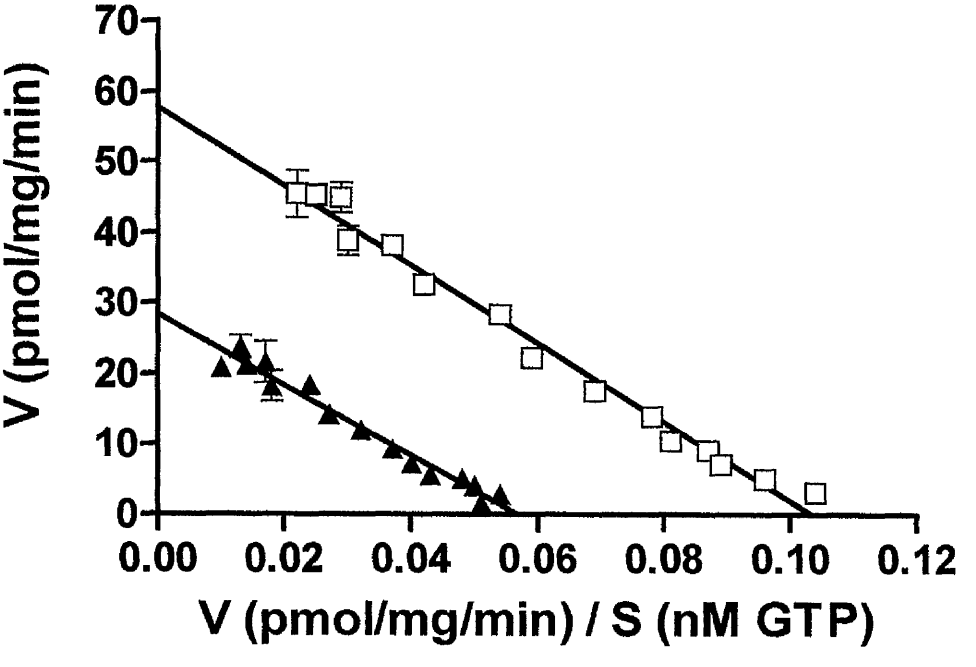
70
60
50
40
30
20
10
0
V (pmol/mg/min)
0.00
0.02
0.04
0.06
0.08
0.10
0.12
V (pmol/mg/min) / S (nM GTP)

Figure 3.11. The kinetics of DADLE-stimulated GTP hydrolysis of transiently expressed hDOR-$G_{i1}\alpha$ (Gly^{351}).

A. DADLE-stimulated high affinity GTP activity at various GTP concentrations

Following transient expression of hDOR-$G_{i1}\alpha$ (Gly^{351}) and prior PTx treatment (25ng/ml, 16h), basal (▲) and DADLE (100 μM)-stimulated (□) high affinity GTPase activity was measured at increasing concentrations of GTP. This is a representative example of three experiments performed.

B. Eadie-Hofstee analysis

An Eadie-Hofstee plot was produced from the data of Figure 3.11A. K_m GTP (basal) was 0.70 ± 0.11 nM and K_m GTP (DADLE) was 0.73 ± 0.07 nM (means ± S.E.M, n=3). GTP turnover number was calculated as 4.9 ± 1.1 min^{-1} (mean ± S.E.M, n=3). This is typical of three experiments performed.

A

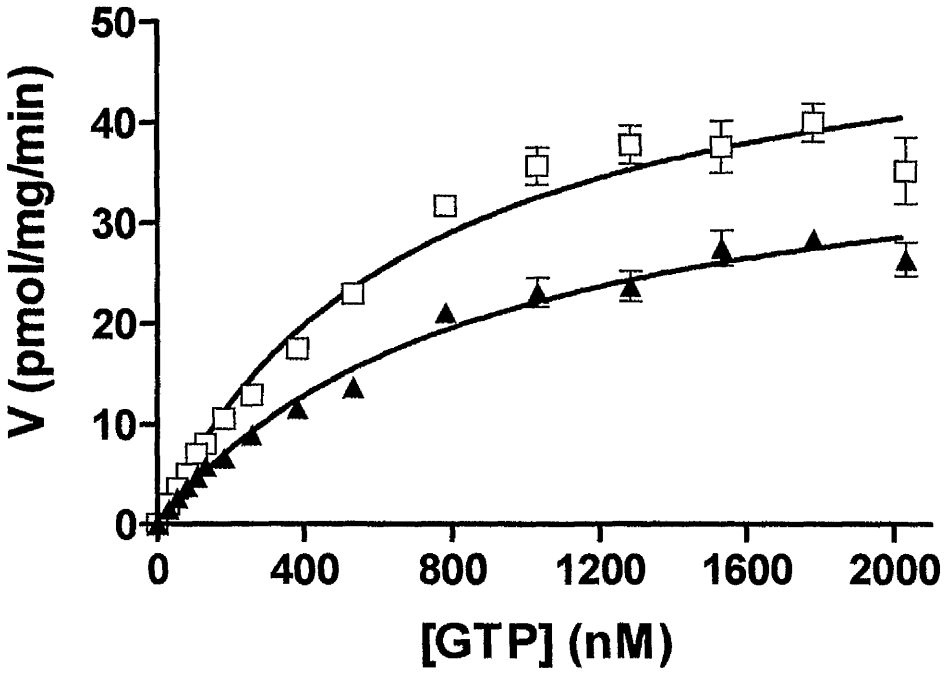
50
40
30
20
10
0
V (pmol/mg/min)
0
400
800
1200
1600
2000
[GTP] (nM)

B

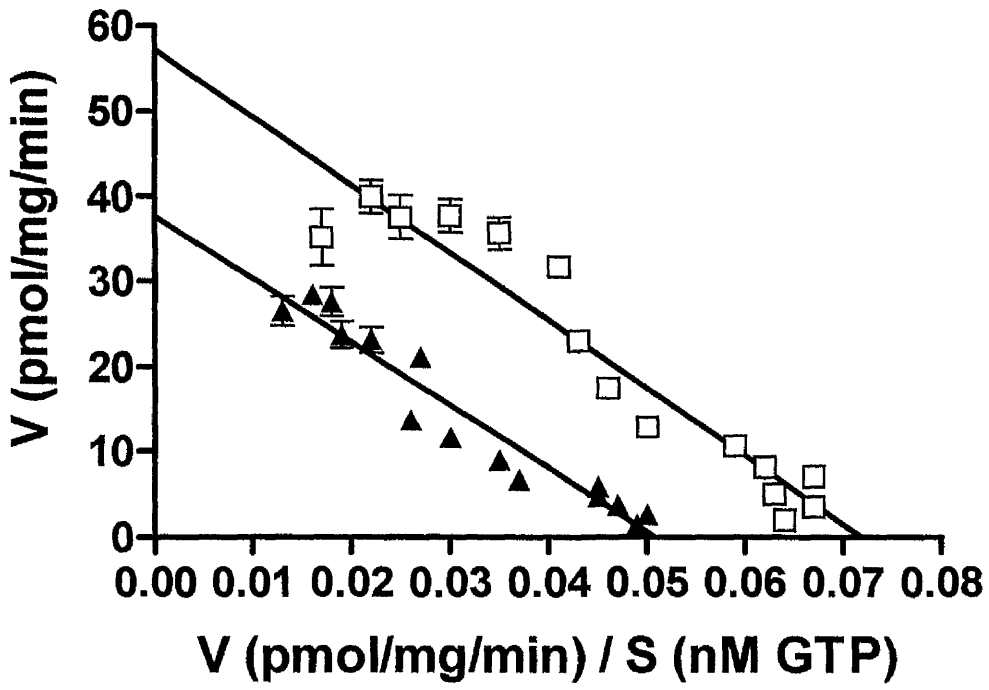
60
50
40
30
20
10
0
V (pmol/mg/min)
0.00 0.01 0.02 0.03 0.04 0.05 0.06 0.07 0.08
V (pmol/mg/min) / S (nM GTP)

Figure 3.12 The kinetics of DADLE-stimulated GTP hydrolysis of transiently expressed hDOR-$G_{o1}\alpha$ (Ile^{351}).

A. DADLE-stimulated high affinity GTP activity at various GTP concentrations

Following transient expression of hDOR-$G_{o1}\alpha$ (Ile^{351}) and prior PTx treatment (25ng/ml, 16h), basal (▲) and DADLE (100 μM)-stimulated (□) high affinity GTPase activity was measured at increasing concentrations of GTP. This is a representative example of three experiments performed.

B. Eadie-Hofstee analysis

An Eadie-Hofstee plot was produced from the data of Figure 3.12A. K_m GTP (basal) was 0.68 ± 0.09 nM and K_m GTP (DADLE) was 0.62 ± 0.10 nM (means ± S.E.M, n=3). GTP turnover number was calculated as 3.0 ± 0.1 min^{-1} (mean ± S.E.M, n=3). This is typical of three experiments performed.

A

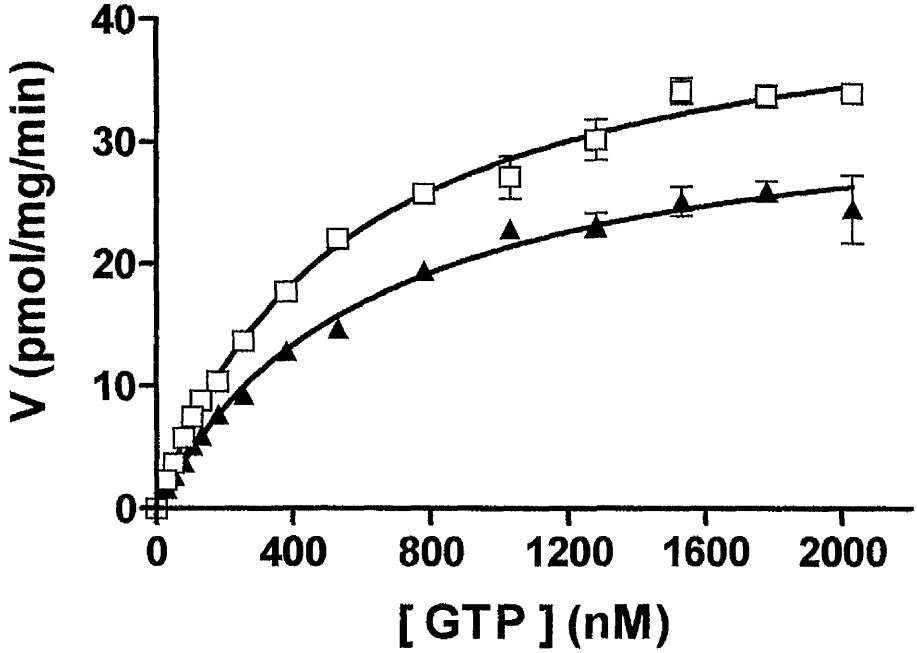
40
30
20
10
0
V (pmol/mg/min)
0
400
800
1200
1600
2000
[GTP] (nM)

B

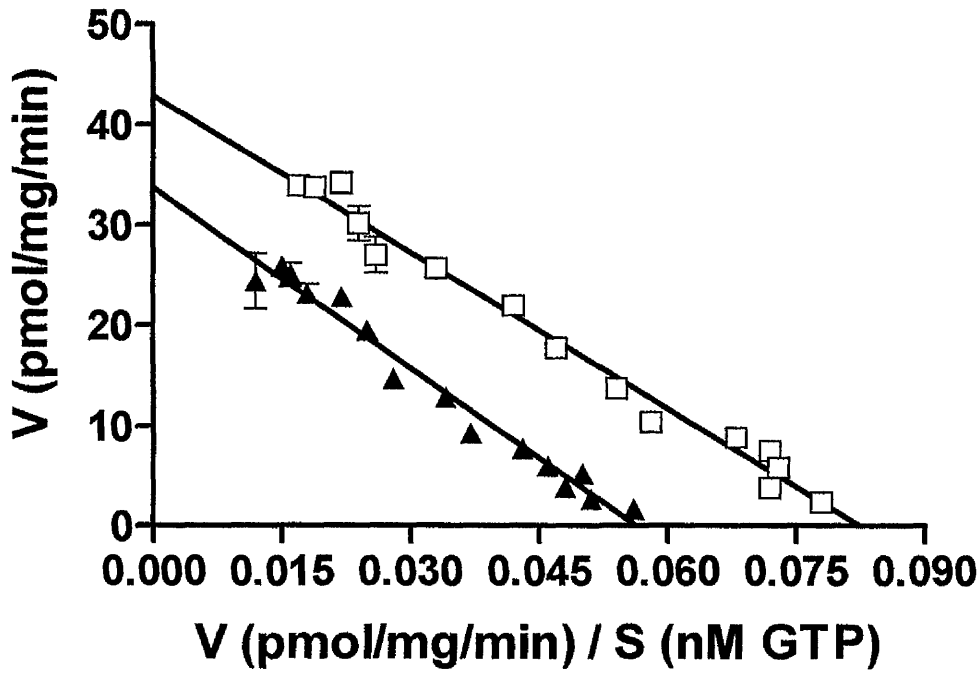
50
40
30
20
10
0
V (pmol/mg/min)
0.000
0.015
0.030
0.045
0.060
0.075
0.090
V (pmol/mg/min) / S (nM GTP)

Figure 3.13. Stable cell lines expressing hDOR-$G_{i1}\alpha$ (Ile^{351}) and hDOR-$G_{o1}\alpha$ (Ile^{351}) fusion proteins

A. Selected clones stably expressing hDOR-$G_{i1}\alpha$ (Ile^{351}).

Following stable expression of the hDOR-$G_{i1}\alpha$ (Ile^{351}) fusion protein in HEK293 cells in an antibiotic selective manner (G418-sulphate, 1mg/ml), clones expressing hDOR-$G_{i1}\alpha$ (Ile^{351}) were expanded. Expression of the fusion protein was assessed using ~ 5 nM [^{3}H] naltrindole binding with 100 μM naloxone used to define non-specific binding. This is a representative example of one experiment performed in triplicate (mean ± S.D.).

B. Selected clones stably expressing hDOR-$G_{o1}\alpha$ (Ile^{351}).

Following stable expression of the hDOR-$G_{o1}\alpha$ (Ile^{351}) fusion protein in HEK293 cells in an antibiotic selective manner (G418-sulphate, 1mg/ml), clones expressing hDOR-$G_{o1}\alpha$ (Ile^{351}) were expanded. Expression of the fusion protein was assessed using ~ 5 nM [^{3}H] naltrindole binding with 100 μM naloxone used to define non-specific binding. This is a representative example of one experiment performed in triplicate (mean ± S.D.).

A

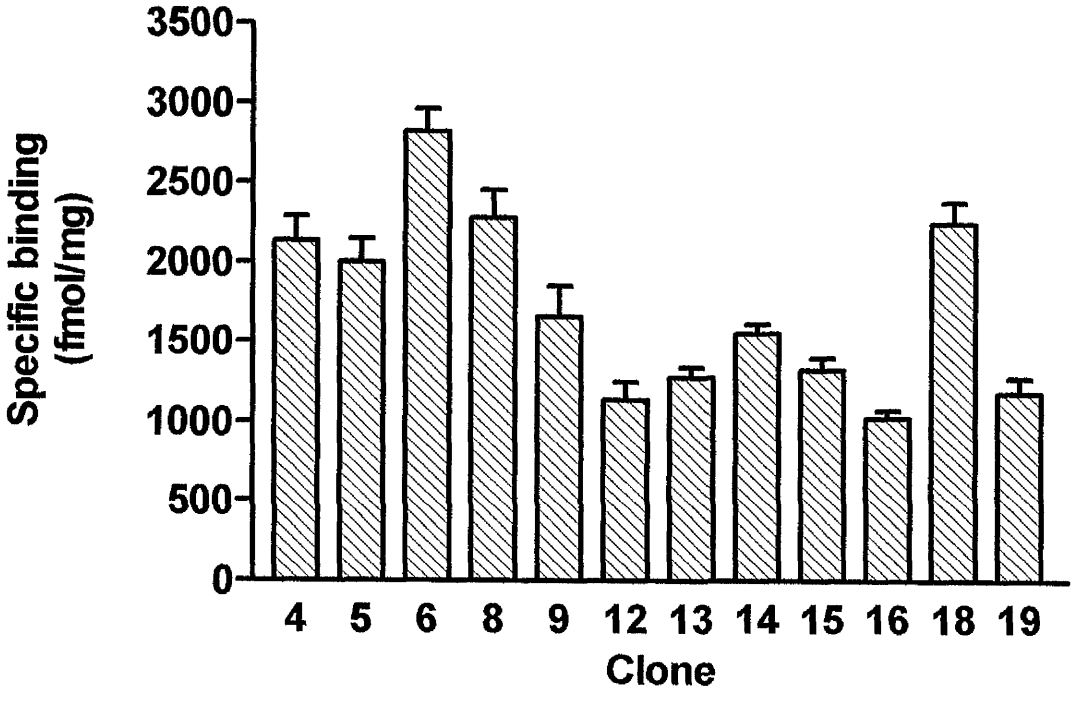
Specific binding (fmol/mg)
3500
3000
2500
2000
1500
1000
500
0
4 5 6 8 9 12 13 14 15 16 18 19
Clone

B

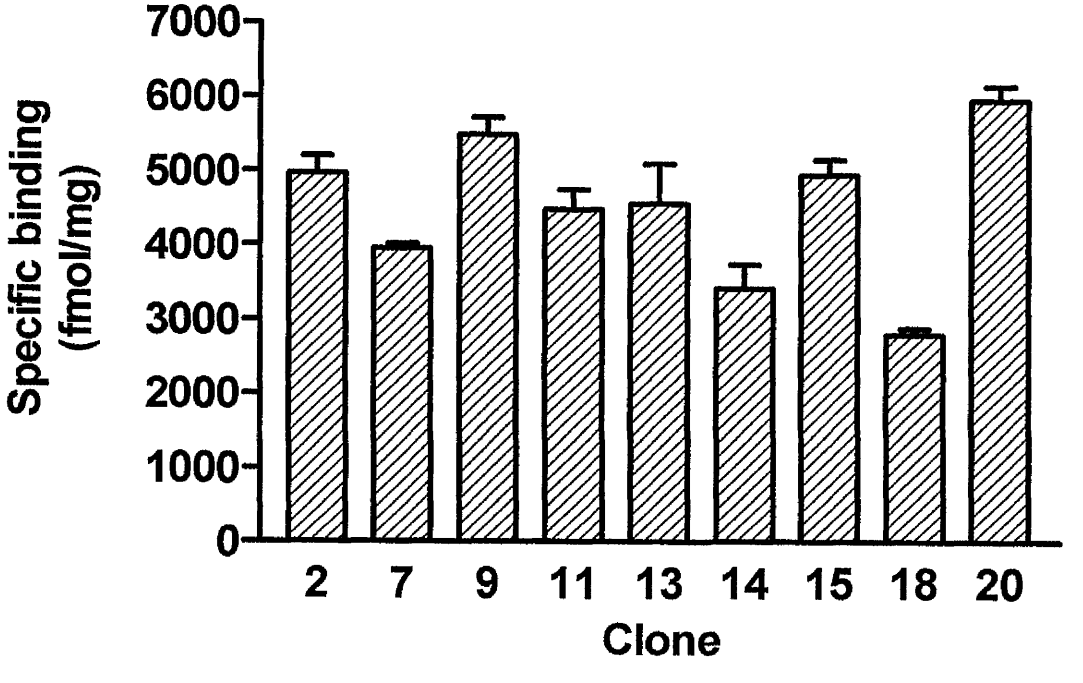
Specific binding (fmol/mg)
7000
6000
5000
4000
3000
2000
1000
0
2 7 9 11 13 14 15 18 20
Clone

Figure 3.14. Correlation between specific [^{3}H] naltrindole binding and DADLE-stimulated GTPase activity of clones stably expressing hDOR-$G_{i1}\alpha$/ $G_{o1}\alpha$ fusion proteins

Correlation between single concentration [^{3}H] naltrindole binding (Figure 3.13A) and maximal concentration DADLE-stimulated GTPase activity of selected clones stably expressing hDOR-$G_{i1}\alpha$ (Ile^{351}) (□) and between single concentration [^{3}H] naltrindole binding (Figure 3.13B) and maximal concentration DADLE–stimulated GTPase activity of selected clones stably expressing hDOR-$G_{o1}\alpha$ (Ile^{351}) (▲).

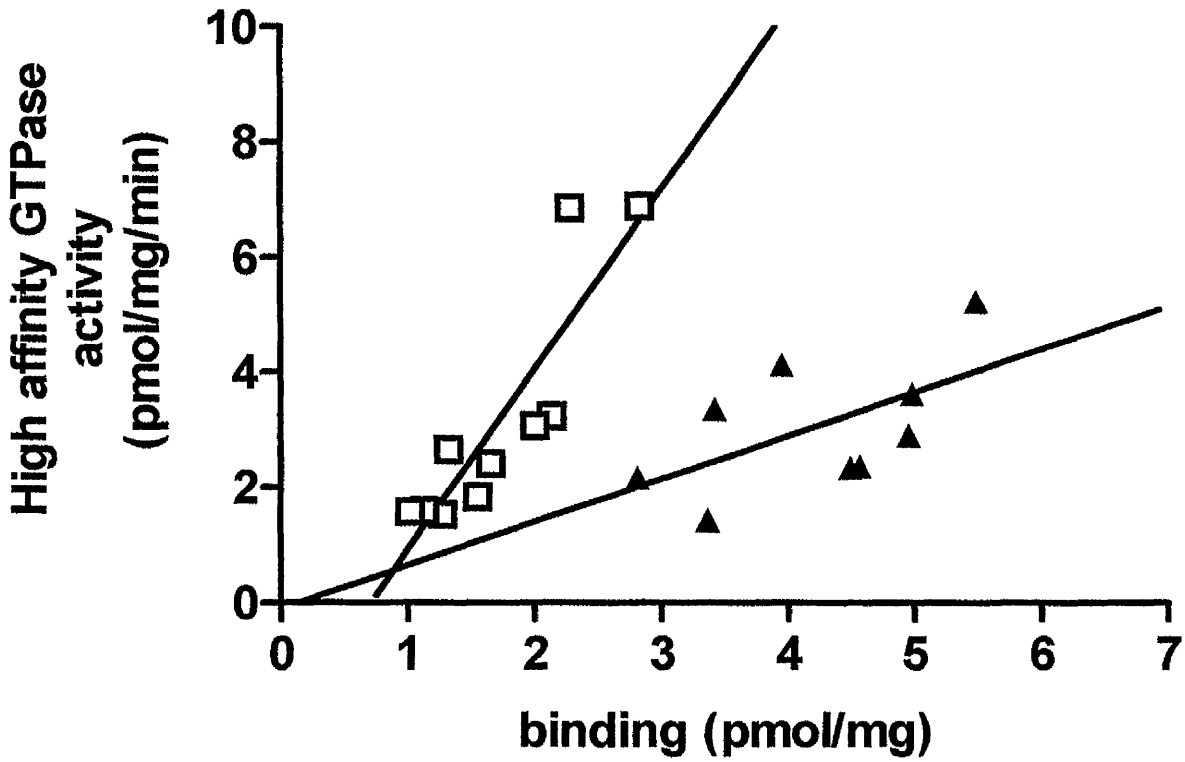
High affinity GTPase activity (pmol/mg/min)
10
8
6
4
2
0
0
1
2
3
4
5
6
7
binding (pmol/mg)

Figure 3.15. Analysis of [^{3}H] naltrindole binding to stably expressed hDOR-$G_{i1}\alpha$ (Ile^{351}).

A. [^{3}H] naltrindole binding studies on membranes stably expressing hDOR-$G_{i1}\alpha$ (Ile^{351}).

Following stable expression of the hDOR-$G_{i1}\alpha$ (Ile^{351}) fusion protein and prior PTx treatment (25ng/ml, 16h), saturation binding studies using [^{3}H] naltrindole were performed on membranes of HEK293T cells at various range of [^{3}H] naltrindole. Non specific binding was assessed in parallel in the presence of 100 μM unlabelled naloxone. B_{max} of hDOR-$G_{i1}\alpha$ (Ile^{351}) varied with passage (3-6 pmol/mg). The K_d of [^{3}H] naltrindole for hDOR-$G_{i1}\alpha$ (Ile^{351}) was estimated as 0.47 ± 0.04 nM. (mean ± S.E.M, n=3). This is a representative example of three experiments performed.

B. Scatchard analysis

Scatchard plot was generated from the data of Figure 3.15A. The slope of the graph provides the negative inverse of K_d ($-1/K_d$), while the X-intercept is the B_{max}. This is a typical example of three experiments performed.

A

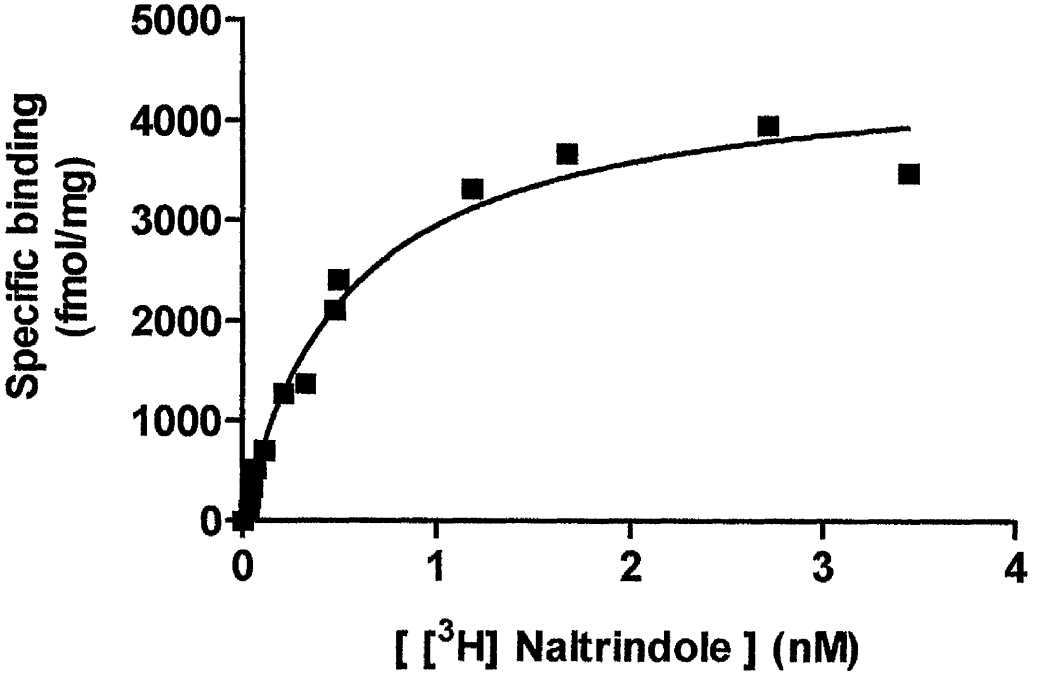
Specific binding
(fmol/mg)
5000
4000
3000
2000
1000
0
0
1
2
3
4
[[3H] Naltrindole] (nM)

B

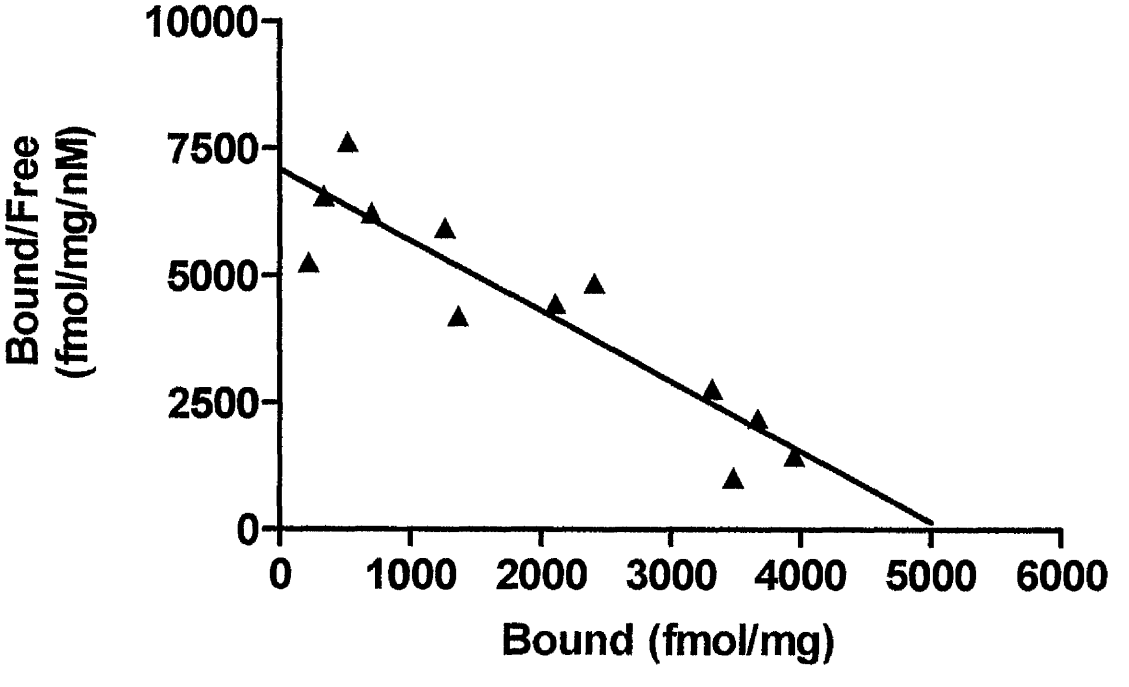
Bound/Free
(fmol/mg/nM)
10000
7500
5000
2500
0
0
1000
2000
3000
4000
5000
6000
Bound (fmol/mg)

Figure 3.16 Analysis of [^{3}H] naltrindole binding on stably expressing hDOR-$G_{o1}\alpha$ (Ile^{351}).

A. [^{3}H] naltrindole binding studies on membranes stably expressing hDOR-$G_{o1}\alpha$ (Ile^{351}).

Following stable expression of hDOR-$Go_1\alpha$ (Ile^{351}) and prior PTx treatment (25ng/ml, 16h), saturation binding studies using [^{3}H] naltrindole were performed on membranes of HEK293T cells at various concentrations of [^{3}H] naltrindole. Non specific binding was assessed in parallel in the presence of 100 μM unlabelled naloxone. B_{max} of hDOR–$G_{o1}\alpha$ (Ile^{351}) varied with passage (5-10 pmol/mg). The K_d of [^{3}H] naltrindole for hDOR–$G_{o1}\alpha$ (Ile^{351}) was estimated as 0.88 ± 0.35 nM (mean ± S.E.M, n=3). This is a representative example of three experiments performed.

B. Scatchard analysis

Scatchard plot was analysed from the Figure 3.16A. The slope of the graph gave the negative inverse of K_d ($-1/K_d$), while the X-intercept is the B_{max}. This is a typical representative of three experiments performed.

A

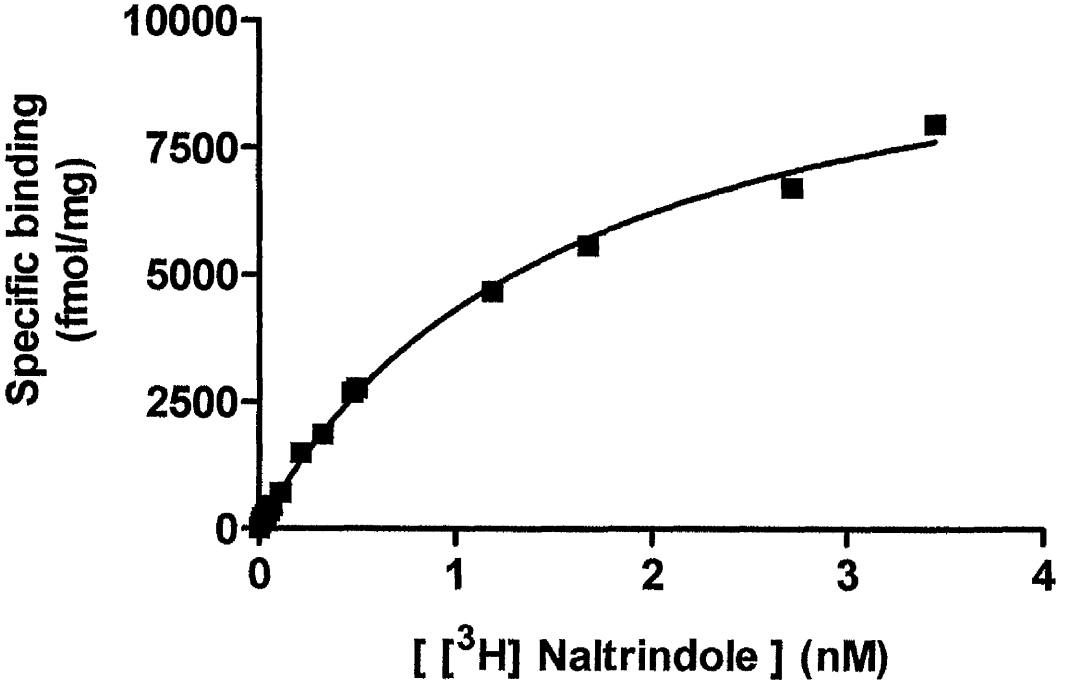
10000
7500
5000
2500
0
Specific binding
(fmol/mg)
0
1
2
3
4
[[3H] Naltrindole] (nM)

B

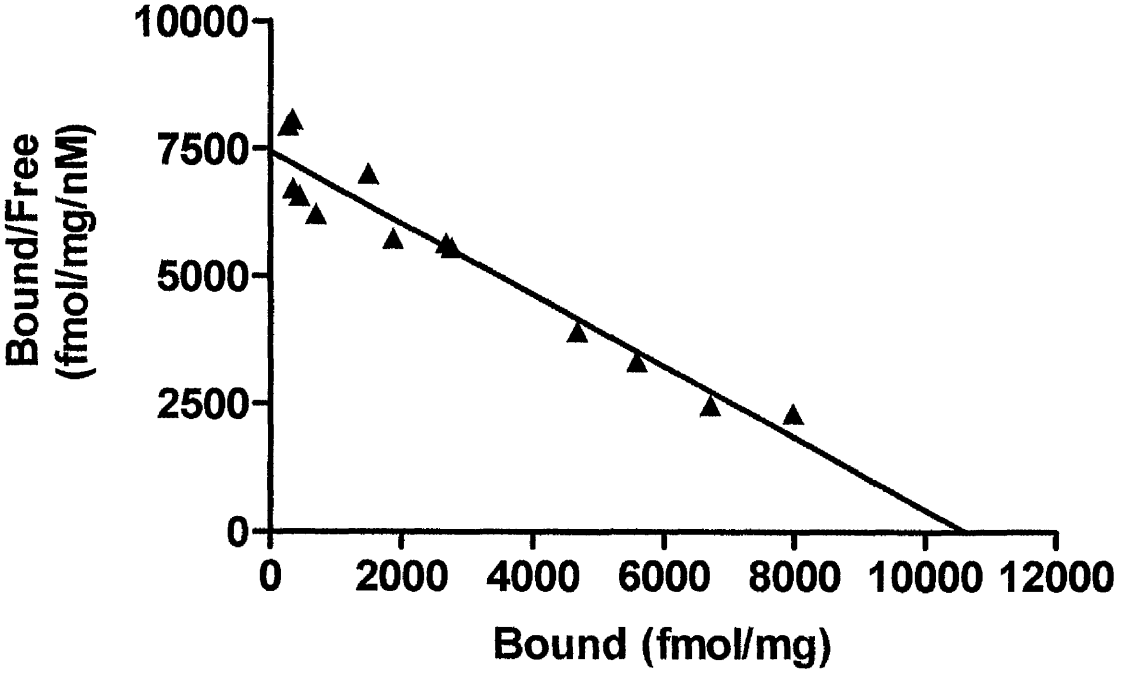
10000
7500
5000
2500
0
Bound/Free
(fmol/mg/nM)
0
2000
4000
6000
8000
10000
12000
Bound (fmol/mg)

Figure 3.17. Deglycosylation of glycosylated forms of hDOR-$G_{o1}\alpha$ (Ile^{351}).

A. Glycosylation

Membranes from HEK293 cells stably expressing hDOR-$G_{o1}\alpha$ (Ile^{351}) were prepared and their protein resolved in 10% SDS-PAGE. Following transfer to nitrocellulose, samples were immunoblotted with antiserum ON1 (specific for the N-terminal hexadecapeptide of $G_{o1}\alpha$). Three bands were detected at increasing concentration of membrane protein (10μl, 7μl, 3μl / lanes 2, 3, 4), but not in mock transfected cells (Lane1), which were glycosylated (Mr 75-95 kDa).

B. Deglycosylation

NGF (N-Glycosidase F, Roche Molecular Biochemicals) was used for structural analysis of N (asparagine)-linked carbohydrate chains of glycoproteins. After the deglycosylation reaction, the protein was analysed on 10% SDS-PAGE, where a shift to a lower apparent molecular mass indicates the removal of aspargine-linked glycan chains. Successful deglycosylated of this fusion protein (Mr 75 kDa, lane2) was obtained. Lane 1, untreated, lane 2, NGF-treated.

A

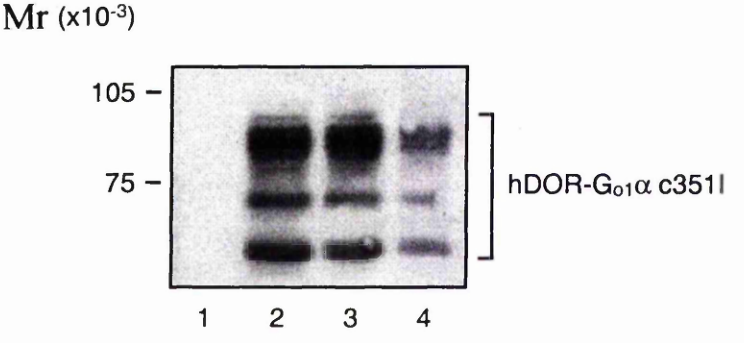
Mr (x10-3)
105 –
75 –
hDOR-Goα c351I
1 2 3 4

B

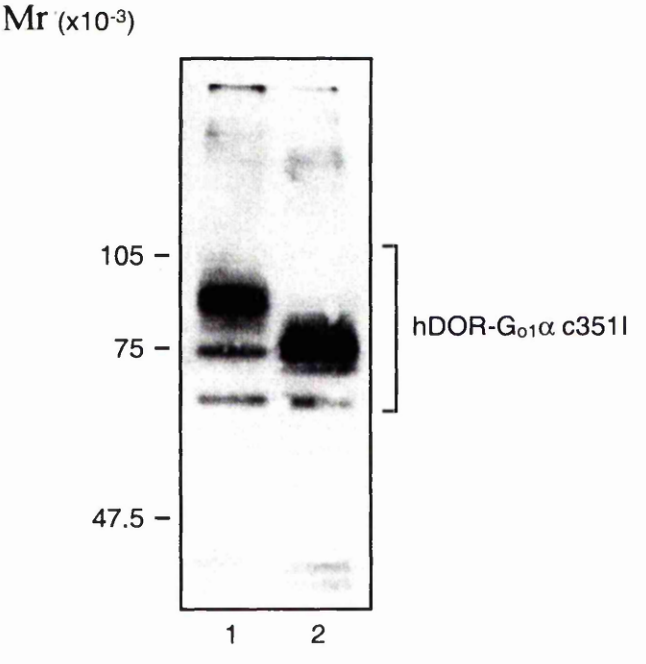
Mr (x10-3)
105 –
75 –
47.5 –
hDOR-Goα c351I
1 2

Figure 3.18. DADLE-stimulated high affinity GTPase activities of stably expressed hDOR-$G_{i1}\alpha/G_{o1}\alpha$.

A. DADLE-stimulated high affinity GTPase activity of stably expressed hDOR-$G_{i1}\alpha$ (Ile^{351}).

Cells stably expressing hDOR-$G_{i1}\alpha$ (Ile^{351}) were PTx treated (25ng/ml, 16h) and DADLE-stimulated high affinity GTPase activity was measured in membrane preparations. The pEC_{50} value was 7.5 ± 0.18 (mean ± S.E.M, n=3).

B. DADLE-stimulated high affinity GTPase activity of stably expressed hDOR-$G_{o1}\alpha$ (Ile^{351}).

Cells stably expressing hDOR-$G_{o1}\alpha$ (Ile^{351}) were PTx treated (25ng/ml, 16h) and DADLE-stimulated high affinity GTPase activity was measured in membrane preparations. The pEC_{50} value was 7.32 ± 0.23 (mean ± S.E.M, n=3).

A

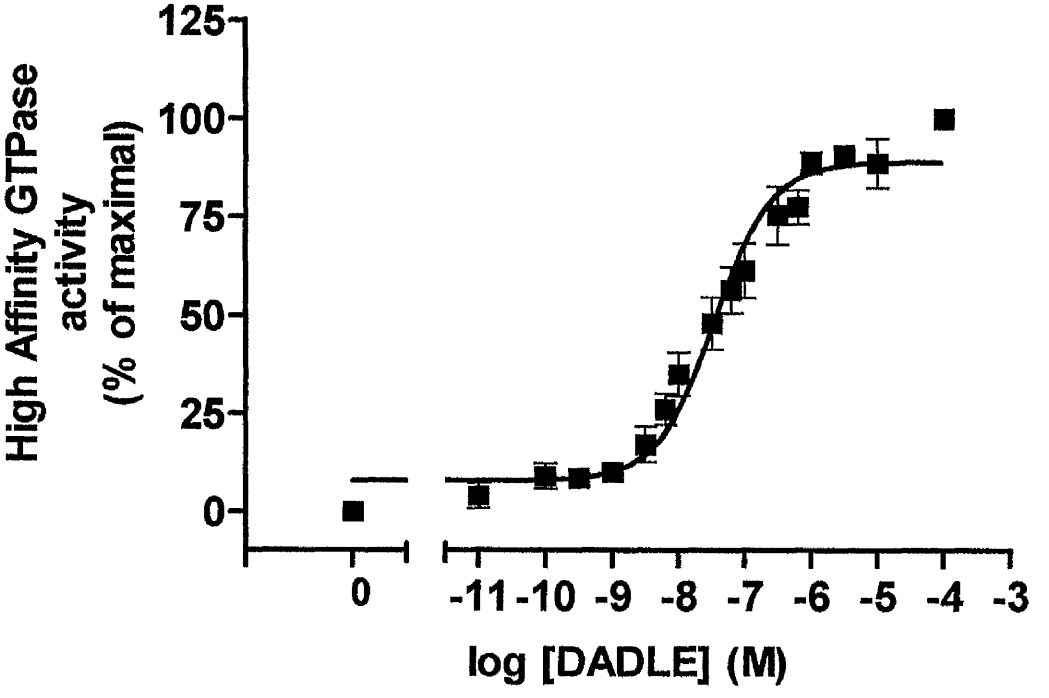
High Affinity GTPase activity (% of maximal)
125
100
75
50
25
0
0
-11 -10 -9 -8 -7 -6 -5 -4 -3
log [DADLE] (M)

B

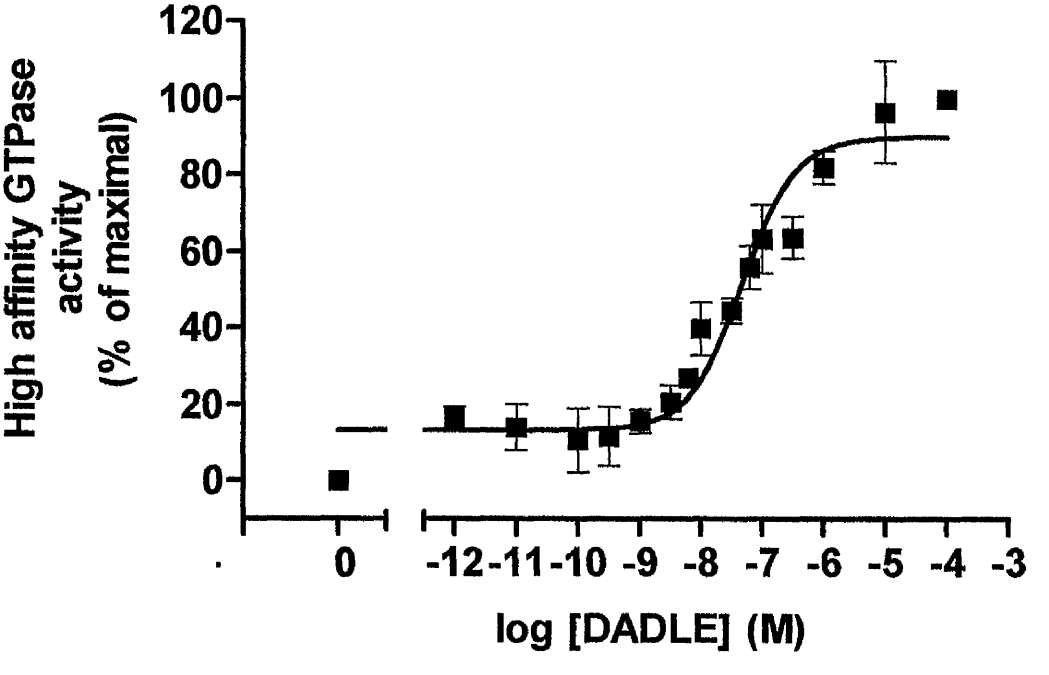
High affinity GTPase activity (% of maximal)
120
100
80
60
40
20
0
0
-12 -11 -10 -9 -8 -7 -6 -5 -4 -3
log [DADLE] (M)

Figure 3.19. The kinetics of DADLE-stimulated GTP hydrolysis of stably expressed hDOR-$G_{i1}\alpha$ (Ile^{351}).

A. DADLE-stimulated high affinity GTP activity at various GTP concentrations

Cells stably expressing hDOR-$G_{i1}\alpha$ (Ile^{351}) were PTx treated (25ng/ml, 16h) and basal (▲) and DADLE (100μM)-stimulated (□) high affinity GTPase activity was measured at increasing concentrations of GTP. This is typical of three experiments performed.

B. Eadie-Hofstee analysis

An Eadie-Hofstee plot was produced from the data of Figure 3.19A. V_{max} was obtained by the difference in y-intercept between the basal (▲) and DADLE-stimulated (□) activity and K_m for GTP was determined by the negative value of the slope of the graph. K_m GTP (basal) was 0.53 ± 0.07 nM and K_m GTP (DADLE) was 0.50 ± 0.08 nM (means ± S.E.M, n=3). GTP turnover number was calculated as 8.07 ± 0.35 min^{-1} (mean ± S.E.M, n=3). This is a typical of three experiments performed.

A

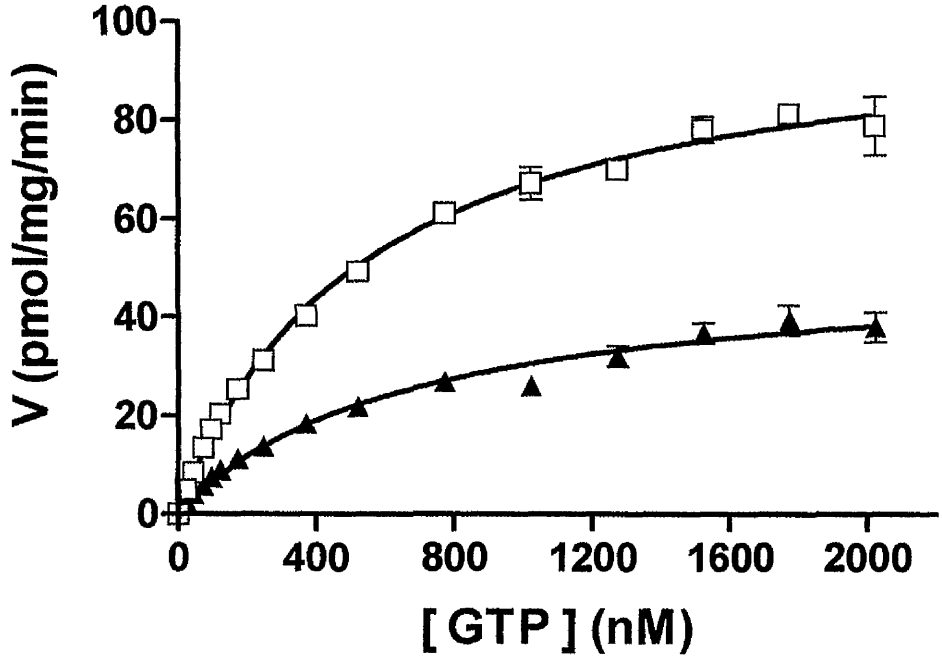
100
80
60
40
20
0
V (pmol/mg/min)
0
400
800
1200
1600
2000
[GTP] (nM)

B

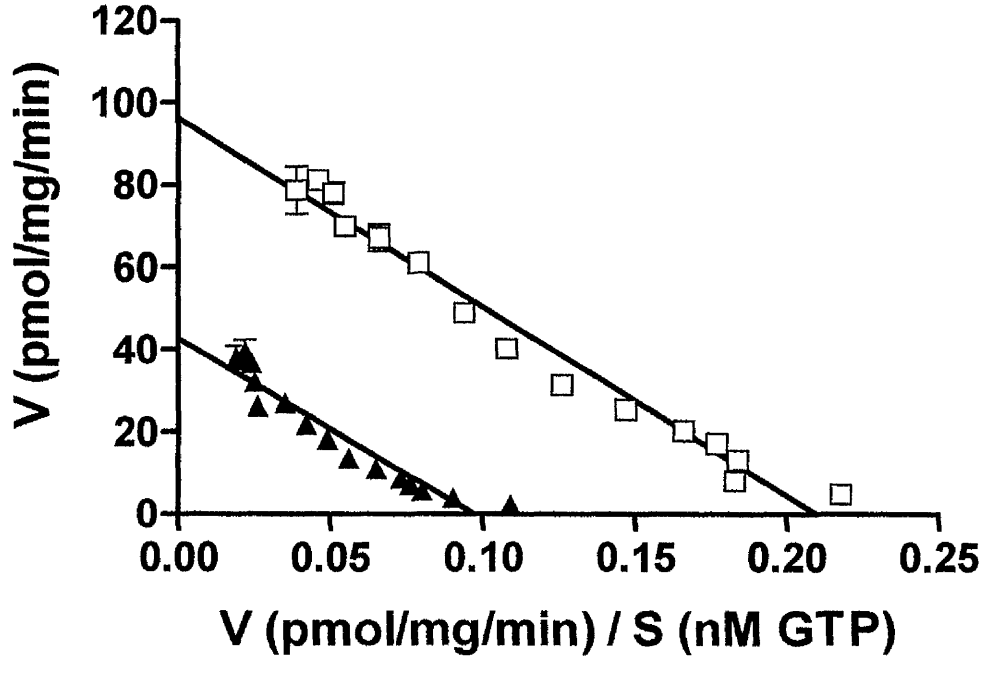
120
100
80
60
40
20
0
V (pmol/mg/min)
0.00
0.05
0.10
0.15
0.20
0.25
V (pmol/mg/min) / S (nM GTP)

Figure 3.20. The kinetics of DADLE-stimulated GTP hydrolysis of stably expressed hDOR-$G_{o1}\alpha$ (Ile^{351}).

A. DADLE-stimulated high affinity GTP activity at various GTP concentrations

Cells stably expressing hDOR-$G_{o1}\alpha$ (Ile^{351}) were PTx treated (25ng/ml, 16h) and basal (▲) and DADLE (100 μM)-stimulated (□) high affinity GTPase activity was measured at increasing concentrations of GTP. This is a typical of three experiments performed.

B. Eadie-Hofstee analysis

An Eadie-Hofstee plot was produced from the data of Figure 3.20A. The K_m GTP (basal) was 0.66 ± 0.09 nM and K_m GTP (DADLE) was 0.47 ± 0.12 nM (means ± S.E.M, n=3). GTP turnover number was calculated as 2.07 ± 0.72 min^{-1} (mean ± S.E.M, n=3). This is a typical of three experiments performed.

A

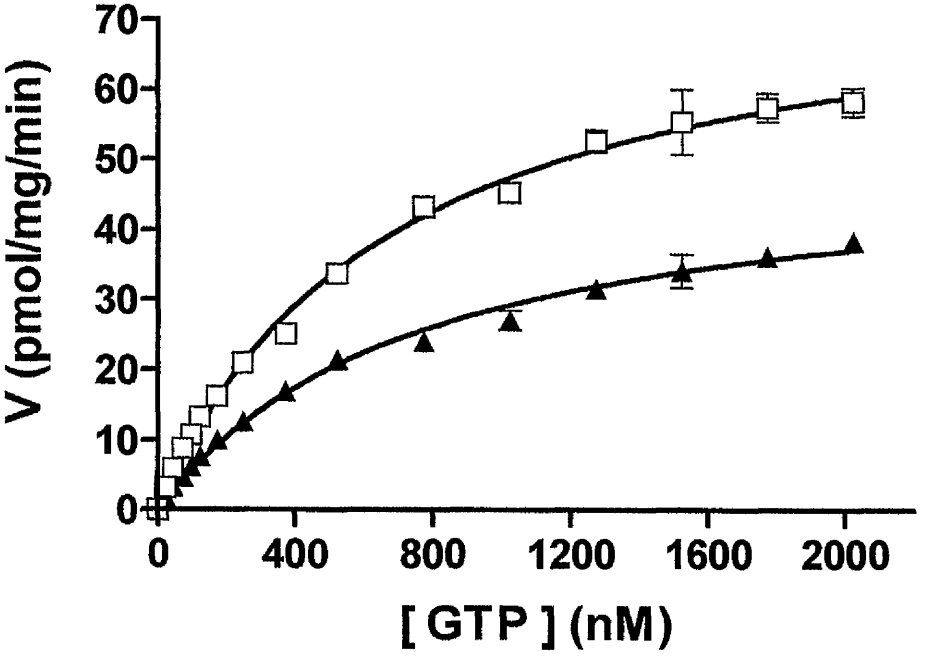
70
60
50
40
30
20
10
0
V (pmol/mg/min)
0
400
800
1200
1600
2000
[GTP] (nM)

B

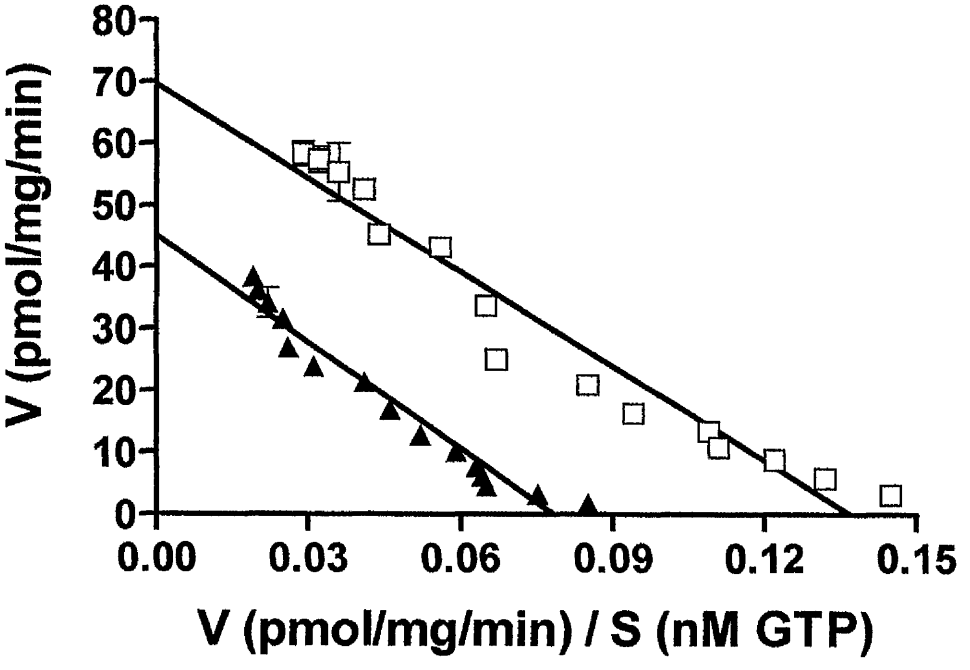
80
70
60
50
40
30
20
10
0
V (pmol/mg/min)
0.00
0.03
0.06
0.09
0.12
0.15
V (pmol/mg/min) / S (nM GTP)

Figure 3.21. Effect of PTx treatment on the high affinity GTPase activity of hDOR-$G_{i1}\alpha$ (Ile^{351}).

Membranes were prepared from a clone stably expressing hDOR-$G_{i1}\alpha$ (Ile^{351}) which was untreated (□) or treated (▲) with PTx (25ng/ml, 16h). DADLE-stimulated GTPase was measured. This is a representative experiment performed in triplicate (mean ± S.D.)

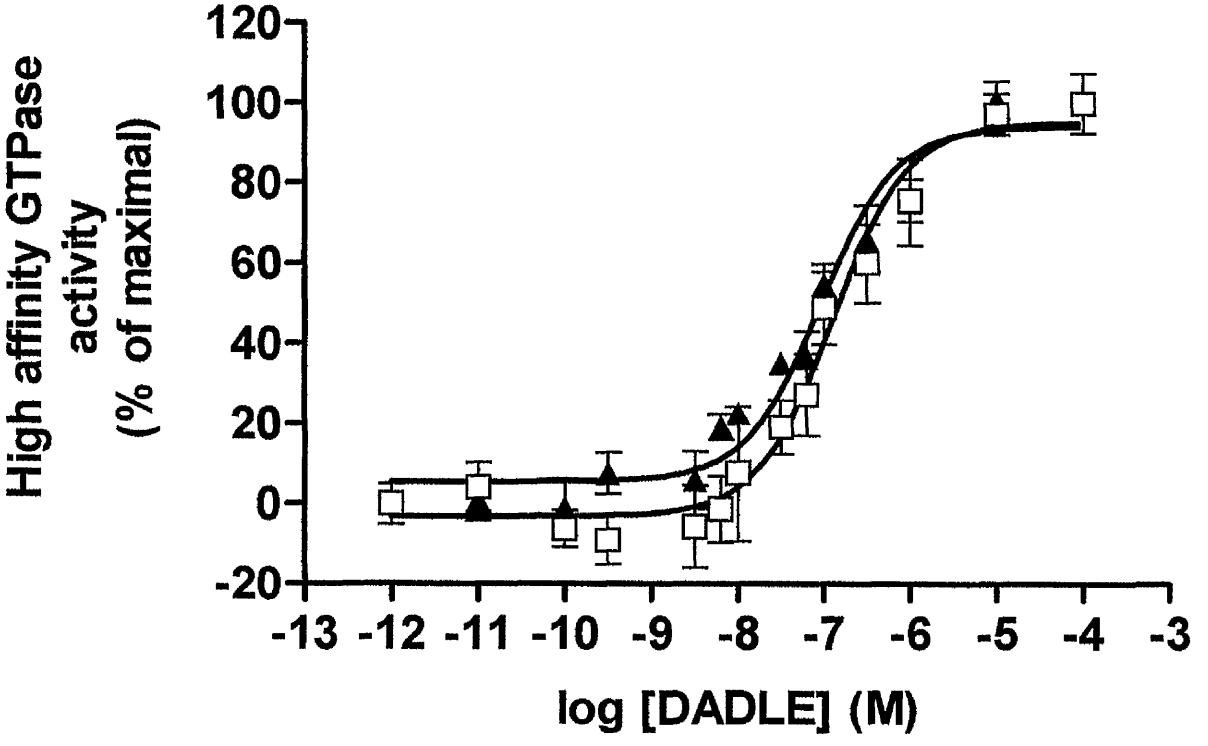
High affinity GTPase activity (% of maximal)
120
100
80
60
40
20
0
-20
-13 -12 -11 -10 -9 -8 -7 -6 -5 -4 -3
log [DADLE] (M)

Figure 3.22 Comparison of DADLE regulation of adenylyl cyclase activity in cells stably expressing hDOR-$G_{i1}\alpha$ (Ile^{351}) and hDOR-$G_{o1}\alpha$ (Ile^{351}) fusion proteins.

A. Effect of hDOR-$G_{i1}\alpha$ (Ile^{351}) on AC activity

Forskolin (50μM) stimulated AC activity was measured in untreated (▲) and PTx (25ng/ml, 16h) treated (□) cells stably expressing hDOR-$G_{i1}\alpha$ (Ile^{351}) as was the effects of increasing concentration of DADLE. The pEC_{50} value for hDOR-$G_{i1}\alpha$ (Ile^{351}) was 10.06 ± 0.38 (mean ± S.E.M, n=3) for untreated and 9.58 ± 0.14 (mean ± S.E.M, n=3) for PTx-treated. This is a typical example of three experiments performed.

B. Effect of hDOR-$G_{o1}\alpha$ (Ile^{351}) on AC activity

Forskolin (50μM) stimulated AC activity was measured in untreated (▲) and PTx (25ng/ml, 16h) treated (□) cells stably expressing hDOR-$G_{o1}\alpha$ (Ile^{351}) as was the effects of increasing concentrations of DADLE. The pEC_{50} value for hDOR–$G_{o1}\alpha$ (Ile^{351}) was 9.84 ± 0.36 (mean ± S.E.M, n=3) for untreated and as 9.32 ± 0.08 (mean ± S.E.M, n=3) for PTx-treated. This is a typical example of three experiments performed.

A

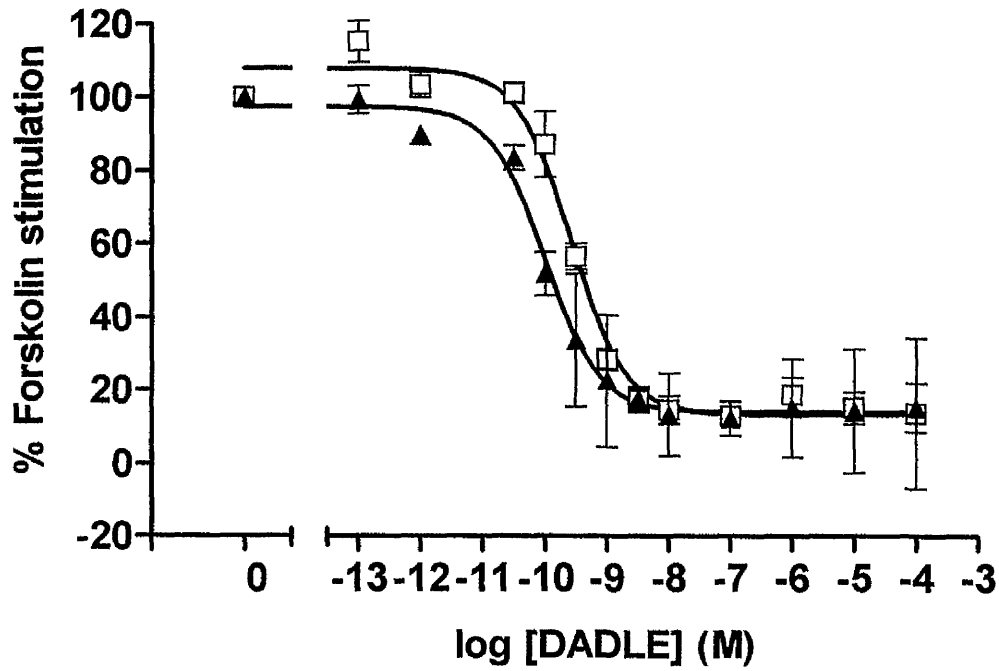
% Forskolin stimulation
120
100
80
60
40
20
0
-20
0
-13 -12 -11 -10 -9 -8 -7 -6 -5 -4 -3
log [DADLE] (M)

B

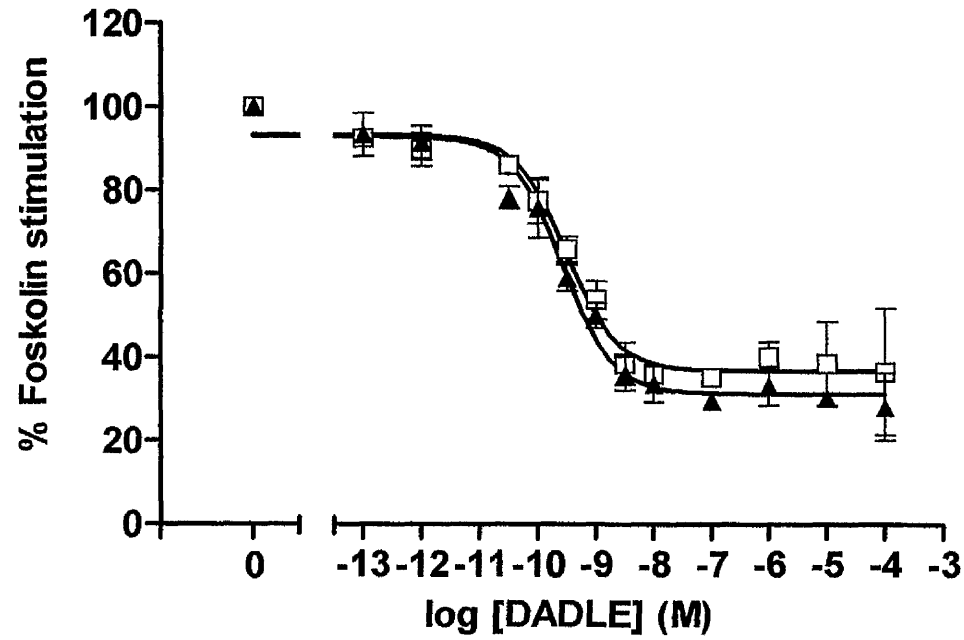
% Foskolin stimulation
120
100
80
60
40
20
0
0
-13 -12 -11 -10 -9 -8 -7 -6 -5 -4 -3
log [DADLE] (M)

Figure 3.23. Graphic representation of the construction of the hMOR-$G_{i1}\alpha$ (Ile^{351}) fusion protein

The cDNA of hMOR-1 was amplified by PCR in order to shorten the 5′ terminal by introducing a *KpnI* site and to remove the stop codon by introducing another *KpnI* site. The sequence amplified by PCR was digested with *KpnI*, purified and ligated into the *KpnI* site of pcDNA3 containing $G_{i1}\alpha$ (Ile^{351}). This fusion protein was fully sequenced prior to use.

Subcloning Strategy

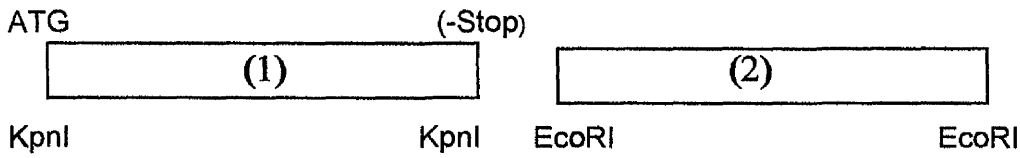

Graphic Representation :

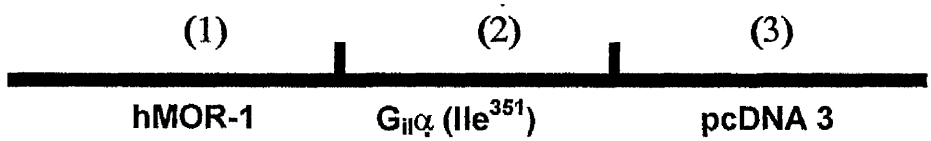

Figure 3.24. Analysis of [^{3}H] diprenorphine binding to transiently expressed hMOR-$G_{i1}\alpha$ (Ile^{351}).

A. [^{3}H] diprenorphine saturation-binding studies to membranes transiently expressing the hMOR-$G_{i1}\alpha$ (Ile^{351}) fusion protein

Following transient expression of the hMOR-$G_{i1}\alpha$ (Ile^{351}) fusion protein and prior PTx treatment (25ng/ml, 16h), [^{3}H] diprenorphine saturation binding studies were performed on membranes of HEK293T cells. This is a representative example of three experiments performed.

B. Scatchard analysis

A Scatchard plot was generated from the data of Figure 3.24A. This is a typical example of three experiments performed in triplicate.

A

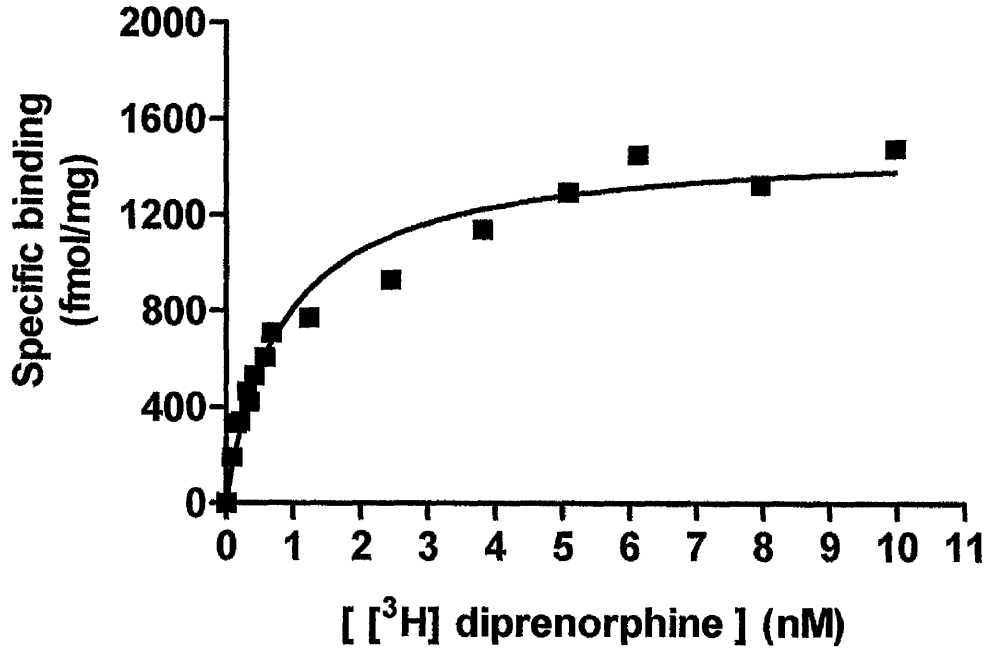
Specific binding (fmol/mg)
2000
1600
1200
800
400
0
0 1 2 3 4 5 6 7 8 9 10 11
[[3H] diprenorphine] (nM)

B

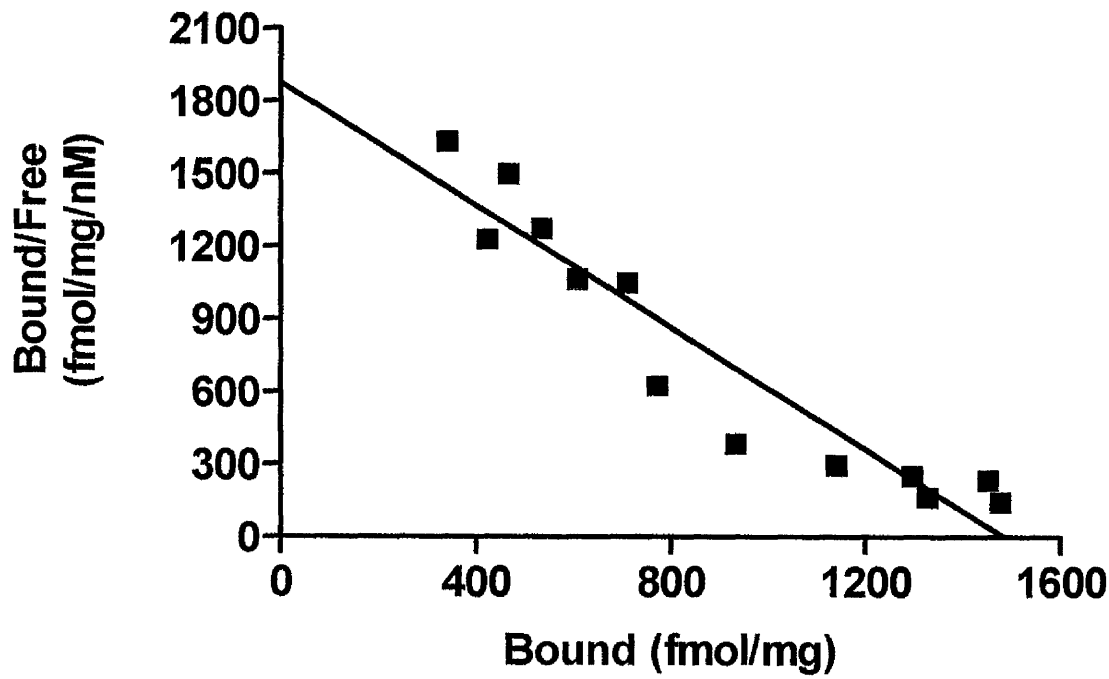
Bound/Free (fmol/mg/nM)
2100
1800
1500
1200
900
600
300
0
0 400 800 1200 1600
Bound (fmol/mg)

Figure 3.25. DADLE stimulates the high affinity GTPase activity of transiently expressed hMOR-$G_{i1}\alpha$ (Ile^{351}).

Following transient expression of hMOR-$G_{i1}\alpha$ (Ile^{351}) and prior PTx treatment (25ng/ml, 16h), high affinity GTPase activity was measured in the presence of varying concentrations of DADLE. Data represent the mean ± S.E.M from three independent experiments.

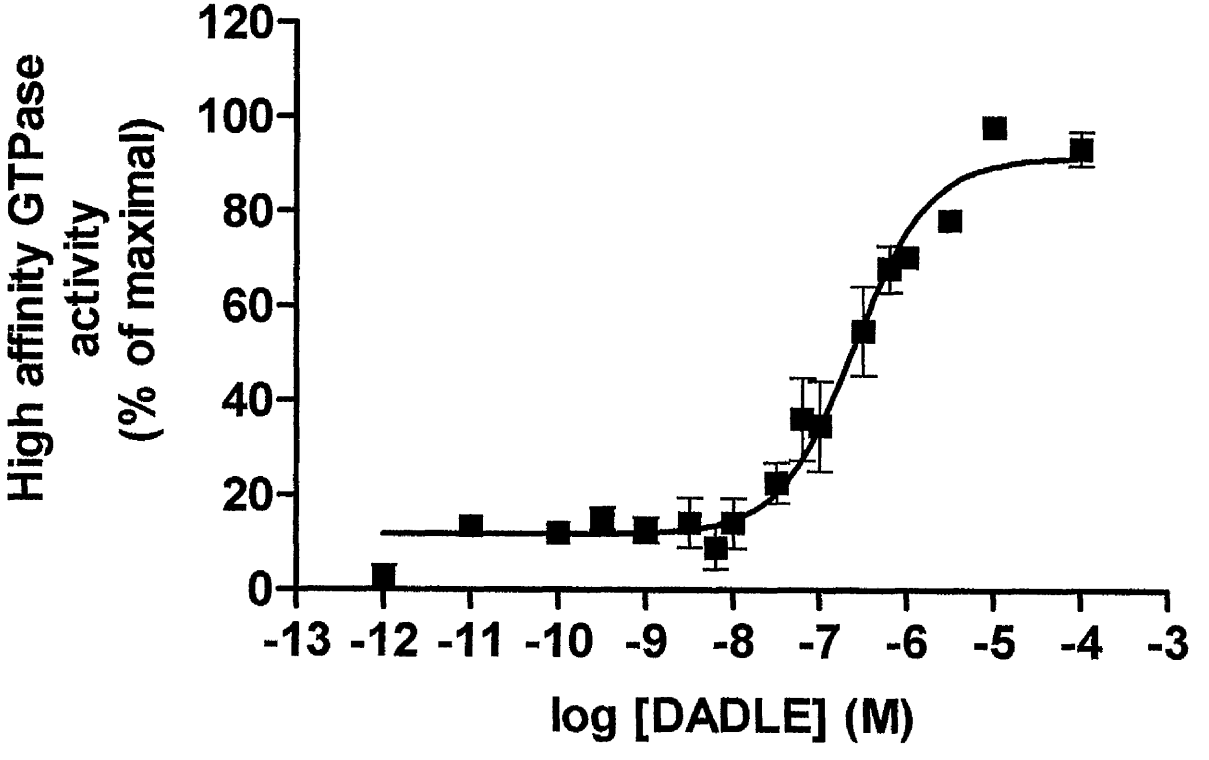
High affinity GTPase activity (% of maximal)
120
100
80
60
40
20
0
-13 -12 -11 -10 -9 -8 -7 -6 -5 -4 -3
log [DADLE] (M)

Figure 3.26. DADLE-stimulated GTP hydrolysis of transiently expressed hMOR-$G_{i1}\alpha$ (Ile^{351}).

A. DADLE-stimulates high affinity GTP activity at various GTP concentrations

Following transient expression of hMOR-$G_{i1}\alpha$ (Ile^{351}) and prior PTx treatment (25ng/ml, 16h), basal (▲) and DADLE (100μM)-stimulated (□) high affinity GTPase activity was measured at increasing concentrations of GTP. This is a representative example of three experiments performed.

B. Eadie-Hofstee analysis

An Eadie-Hofstee plot was produced from the data of Figure 3.26A. This is typical of three experiments performed.

A

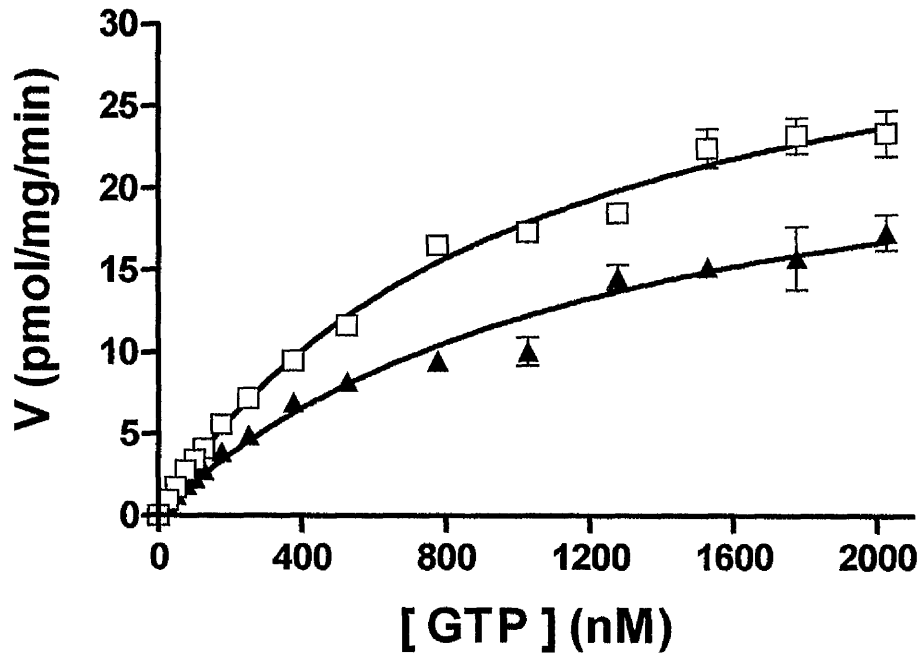
30
25
20
15
10
5
0
V (pmol/mg/min)
0
400
800
1200
1600
2000
[GTP] (nM)

B

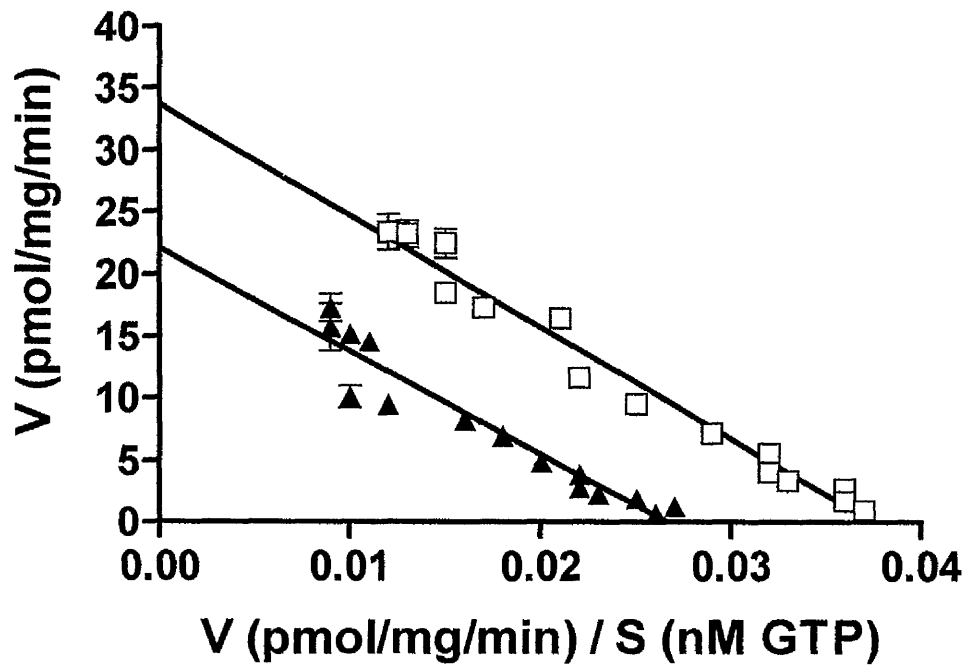
40
35
30
25
20
15
10
5
0
V (pmol/mg/min)
0.00
0.01
0.02
0.03
0.04
V (pmol/mg/min) / S (nM GTP)

CHAPTER IV

Control of the efficiency of agonist-induced information transfer and stability of the ternary complexes containing the δ-opioid receptor and the α-subunits of G_{i1} and G_{o1} by mutation of a receptor/G protein contact interface.

INTRODUCTION (Chapter 4)

The δ, μ and κ opioid receptors are highly homologous, all members of the GPCR superfamily (Knapp *et al.*, 1995: Connor and Christie, 1999: Law *et al.*, 2000). Each mediates the bulk of its effects via activation of members of the Gi family of heterotrimeric G proteins (Connor and Christie, 1999: Law *et al.*, 2000). These opioid receptors can activate both $G_{o1}\alpha$ and $G_{i1}\alpha$, which are closely related, and highly expressed in the central nervous system. Since the initial pharmacological identification of the DOR, considerable effort has been directed toward understanding the signal transduction pathways that couple this receptor to analgesia and other functional responses. It is well established that most DOR-mediated events are dependent on the activity of PTx-sensitive G proteins. It is also well established that DOR-selective ligands inhibit intracellular cAMP levels and modulate the activity of voltage-gated calcium and potassium channels.

Evidence from a wide range of experimental approaches has indicated that the C-terminal region of G protein α subunits plays a key role in the selectivity of interactions with members of the family of GPCRs (Hamm, 1998: Schonerberg *et al.*, 1999: Wess, 1998: Gether and Kobilka, 1998). These include that the *unc* mutation of Gsα, which results from an Arg-Pro alteration 6 amino acids from the C-terminus, prevents productive interactions with GPCRs (Sullivan *et al.*, 1987) and that chimaeric G proteins, in which the extreme C-terminal region is exchanged, alter GPCR coupling specificity (Milligan and Rees, 1999). Through alanine scan

mutagenesis, Osawa and Weiss (1995) identified several residues in the C-terminus of Gtα which affect coupling of the G protein with its cognate receptor. One of the residues identified by Osawa and Weiss (1995) was a cysteine residue, located four amino acids from the C-terminus. Substitution of this residue for tyrosine (C347Y) was seen to result in a loss of G protein/receptor coupling. Similarly, ADP-ribosylation of this residue by PTx has been shown to prevent the coupling of receptor and G protein. Moreover, substitution of the equivalent cysteine residue by glycine in $G_{i1}\alpha$ (Senogles, 1994) or serine in $G_{i3}\alpha$ (Hunt *et al.*, 1994) has been shown to result in a less marked decrease in G protein/receptor coupling.

The importance of C-terminal residues of Gα proteins in receptor coupling was further demonstrated by Conklin *et al* (1993a) when they generated $Gq\alpha/G_{i2}\alpha$ chimeric proteins by replacing 1 to 23 amino acids of the C-terminal region of Gqα with those of $G_{i2}\alpha$. When these chimeric G proteins were co-expressed with A_1 adenosine or D_2 dopamine receptors, which are Giα coupled receptors, functional coupling in HEK293 cells was shown by elevation of agonist stimulated PLC activity. The critical C-terminal residues involved in receptor coupling were further defined to be at the –3 and –4 position from the C-terminus of Gα, using mutation studies of a Gqα/Gzα chimera (Conklin *et al.*, 1996). However, in a study of other chimeric G proteins with substitutions of their extreme C-terminus, it was apparent that not all GPCRs were able to couple as efficiently. For example, replacement of C-terminal amino acids of Gqα with the equivalent Gsα sequence permitted V_2 vasopressin receptor but not β_2-adrenergic receptor (both are Gs coupled GPCRs) to stimulate PLC. Similar replacement of Gsα amino acids with those from Gqα permitted

bombesin and V1a vasopressin receptors but not the oxytocin receptor (all are Gq coupled GPCRs) to stimulate AC (Conklin *et al.*, 1996).

In 1997, Medici *et al.*, expressed a fusion protein between the α-factor receptor (Ste2) and the yeast Gα subunit (Gpa1) into *Saccharomyces cerevisiae* devoid of endogenous *STE2* and *GPA1* genes. In *GPA1* gene deleted yeast cells, the free Gβγ complex constitutively activates the pheromone response pathway, which leads to growth inhibition, and finally lethality in haploid cells. The fusion protein Ste2-Gpa1 was transformed into Gpa1 deficient yeast cells and was able to function as normal Gpa1 by binding Gβγ complex, and hence allowed normal growth. In another fusion protein, the C-terminal portion of Gpa1 was replaced by the corresponding domain of mammalian Gsα. This chimeric protein consists of the N-terminal 362 a.a of yeast Gpa1 and C-terminal 128 a.a of rat Gsα. This chimeric Gpa1-Gsα restored signal transduction in Gpa1-deficient cells only when fused to Ste2. Thus, the function of the G protein C-terminus was mainly to bring Gpa1 in close vicinity to Ste2. It was concluded that the C-terminus of Gα may not have a particular role in transmitting signal from the receptor, but it mainly responsible for ensuring close contact between the receptor and G protein.

In 1999, Fong and Milligan constructed a fusion protein between a FLAG-epitope-tagged human IP prostanoid receptor (FhIPR) and the chimaeric Gα subunit, G_{i1}/Gs6α in which the last 6 a.a of $G_{i1}α$ were replaced with those of Gsα. In this study, functional activities were compared between the freely interacting components and three FhIPR-Gα fusion proteins (FhIPR-Gsα, FhIPR-$G_{i1}α$, FhIPR-G_{i1}/Gs6α) using both [^{35}S] GTPγS binding assays and high affinity GTPase assays. The importance of the C-terminus of Gsα was demonstrated in restoring the coupling

between FhlPR and Gα subunit. Furthermore, unlike the work of Medici *et al*, 1997, these studies support a maintained central role for the G protein C-terminus in GPCR interactions within the fusion protein context.

In fusion proteins, the GPCR C-terminus serves as a tether between the GPCR core and Gα. The length of the C-terminus of different GPCRs is extremely variable (Reneke *et al.*, 1988). The C-termini of the α_{2A}AR and β_2AR comprise 25 and 72 amino acids respectively. This large difference in the length of the C-terminus could significantly impact on receptor-G protein and G protein-effector coupling in fusion proteins. For example, the properties of fusion proteins in which 26 [β_2AR(Δ26)-Gsα_L] or 70 [β_2AR(Δ70)-Gsα_L] residues of the β_2AR C-terminus were deleted were examined and compared with the previously described β_2ARGsα (Wenzel-Seifert *et al.*, 1998). Deletions in the β_2AR C-terminus strongly reduced steady-state GTP hydrolysis, GTPγ[^{35}S] binding activity and AC activity. They concluded that deletion of the receptor C-terminus in β_2ARGsα fusion proteins decreased the mobility of Gsα relative to receptor and thus enhanced basal and agonist-regulated AC activity by slowing down G protein inactivation. In other words, restricting the mobility of G proteins relative to receptors represents a potential mechanism by which signalling efficiency can be modulated.

Conformational changes in this region are associated with G protein activation (Yang *et al.*, 1999). The Gi-family G proteins share a common cysteine residue 4 amino acids from the C-terminus which is the site of action of the ADP-

ribosyltransferase activity of PTx (Milligan, 1998). This modification prevents effective interactions between GPCRs and these G proteins. However, as it is routine for cells to express multiple Gi-family G proteins the molecular identity of the G protein(s) responsible cannot be determined from this alone (Milligan, 1988). In general, treatment of cells expressing an opioid receptor with PTx frequently prevents downstream signalling by opioid agonists (Connor and Christie, 1999).

Many studies have employed mutants of these proteins in which the PTx-sensitive Cys has been altered (Senogles *et al.*, 1994: Chuprun *et al.*, 1997: Yamaguchi *et al.*, 1997: Wise *et al.*, 1997b). This has allowed the elimination of potential interactions of GPCRs with endogenously expressed forms of Gi by prior PTx treatment and analysis of interactions by reconstitution of function provided by the mutated G protein. In studies with the α_{2A}-adrenoceptor Bahia *et al.*, (1998) co-expressed this GPCR along with forms of $G_{i1}\alpha$ in which the PTx-sensitive Cys was replaced by all of the other naturally occurring amino acids. They observed a wide range of capacity of the agonist-occupied receptor to activate the modified forms of the G protein.

Over the years a range of approaches have been taken to explore potential selectivity of different Gi-family G proteins to both interact with opioid receptors and to regulate signal transduction cascades. These include the use of G protein subtype selective antisera (Mckenzie and Milligan, 1990: Georgoussi *et al.*, 1995: Murphy and Makhlouf, 1996: Chalecka-Franaszek *et al.*, 2000), reconstitution studies with purified G proteins (Chan *et al.*, 1995) and strategies which incorporate a covalent label only into G proteins which have become activated by a receptor (Milligan and Mckenzie, 1988: Roerig *et al.*, 1992: Laugwitz *et al.,* 1993: Prather *et al.*, 1994: Chakrabarti *et al.*, 1995). However, it is difficult to explore quantitative aspects of possible

differences in receptor activation of related G proteins using any of these methods. Despite this a range of studies have suggested differential effects of either opioid receptor subtypes to activate the same G protein (Laugwitz *et al.,* 1993: Lee *et al.*, 1998) or of a single receptor subtype to activate closely related G proteins (Laugwitz *et al.,* 1993: Kohno *et al.*, 2000), alteration in the identity of the G proteins associated with opioid receptors when they become activated (Law and Reisine, 1997) or different coupling efficiencies of an opioid receptor to G proteins in different brain regions (Maher *et al.*, 2000). In contrast to this literature, a recent review (Connor and Christie, 1999) concluded that ''notions that different types of opioid receptors intrinsically couple preferentially to one type of effector rather than another should be discarded''.

For the above reasons, both we and a number of other groups have generated fusion proteins between GPCRs and G protein α subunits in which single ORF containing both GPCR and G protein function are produced (Seifert *et al.*, 1999: Milligan, 2000). These comprise a single ORF such that following removal of the stop codon from a DNA encoding a GPCR the G protein α subunit is attached in-frame and thus a single polypeptide encoding both functionalities can be expressed and analysed. The use of such fusion proteins has recently been extensively reviewed (Seifert *et al.*, 1999: Milligan, 2000).

Some benefits and successful examples of this strategy have already been presented in Chapter III. Several researchers, including Colquhoun, (1998) have concluded that specific features of the fusion proteins make them unique tools for investigating a range of pharmacological questions. This has been used for understanding the basis of ligand efficacy in terms of information transfer between the proteins (Carr *et al.*, 1998: Jackson *et al.*, 1999). Secondly, it also has been used to

examine the quantitative effects of point mutations in GPCR and G proteins on the affinity of their interactions (Waldhoer *et al.*, 1999). Using fused tandems of the A_1-adenosine receptor and G protein α-subunits [A_1-$G_{i1}\alpha$ (wild type), A_1-$G_{i1}\alpha$ (Ile^{351}), A_1-$G_{i1}\alpha$ (Gly^{351})], the kinetics of high affinity agonist binding on the ternary complex between agonist, receptor and G protein was investigated as was the importance of Cys^{351} of G proteins for regulating the affinity between the receptor and mutated G proteins.

Most intercellular signal molecules exert their effects through GPCRs that couple to heterotrimeric G proteins, which in turn regulate the activity of effector systems (Gilman, 1987). The extended ternary complex model of receptor activation assumes that GPCRs exist either in an inactive ''R'' state or an active ''R*'' state (Lefkowitz *et al.*, 1993: Leff, 1995). GPCRs can isomerise from R to R* spontaneously, and this imbues constitutive activity to the system. Receptor agonists stabilise the R* state and increase basal G protein activity, whereas inverse agonists stabilise the R state and reduce basal G protein activity (Lefkowitz *et al.*, 1993: Leff, 1995). Neutral antagonists bind equally well to both R and R*, and thus do not alter either the equilibrium between the two states or effector activity.

The basic principle underlying the use of agonist-binding to detect receptor/G protein interactions is that any parameter of the system (for example, agonist affinity) which changes with the conformation of the receptor may be used as a monitor of RG coupling. It is known that receptors exist in two states, R (receptor alone) and RG (receptor coupled to the G protein). The former has a low affinity for agonists, while the latter has a high affinity.

In order to detect high affinity agonist binding in binding assays (either direct or competition), it is necessary to eliminate contamination of the membrane preparation by endogenous GTP or GDP. High affinity agonist binding is measured in radioligand binding assays that employ cell membrane preparations that have been washed to remove guanine nucleotide. The G protein in the agonist high-affinity ternary complex is in the trimeric form (α-subunit coupled to the $\beta\gamma$-dimer). GDP strongly stabilises the trimeric form of the G protein. In binding assays, the concentration of free GDP could be low enough to limit the association of the G protein α subunit and $\beta\gamma$ dimer so that only a fraction of the G protein is in a form that can interact with the receptor to form the high affinity agonist binding state.

Electrostatic, direct hydrogen-bond and van der Waals interactions between two molecules in an aqueous environment are not particularly favorable energetically because there are comparable competing interactions between the molecules in question and the water surrounding them. Water is a very poor solvent for nonpolar molecules compared with most organic liquids. Nonpolar molecules cannot participate in the hydrogen bonding that appears to be so important in liquid water, and aqueous solutions of such molecules have many anomalous physical properties. This relative absence of hydrogen bonds between nonpolar molecules and water causes interactions among the nonpolar molecules: the water causes enhanced interactions among the nonpolar groups themselves, which are much more favorable than it would be the case in ordered solvents. In conclusion nonpolar molecules greatly prefer nonpolar environments. This preference of nonpolar atoms for nonaqueous environments has come to be known as the **hydrophobic interaction.** It is a major factor in the

stabilities of proteins, nucleic acids, and membranes, and it has some unusual characteristics. The hydrophobicities of the individual amino acid side chains have been measured experimentally in a variety of ways, using the free amino acids and amino acids with the amino and carboxyl groups engaged in molecular bonding.

In co-transfection studies with the porcine α_{2A}-adrenoceptor and forms of $G_{i1}\alpha$ in which Cys^{351} was replaced by all other 19 possible amino acids (Bahia *et al.*, 1998), the agonist UK14304 displayed a spectrum of capacity to activate the modified G proteins. This capacity correlated highly with the hydrophobicity of the different amino acids positioned at residue ^{351}. Furthermore, mutationally modified forms of fused $G_i\alpha$ subunits designed to be resistant to the actions of PTx have been used to examine potential selectivity of coupling with a range of other GPCRs. In 1999, Jackson *et al.*, examined the relative intrinsic activity of a series of partial agonists at three distinct fusion proteins that contained the porcine α_{2A}-adrenoceptor and forms of $G_{i1}\alpha$ in which residue ^{351} was either Gly, Cys or Ile. Similar studies in which fusion proteins were constructed between the human 5-HT_{1A} receptor and residue ^{351} mutants of $G_{o1}\alpha$ have also demonstrated variation in agonist relative intrinsic activity with modification of this residue (Dupuis *et al.*, 1999). Furthermore, Leaney and Tinker, (2000) examined the role of isoforms of PTx-sensitive G protein α subunits ($G_{i1}\alpha$, $G_{I2}\alpha$, $G_{i3}\alpha$ and $G_{o1}\alpha$) in mediating coupling between various receptor systems (A_1, α_{2A}, D_{2S}, M_4, $GABA_B1a+2$, and $GABA_B1b+2$) and the cloned neuronal ion channel effectors (Kir3.1+3.2A).

With the benefits of the fusion protein strategy the characteristics of the ternary complex of receptor, agonist and G protein was investigated using high affinity agonist binding studies. Herein, fusion proteins between the hDOR and a range of modified forms of $G_{i1}\alpha$ have been employed to explore the effect of G protein mutation on agonist-GPCR-G protein ternary complex formation and dissociation and the stability of this ternary complex in GPCR to G protein information transfer.

RESULTS (Chapter 4)

Structure of amino acids

Every protein can be viewed as a polymer of amino acids. There are 20 common amino acids. The central carbon is covalently bonded on one side to an amino group (NH_2) and one the other side to a carboxyl group (COOH). A third bond is always hydrogen, and the fourth bond is to a variable side chain (R). **Figure 4.1** introduces the structure of 8 different amino acids that I have used in all my experiments for the hDOR-Gα fusion protein mutants.

[^{3}H] DADLE binding to hDOR and hDOR-$G_{i1}\alpha$ (Ile^{351})/-$G_{o1}\alpha$ (Ile^{351}) fusion proteins

I. Analysis of [^{3}H] DADLE binding to stably expressed isolated hDOR

Agonist-induced exchange of GTP for GDP on a G protein is accepted as the rate-limiting step of the GTP exchange and hydrolysis cycle and reflects enhanced dissociation of GDP from the nucleotide binding site (Gilman *et al.*, 1987). Thus, agonist stimulation of subsequent GTPase activity provides a direct monitor of G protein activation by the agonist-occupied receptor (Gierschik *et al.*, 1994). As the addition of agonist reduces the affinity of the G protein for GDP, then increasing concentrations of GDP would be expected to reduce the binding affinity of [^{3}H] agonist for the receptor. In preliminary membrane binding experiments, [^{3}H] naltrindole and [^{3}H] DADLE saturation binding studies were performed on stably expressed hDOR cell lines **(Figures 4.2A, 4.3A).** Scatchard conversions were obtained from the direct saturation experiments. K_d of [^{3}H] naltrindole was estimated as 0.54 ± 0.36 nM (mean ± range, n=2) and that of [^{3}H] DADLE was 0.85 ± 0.18 nM (mean ± range, n=2) **(Figures 4.2B, 4.3B).** The effectiveness of PTx treatment was optimised for PTx amount (50, 100 ng/ml) and incubation time (12, 24 h) **(Figure 4.4).** In membrane binding experiments which used a single concentration of the agonist [^{3}H] DADLE, addition of GDP caused a concentration-dependent reduction in levels of [^{3}H] DADLE binding to the stably expressed hDOR in HEK293 cells **(Figure 4.5A).** PTx treatment (100 ng/ml, 24h) of cells expressing the hDOR prior to membrane preparation also reduced the level of [^{3}H] DADLE binding. This was to a similar extent as produced by maximally effective concentrations of GDP and following PTx treatment GDP

produced no further reduction in [^{3}H] DADLE (5 nM) binding. In contrast, the binding of the hDOR antagonist [^{3}H] naltrindole (4 nM) to membranes was not reduced by the presence of GDP **(Figure 4.5B).** Prior PTx treatment actually increased levels of binding of [^{3}H] naltrindole by increasing the total number of binding sites **(Figures 4.5B, 4.5C).** Further [^{3}H] naltrindole saturation binding experiments were performed on membranes of untreated and of PTx treated (25ng/ml, 16h) cells stably expressed either hDOR (data not shown) and hDOR-$G_{i1}\alpha$ (Ile^{351}) **(Figure 4.5C).** There was a little change for the hDOR but a significant up-regulation for hDOR-$G_{i1}\alpha$ (Ile^{351}). This showed an increase of receptor number (B_{max}) without alteration of K_d for [^{3}H] naltrindole. In addition, [^{3}H] naltrindole binding at a single concentration of radioligand to membranes of stably expressed hDOR (PTx untreated) was displaced with unlabelled DADLE in a concentration-dependent fashion (data not shown). According to the two-state receptor theory, it could be expected to see the presence of two binding affinity sites. However, it was not possible to detect two such sites. However, in the presence of the poorly hydrolysed analogue of Gpp[NH]p (100 μM) the IC_{50} value for DADLE was moved to higher concentration, which indicated a reduction of binding affinity of DADLE to the hDOR.

II. Analysis of [^{3}H] DADLE binding to stably expressed hDOR-$G_{i1}\alpha$ (Ile^{351}) fusion protein

In preliminary membrane binding experiments, [^{3}H] naltrindole saturation binding experiments were performed on the stably expressed hDOR-$G_{i1}\alpha$ (Ile^{351}) fusion protein (clone no.6) **(Figure 4.6).** The K_d of [^{3}H] naltrindole was 0.47 ± 0.04 nM (mean ± S.E.M, n=3). In addition, [^{3}H] DADLE saturation binding experiments were performed on this stable cell line **(Figure 4.7).** Unlike the isolated receptor, as was expected from the two state receptor theory, both high affinity and low affinity states of [^{3}H] DADLE for this fusion protein could be detected. The K_H of [^{3}H] DADLE was 0.60± 0.16 nM (mean ± S.E.M, n=3). Furthermore, [^{3}H] DADLE binding to membranes of untreated **(Figure 4.8A)** and PTx treated **(Figure 4.8B)** (25ng/ml, 16h) of this cell line was displaced by GDP in a concentration-dependent fashion. Moreover, like the isolated receptor, DADLE had the capacity to compete with [^{3}H] naltrindole to bind to the hDOR-$G_{i1}\alpha$ (Ile^{351}) fusion protein in membranes of PTx treated cells. In the absence of guanine nucleotides, two sites with distinct affinities for DADLE were observed (pKi high affinity = 9.3 ± 0.19, pKi low affinity = 6.5 ± 0.22, means ± S.E.M, n=3), whereas in the presence of either GDP **(Figure 4.9),** or the poorly hydrolysed analogue of GTP, Gpp[NH]p (data not shown) (both 100 μM) a monophasic competition curve (pKi = 6.5 ± 0.25, mean ± S.E.M, n=3) was obtained in which only the low affinity site for DADLE was observed. In contrast, membranes of untreated **(Figure 4. 10A)** and PTx treated **(Figure 4.10B)** cells were prepared and the binding of [^{3}H] naltrindole to the hDOR-$G_{i1}\alpha$ (Ile^{351}) was monitored as GDP concentration was increased. Surprisingly, an increase in [^{3}H] naltrindole binding was detected in both cases. Further [^{3}H]

naltrindole saturation binding experiments were performed on membranes in the presence and the absence of GDP **(Figure 4.10C).** An increase of receptor number was detected without alteration of K_d for [^{3}H] naltrindole.

Table 4.1. Summary of characterisation of stably expressed hDOR-$G_{i1}\alpha$ (Ile^{351}) fusion protein

	hDOR-$G_{i1}\alpha$ (Ile^{351})
K_d for [^{3}H] naltrindole (nM)	0.47 ± 0.04
K_H for [^{3}H] DADLE (nM)	0.60 ± 0.16
pKi high affinity for DADLE	9.3 ± 0.19
pKi low affinity for DADLE	6.5 ± 0.22***

Data represent means ± S.E.M from three independent experiments

*** This data is significantly different from pKi high affinity ($P < 0.0001$).

III. Analysis of [^{3}H] DADLE binding to stably expressed hDOR-$G_{o1}\alpha$ (Ile^{351}) fusion protein

In preliminary membrane binding experiments, [^{3}H] naltrindole saturation binding experiments were performed on the stably expressed hDOR-$G_{o1}\alpha$ (Ile^{351}) fusion protein (clone no.9) **(Figure 4.11).** The K_d of [^{3}H] naltrindole was 0.88 ± 0.35 nM (mean ± S.E.M, n=3). In addition, [^{3}H] DADLE saturation binding experiments were performed on this stable cell line **(Figure 4.12).** Like the hDOR-$G_{i1}\alpha$ (Ile^{351}) fusion protein, two distinct binding affinity sites for [^{3}H] DADLE were detected with this construct. The K_H of [^{3}H] DADLE was 0.75 ± 0.03 nM (mean ± range, n=2). [^{3}H] DADLE binding to membranes of untreated **(Figure 4.13A)** and PTx treated **(Figure 4.13B)** (25ng/ml, 16h) cells was displaced by GDP in a concentration-dependent fashion. Moreover, as with the isolated receptor and the hDOR-$G_{i1}\alpha$ (Ile^{351}) fusion protein, DADLE had the capacity to compete with [^{3}H] naltrindole to bind to the hDOR-$G_{o1}\alpha$ (Ile^{351}) fusion protein in membranes of PTx treated cells. However, in membranes of untreated **(Figure 4. 14A)** and PTx treated **(Figure 4.14B)** cells binding of [^{3}H] naltrindole to the hDOR-$G_{o1}\alpha$ (Ile^{351}) was not affected by GDP.

Table 4.2. Summary of characterisation of stably expressed hDOR-$G_{o1}\alpha$ (Ile^{351}) fusion protein

	hDOR-$G_{o1}\alpha$ (Ile^{351})
K_d for [^{3}H] naltrindole (nM)	0.88 ± 0.35
K_H for [^{3}H] DADLE (nM)	0.75 ± 0.03*

Data represent means ± S.E.M from three independent experiments

***Results are presented as mean ± range from 2 independent experiments.**

[^{3}H] DADLE binding to hDOR-$G_{i1}\alpha$ (Xaa^{351})/-$G_{o1}\alpha$ (Xaa^{351}) fusion proteins

I. Analysis of [^{3}H] DADLE binding to transiently expressed hDOR-$G_{i1}\alpha$ (Xaa^{351}) fusion proteins

Chimeric cDNAs encoding fusion proteins between the hDOR and the α subunit of G_{i1} were produced using a range of forms of $G_{i1}\alpha$ in which the PTx-sensitive Cys^{351} was replaced with other amino acids **(Figures 3.1A, 3.1B).** All of the constructs could be transiently expressed in HEK293T cells as monitored by the appearance of specific binding sites for [^{3}H] naltrindole **(Figure 3.5).** Although levels of expression of the constructs varied between individual transfections there was no specific pattern of expression associated with the identity of the G protein mutant. Saturation binding studies using [^{3}H] naltrindole indicated this ligand was bound with high affinity (K_d, 0.2-0.8 nM) by all the constructs **(Figures 3.6, 3.7).** The capacity of GDP to modulate [^{3}H] DADLE binding (1nM) was then explored in membranes of PTx-treated HEK293T cells following transient expression of 8 distinct forms of the hDOR-$G_{i1}\alpha$ fusion protein in which $residue^{351}$ of the G protein element was Ile, Leu, Phe, Val, Ala, Ser, Gly or Arg. In all cases the binding of [^{3}H] DADLE was reduced in a concentration-dependent fashion by GDP. However, the EC_{50} for GDP varied by more than 10 fold between the different constructs **(Figure 4.15A)** and the pEC_{50} for GDP was correlated strongly with the n-octanol/H_2O partition co-efficient of $residue^{351}$ (a measure of their hydrophobicity) ($R^2 \rightarrow 0.7421$) **(Figure 4.15B).** This was similar to studies with the α_{2A}-adrenoceptor (Bahia *et al.*, 1998) which co-expressed this GPCR

along with forms of $G_{i1}\alpha$ in which the PTx-sensitive Cys was replaced by all of the other naturally occurring 19 amino acids.

II. Analysis of [^{3}H] DADLE binding to transiently expressed hDOR-$G_{o1}\alpha$ (Xaa^{351}) fusion proteins

Using the same approach as for the fusion protein mutants between the hDOR and the forms of the PTx-resistant α subunit of G_{i1}, chimeric cDNAs of hDOR and PTx-resistant $G_{o1}\alpha$ also were produced **(Figure 3.3).** These constructs could be transiently expressed in HEK293T cells as monitored by the appearance of specific binding sites for [^{3}H] naltrindole **(Figure 3.5).** Saturation binding studies using [^{3}H] naltrindole indicated this ligand was bound with high affinity (K_d, 0.2-0.8 nM) by these constructs **(Figures 3.6, 3.7).** The capacity of GDP to modulate [^{3}H] DADLE binding (1nM) was then explored in membranes of PTx-treated HEK293T cells following transient expression of 3 distinct forms of the hDOR-$G_{o1}\alpha$ fusion protein in which residue^{351} of the G protein element was Ile, Leu or Gly. In all cases the binding of [^{3}H] DADLE was reduced in a concentration-dependent fashion by GDP **(Figure 4.16A)** and the pEC_{50} for GDP was correlated with the n-octanol/H_2O partition co-efficient of residue^{351} **(Figure 4.16B)** as noted earlier for the hDOR-G_{i1} (Xaa^{351}) fusion protein mutants **(Figure 4.15B).**

Comparison of the kinetics of [^{3}H] DADLE binding to hDOR-$G_{i1}\alpha$ (Ile^{351})/-$G_{i1}\alpha$ (Gly^{351}) fusion proteins

I. Comparison of potency of GDP and suramin to modulate [^{3}H] DADLE binding to hDOR-$G_{i1}\alpha$ fusion proteins

From Figures 4.15A, 4.15B, hDOR-$G_{i1}\alpha$ fusion proteins containing either Ile or Gly at residue^{351} were selected to compare the precise kinetics of [^{3}H] DADLE binding to the fusion proteins [hDOR-$G_{i1}\alpha$ (Ile^{351}), highest potency for GDP: hDOR-$G_{i1}\alpha$ (Gly^{351}), one example of low potency for GDP]. Membranes from cells transiently expressed hDOR-$G_{i1}\alpha$ (Ile^{351})/-$G_{i1}\alpha$ (Gly^{351}) were prepared and [^{3}H] DADLE binding experiments were carried at increasing concentrations of GDP, which were able to reduce the binding of agonist to both fusion proteins **(Figure 4.17A).** GDP was more potent at the hDOR-$G_{i1}\alpha$ (Gly^{351}) fusion protein (pIC50 = 6.58 ± 0.16, mean ± S.E.M, n=3) than at the hDOR-$G_{i1}\alpha$ (Ile^{351}) fusion protein (pIC50 = 5.78 ± 0.1, mean ± S.E.M, n=3). These values are significantly different (** $P< 0.005$). By contrast, the binding of [^{3}H] naltrindole to either transiently expressed fusion protein was not reduced by GDP **(Figure 4.17B).**

Suramin has been described as a G protein antagonist (Beindl *et al.*, 1996: Freissmuth *et al.*, 1999) as it is able to interfere with information transfer from GPCR to G protein without acting as a competitive antagonist at the GPCR ligand binding site (Beindl *et al.*, 1996: Freissmuth *et al.*, 1999). Increasing concentrations of suramin were also able to limit the binding of [^{3}H] DADLE **(Figure 4.18A)** to the Ile and Gly containing hDOR-$G_{i1}\alpha$ fusion proteins. As with GDP, suramin was more potent at the

hDOR-$G_{i1}\alpha$ (Gly^{351}) fusion protein (pIC50 = 5.28 ± 0.15, mean ± S.E.M, n=3) than at the hDOR-$G_{i1}\alpha$ (Ile^{351}) fusion protein (pIC50 = 4.67 ± 0.15, mean ± S.E.M, n=3) **(Figure 4.18A).** These values are significantly different (**P < 0.01). This effect of suramin did not reflect direct competition at the ligand binding site as the binding of [^{3}H] naltrindole was not reduced by suramin **(Figure 4.18B).**

Table 4.3. Comparison of the potency of GDP and suramin to inhibit [^{3}H] DADLE binding to the hDOR-$G_{i1}\alpha$ fusion proteins

Potency (pIC_{50} values)	hDOR-$G_{i1}\alpha$ (Ile^{351})	hDOR-$G_{i1}\alpha$ (Gly^{351})
GDP	5.78 ± 0.10	6.58 ± 0.16**
Suramin	4.67 ± 0.15	5.28 ± 0.15**

Experiments were performed with 1 nM [^{3}H] DADLE.

Data represent means ± S.E.M from 3 independent experiments

** **Significantly different from the hDOR-$G_{i1}\alpha$ (Ile^{351}), P < 0.005 for GDP, P < 0.01 for suramin.**

II. Association and dissociation kinetics of [^{3}H] DADLE binding to hDOR-$G_{i1}\alpha$ fusion proteins

To explore the basis for the difference in GDP effects on [^{3}H] DADLE binding hDOR-$G_{i1}\alpha$ fusion proteins containing Ile or Gly at residue^{351} of the G protein element were used. The binding rate of [^{3}H] DADLE (1.2 nM at 25 ° C) to these constructs was indistinguishable with $K_{observed} = 0.27 \pm 0.04$ min^{-1} for Gly and 0.25 ± 0.06 min^{-1} for the Ile containing construct (means ± S.E.M, n=3) **(Figure 4.19A, Table 4.4).**

However, following attainment of steady-state levels of [^{3}H] DADLE binding, addition of a marked excess of the opioid antagonist naloxone (10μM) demonstrated the rate of dissociation of [^{3}H] DADLE to be distinct, with the Gly containing construct ($K_{off} = 0.183 \pm 0.023$* min^{-1}) substantially greater than the Ile-containing one ($K_{off} = 0.072 \pm 0.009$ min^{-1}) **(Figure 4.19B, Table 4.4).** These values are significantly different (*$P < 0.01$).

These values produced a kinetically estimated K_d for [^{3}H] DADLE of 0.5 nM for the Ile^{351} construct but a 5 fold higher value (2.5 nM) for the Gly^{351} containing fusion protein **(Table 4.4).**

I would like to describe more precisely how these estimates of K_d were calculated.

- For hDOR-$G_{i1}\alpha$ (Ile^{351}) (PTx treated, 25ng/ml, 16h)

[^{3}H] DADLE (1.2 nM at 25 ° C)

$K_{off} = 0.072 \pm 0.009$ min^{-1}

$K_{observed} = 0.25 \pm 0.06$ min^{-1}

According to the equation,

$$K_{on} = \frac{K_{ob} - K_{off}}{[\text{radioligand}]\ (\text{nM})}$$

$$K_{on} = \frac{0.25 - 0.072}{1.2} = 0.144\ \text{nM}^{-1}\ \text{min}^{-1}$$

$$K_d = \frac{K_{off}}{K_{on}} = \frac{0.072}{0.144} = 0.5\ \text{nM}$$

- hDOR-$G_{i1}\alpha$ (Gly^{351}) (PTx treated, 25ng/ml, 16h)

[^{3}H] DADLE (1.2 nM at 25 ° C)

$K_{off} = 0.183 \pm 0.023\ \text{min}^{-1}$

$K_{observed} = 0.27 \pm 0.038\ \text{min}^{-1}$

According to the equation,

$$K_{on} = \frac{K_{ob} - K_{off}}{[\text{radioligand}]\ (\text{nM})}$$

$$K_{on} = \frac{0.27 - 0.183}{1.2} = 0.072\ \text{nM}^{-1}\ \text{min}^{-1}$$

$$K_d = \frac{K_{off}}{K_{on}} = \frac{0.183}{0.072} = 2.5\ \text{nM}$$

Equivalent differences between the constructs were obtained whether the kinetic assays were performed at 25°C or 37°C or if dissociation was monitored following addition of an excess of antagonist or by limiting dilution of the assay (data not shown).

Very similar values for these two constructs were obtained from direct equilibrium [^{3}H] DADLE saturation binding studies **(Figures 4.20A, 4.21A, Table**

4.4). The K_d for direct [^{3}H] DADLE saturation binding for hDOR-$G_{i1}\alpha$ (Ile^{351}) was 0.68 ± 0.05 nM and that for hDOR-$G_{i1}\alpha$ (Gly^{351}) was 2.1 ± 0.38* nM (means ± S.E.M, n=3) **(Figures 4.20B, 4.21B, Table 4.4).** These values are significantly different (*P < 0.01).

Table. 4.4. Association and dissociation kinetics of the binding of [^{3}H] DADLE to hDOR-$G_{i1}\alpha$ fusion proteins

	hDOR-$G_{i1}\alpha$ (Ile^{351})	hDOR-$G_{i1}\alpha$ (Gly^{351})
$K_{observed}$ (min^{-1})	0.245 ± 0.057	0.27 ± 0.038
K_{on} (nM^{-1}/min^{-1})	0.150 ± 0.043	0.066 ± 0.019*
K_{off} (min^{-1})	0.072 ± 0.009	0.183 ± 0.023*
Dissociation ($t_{1/2}$) (min)	10.1 ± 1.2	3.9 ± 0.42*
K_d (nM) kinetic measure	0.50	2.54
K_d (nM) equilibrium binding	0.68 ± 0.05	2.1 ± 0.38*

Kinetic experiments were performed with [^{3}H] DADLE (1.2nM, 25 °C).

Dissociation experiments were monitored following the addition of naloxone (10 μM).

Data represent means ± S.E.M from 3 independent experiments.

***Significantly different, P < 0.01.**

*** Significantly different, P < 0.05.**

DISCUSSION (Chapter 4)

Addition of agonist reduces the affinity of the G protein for GDP and increasing concentrations of GDP reduced the binding affinity of [^{3}H] DADLE for the hDOR and hDOR-$G_{i1}\alpha$ (Ile^{351})/-$G_{o1}\alpha$ (Ile^{351}).

I have taken advantage of a fusion protein strategy in which either $G_{o1}\alpha$ or $G_{i1}\alpha$ were linked directly to the C-terminal tail of the hDOR. In a variety of studies mutated forms of G protein α subunit cDNAs have been produced to allow expression of fusion proteins between a GPCR and the G protein. The benefits of this strategy have recently been extensively reviewed (Milligan, 2000: Seifert *et al.*, 1999). This ensures that the proximity of the receptor to each G protein is identical, that they are expressed in equal ratios and most importantly that the levels of each G protein can be easily measured (Seifert *et al.*, 1999: Milligan, 2000). As the fusion proteins have a 1:1 stoichiometry of receptor to G protein, saturation binding studies with an antagonist ligand provide direct measures of G protein, as well as receptor, expression levels.

It is well known that agonists can demonstrate high affinity for receptor states due to the promotion of G protein coupling. This leads to differences in the apparent amount of total receptor density when measured with antagonist radioligands (where the complete receptor population is measured) and agonist radioligands (where only G protein complexed receptors are generally measured). For example, in human brain, the α_2-adrenoceptor agonist radioligand [^{3}H] clonidine measures a high-affinity

binding density of 47 fmol/mg of protein, while a radioligand antagonist [^{3}H] RX821002 measures a considerably larger number (95 fmol/mg of protein) (Kenakin, 1997).

Table 4.5. Properties of antagonist and agonist radioligands

Radioligand	Properties	Uses
Antagonist	① high-affinity ② low dissociation rate-constant ③ insensitive to conformational state	① determining total receptor numbers ② competition experiments with unlabelled compounds
Agonist	① high and low affinity binding sensitive to conformational state	① identifying RG coupling

In 1999, Waldhoer *et al.*, using the fusion protein strategy, examined the kinetics of ternary complex formation with fusion proteins composed of the A_1-adenosine receptor and G protein α–subunits. Binding of the agonist to form a ternary complex with the GPCR and G protein decreased the binding affinity of GDP for the G protein. The ability of GDP to suppress the formation of the ternary complex was examined. Because the activated receptor reduces the affinity of the G protein for GDP (by promoting GDP release), an excess of GDP conversely lowers the affinity of the G protein for the receptor (Hepler and Gilman, 1992). Seifert *et al.*, (1999), using a β_2AR-Gs fusion protein, examined the effects of different purine nucleotides [GTP, ITP, and XTP] on receptor/G protein coupling. They demonstrated that these purine nucleotides were useful tools to detect ligand-specific G protein-coupling states of receptors. They concluded that the efficacy and potency of a panel of β_2AR ligands

are affected by the nucleotide bound to Gsα and that purine nucleotides differentially disrupt the ternary complex stabilised by different ligands, supporting the concept of multiple active receptor conformations.

In preliminary binding experiments utilising the stable expressed isolated hDOR, [^{3}H] naltrindole and [^{3}H] DADLE saturation binding experiments were performed. **Figure 4.2 and Figure 4.3** are representative [^{3}H] naltrindole and [^{3}H] DADLE saturation binding experiments respectively. Membranes expressing this receptor were prepared and their B_{max} and K_d for ligand measured. The K_d for [^{3}H] naltrindole at hDOR was 0.54 ± 0.36 nM (mean ± range, n=2) and that for [^{3}H] DADLE was 0.85 ± 0.18 nM (mean ± range, n=2). **Figure 4.4** was one independent experiment to show the effectiveness of PTx treatment on [^{3}H] DADLE binding to the stably expressed hDOR. Binding affinity of [^{3}H] DADLE was decreased with increasing concentrations of GDP. However no effect of GDP was observed following PTx treatment, which caused a decrease of apparent receptor number for [^{3}H] DADLE **(Figure 4.5A).** The effects of pre-treatment of the cells with PTx or addition of GDP (100 μM) to membranes on the binding of [^{3}H] DADLE and [^{3}H] naltrindole was assessed **(Figure 4.5B).** It was observed that the specific binding of a single concentration of the agonist [^{3}H] DADLE, but not the antagonist [^{3}H] naltrindole, was reduced substantially by both treatments. However, these two elements were not additive, as GDP had no further effect following PTx treatment. There was an increase of specific binding of [^{3}H] naltrindole after PTx treatment of cells expressing the hDOR. In order to explain this [^{3}H] naltrindole saturation binding studies to the stably expressed hDOR-$G_{i1}\alpha$ (Ile^{351}) was performed on membranes of PTx untreated and pre-treated (25ng/ml, 16h) cells. These demonstrated up-regulation of receptor with PTx treatment **(Figure**

4.5C).

I selected Ile for the replacement for the bulk of the experiments as it had previously been demonstrated that positioning of a hydrophobic amino acid at this location provides the most effective interface between GPCR and G protein (Bahia *et al.*, 1998). Two stable cell lines of the hDOR-$G_{i1}\alpha$ (Ile^{351}) (Clone no.6) and hDOR-$G_{o1}\alpha$ (Ile^{351}) (clone no.9) were established **(Figure 3.13). Figure 4.6 and Figure 4.7** are representative [^{3}H] naltrindole and [^{3}H] DADLE saturation binding experiments for hDOR-$G_{i1}\alpha$ (Ile^{351}). The K_d for [^{3}H] naltrindole at hDOR-$G_{i1}\alpha$ (Ile^{351}) after PTx treatment (25ng/ml, 16h) was 0.47 ± 0.04 nM (mean ± S.E.M, n=3). As expected from two-state receptor theory, both high affinity and low affinity states were detected from direct [^{3}H] DADLE saturation-binding curves. Conversion of binding data to a Scatchard plot showed the high affinity site for [^{3}H] DADLE for this construct as 0.60 ± 0.16 nM (mean ± S.E.M, n=3). It was surprised to see the clear two site binding states with this construct. Classically it has been difficult problem to detect these two site states in expressed isolated receptor. I think that it was possible because the structure of fusion protein has 1:1 fixed stoichiometry, which provides same ratio between receptor and fused G protein, compared to only receptor expression in the cell lines. Binding of [^{3}H] DADLE on membranes of this cell line with PTx untreated and pre-treated was decreased with increasing concentrations of GDP. However no effect of the binding of [^{3}H] DADLE was observed following PTx treatment, which showed to be resistant by PTx treatment into this construct **(Figures 4.8A, 4.8B).**

With the displacement experiment, the above results were confirmed in studies in which the binding of [^{3}H] naltrindole to the hDOR-$G_{i1}\alpha$ (Ile^{351}) fusion protein was

competed for by increasing concentrations of DADLE **(Figure 4.9, Table 4.1).** In the absence of added guanine nucleotides, two clearly distinct affinity states for DADLE (pKi high affinity, 9.3 ± 0.19; pKi low affinity, 6.5 ± 0.22, means ± S.E.M, n=3, P < 0.0001***) were identified whereas in the presence of either Gpp[NH]p or GDP a monophasic displacement curve was obtained (pKi = 6.5 ± 0.25, mean ± S.E.M, n=3) corresponding to a low affinity state for DADLE. Although this is a classical expectation from two-state receptor theory, the expression of this feature in the fusion protein was substantially more pronounced than is often observed in such studies with co-expressed but separate receptors and G proteins, with the K_i values for DADLE differing by over 200 fold. The estimated % of high affinity agonist binding sites in the absence of guanine nucleotides (42-46%) was also substantial, suggesting that the proximity of GPCR and G protein within the fusion construct encouraged these interactions. When a similar experiment was tried on membranes stably expressing the isolated hDOR, two agonist affinity sites were not clearly distinct in the absence of guanine nucleotides but the displacement was moved to lower affinity in the presence of Gpp[NH]p (data not shown). Distinct agonist affinity states of a β_2AR-Gsα fusion protein have also recently been monitored in ligand binding studies (Seifert *et al.*, 1999: Seifert *et al.*, 1999: Wenzel-Seifert and Seifert, 2000). The effect of guanine nucleotides on such agonist competition curves is to decrease the affinity and increase the Hill slope from the biphasic to the monophasic curves. In a two-site model, nucleotides decrease the affinity of the agonist at the high affinity site or decrease the proportion of high-affinity sites. This indicates that the agonist ligand can sense the difference between two states of the hDOR-$G_{i1}\alpha$ fusion proteins even though the protein partners cannot formally separate.

Binding of [^{3}H] naltrindole to hDOR-$G_{i1}\alpha$ (Ile^{351}) in PTx untreated and treated

membranes (25ng/ml, 16h) **(Figures 4.10A, 4.10B)** was performed at increasing concentrations of GDP. Surprisingly two independent experiments showed an increase of receptor binding at high concentrations of GDP. However no effect of the binding of [^{3}H] naltrindole was observed following PTx treatment. To explain this result, further [^{3}H] naltrindole saturation binding studies were performed on membranes of stably expressed hDOR-$G_{i1}\alpha$ (Ile^{351}) in the absence and the presence of 100 μM GDP, which also resulted in an increase of receptor binding for [^{3}H] naltrindole with minor alteration of the K_d in the presence of GDP **(Figure 4.10C).** I would like to give some possible reasons. According to my previous result, the K_d for [^{3}H] naltrindole for the hDOR-$G_{i1}\alpha$ (Ile^{351}) fusion protein (0.77 ± 0.12 nM, mean ± S.E.M, n=3) was about 6 times higher than for the hDOR-$G_{i1}\alpha$ (Gly^{351}) fusion protein (0.13 ± 0.02 nM, mean ± S.E.M, n=3) (***P< 0.001) **(Table 3.1).** It has been considered that naltrindole is a neutral δ-antagonist and it can prevent the activity of an inverse agonist (Neilan *et al.*, 1999). One possibility to explain these different K_d values for the same receptor is that naltrindole behaves as an inverse agonist on the hDOR-$G_{i1}\alpha$ (Ile^{351}) fusion protein, which may have greater constitutive activity due to the mutation to the strong hydrophobic, aliphatic amino acid, Ile, but not on the Gly^{351} residue containing fusion protein. In support of the above explanation, spiperone has been described as an inverse agonist at the human 5-HT_{1A} receptor, able to reduce basal, agonist-independent, signal transduction (Barr and Manning, 1997). Spiperone functioned as an inverse agonist in membranes expressing the 5-HT_{1A}-$G_{i1}\alpha$ (wild type) fusion protein and in those expressing 5-HT_{1A}-$G_{i1}\alpha$ (Ile^{351}) but not a 5-HT_{1A}-$G_{i1}\alpha$ (Gly^{351}) fusion protein (Kellet *et al.*, 1999). Therefore I think that these increases are because of an inverse agonistic property of naltrindole for the stably expressed hDOR-$G_{i1}\alpha$

(Ile^{351}). However I was unable to observe such an effect following transient expression of hDOR-$G_{i1}\alpha$ (Ile^{351}) (data not shown) or stable expression of hDOR-$G_{o1}\alpha$ (Ile^{351}) **(Figure 4.14).**

[^{3}H] naltrindole and [^{3}H] DADLE saturation binding studies were carried for the stably expressed hDOR-$G_{o1}\alpha$ (Ile^{351}) fusion protein. **Figure 4.11 and Figure 4.12** are representative [^{3}H] naltrindole and [^{3}H] DADLE saturation binding experiments. The K_d for [^{3}H] naltrindole at hDOR-$G_{o1}\alpha$ (Ile^{351}) after PTx treatment (25ng/ml, 16h) was 0.88 ± 0.35 nM (mean ± S.E.M, n=3). Both high affinity and low affinity sites were detected from direct [^{3}H] DADLE saturation-binding studies. Conversion of binding data to Scatchard plots showed the high affinity site for [^{3}H] DADLE at hDOR-$G_{o1}\alpha$ (Ile^{351}) as 0.75 ± 0.03 nM (mean ± range, n=2). Binding of [^{3}H] DADLE was decreased with increasing concentrations of GDP in both untreated and PTx treated membranes. However no effect on the binding of [^{3}H] DADLE was observed following PTx treatment **(Figures 4.13A, 4.13B).** The binding studies of [^{3}H] naltrindole to hDOR-$G_{o1}\alpha$ (Ile^{351}) with PTx untreated **(Figure 4.14A)** and treatment (25ng/ml, 16h) **(Figure 4.14B)** were performed with increasing concentrations of GDP. No GDP effect was observed on the binding of [^{3}H] naltrindole and PTx treatment had no effect on the binding of [^{3}H] naltrindole, which was different from the observation from the hDOR-$G_{i1}\alpha$ (Ile^{351}). Binding of [^{3}H] naltrindole to the hDOR-$G_{o1}\alpha$ (Ile^{351}) was competed for by increasing concentrations of DADLE in the absence of added guanine nucleotides and the presence of either Gpp[NH]p or GDP (data not shown).

The capacity of GDP to modulate [^{3}H] DADLE binding to membranes of PTx-treated HEK293T cells following transient expression of hDOR-$G_{i1}\alpha$ (Xaa^{351})/-$G_{o1}\alpha$ (Xaa^{351}) fusion protein mutants

Agonist-induced information transfer from GPCR to G protein is dependent upon the capacity of the ligand to promote the dissociation of GDP from the nucleotide-binding pocket of the G protein and thus allow exchange for GTP. As this is the rate limiting step of the cycle of G protein activation and deactivation (Gilman, 1987) it can be monitored by following the subsequent rate of hydrolysis of GTP.

In the current studies, I demonstrated that the identity of residue^{351} of $G_{i1}\alpha$ alters both the effectiveness of agonist-induced activation of the G protein by the hDOR and determines the stability of a ternary complex between agonist, hDOR and $G_{i1}\alpha$ by altering its rate of dissociation. These two features are likely to be inherently related as effective maintenance of the ternary complex is required to allow agonist-induced information transfer between the partner proteins. A recent novel insight derived from GPCR-G protein fusion proteins containing point mutations in the G protein C-terminal region is how these alter the affinity of interaction between the GPCR and G protein (Waldhoer *et al.*, 1999). In these studies, two approaches were used to estimate the affinity of the receptor for the mutated G protein moiety in the tandem. First, the ability of GDP to suppress the formation of the ternary complex was determined. Because the activated receptor reduces the affinity of the G protein for GDP (by promoting GDP release), an excess of GDP conversely lowers the affinity of the G protein for the receptor (Hepler and Gilman, 1992). The inhibition of high

affinity binding of (–)-N^6-3[^{125}I](iodo-4-hydroxy phenylisopropyl adenosine, to membranes prepared from HEK293 cells expressing A_1-$G_{i1}\alpha$ (wild type) as well as the A_1-$G_{i1}\alpha$ (Ile^{351}) and A_1-$G_{i1}\alpha$ (Gly^{351}) fusion proteins by GDP was then observed. The second approach relied on the use of suramin, a G protein antagonist, which binds directly to G protein α-subunits (Freissmuth *et al.*, 1996) and competes with the activated receptor for binding to the G protein. High affinity agonist binding to A_1-$G_{i1}\alpha$ fusion proteins mutated at Cys^{351} of the $G_{i1}\alpha$ moiety was suppressed by suramin as well. It was concluded that $G_{i1}\alpha$ (Gly^{351}) exhibited the lowest affinity for the A_1 adenosine receptor. Such results are consistent with the rank order of affinity of the A_1 adenosine receptor for this G protein being greatest for wild type and lowest for $G_{i1}\alpha$ (Gly^{351}). Equivalent experiments on a range of hDOR-$G_{i1}\alpha$ fusion containing only a variation of the amino acids (Ile, Ala, Gly, Ser, Arg, Val, Leu, Phe) at this position produced a picture in which there was strong correlation between the partition coefficient of each amino acids between n-octanol and H_2O (a measure of their hydrophobicity) and the pEC_{50} for GDP-mediated reduction in [^{3}H] DADLE binding ($R^2 \rightarrow 0.7421$) **(Figures 4.15A, 4.15B).** Similar experiments with hDOR-$G_{o1}\alpha$ fusion proteins containing different amino acids (Ile, Leu, Gly) were performed. This also resulted in a correlation between the partition coefficient of each amino acids between n-octanol and H_2O and the pEC_{50} for GDP-mediated reduction in [^{3}H] DADLE binding **(Figures 4.16A, 4.16B),** although with only 3 amino acids tested it is not possible to argue the importance of these observations.

Comparison of the kinetics of [^{3}H] DADLE binding to hDOR-$G_{i1}\alpha$ (Ile^{351})/-$G_{i1}\alpha$ (Gly^{351}) fusion proteins.

I selected the hDOR-$G_{i1}\alpha$ (Ile^{351}) and hDOR-$G_{i1}\alpha$ (Gly^{351}) fusion proteins as marked examples of the observed differences in GDP regulation of [^{3}H] DADLE binding. In 1999, Waldhoer *et al.*, using the fusion protein strategy, showed that the association of receptor and G protein is not rate-limiting; in contrast, the stability of the ternary complex is limited by the dissociation rate of the G protein. In other words, this suggested that the fidelity of receptor-G protein coupling is achieved by a kinetic proof-reading mechanism.

In these studies, I explored the stability of ternary complexes of two different mutant fusion proteins by measuring the association and dissociation kinetics of agonist binding. Previously PTx treatment had no effect on the binding of [^{3}H] DADLE to either the hDOR-$G_{i1}\alpha$ (Ile^{351}) or hDOR-$G_{i1}\alpha$ (Gly^{351}) fusion proteins as these are resistant to the actions of the toxin. However, in both cases increasing concentrations of GDP again reduced [^{3}H] DADLE binding **(Figure 4.17A).** It was obvious that higher concentrations of GDP were required to restrict the binding of [^{3}H] DADLE to the hDOR-$G_{i1}\alpha$ (Ile^{351}) fusion protein than to the one containing $G_{i1}\alpha$ (Gly^{351}) (pIC_{50} values for Ile = 5.78 ± 0.1, for Gly = 6.58 ± 0.16, means ± S.E.M, n=3). Again, GDP did not reduce the binding of [^{3}H] naltrindole to these fusion proteins **(Figure 4.17B).** These results provided clear evidence for differences in the ternary complex of DADLE-hDOR-$G_{i1}\alpha$ due to the single amino acid alteration. Similar results in terms of agonist binding have been observed recently for the A_1

adenosine receptor (Waldhoer *et al.,* 1999) and used as evidence that the stability of the ternary complex is determined by the dissociation rate of the G protein. This is supported further by the difference in EC_{50} for the G protein antagonist suramin (Beindl *et al.,* 1996: Freissmuth *et al.*, 1999) to inhibit [^{3}H] DADLE binding to the Gly^{351} and Ile^{351} hDOR-containing fusion proteins and indicate greater affinity of interaction between hDOR and Ile^{351} $G_{i1}\alpha$ than between hDOR and Gly^{351} $G_{i1}\alpha$ **(Figure 4.18A)**. Previous studies with the $5HT_{1A}$ receptor have shown this receptor to display constitutive, agonist-independent, capacity to activate Ile^{351} $G_{i1}\alpha$ but not Gly^{351} $G_{i1}\alpha$ (Kellet *et al.,* 1999) and there is increased relative intrinsic activity of partial agonists at the α_{2A}-adrenoceptor to activate Ile^{351} $G_{i1}\alpha$ compared to Gly^{351} $G_{i1}\alpha$ (Jackson *et al.*, 1999). Such observations further demonstrate the importance of the nature of this interface for protein-protein interactions between GPCR and G protein and that these interactions, which can be monitored by ternary complex stability, determine the effectiveness of information transfer from the GPCR to G protein. Also, as for GDP, suramin did not reduce the binding of [^{3}H] naltrindole to these fusion proteins **(Figure 4.18B).**

Association (on-rate) binding experiments were used to determine the K_{on}. Such experiments are effected by the concentration of radioligand, dissociation rate constant (K_{off}) and temperature. K_{on} is usually expressed in units of $Molar^{-1}$ min^{-1}. I have used the following equation.

$$K_{on} = \frac{K_{ob} - K_{off}}{[\text{radioligand}]}$$

Association experiments for [^{3}H] DADLE were carried for various times at 25 °C with prior PTx treatment of cells transiently expressing two selective mutants. I was able to measure the K_{ob}, observed rate constant (min^{-1}) from the direct association experiments. Calculated K_{ob} of these two fusion protein mutants was not significantly different.

Dissociation binding experiments measured the "off-rate" for radioligand dissociation from the receptor. Initially ligand and receptor were allowed to bind to equilibrium. At that point, a very high concentration of an unlabeled ligand was added or the sample diluted by incubation to a large volume. The K_{off} is expressed in units of inverse time. This also helps to calculate the $t_{1/2}$, half-life for dissociation as 0.6931/ K_{off}.

Dissociation experiments for [^{3}H] DADLE were performed for various times at 25 ° C with prior PTx treatment, by adding an excess of an antagonist (10 μM naloxone). The measured K_{off} and $t_{1/2}$ were significantly different between these two fusion proteins.

These values, K_{on} and K_{off}, I was then used to combine them to calculate the K_d of receptor binding.

$$K_d = \frac{K_{off}}{K_{on}}$$

The units are consistent: K_{off} is in units of min^{-1}; K_{on} is in units of $M^{-1}min^{-1}$, so K_d is in units of M.

In order to calculate the high affinity K_i value for the competition binding of [^{3}H] naltrindole for hDOR-$G_{i1}\alpha$ (Ile^{351}), I have used the following equation.

$$K_i = \frac{IC_{50}}{1 + \frac{[\text{radioligand}]}{K_d}}$$

The association kinetics of [^{3}H] DADLE to these two fusion proteins were not different but upon reaching [^{3}H] DADLE binding steady-state, addition of an excess of an antagonist allowed dissociation kinetics of [^{3}H] DADLE to be monitored. It was clear that, under the conditions employed, dissociation of this ligand was substantially more rapid from the Gly^{351} containing fusion protein and this corresponded to a 5-fold difference in the dissociation constant for [^{3}H] DADLE **(Figures 4.19A, 4.19B, Table 4.4).** Equivalent variation in the measured K_d for [^{3}H] DADLE was obtained in equilibrium saturation binding assays **(Figures 4.20, 4.21, Table 4.4).** Furthermore, the measured K_d for [^{3}H] DADLE binding to the hDOR-$G_{i1}\alpha$ (Ile^{351}) fusion protein was very similar to the K_i for binding (0.25-0.91 nM) of this ligand to the agonist high affinity state of the fusion protein estimated from competition binding studies with [^{3}H] naltrindole.

Figure 4.1. Structure of amino acids

Group I. Amino acids with apolar R groups

Alanine

Ala, A

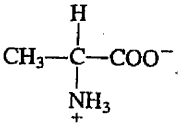

Valine

Val, V

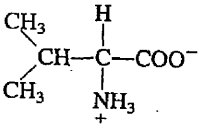

Leucine

Leu, L

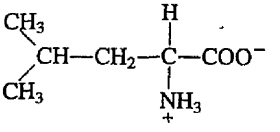

Isoleucine

Ile, I

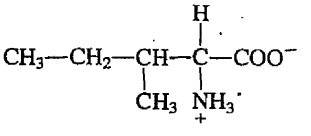

Phenylalanine

Phe, F

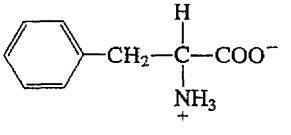

Group II. Amino acids with uncharged polar R groups

Glycine

Gly, G

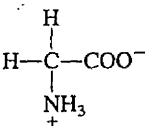

Serine

Ser, S

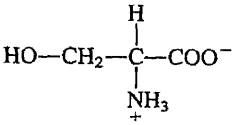

Cysteine

Cys, C

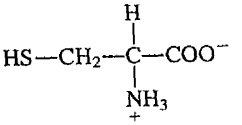

Group III. Amino acids with charged R groups

Arginine

Arg, R

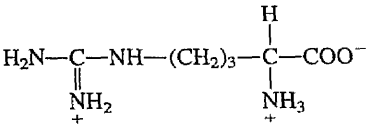

Adapted from Biochemistry, page 62 (Fourth edition)

(written by Geoffrey L. Zubay)

Figure 4.2. Analysis of [^{3}H] naltrindole binding to stably expressed hDOR

A. [^{3}H] naltrindole binding studies on membranes stably expressing hDOR

Following stable expression of the hDOR, saturation binding studies using [^{3}H] naltrindole were performed on membranes of HEK293 cells. Non specific binding was assessed in parallel in the presence of 100 μM naloxone. Bmax of hDOR varied between 1-2 pmol/mg with different passages. The K_d of [^{3}H] naltrindole for hDOR was estimated as 0.54 ± 0.36 nM. (mean ± range, n=2). This is a representative example of two experiments performed.

B. Scatchard analysis

A Scatchard plot was generated from the data of Figure 4.2A.

A

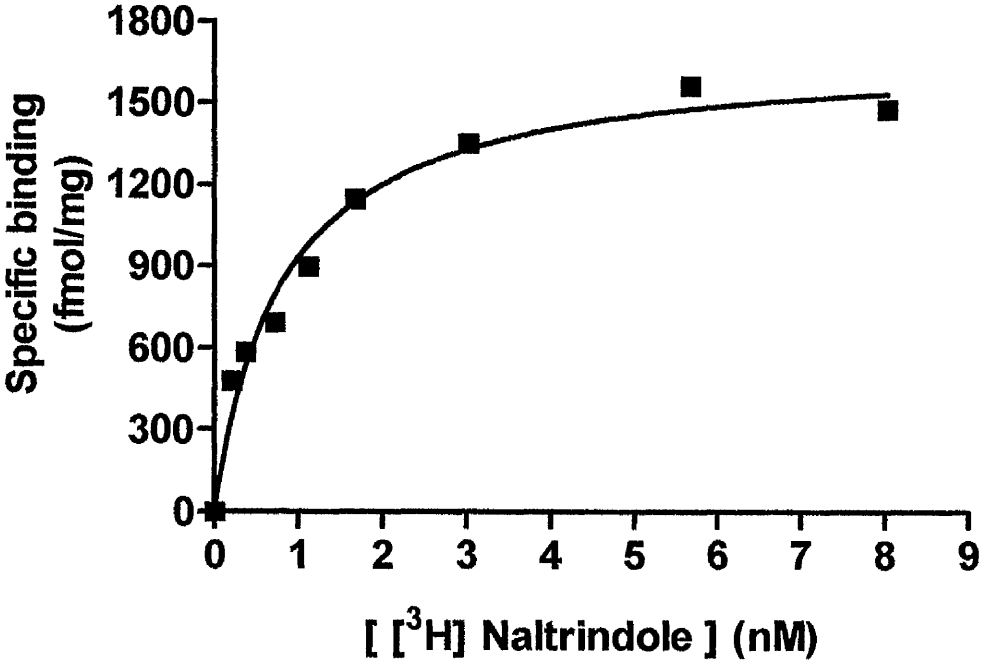
Specific binding
(fmol/mg)
1800
1500
1200
900
600
300
0
0
1
2
3
4
5
6
7
8
9
[[3H] Naltrindole] (nM)

B

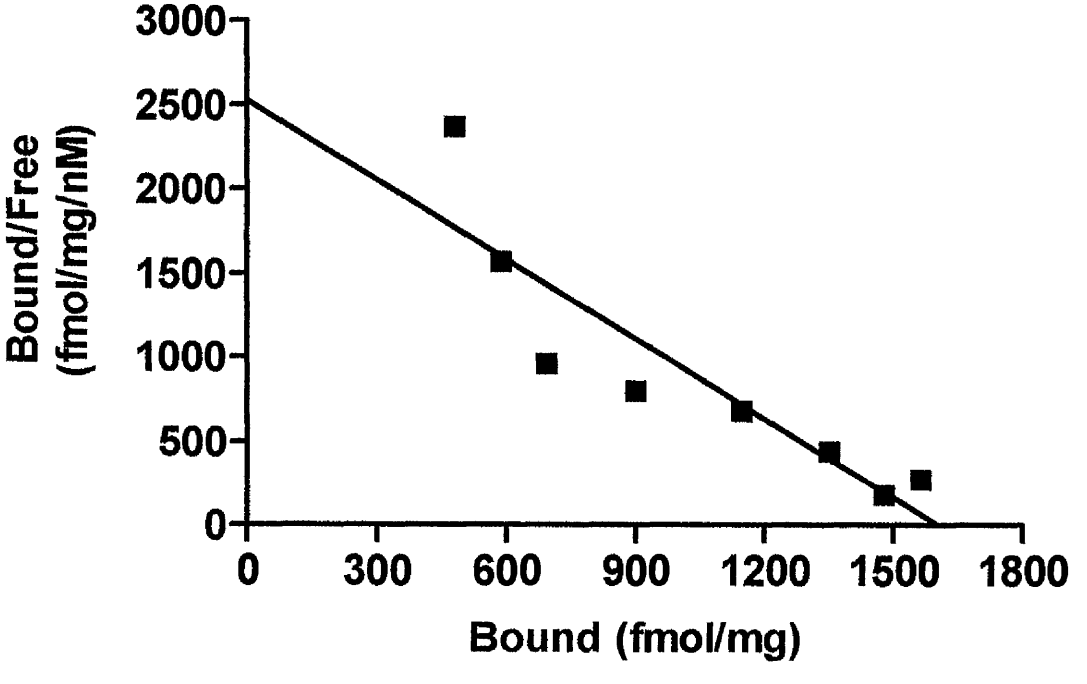
Bound/Free
(fmol/mg/nM)
3000
2500
2000
1500
1000
500
0
0
300
600
900
1200
1500
1800
Bound (fmol/mg)

Figure 4.3. Analysis of [^{3}H] DADLE binding to stably expressed hDOR

A. [^{3}H] DADLE binding studies on membranes stably expressing hDOR

Following stable expression of the hDOR, saturation binding studies using [^{3}H] DADLE were performed on membranes of HEK293 cells. Non specific binding was assessed in parallel in the presence of 10 μM DADLE. The K_d of [^{3}H] DADLE for hDOR was estimated as 0.85 ± 0.18 nM (mean ± range, n=2). This is a representative example of two experiments performed.

B. Scatchard analysis

A Scatchard plot was generated from the data of Figure 4.3A.

A

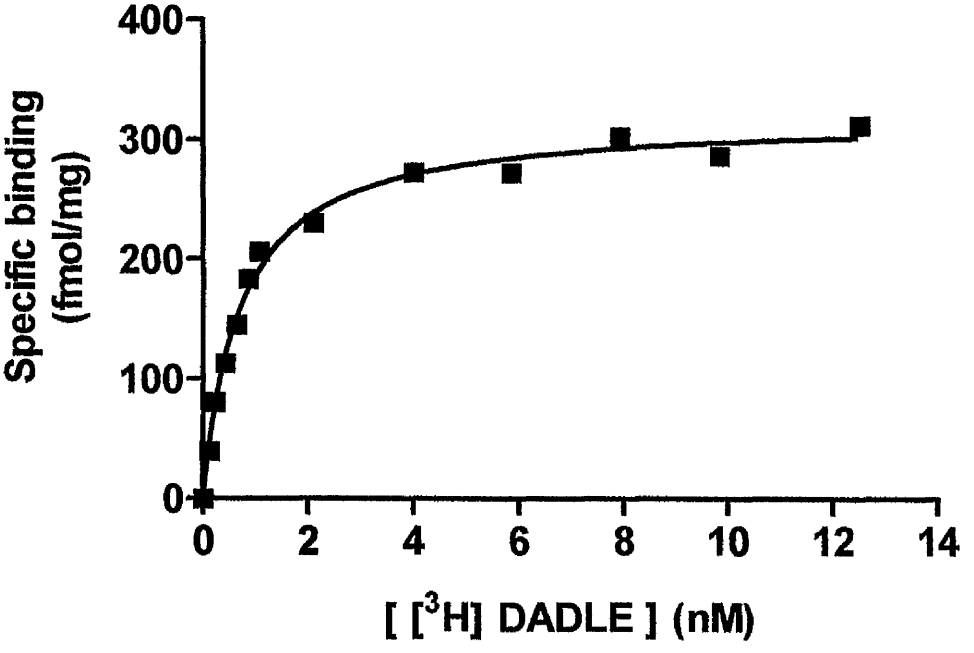
Specific binding
(fmol/mg)
400
300
200
100
0
0
2
4
6
8
10
12
14
[[3H] DADLE] (nM)

B

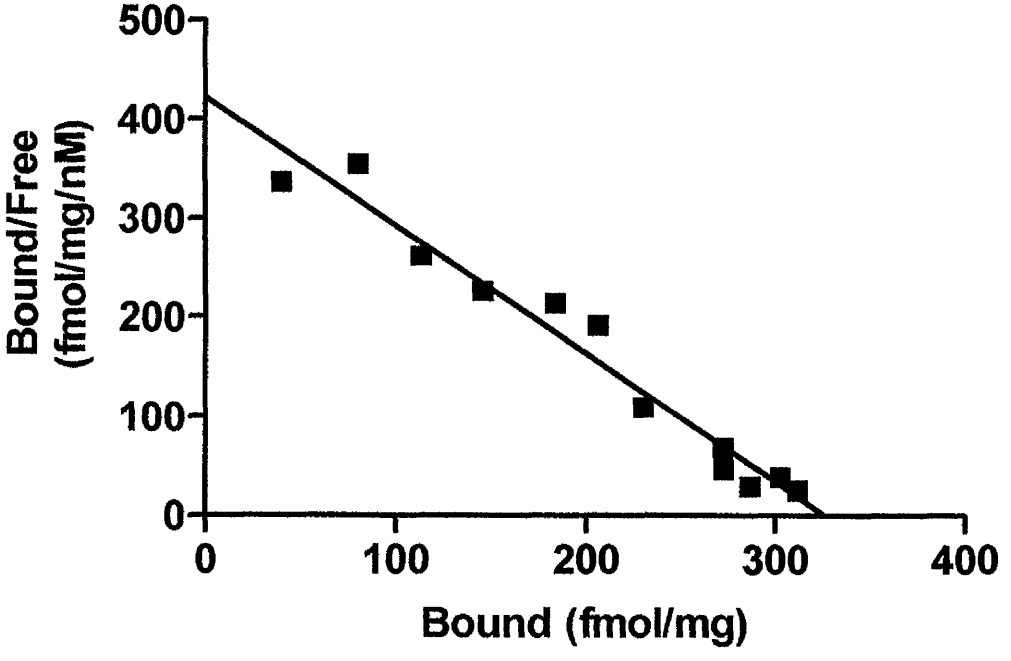
Bound/Free
(fmol/mg/nM)
500
400
300
200
100
0
0
100
200
300
400
Bound (fmol/mg)

Figure 4.4. Effect of PTx treatment on stably expressed hDOR

A. Effect of PTx treatment on [^{3}H] DADLE binding in membranes stably expressing hDOR

Following stable expression of the hDOR and prior PTx treatment with increasing incubation time [50ng/12h,100ng/12h, 50ng/24h, 100ng/24h], [^{3}H] DADLE binding studies were performed on membranes of hDOR. This is one typical experiment performed.

B. Conversion to percentage from Figure 4.4A

The data from Figure 4.4A was converted to percentage (%).

A

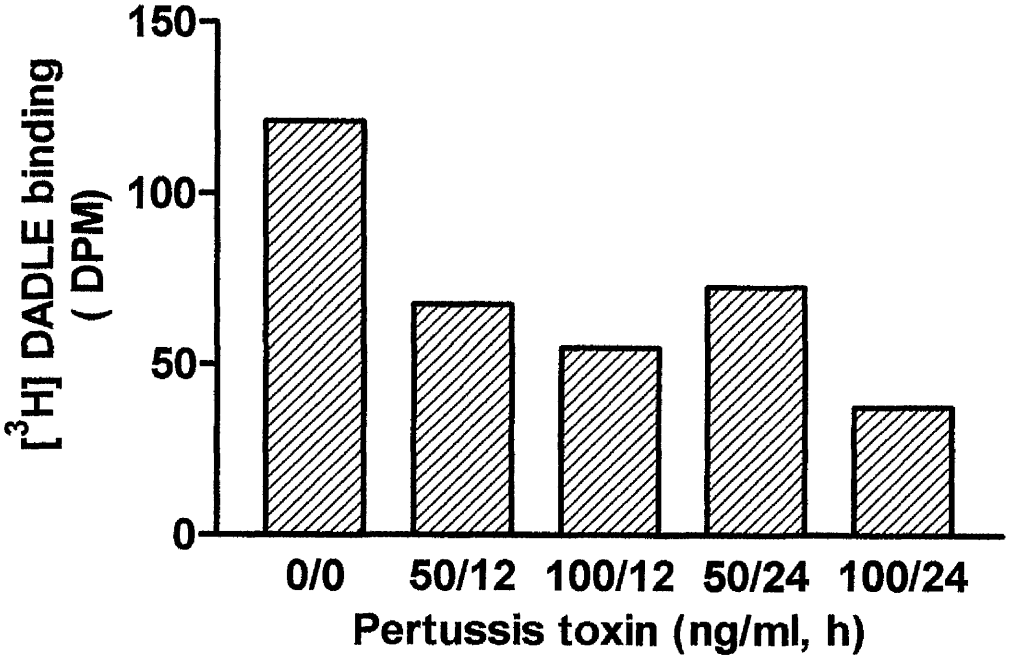
150
100
50
0
[3H] DADLE binding
(DPM)
0/0
50/12
100/12
50/24
100/24
Pertussis toxin (ng/ml, h)

B

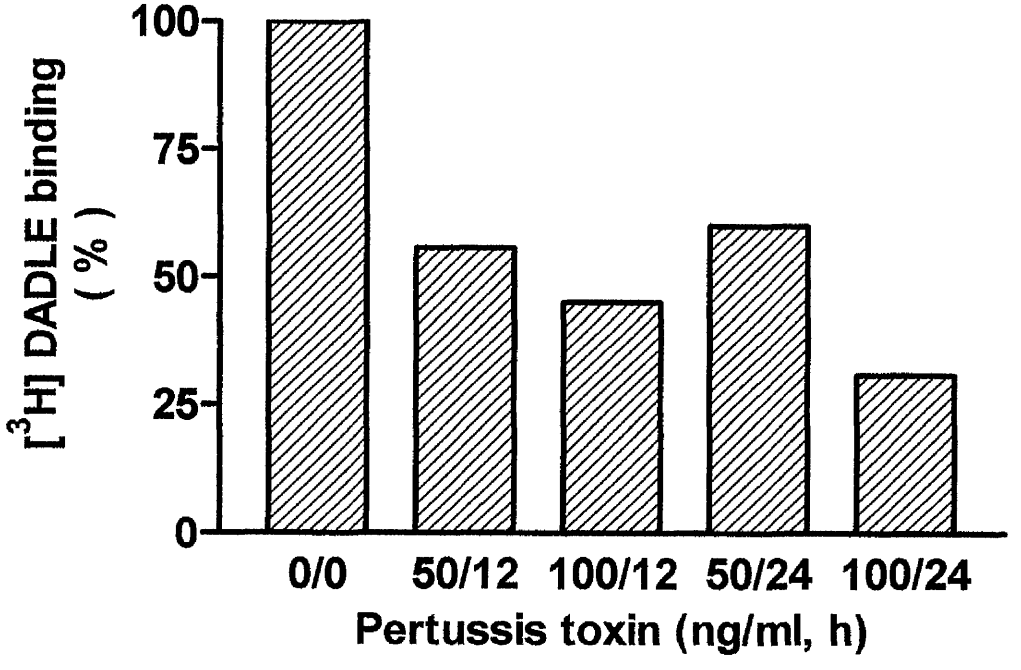
100
75
50
25
0
[3H] DADLE binding
(%)
0/0
50/12
100/12
50/24
100/24
Pertussis toxin (ng/ml, h)

Figure 4.5. [^{3}H] DADLE and [^{3}H] naltrindole binding studies for stably expressed hDOR at increasing concentrations of GDP

A. Reduction of binding of [^{3}H] DADLE at increasing concentrations of GDP

Following stable expression of hDOR, PTx untreated (■) or treated (□) (100ng/ml, 24h) membranes were prepared. The specific binding of [^{3}H] DADLE (4.5 nM) was assessed at increasing concentrations of GDP. Non specific binding was assessed in parallel in the presence of 10 μM unlabelled DADLE. Data are shown from a representative experiment.

B. Effects of GDP and PTx treatment on the binding of [^{3}H] DADLE and [^{3}H] naltrindole to the hDOR

The effects of pre-treatment (100ng/ml, 24h) of the cells with PTx or addition of GDP (100 μM) to membranes on the binding of [^{3}H] DADLE (5 nM) and [^{3}H] naltrindole (4 nM) was assessed. Results are presented as mean ± range from 2 independent experiments (** $P < 0.05$, *** $P < 0.01$).

C. Effects of PTx treatment on [^{3}H] naltrindole binding to stably expressing hDOR-$G_{i1}\alpha$ (Ile^{351}).

Following stable expression of hDOR-$G_{i1}\alpha$ (Ile^{351}), PTx untreated (▲) or treated (□) (25ng/ml, 16h) membranes were prepared. Saturation binding studies using [^{3}H] naltrindole were performed on membranes of HEK293 cells. Non specific binding was assessed in parallel in the presence of 100 μM naloxone. Data are shown from a representative experiment.

A

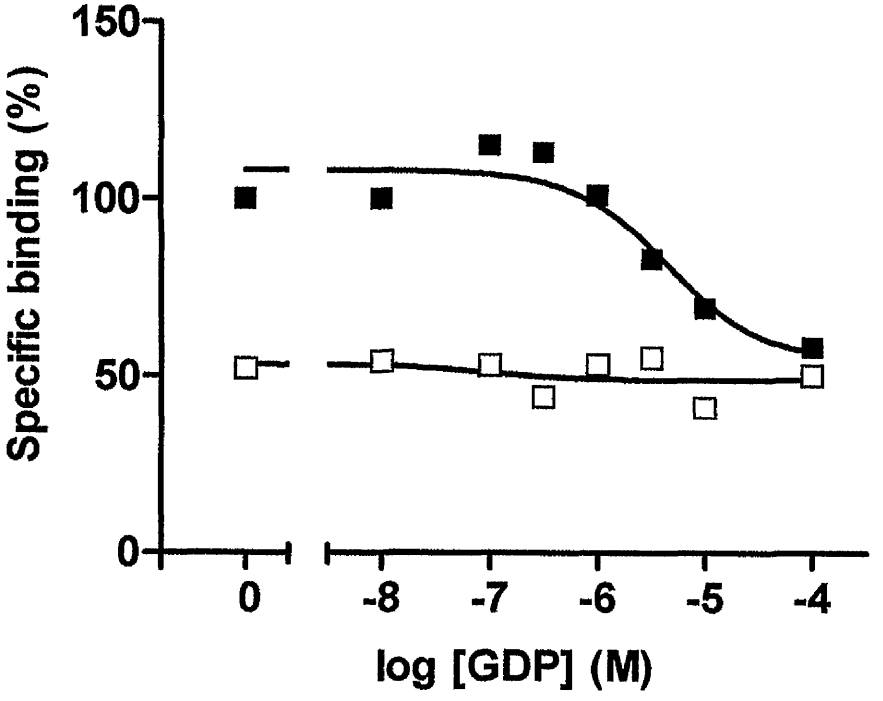
150
100
50
0
Specific binding (%)
0
-8
-7
-6
-5
-4
log [GDP] (M)

B

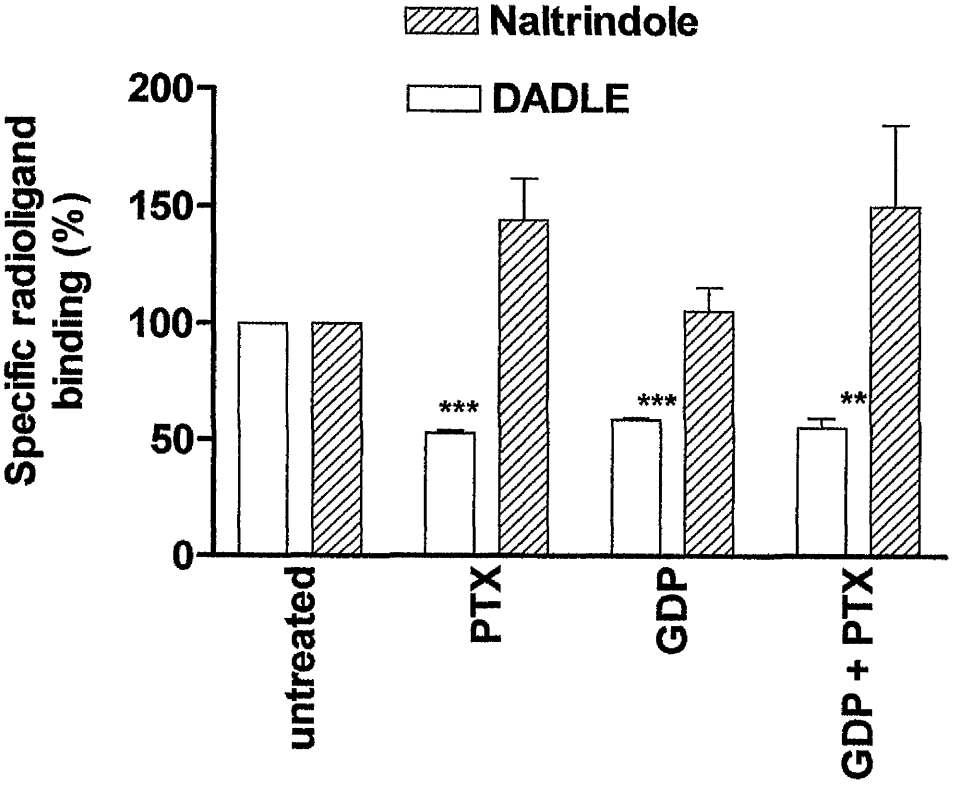
Naltrindole
DADLE
200
150
100
50
0
Specific radioligand binding (%)
***
***
**
untreated
PTX
GDP
GDP + PTX

C

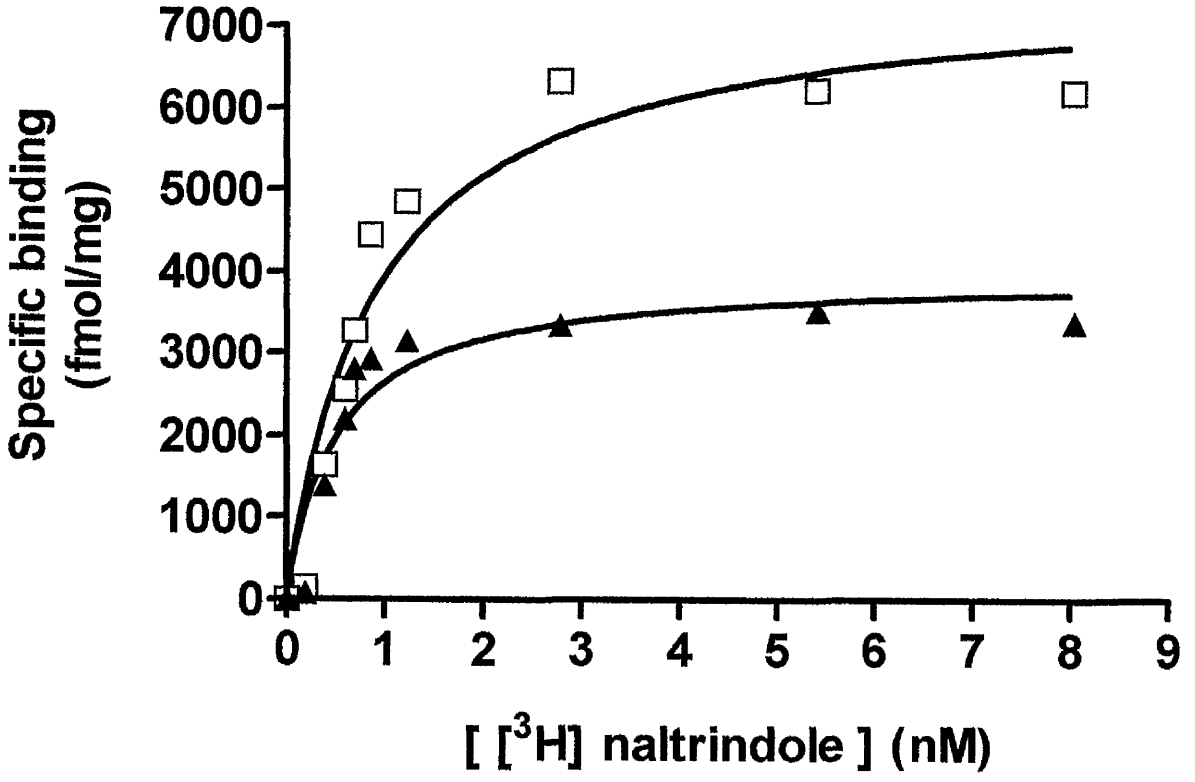
Specific binding
(fmol/mg)
7000
6000
5000
4000
3000
2000
1000
0
0
1
2
3
4
5
6
7
8
9
[[3H] naltrindole] (nM)

Figure 4.6. Analysis of [^{3}H] naltrindole binding to stably expressed hDOR-$G_{i1}\alpha$ (Ile^{351}).

A. [^{3}H] naltrindole binding studies on membranes stably expressing hDOR-$G_{i1}\alpha$ (Ile^{351}).

Following stable expression of the hDOR-$G_{i1}\alpha$ (Ile^{351}) fusion protein and prior PTx treatment (25ng/ml, 16h), saturation binding studies using [^{3}H] naltrindole were performed on membranes of HEK293 cells. Non specific binding was assessed in parallel in the presence of 100 μM naloxone. This is a representative example of three performed.

B. Scatchard analysis

A Scatchard plot was generated from the data of Figure 4.6A.

A

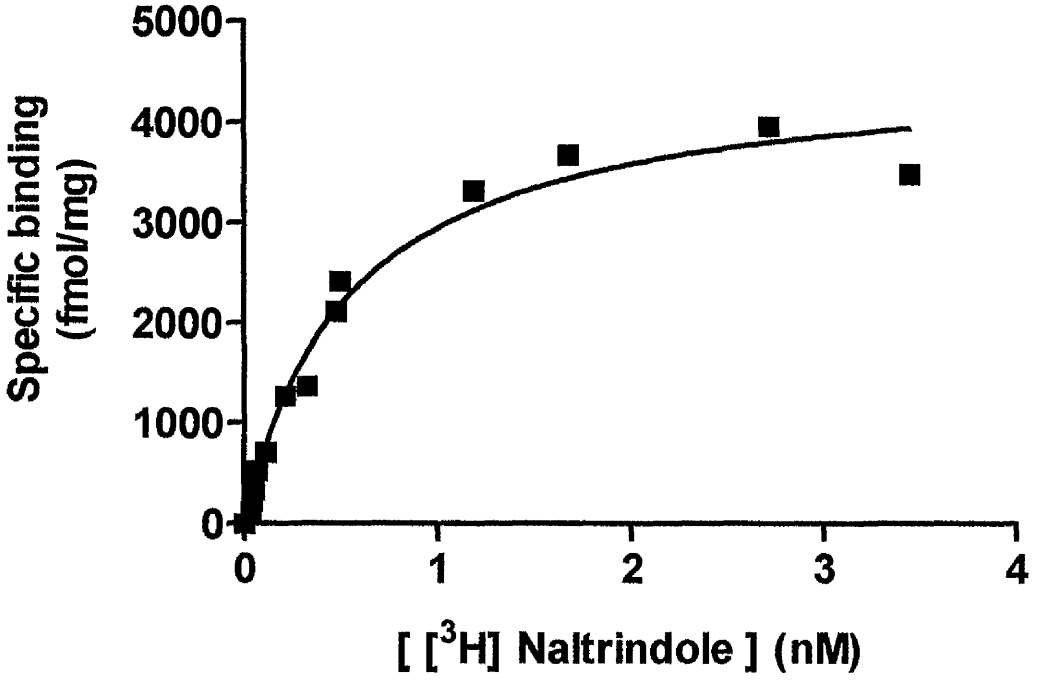
5000
4000
3000
2000
1000
0
Specific binding
(fmol/mg)
0
1
2
3
4
[[3H] Naltrindole] (nM)

B

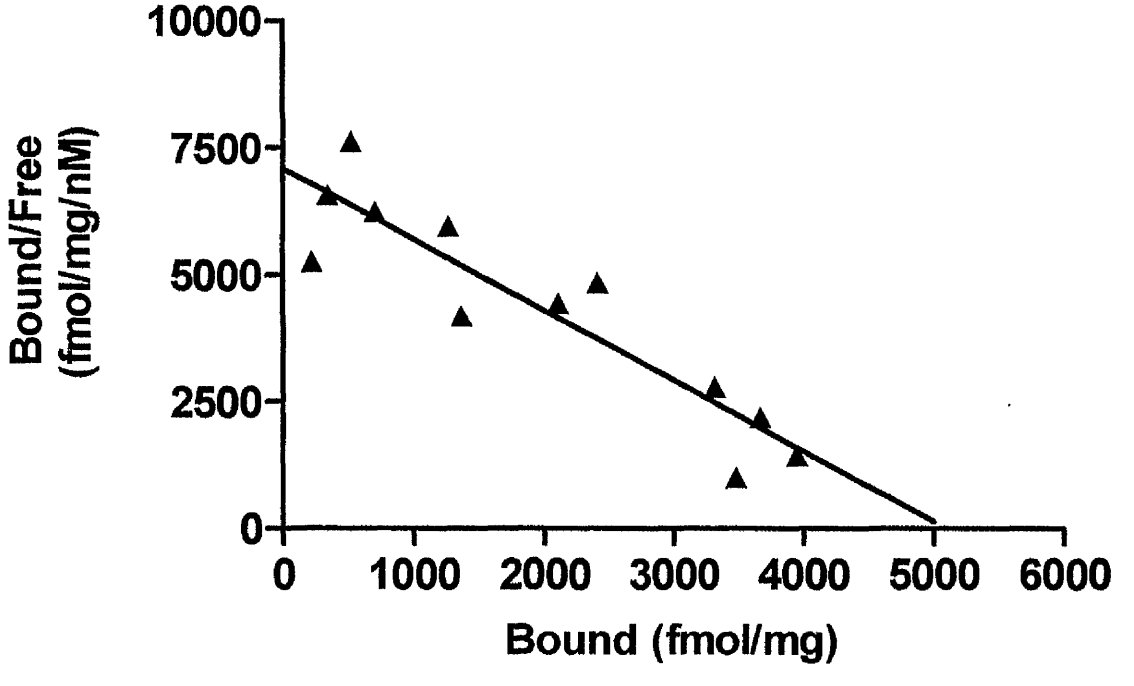
10000
7500
5000
2500
0
Bound/Free
(fmol/mg/nM)
0
1000
2000
3000
4000
5000
6000
Bound (fmol/mg)

Figure 4.7 Analysis of [^{3}H] DADLE binding to stably expressed hDOR-$G_{i1}\alpha$ (Ile^{351}).

A. [^{3}H] DADLE binding studies on membranes stably expressing hDOR-$G_{i1}\alpha$ (Ile^{351}).

Following stable expression of the hDOR-$G_{i1}\alpha$ (Ile^{351}) fusion protein and prior PTx treatment (25ng/ml, 16h), saturation binding studies using [^{3}H] DADLE were performed on membranes of HEK293 cells. Non specific binding was assessed in parallel in the presence of 10 μM DADLE. Both high affinity and low affinity binding sites for [^{3}H] DADLE were detected. This is a representative example of three experiments performed.

B. Scatchard analysis

A Scatchard plot was generated from the data of Figure 4.7A.

A

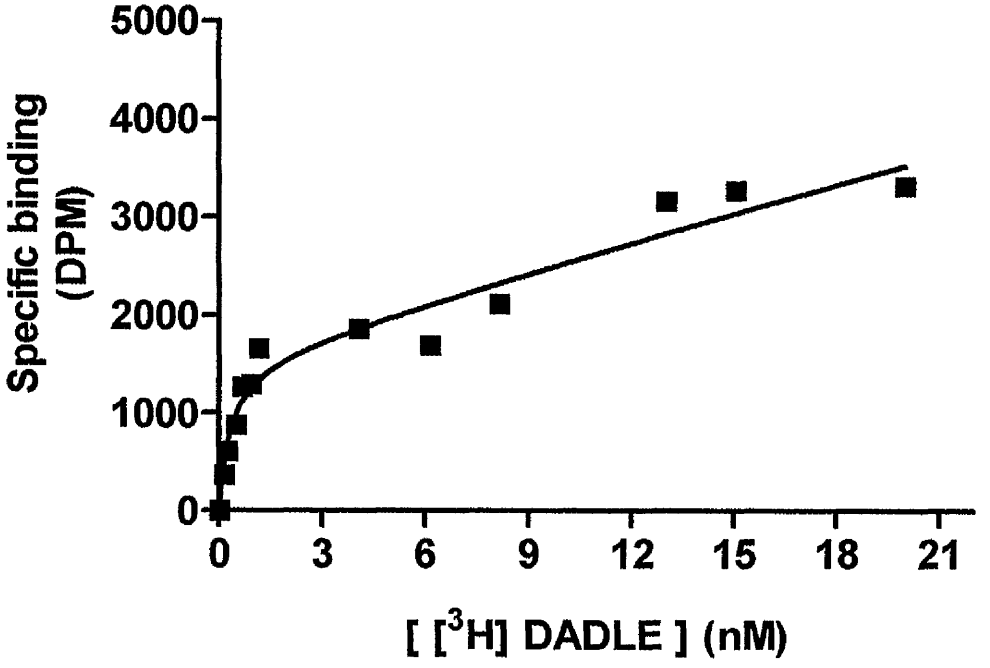
5000
4000
3000
2000
1000
0
Specific binding (DPM)
0
3
6
9
12
15
18
21
[[3H] DADLE] (nM)

B

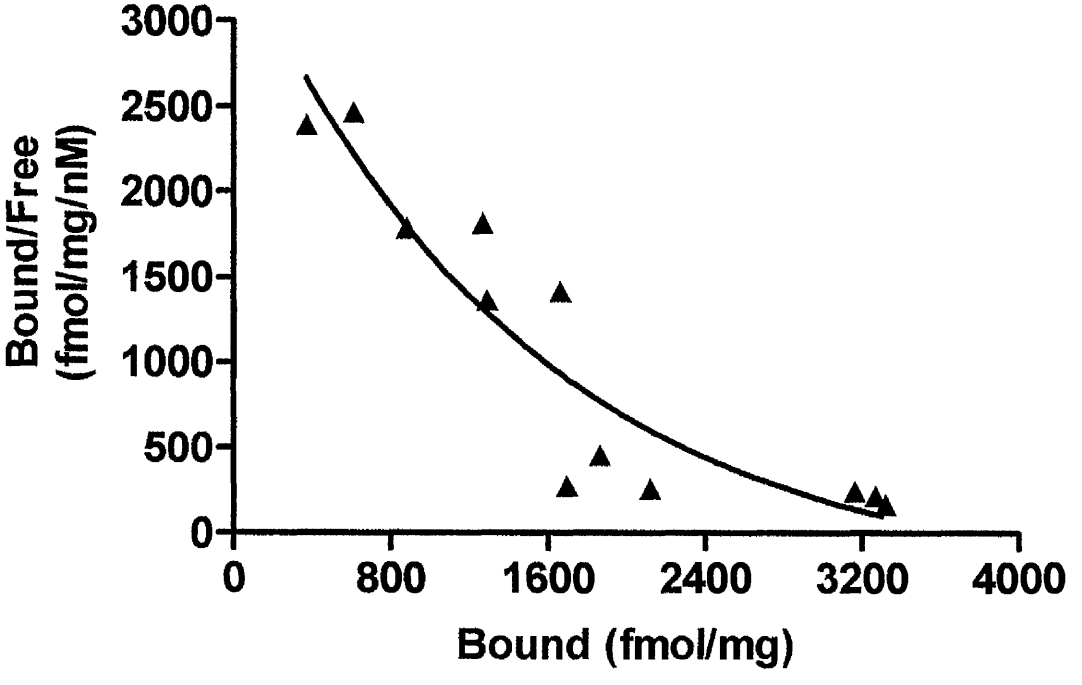
3000
2500
2000
1500
1000
500
0
Bound/Free (fmol/mg/nM)
0
800
1600
2400
3200
4000
Bound (fmol/mg)

Figure 4.8. Increasing concentrations of GDP reduce the binding of [^{3}H] DADLE to the hDOR $G_{i1}\alpha$ (Ile^{351}).

A. [^{3}H] DADLE binding studies on membranes stably expressing hDOR-$G_{i1}\alpha$ (Ile^{351}).

Following stable expression of the hDOR-$G_{i1}\alpha$ (Ile^{351}) fusion protein membranes of HEK293 cells were prepared without PTx treatment. The binding of [^{3}H] DADLE (0.5 nM) was performed at various concentrations of GDP. Data are shown from a representative experiment.

B. [^{3}H] DADLE binding studies on membranes stably expressing hDOR-$G_{i1}\alpha$ (Ile^{351}): Effect of PTx treatment.

Following stable expression of the hDOR-$G_{i1}\alpha$ (Ile^{351}) fusion protein and prior PTx treatment (25ng/ml, 16h), membranes were prepared. The binding of [^{3}H] DADLE (1.1 nM) was measured at various concentrations of GDP. Data are shown from a representative experiment.

A

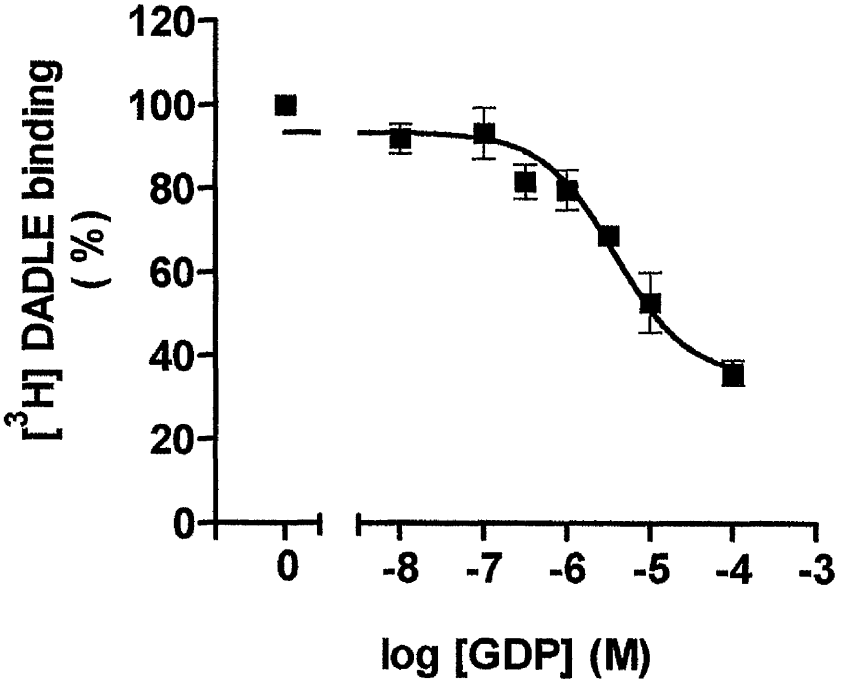
120
100
80
60
40
20
0
[3H] DADLE binding (%)
0
-8
-7
-6
-5
-4
-3
log [GDP] (M)

B

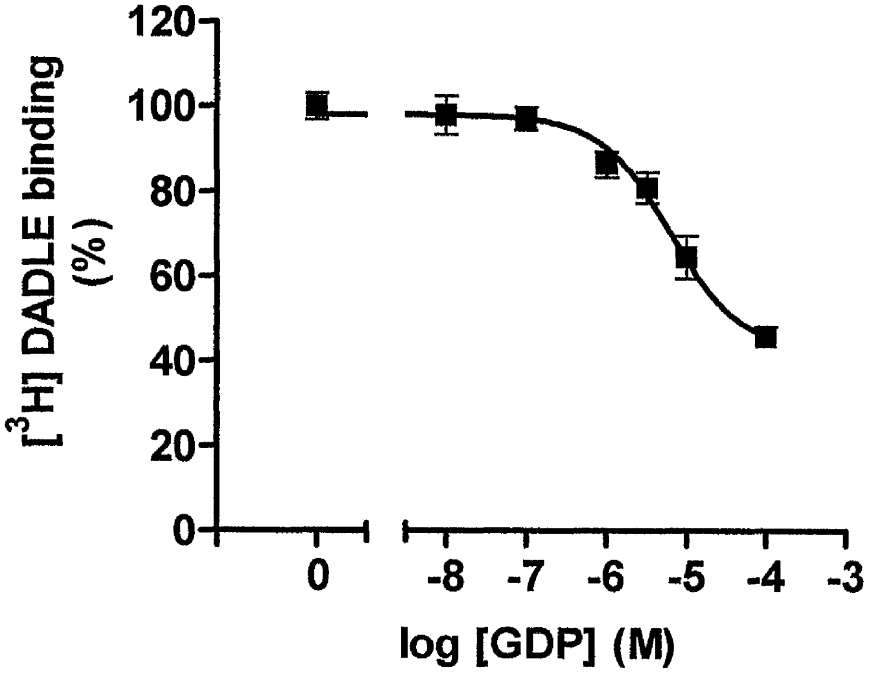
120
100
80
60
40
20
0
[3H] DADLE binding (%)
0
-8
-7
-6
-5
-4
-3
log [GDP] (M)

Figure 4.9. The ability of DADLE to displace [^{3}H] naltrindole binding in membranes stably expressed hDOR-$G_{i1}\alpha$ (Ile^{351}).

The specific binding of [^{3}H] naltrindole (1.2 nM) to the hDOR-$G_{i1}\alpha$ (Ile^{351}) fusion protein in membranes of PTx treated cells was assessed in the presence of varying concentrations of DADLE in the absence of added guanine nucleotides (□) and in the presence of 100 μM GDP (▲). In the absence of guanine nucleotides, two sites with distinct affinities for DADLE were observed with pKi high affinity = 9.3 ± 0.19, pKi low affinity = 6.5 ± 0.22, means ± S.E.M, n=3), whereas in the presence of GDP (100 μM) a monophasic competition curve (pKi low affinity = 6.5 ± 0.25, mean ± S.E.M, n=3) was obtained. Data are from a representative experiment.

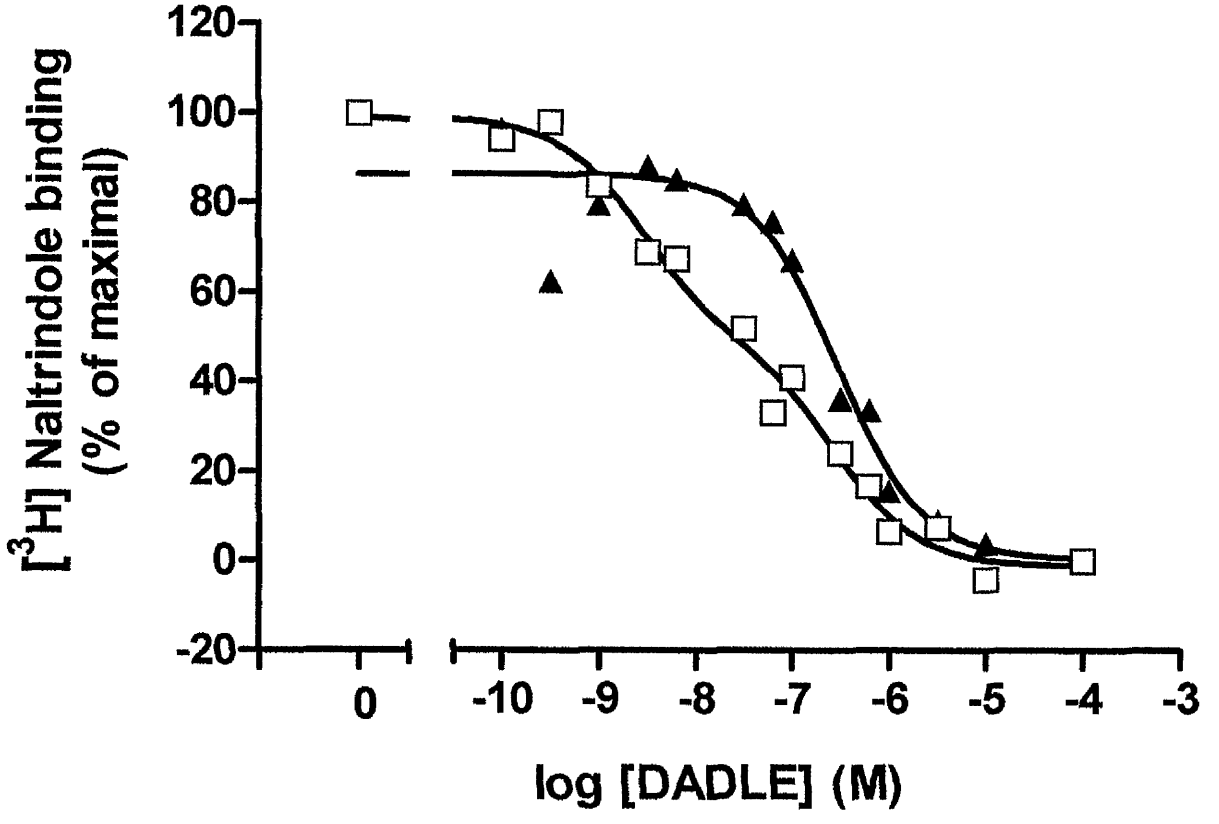
[3H] Naltrindole binding
(% of maximal)
120
100
80
60
40
20
0
-20
0
-10
-9
-8
-7
-6
-5
-4
-3
log [DADLE] (M)

Figure 4.10. Increasing concentrations of GDP do not reduce the binding of [^{3}H] naltrindole for the hDOR $G_{i1}\alpha$ (Ile^{351}).

A. [^{3}H] naltrindole binding studies on membranes stably expressing hDOR-$G_{i1}\alpha$ (Ile^{351}).

Following stable expression of the hDOR-$G_{i1}\alpha$ (Ile^{351}) fusion protein membranes of HEK293 cells were prepared. The binding of [^{3}H] naltrindole (4 nM) was performed at various concentrations of GDP. Data are shown from a representative experiment.

B. [^{3}H] naltrindole binding studies on membranes stably expressing hDOR-$G_{i1}\alpha$ (Ile^{351}): Effect of PTx treatment

Following stable expression of the hDOR-$G_{i1}\alpha$ (Ile^{351}) fusion protein and prior PTx treatment (25ng/ml, 16h), membranes of HEK293 cells were prepared. The binding of [^{3}H] naltrindole (4 nM) was performed at various concentrations of GDP. Data are shown from a representative experiment.

C. Effect of GDP on [^{3}H] naltrindole binding on membranes stably expressing hDOR-$G_{i1}\alpha$ (Ile^{351}).

Following stable expression of the hDOR-$G_{i1}\alpha$ (Ile^{351}) fusion protein, saturation binding studies using [^{3}H] naltrindole were performed on membranes of HEK293 cells in the absence of GDP (▲) and in the presence of 100 μM GDP (□). Non specific binding was assessed in parallel in the presence of 100 μM naloxone. Data are shown from a representative experiment.

A

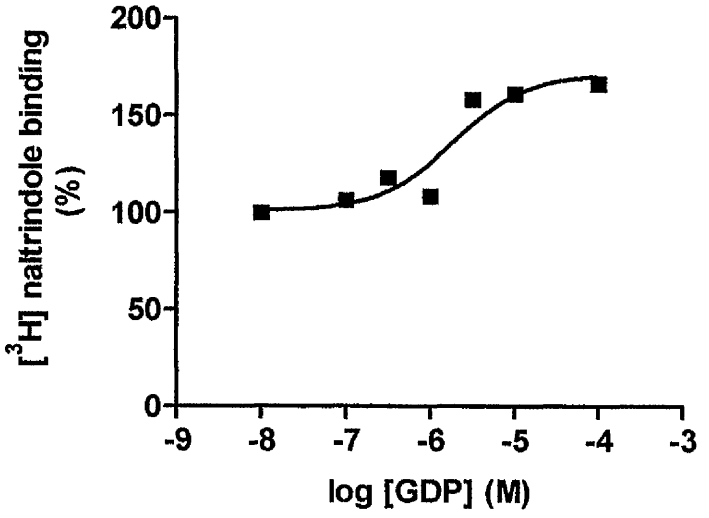
[3H] naltrindole binding (%)
200
150
100
50
0
-9
-8
-7
-6
-5
-4
-3
log [GDP] (M)

B

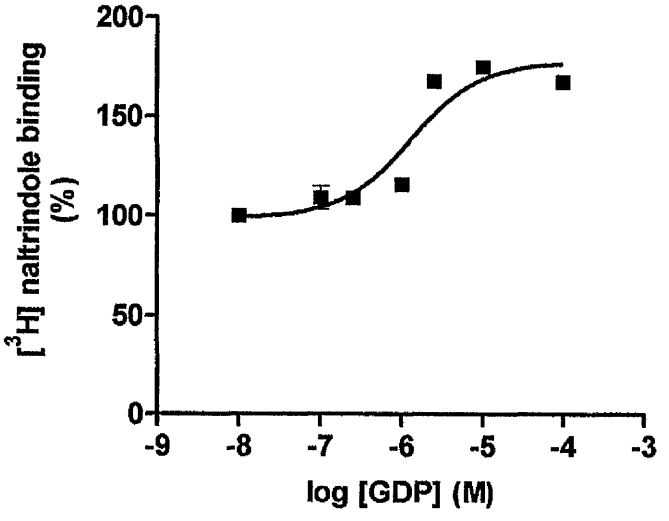
[3H] naltrindole binding (%)
200
150
100
50
0
-9
-8
-7
-6
-5
-4
-3
log [GDP] (M)

C

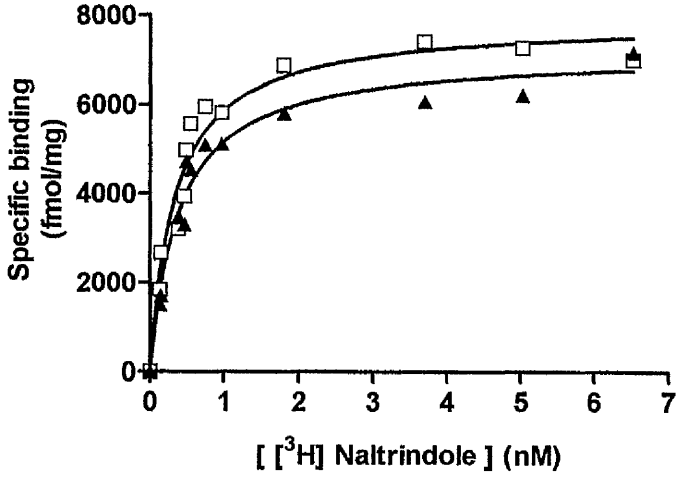
Specific binding (fmol/mg)
8000
6000
4000
2000
0
0
1
2
3
4
5
6
7
[[3H] Naltrindole] (nM)

Figure 4.11. Analysis of [^{3}H] naltrindole binding to stably expressed hDOR-$G_{o1}\alpha$ (Ile^{351}).

A. [^{3}H] naltrindole binding studies on membranes stably expressing hDOR-$G_{o1}\alpha$ (Ile^{351}).

Following stable expression of the hDOR-$G_{o1}\alpha$ (Ile^{351}) fusion protein and prior PTx treatment (25ng/ml, 16h), saturation binding studies using [^{3}H] naltrindole were performed on membranes of HEK293 cells. Non specific binding was assessed in parallel in the presence of 100 μM naloxone. This is a representative example of three experiments performed.

B. Scatchard analysis

A Scatchard plot was generated from the data of Figure 4.11A.

A

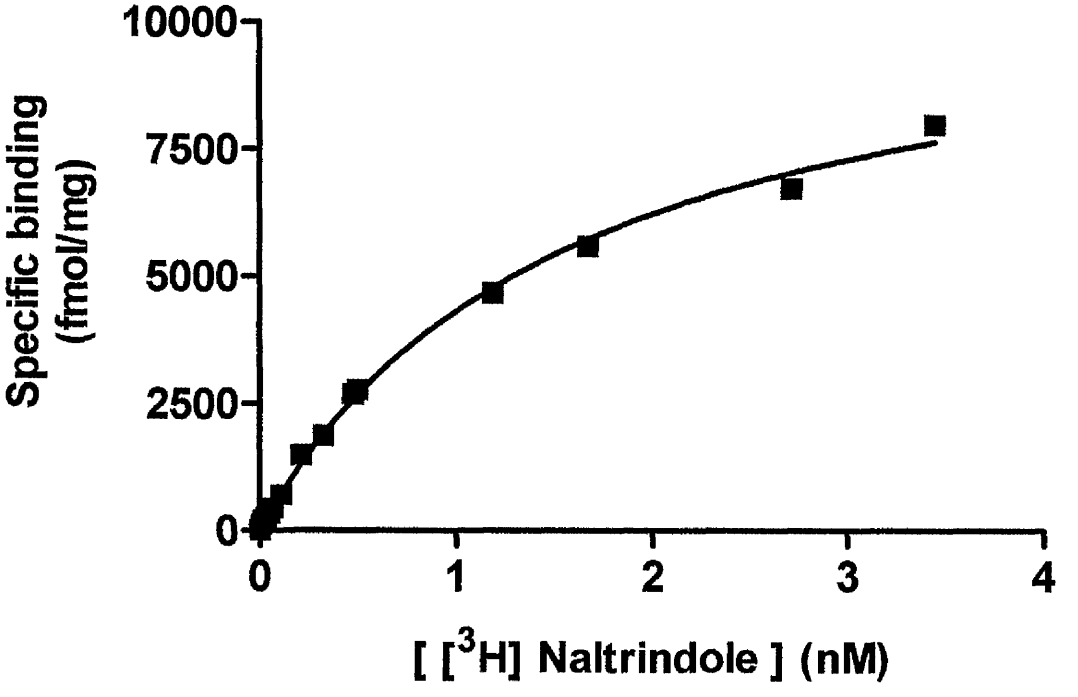
10000
7500
5000
2500
0
Specific binding
(fmol/mg)
0
1
2
3
4
[[3H] Naltrindole] (nM)

B

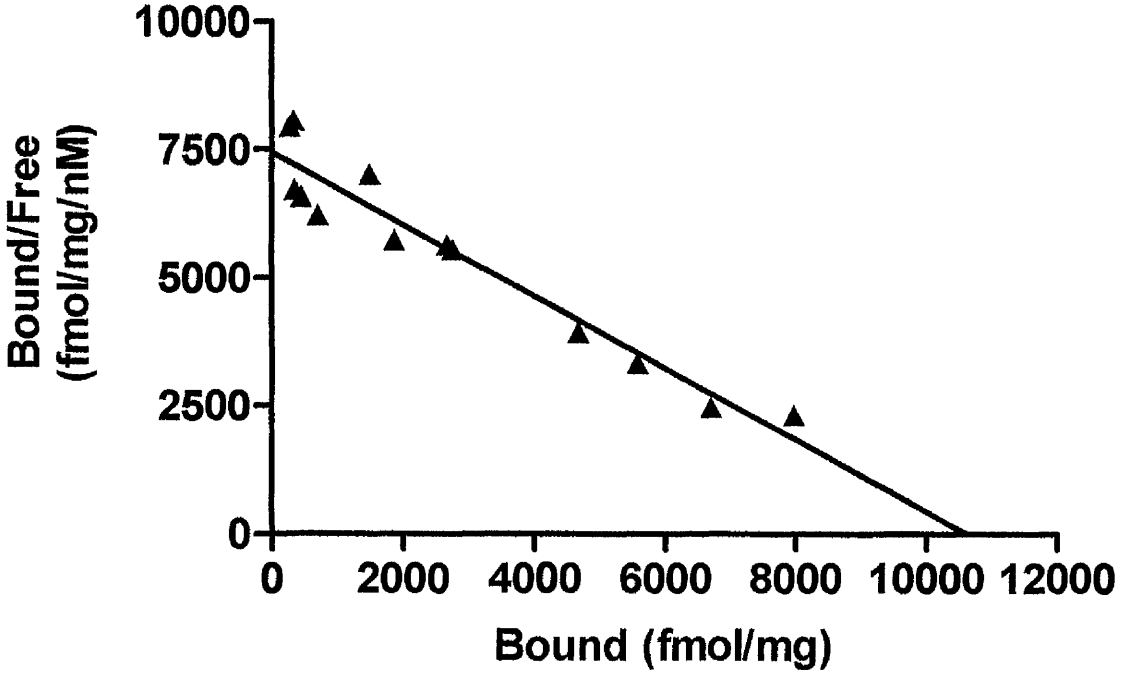
10000
7500
5000
2500
0
Bound/Free
(fmol/mg/nM)
0
2000
4000
6000
8000
10000
12000
Bound (fmol/mg)

Figure 4.12. Analysis of [^{3}H] DADLE binding to stably expressed hDOR-$G_{o1}\alpha$ (Ile^{351}).

A. [^{3}H] DADLE binding studies on membranes stably expressing hDOR-$G_{o1}\alpha$ (Ile^{351}).

Following stable expression of the hDOR-$G_{o1}\alpha$ (Ile^{351}) fusion protein and prior PTx treatment (25ng/ml, 16h), saturation binding studies using [^{3}H] DADLE were performed on membranes of HEK293 cells. Non specific binding was assessed in parallel in the presence of 10 μM DADLE. Both high affinity and low affinity binding sites for [^{3}H] DADLE were detected. The K_H of [^{3}H] DADLE for hDOR-$G_{o1}\alpha$ (Ile^{351}) was estimated as 0.75 ± 0.03 nM.(mean ± range, n=2). This is a representative example of two experiments performed.

B. Scatchard analysis

A Scatchard plot was generated from the data of Figure 4.12A.

A

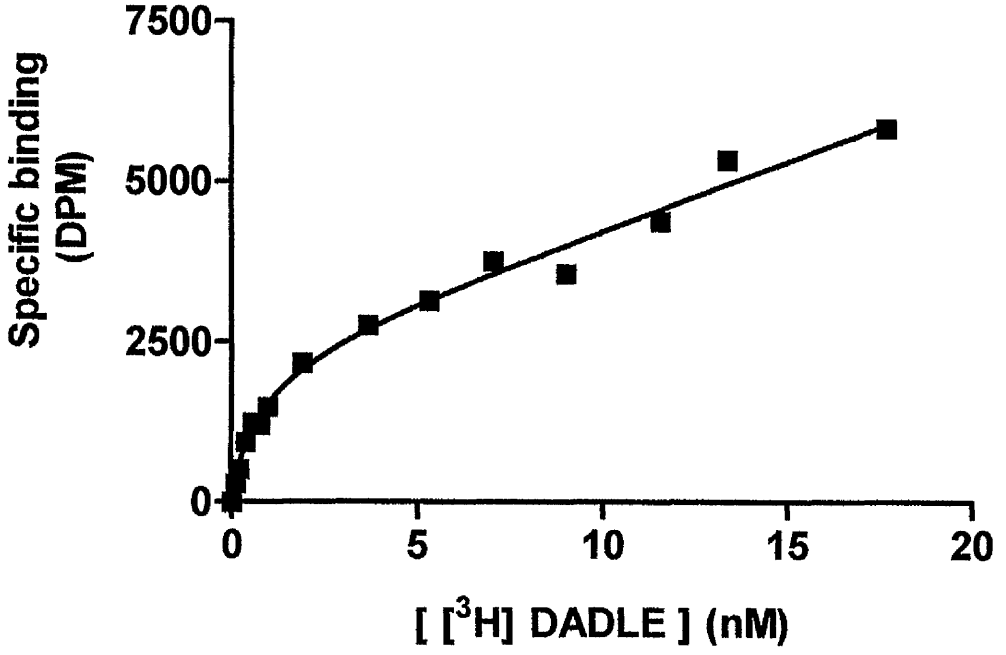
7500
5000
2500
0
Specific binding (DPM)
0
5
10
15
20
[[3H] DADLE] (nM)

B

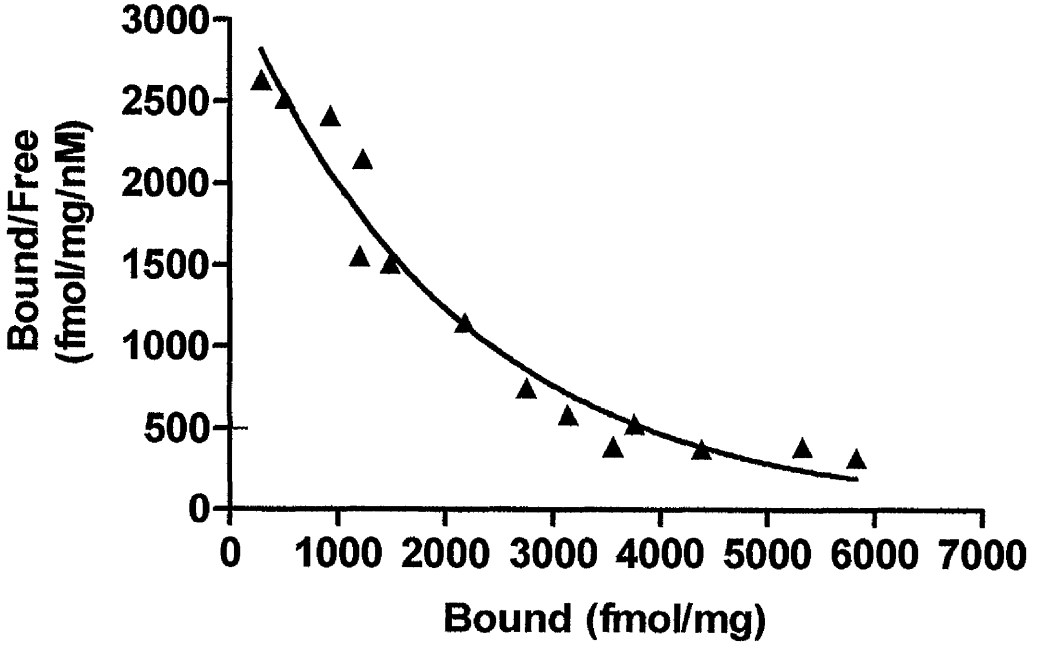
3000
2500
2000
1500
1000
500
0
Bound/Free (fmol/mg/nM)
0
1000
2000
3000
4000
5000
6000
7000
Bound (fmol/mg)

Figure 4.13. Increasing concentrations of GDP reduce the binding affinity of [^{3}H] DADLE for hDOR $G_{o1}\alpha$ (Ile^{351}).

A. [^{3}H] DADLE binding studies on PTx untreated membranes stably expressing hDOR-$G_{o1}\alpha$ (Ile^{351}).

Following stable expression of the hDOR-$G_{o1}\alpha$ (Ile^{351}) fusion protein membranes of HEK293 cells were prepared. The binding of [^{3}H] DADLE (1.2 nM) was performed at various concentrations of GDP. Data are shown from a representative experiment.

B. [^{3}H] DADLE binding studies on membranes stably expressing hDOR-$G_{o1}\alpha$ (Ile^{351}): Effect of PTx treatment

Following stable expression of the hDOR-$G_{o1}\alpha$ (Ile^{351}) fusion protein and prior PTx treatment (25ng/ml, 16h), membranes of HEK293 cells were prepared. The binding of [^{3}H] DADLE (1.2 nM) was performed at various concentrations of GDP. Data are shown from a representative experiment.

A

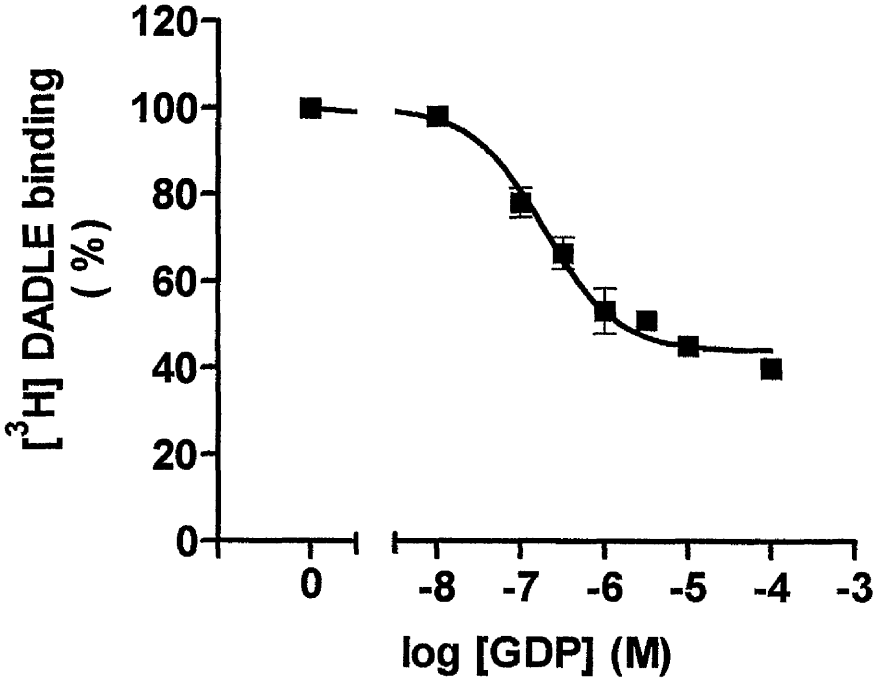
120
100
80
60
40
20
0
[3H] DADLE binding (%)
0
-8
-7
-6
-5
-4
-3
log [GDP] (M)

B

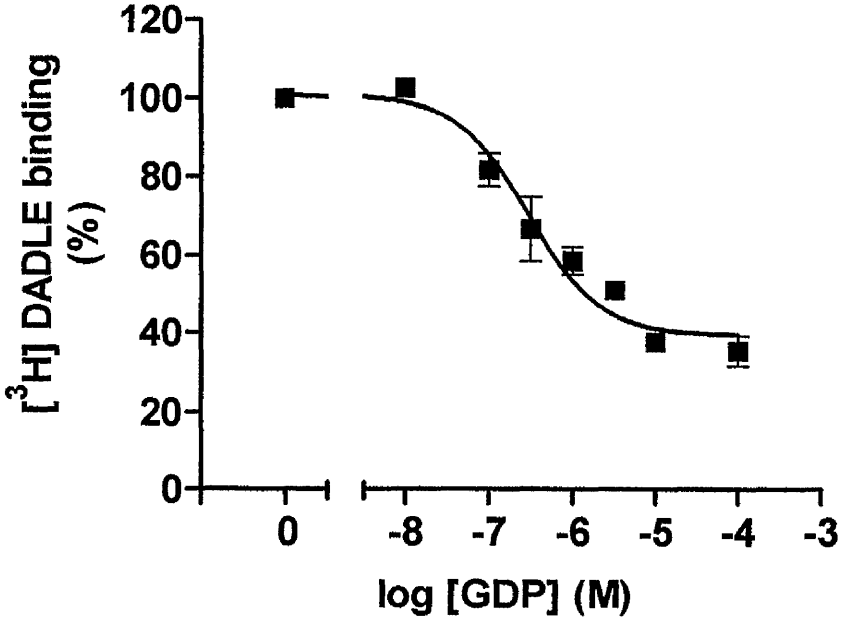
120
100
80
60
40
20
0
[3H] DADLE binding (%)
0
-8
-7
-6
-5
-4
-3
log [GDP] (M)

Figure 4.14. Increasing concentrations of GDP do not reduce the binding of [^{3}H] naltrindole for the hDOR $G_{o1}\alpha$ (Ile^{351}).

A. [^{3}H] naltrindole binding studies on PTx untreated membranes stably expressing hDOR-$G_{o1}\alpha$ (Ile^{351}).

Following stable expression of the hDOR-$G_{o1}\alpha$ (Ile^{351}) fusion protein membranes of HEK293 cells were prepared. The binding of [^{3}H] naltrindole (4.8 nM) was performed at various concentrations of GDP. Data are shown from a representative experiment.

B. [^{3}H] naltrindole binding studies on membranes stably expressing hDOR-$G_{o1}\alpha$ (Ile^{351}): Effect of PTx treatment

Following stable expression of the hDOR-$G_{o1}\alpha$ (Ile^{351}) fusion protein and prior PTx treatment (25ng/ml, 16h), membranes of HEK293 cells were prepared. The binding of [^{3}H] naltrindole (4.8 nM) was performed at various concentrations of GDP. Data are shown from a representative experiment.

A

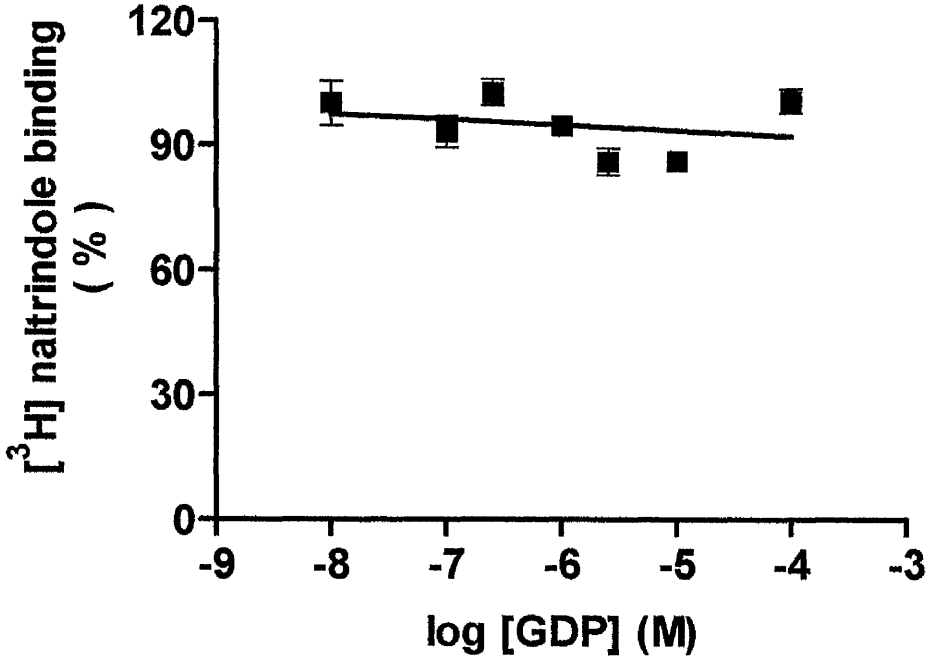
120
90
60
30
0
-9
-8
-7
-6
-5
-4
-3
[3H] naltrindole binding
(%)
log [GDP] (M)

B

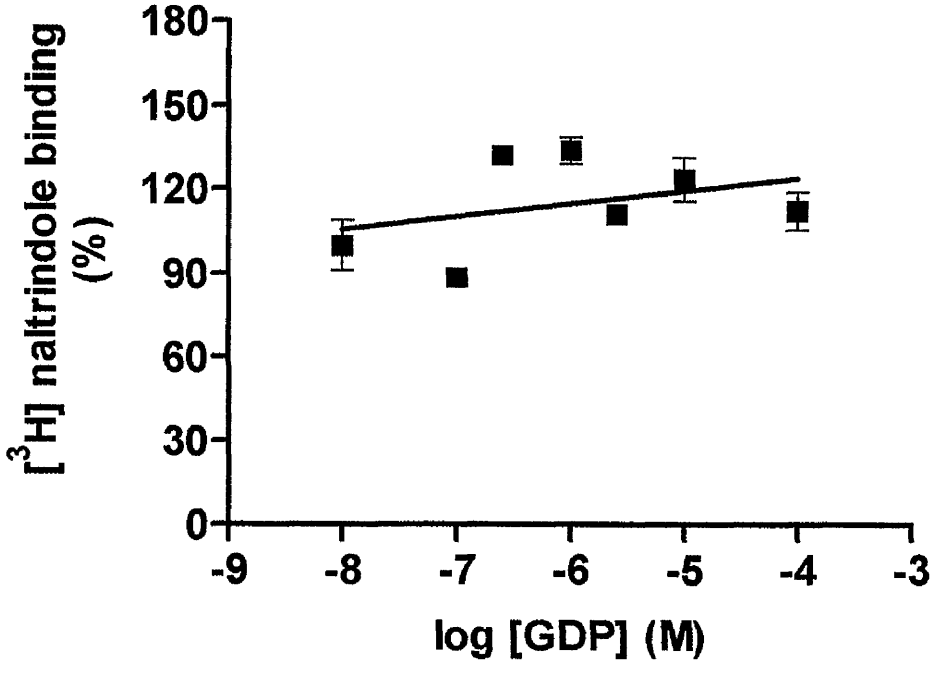
180
150
120
90
60
30
0
-9
-8
-7
-6
-5
-4
-3
[3H] naltrindole binding
(%)
log [GDP] (M)

Figure 4.15. Effect of residue^{351} of $G_{i1}\alpha$ on the potency of GDP to regulate [^{3}H] DADLE binding to hDOR-$G_{i1}\alpha$ (Xaa ^{351}) fusion protein mutants.

A. [^{3}H] DADLE binding studies on membranes transiently expressing hDOR-G_{i1} (Xaa ^{351}) fusion protein mutants.

Following transient expression of hDOR-$G_{i1}\alpha$ (Xaa ^{351}) fusion protein mutants in which residue^{351} of $G_{i1}\alpha$ was - Ile, Ala, Gly, Ser, Arg, Val, Leu or Phe – and prior PTx treatment (25ng/ml, 16h), membranes of HEK293T cells were prepared. [^{3}H] DADLE binding (1 nM) was measured at increasing concentrations of GDP. Data are shown from a representative experiment ($R^2 \rightarrow 0.7421$).

B. The pEC_{50} values for GDP-mediated reduction in the specific binding of [^{3}H] DADLE to hDOR-G_{i1} (Xaa ^{351}) fusion protein mutants.

The pEC_{50} values for GDP-mediated reduction in the specific binding of [^{3}H] DADLE was correlated with the n-octanol/H_20 partition co-efficients (Bahia *et al.*, 1998) of residue ^{351} of G_{i1} α in the fusion proteins. Amino acids are designated by the standard one letter code.

A

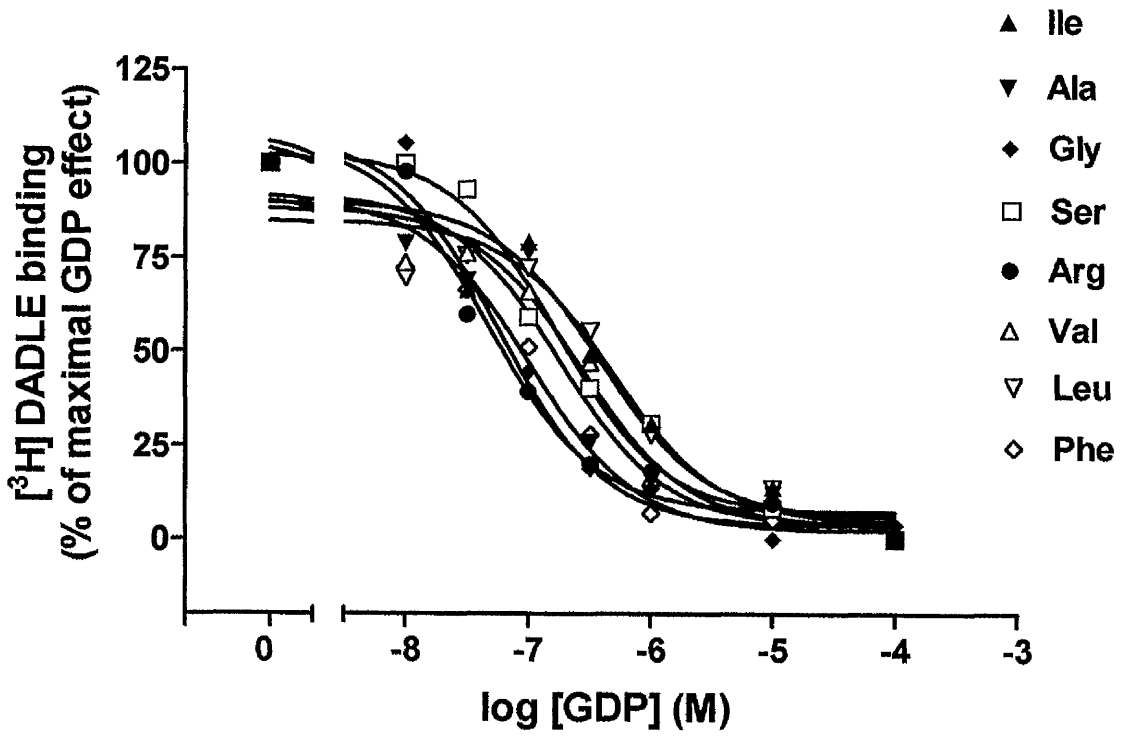
Ile
Ala
Gly
Ser
Arg
Val
Leu
Phe
[3H] DADLE binding
(% of maximal GDP effect)
125
100
75
50
25
0
0
-8
-7
-6
-5
-4
-3
log [GDP] (M)

B

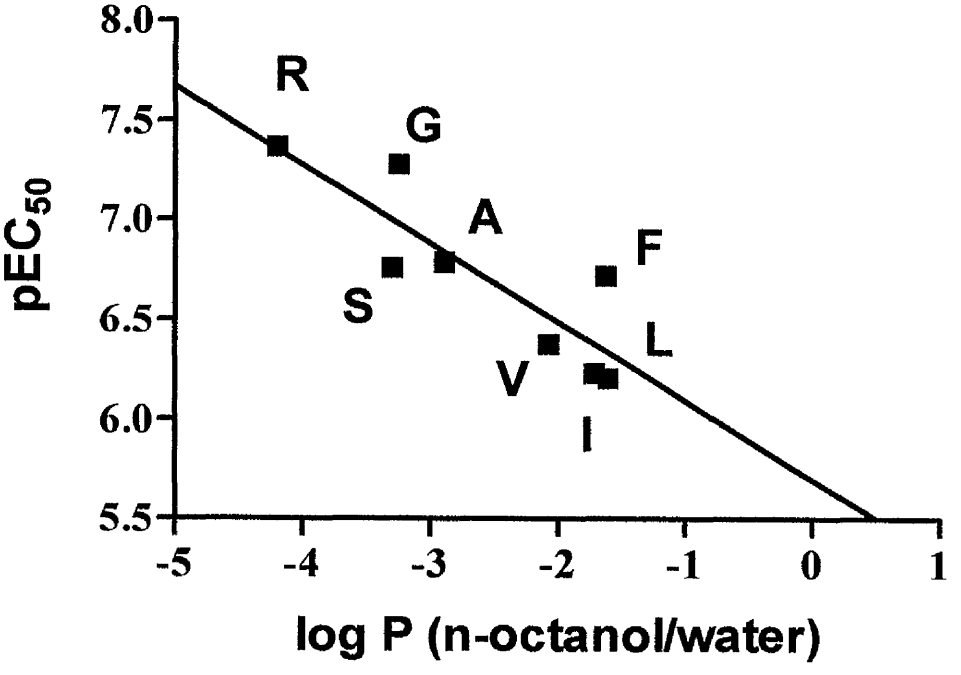
8.0
7.5
7.0
6.5
6.0
5.5
pEC50
R
G
A
S
F
L
V
I
-5
-4
-3
-2
-1
0
1
log P (n-octanol/water)

Figure 4.16. Effect of residue^{351} of $G_{o1}\alpha$ on the potency of GDP to regulate [^{3}H] DADLE binding to hDOR-$G_{o1}\alpha$ (Xaa ^{351}) fusion protein mutants.

A. [^{3}H] DADLE binding studies on membranes transiently expressing hDOR-G_{o1} (Xaa ^{351}) fusion protein mutants.

Following transient expression of hDOR-$G_{o1}\alpha$ (Xaa ^{351}) fusion protein mutants in which residue^{351} of $G_{o1}\alpha$ was - Ile, Leu or Gly – and prior PTx treatment (25ng/ml, 16h), membranes of HEK293T cells were prepared. [^{3}H] DADLE binding (1 nM) was measured at increasing concentrations of GDP. Data are shown from a representative experiment.

B. The pEC_{50} values for GDP-mediated reduction in the specific binding of [^{3}H] DADLE on hDOR-G_{o1} (Xaa ^{351}) fusion protein mutants.

The pEC_{50} values for GDP-mediated reduction in the specific binding of [^{3}H] DADLE was correlated with the n-octanol/H_20 partition co-efficients (Bahia *et al*, 1998) of residue ^{351} of $G_{o1}\alpha$ in the fusion proteins. Amino acids are designated by the standard one letter code.

A

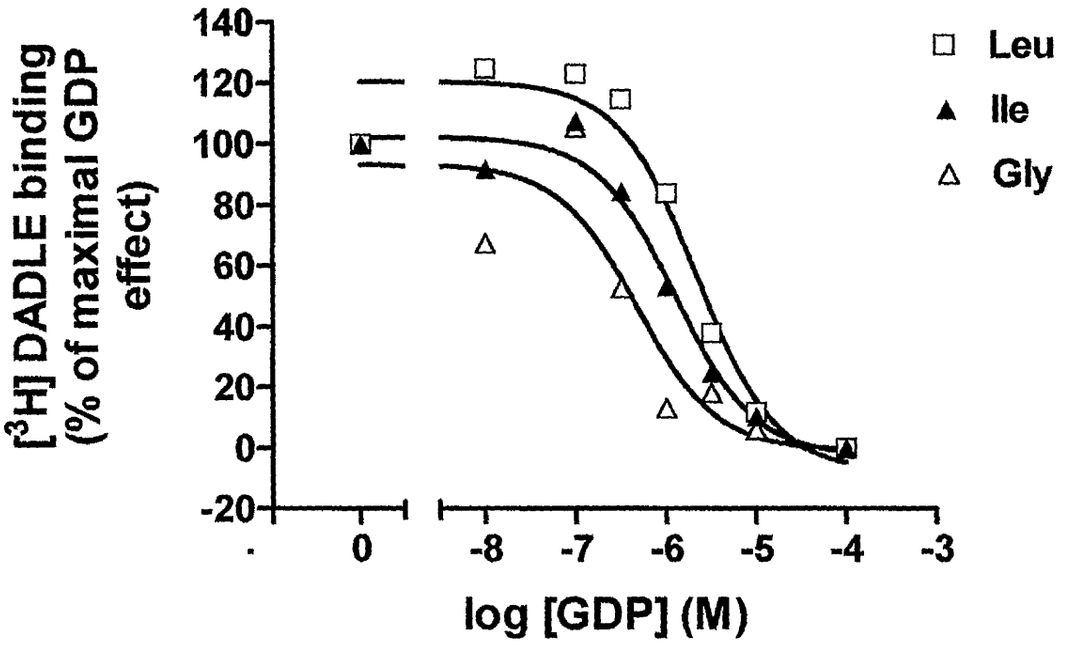
[3H] DADLE binding (% of maximal GDP effect)
140
120
100
80
60
40
20
0
-20
0
-8
-7
-6
-5
-4
-3
log [GDP] (M)
Leu
Ile
Gly

B

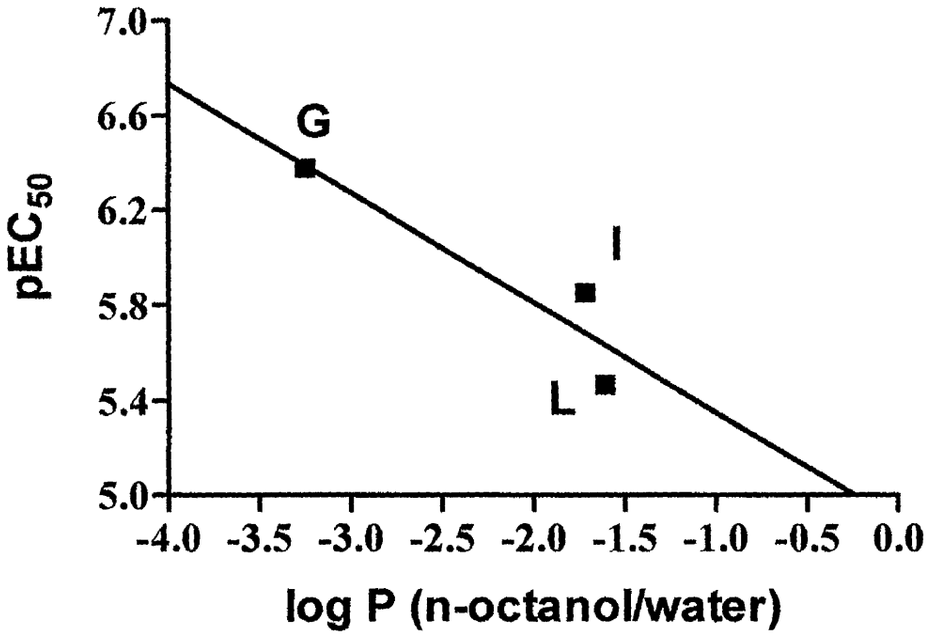
pEC50
7.0
6.6
6.2
5.8
5.4
5.0
G
I
L
-4.0
-3.5
-3.0
-2.5
-2.0
-1.5
-1.0
-0.5
0.0
log P (n-octanol/water)

Figure 4.17. Comparison of GDP effects on binding of [^{3}H] DADLE and [^{3}H] naltrindole to the hDOR-$G_{i1}\alpha$ (Ile ^{351})/-$G_{i1}\alpha$ (Gly ^{351}) fusion proteins.

A. [^{3}H] DADLE binding studies on membranes transiently expressing hDOR-$G_{i1}\alpha$ (Ile ^{351})/-$G_{i1}\alpha$ (Gly ^{351}) fusion proteins

Following transient expression of hDOR-$G_{i1}\alpha$ (Ile ^{351}) (□) and hDOR-$G_{i1}\alpha$ (Gly ^{351}) (▲) fusion proteins and prior PTx pre-treatment (25ng/ml, 16h), membranes of HEK293T cells were prepared. [^{3}H] DADLE binding (1 nM) was measured at increasing concentration of GDP. The pIC_{50} value was 5.78 ± 0.10 for hDOR-$G_{i1}\alpha$ (Ile ^{351}) and 6.58 ± 0.16 for hDOR-$G_{i1}\alpha$ (Gly^{351}) (means ± S.E.M, n=3). These values are significantly different (**P < 0.005).

B. [^{3}H] naltrindole binding studies on membranes transiently expressing hDOR-$G_{i1}\alpha$ (Ile ^{351})/-$G_{i1}\alpha$ (Gly ^{351}) fusion proteins

Following transient expression of hDOR-$G_{i1}\alpha$ (Ile ^{351}) (□) and hDOR-$G_{i1}\alpha$ (Gly ^{351}) (▲) fusion proteins and prior PTx pre-treatment (25ng/ml, 16h), membranes of HEK293T cells were prepared. The specific binding of [^{3}H] naltrindole (2.2 nM) was measured at increasing concentration of GDP. Data represent the mean ± S.E.M from three independent experiments.

A

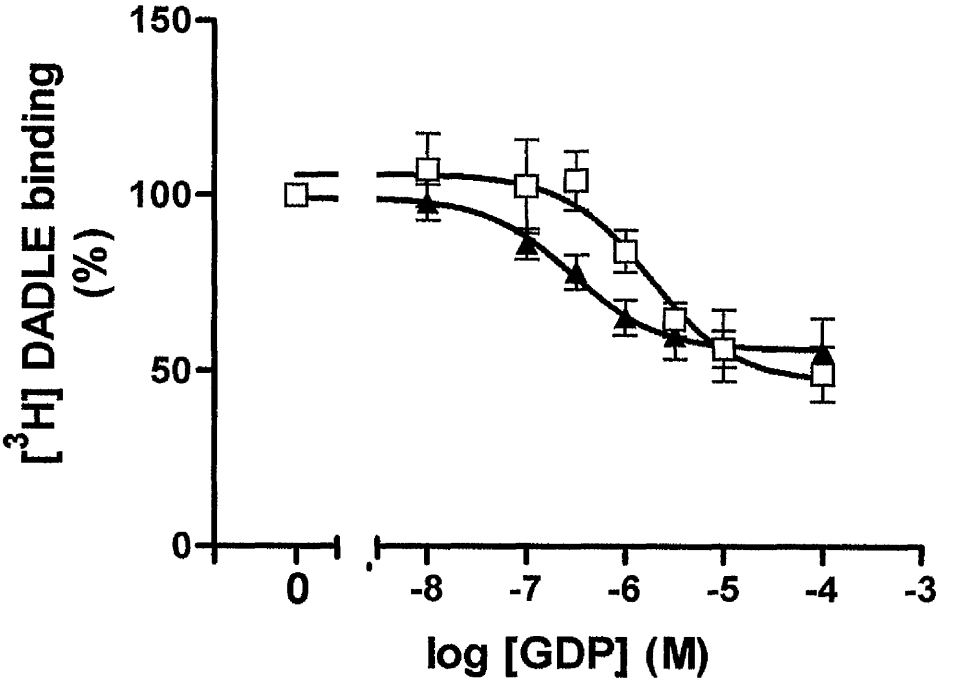
150
100
50
0
[3H] DADLE binding (%)
0
-8
-7
-6
-5
-4
-3
log [GDP] (M)

B

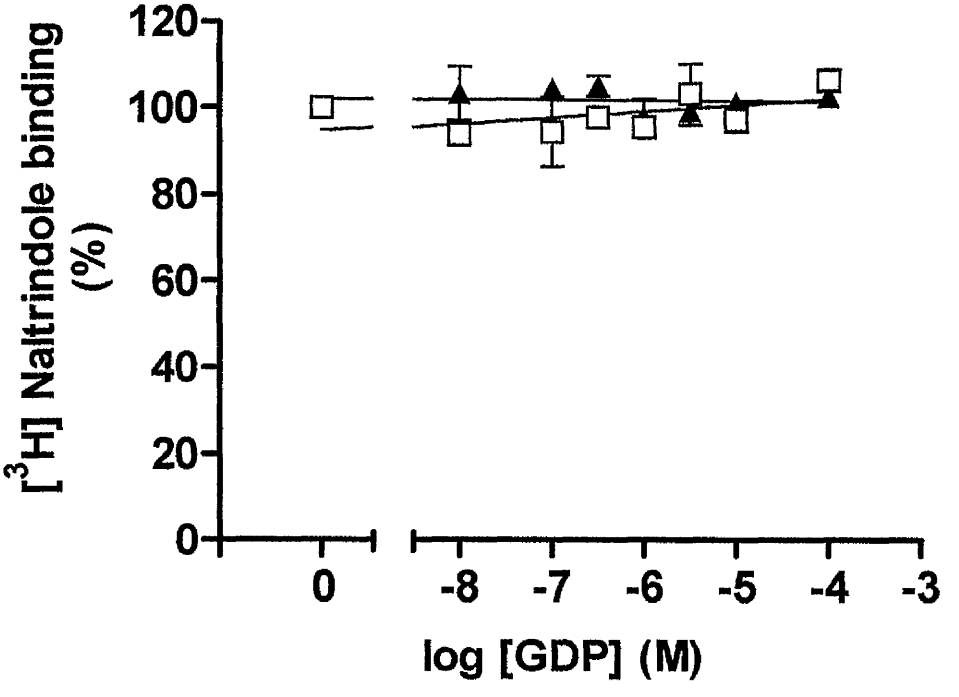
120
100
80
60
40
20
0
[3H] Naltrindole binding (%)
0
-8
-7
-6
-5
-4
-3
log [GDP] (M)

Figure 4.18. The G protein antagonist suramin selectively uncouples a hDOR-$G_{i1}\alpha$ fusion protein containing Gly at $G_{i1}\alpha$ residue ^{351}.

A. [^{3}H] DADLE binding studies on membranes transiently expressing hDOR-$G_{i1}\alpha$ (Ile ^{351})/-$G_{i1}\alpha$ (Gly ^{351}) fusion proteins

Following transient expression of hDOR-$G_{i1}\alpha$ (Ile ^{351}) (□) and hDOR-$G_{i1}\alpha$ (Gly ^{351}) (▲) fusion proteins and prior PTx pre-treatment (25ng/ml, 16h), membranes of HEK293T cells were prepared. [^{3}H] DADLE binding (1 nM) was measured at increasing concentration of suramin. The pIC_{50} value was 4.67 ± 0.15 for hDOR-$G_{i1}\alpha$ (Ile ^{351}) and 5.28 ± 0.15 for hDOR-$G_{i1}\alpha$ (Gly^{351}) (means ± S.E.M, n=3). These values are significantly different (**$P < 0.01$).

B. [^{3}H] naltrindole binding studies on membranes transiently expressing hDOR-$G_{i1}\alpha$ (Ile ^{351})/-$G_{i1}\alpha$ (Gly ^{351}) fusion proteins

Following transient expression of hDOR-$G_{i1}\alpha$ (Ile ^{351}) (□) and hDOR-$G_{i1}\alpha$ (Gly ^{351}) (▲) fusion proteins and prior PTx pre-treatment (25ng/ml, 16h), membranes of HEK293T cells were prepared. The specific binding of [^{3}H] naltrindole binding (2.3 nM) was measured at increasing concentration of suramin. Data represent the mean ± S.E.M from three independent experiments.

A

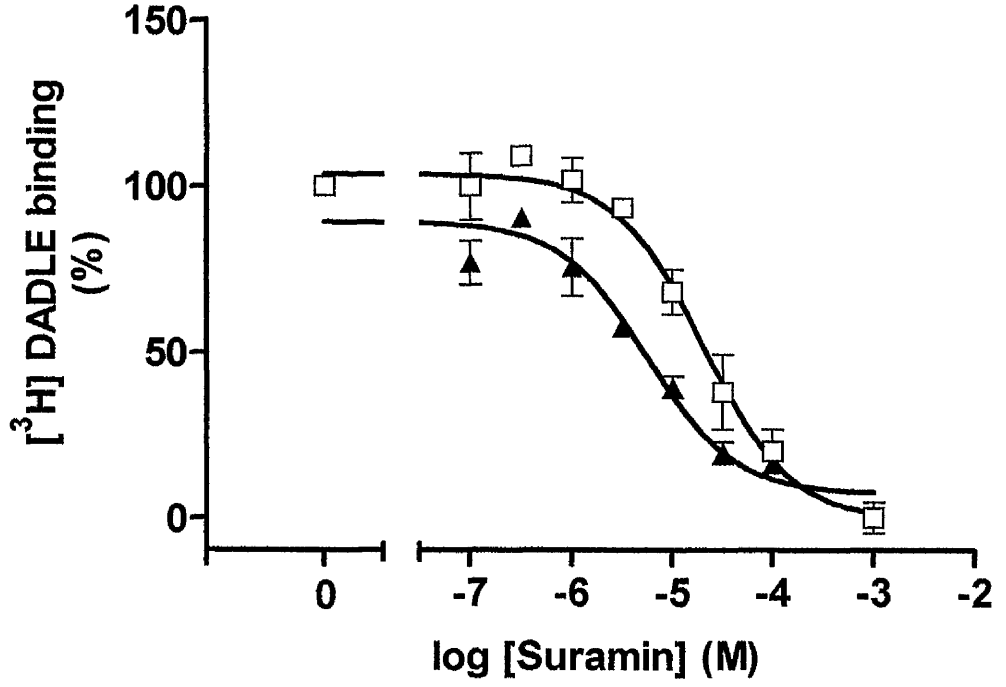
150
100
50
0
[3H] DADLE binding (%)
0
-7
-6
-5
-4
-3
-2
log [Suramin] (M)

B

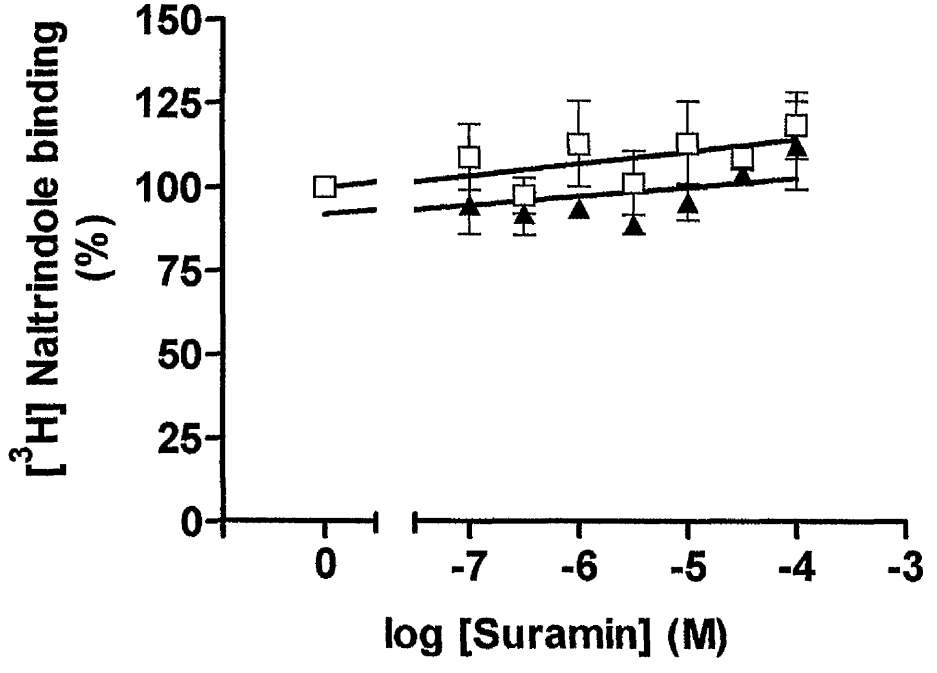
150
125
100
75
50
25
0
[3H] Naltrindole binding (%)
0
-7
-6
-5
-4
-3
log [Suramin] (M)

Figure 4.19. Association and dissociation kinetics of the binding of [^{3}H] DADLE to hDOR-$G_{i1}\alpha$ (Ile ^{351})/-$G_{i1}\alpha$ (Gly ^{351}).

A. Association kinetics of the binding of [^{3}H] DADLE to membranes transiently expressing hDOR-$G_{i1}\alpha$ (Ile ^{351})/-$G_{i1}\alpha$ (Gly ^{351}) fusion proteins

Following transient expression of hDOR-$G_{i1}\alpha$ (Ile ^{351}) (□) and hDOR-$G_{i1}\alpha$ (Gly ^{351}) (▲) fusion proteins and prior PTx pre-treatment (25ng/ml, 16h), membranes of HEK293T cells was prepared. The kinetics of association of [^{3}H] DADLE binding (1.2 nM) to the hDOR-$G_{i1}\alpha$ fusion proteins was monitored at 25°C. Data represent the mean ± S.E.M from three independent experiments.

B. Dissociation kinetics of the binding of [^{3}H] DADLE to membranes transiently expressing hDOR-G_{i1} (Ile ^{351})/-G_{i1} (Gly ^{351}) fusion proteins

Following transient expression of hDOR-G_{i1} (Ile ^{351}) (□) and hDOR-G_{i1} (Gly ^{351}) (▲) fusion proteins and prior PTx pre-treatment (25ng/ml, 16h), membranes of HEK293T cells was prepared and following attainment of steady-state binding of [^{3}H] DADLE to the two fusion proteins the antagonist naloxone (10 μM) was added at 25 ° C. The kinetics of dissociation of [^{3}H] DADLE were monitored. Data represent the mean ± S.E.M from three independent experiments.

A

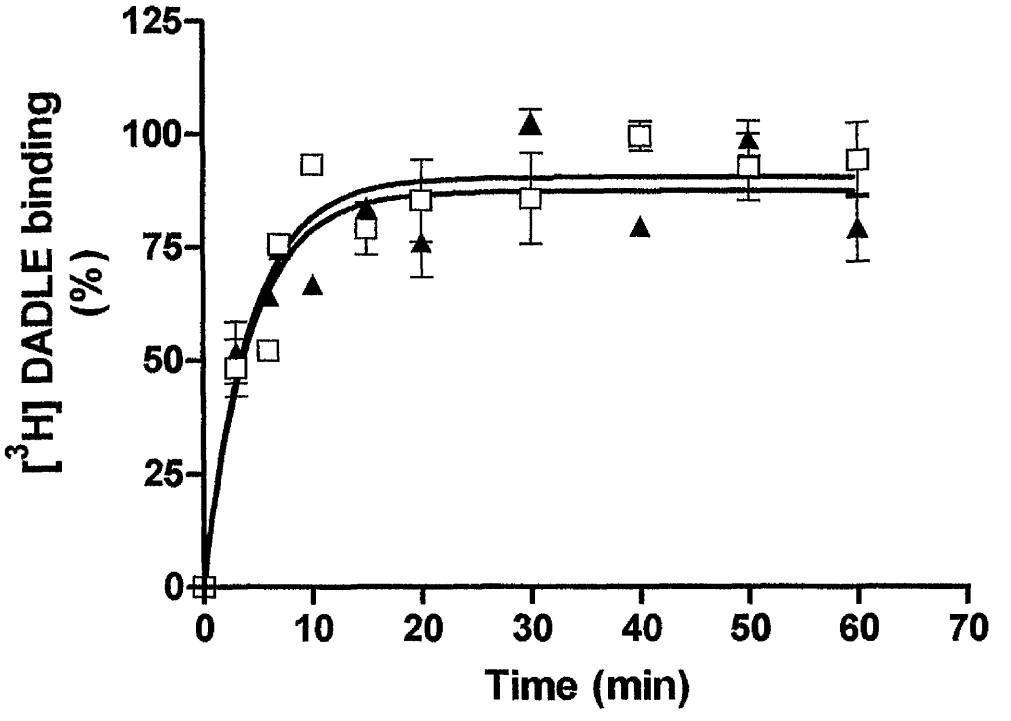
125
100
75
50
25
0
[3H] DADLE binding (%)
0
10
20
30
40
50
60
70
Time (min)

B

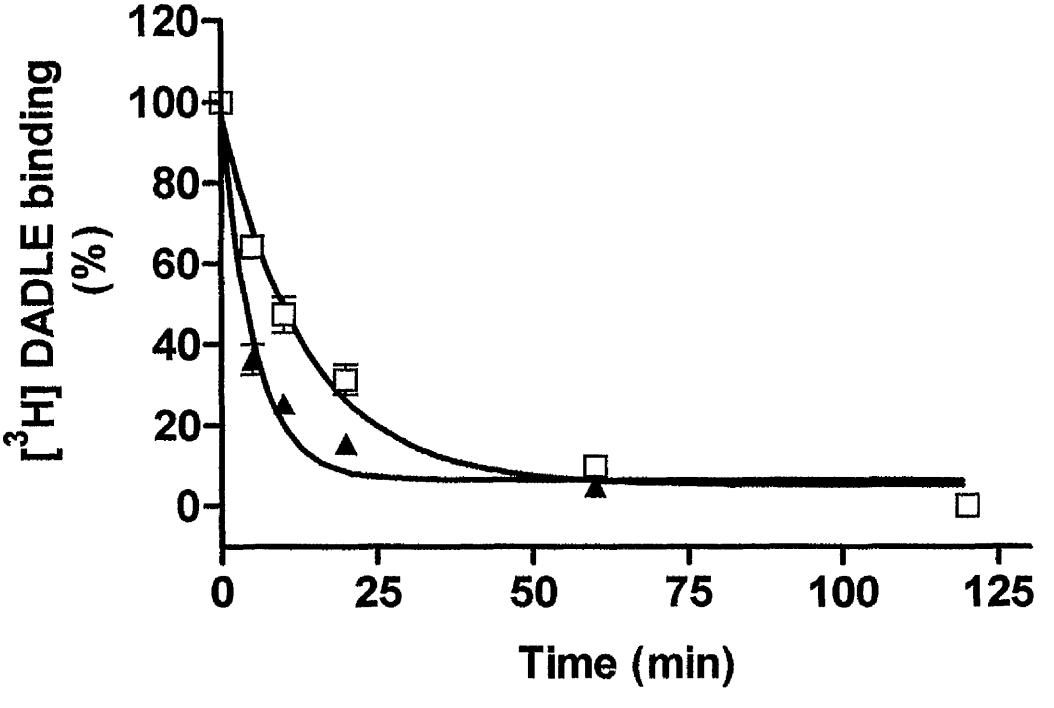
120
100
80
60
40
20
0
[3H] DADLE binding (%)
0
25
50
75
100
125
Time (min)

Figure 4.20. Analysis of [^{3}H] DADLE binding to transiently expressed hDOR-$G_{i1}\alpha$ (Ile^{351}).

A. [^{3}H] DADLE binding studies to membranes transiently expressing hDOR-$G_{i1}\alpha$ (Ile^{351}).

Following transient expression of the hDOR-$G_{i1}\alpha$ (Ile^{351}) fusion protein and prior PTx treatment (25ng/ml, 16h), saturation binding studies using [^{3}H] DADLE were performed on membranes of HEK293T cells. Non specific binding was assessed in parallel in the presence of 10 μM DADLE. The K_H of [^{3}H] DADLE for hDOR-$G_{i1}\alpha$ (Ile^{351}) was estimated as 0.68 ± 0.05 nM (mean ± S.E.M, n=3). This is a representative experiment.

B. Scatchard analysis

A Scatchard plot was generated from the data of Figure 4.20A.

A

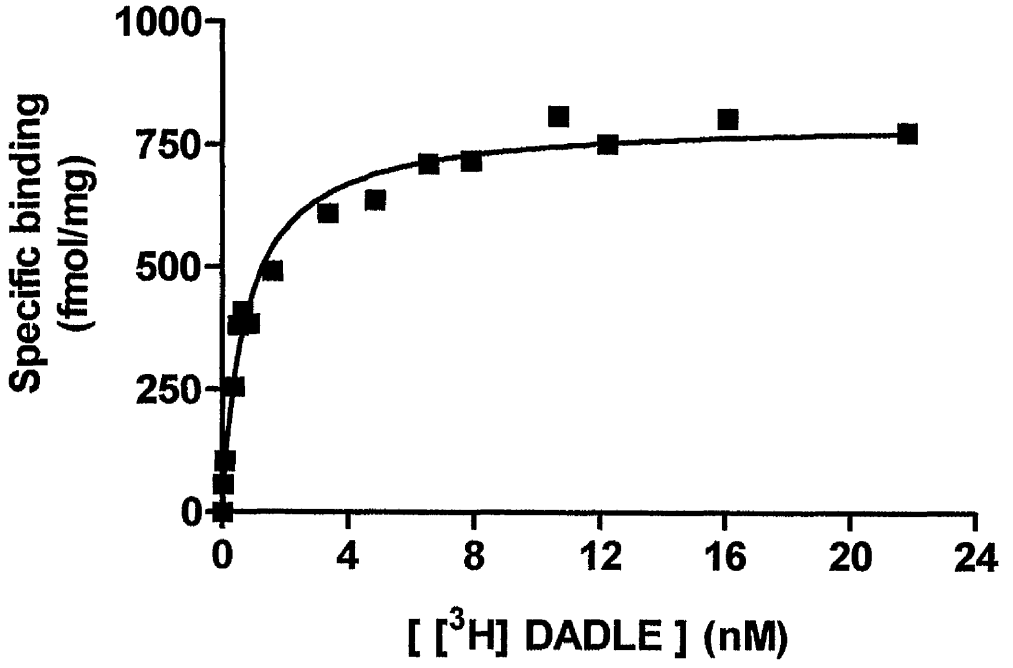
Specific binding (fmol/mg)
1000
750
500
250
0
0
4
8
12
16
20
24
[[3H] DADLE] (nM)

B

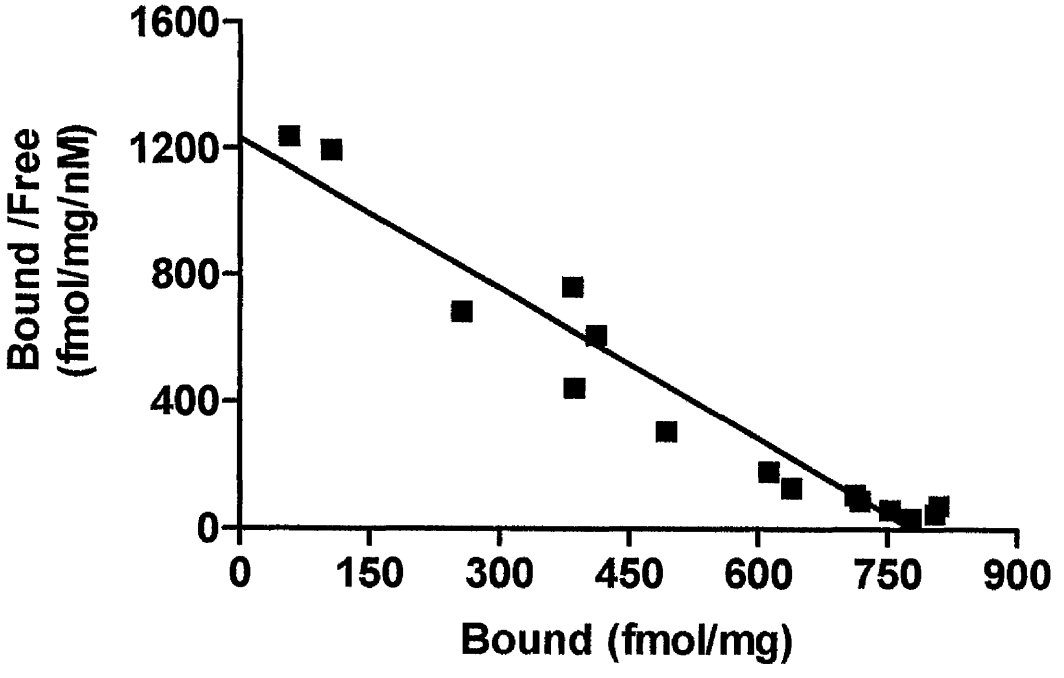
Bound /Free (fmol/mg/nM)
1600
1200
800
400
0
0
150
300
450
600
750
900
Bound (fmol/mg)

Figure 4.21 Analysis of [^{3}H] DADLE binding to transiently expressed hDOR-$G_{i1}\alpha$ (Gly^{351}).

A. [^{3}H] DADLE binding studies on membranes transiently expressing hDOR-$G_{i1}\alpha$ (Gly^{351}).

Following transient expression of the hDOR-$G_{i1}\alpha$ (Gly^{351}) fusion protein and prior PTx treatment (25ng/ml, 16h), saturation binding studies using [^{3}H] DADLE were performed on membranes of HEK293T cells. Non specific binding was assessed in parallel in the presence of 10 μM DADLE. The K_H of [^{3}H] DADLE for hDOR-$G_{i1}\alpha$ (Gly^{351}) was estimated as 2.1 ± 0.38* nM (mean ± S.E.M, n=3). This is a representative experiment. This value is significantly different from the hDOR-$G_{i1}\alpha$ (Ile^{351}) (*$P < 0.01$).

B. Scatchard analysis

A Scatchard plot was generated from the data of Figure 4.21A.

A

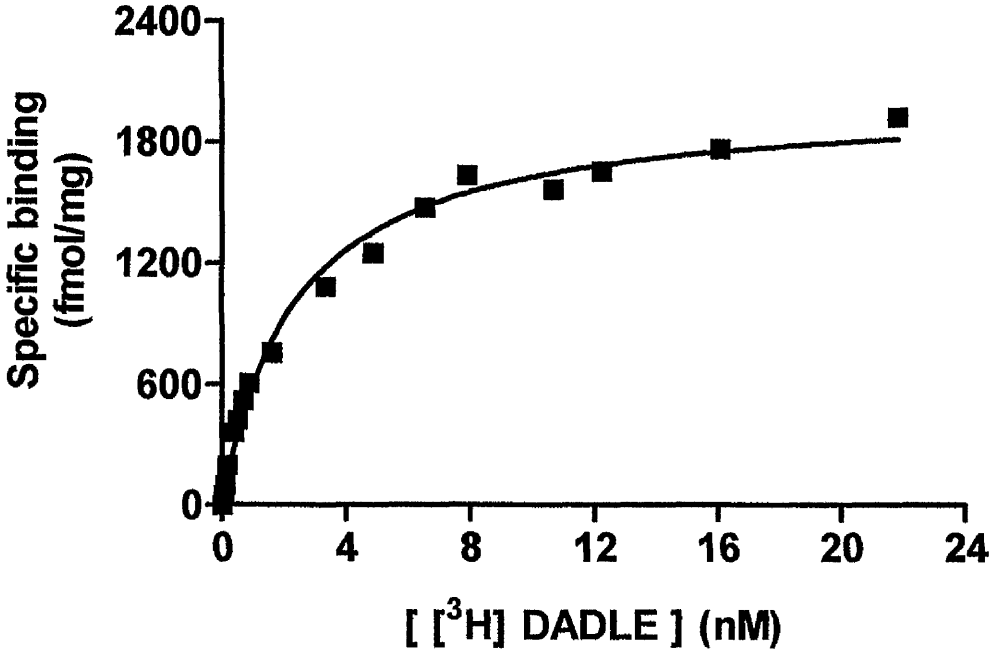
Specific binding (fmol/mg)
2400
1800
1200
600
0
0
4
8
12
16
20
24
[[3H] DADLE] (nM)

B

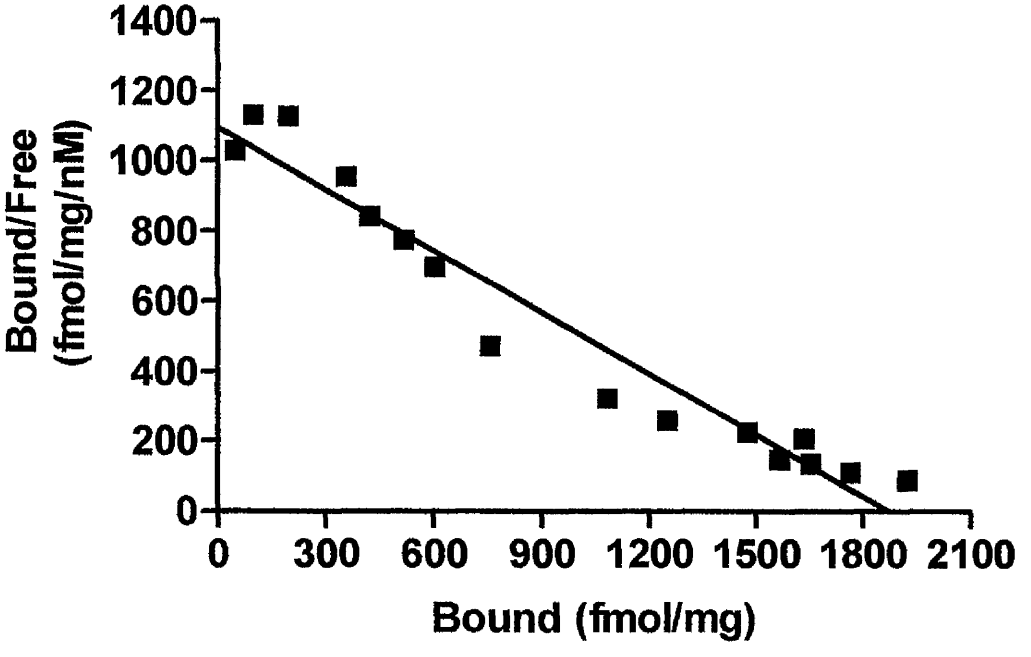
Bound/Free (fmol/mg/nM)
1400
1200
1000
800
600
400
200
0
0
300
600
900
1200
1500
1800
2100
Bound (fmol/mg)

CHAPTER V

Final discussion

FINAL DISCUSSION (CHAPTER V)

GPCRs transduce extracellular signals into the cell by activating heterotrimeric G proteins. Agonist-induced information transfer from GPCR to G protein is dependent upon the capacity of the ligand to promote the dissociation of GDP from the nucleotide binding pocket of the G protein and thus allow exchange for GTP, which is the rate limiting step in the cycle of G protein activation and deactivation (Gilman, 1987).

There are many aspects of opioid receptors that still remain poorly understood. To understand hDOR signalling, I have taken advantage of a fusion protein strategy in which either $G_{o1}\alpha$ or $G_{i1}\alpha$ were linked directly to the C-terminal tail of the hDOR. The benefits of this strategy have recently been extensively reviewed and include that it ensures the proximity of the receptor to each G protein is identical, that they are expressed in equal ratios and, most importantly, that the levels of each G protein can be easily measured (Seifert *et al.*, 1999; Milligan, 2000). As the fusion proteins have a 1:1 stoichiometry of receptor to G protein, saturation binding studies with an antagonist ligand provide direct measures of G protein, as well as receptor, expression levels.

In membranes provided from clones of HEK293 cells transiently/ stably expressing either hDOR-$G_{i1}\alpha$ (Ile^{351}) or hDOR-$G_{o1}\alpha$ (Ile^{351}) the agonist DADLE stimulated high affinity GTPase activity with similar potency. Both constructs were designed to be resistant to the ADP-ribosyltransferase activity of PTx as the target

cysteine of the G protein sequence: (Cys^{351}) was replaced by Ile. It has previously been demonstrated that positioning of a hydrophobic amino acid at this location provides the most effective interface between GPCR and G protein (Bahia *et al.*, 1998). Therefore, agonist-stimulated GTPase activity following PTx treatment of cells must reflect activation of the G protein within the fusion construct and not stimulation of the pool of endogenously expressed G_i-family proteins because these are crippled by this treatment.

In the present studies I have utilised an approach in which receptor-mediated guanine nucleotide exchange on a G protein can be measured at V_{max}. Measures of agonist-stimulated GTPase activity at various concentrations of GTP demonstrated the effect of agonist to represent an increase in V_{max} without altering the apparent affinity (K_m) of the fusion protein for substrate. There was a marked difference between the DADLE-induced GTP turnover number for the two fusion proteins, with the value for hDOR-$G_{i1}\alpha$ (Ile^{351}) being more than 3 times greater than for hDOR-$G_{o1}\alpha$ (Ile^{351}), which was true whether examining transient or stable expression of the constructs. It thus appears that activation of $G_{i1}\alpha$ by the hDOR is more efficient than for $G_{o1}\alpha$. This conclusion is further supported by the observation that isolated $G_{o1}\alpha$ releases GDP more effectively than $G_{i1}\alpha$ and thus in the basal state might be expected to produce greater rather than lower levels of guanine nucleotide exchange (Remmers *et al.*, 1999). It must thus be anticipated that given equal access to the hDOR and equal expression levels of the two G proteins in a single neuron agonists at this receptor will more efficiently regulate downstream targets of $G_{i1}\alpha$.

Both the hDOR-$G_{i1}\alpha$ (Ile^{351}) and hDOR-$G_{o1}\alpha$ (Ile^{351}) fusion proteins were able to inhibit forskolin-stimulated adenylyl cyclase activity in a PTx-insensitive and agonist concentration-dependent manner. These results indicate a clear capacity of both these fusion proteins to regulate downstream effectors. However, I did not address directly whether these effects are produced by the hDOR-linked $G\alpha$ subunits or via β/γ complexes released from the fusion proteins upon agonist activation. Such fusion proteins have been shown directly to interact with β/γ complexes by a variety of approaches (Bertin *et al.*, 1994; Wise *et al.*, 1997b; Small *et al.*, 2000). The potency of DADLE to inhibit AC activity was substantially greater than to stimulate GTPase activity. It is unclear whether this reflects a need for only a small level of agonist-occupancy of the fusion constructs to maximally inhibit AC activity or relates to the very different conditions used for the two assays. Moreover, I wished to assess the relative capacity of two distinct opioid receptor subtypes to activate the same G protein. For this reason, I also generated a hMOR-$G_{i1}\alpha$ (Ile^{351}) fusion protein, transiently expressed this in HEK293 cells and compared in parallel its activation by DADLE with the hDOR-$G_{i1}\alpha$ (Ile^{351}). GTP turnover number of $G_{i1}\alpha$ (Ile^{351}) following maximal occupation of the hMOR-1 by DADLE was not different from that produced by the hDOR. These results indicate that the hMOR-1 activates $G_{i1}\alpha$ as efficiently as the hDOR, at least when DADLE is used as the common agonist ligand.

I was also able to demonstrate that the identity of $residue^{351}$ of $G_{i1}\alpha$ alters both the effectiveness of agonist-induced activation of the G protein by the hDOR and determines the stability of a ternary complex between agonist, hDOR and $G_{i1}\alpha$ by altering its rate of dissociation. These two features are likely to be inherently related as

effective maintenance of the ternary complex is required to allow agonist-induced information transfer between the partner proteins.

In preliminary binding experiments utilising only the isolated hDOR, I observed that the level of binding of a single concentration of the agonist [^{3}H] DADLE, but not of the antagonist [^{3}H] naltrindole, was reduced substantially by both PTx pretreatment of cells and by addition of increasing concentrations of GDP to cell membranes. Furthermore, these two elements were not additive as GDP had no further effect following PTx treatment.

I was surprised to detect two binding states for DADLE to the hDOR-$G_{i1}\alpha$ (Ile^{351}) fusion protein. Expression of this feature in the fusion protein was substantially more pronounced than is often observed in such studies with co-expressed but separate receptors and G proteins, with the K_i values for DADLE differing by over 200 fold. In the absence of added guanine nucleotides, two clearly distinct affinity states for DADLE were identified whereas in the presence of either Gpp[NH]p or GDP a monophasic displacement curve was obtained corresponding to a low affinity state for DADLE. This indicates that the agonist ligand can sense the difference between two states of the hDOR-$G_{i1}\alpha$ fusion proteins even though the protein partners cannot formally separate.

The effects of point mutations at $cysteine^{351}$ in G_{i1} on the behaviour of fusion proteins constructed between the hDOR and G_{i1} were further investigated. Equivalent experiments on a range of hDOR-$G_{i1}\alpha$ fusions containing only a variation of the amino acid at this position produced a picture in which there was good correlation for

the partition coefficient of each amino acid between n-octanol and H_2O (a measure of their hydrophobicity) and the pEC_{50} for GDP-mediated reduction in [^{3}H] DADLE binding. By contrast, GDP did not reduce the binding of the antagonist [^{3}H] naltrindole to these fusion proteins. These results provided clear evidence for differences in the ternary complex of DADLE-hDOR-$G_{i1}\alpha$ due to a single amino acid alteration in the G protein.

I selected the hDOR-$G_{i1}\alpha$ (Ile^{351}) and hDOR-$G_{i1}\alpha$ (Gly^{351}) fusion proteins as marked examples of the observed differences in GDP regulation of [^{3}H] DADLE binding. PTx treatment had no effect on the binding of [^{3}H] DADLE to either the hDOR-$G_{i1}\alpha$ (Ile^{351}) or hDOR-$G_{i1}\alpha$ (Gly^{351}) fusion proteins as these are resistant to the actions of the toxin. However, in both cases increasing concentrations of GDP reduced [^{3}H] DADLE binding. It was obvious that higher concentrations of GDP were required to restrict the binding of [^{3}H] DADLE to the hDOR-$G_{i1}\alpha$ (Ile^{351}) fusion protein than the one containing $G_{i1}\alpha$ (Gly^{351}). The association kinetics of [^{3}H] DADLE to these two fusion proteins were not different but upon reaching [^{3}H] DADLE binding steady-state, addition of an excess of an antagonist allowed the dissociation kinetics of [^{3}H] DADLE to be monitored. Under the conditions employed, dissociation of this ligand was substantially more rapid from the Gly^{351} containing fusion than from the one in which it was replaced by Ile and that these differences corresponded to a 5-fold difference in the dissociation constant for [^{3}H] DADLE. Equivalent variation in the measured K_d for [^{3}H] DADLE was obtained in equilibrium saturation binding assays. Measured K_d for [^{3}H] DADLE binding to the hDOR-$G_{i1}\alpha$ (Ile^{351}) fusion protein was very similar to the pK_i for binding (9.3 ± 0.19,

means ± S.E.M) of this ligand to the agonist high affinity state of the fusion protein estimated from competition binding studies with [^{3}H] naltrindole. The G protein antagonist suramin displayed higher potency to inhibit [^{3}H] DADLE binding to the Gly^{351} than to the Ile^{351} hDOR-containing fusion protein, which is consistent with greater affinity of interactions between hDOR and $G_{i1}\alpha$ (Ile^{351}) than between hDOR and $G_{i1}\alpha$ (Gly^{351}). Previous studies with the $5HT_{1A}$ receptor have shown this receptor to display constitutive, agonist-independent capacity to activate $G_{i1}\alpha$ (Ile^{351}) but not $G_{i1}\alpha$ (Gly^{351}) and there is increased relative intrinsic activity of partial agonists at the α_{2A}-adrenoceptor to activate $G_{i1}\alpha$ (Ile^{351}) compared to $G_{i1}\alpha$ (Gly^{351}). Such observations demonstrate the importance of the nature of this interface for protein-protein interactions between GPCR and G protein and that these interactions, which can be monitored by ternary complex stability, determine the effectiveness of information transfer from the GPCR to G protein. In other words, $cysteine^{351}$ is critical for stabilising the ternary complex.

List of publications

LIST OF PUBLICATIONS

- Control of the efficiency of agonist-induced information transfer and stability of the ternary complex containing the δ-opioid receptor and the α subunit of G_{i1} by mutation of a receptor/G protein contact interface.

  Hyo-Eun Moon, Daljit S. Bahia, Antonella Cavalli, Marcel Hoffmann and Graeme Milligan.

  (*Submiited to Neuropharmacology).*

- The human δ opioid receptor activates $G_{i1}\alpha$ more efficiently than $G_{o1}\alpha$.

  Hyo-Eun Moon, Daljit S. Bahia, Antonella Cavalli, Marcel Hoffmann, Dominigue Massotte and Graeme Milligan. (2001) *Journal of Neurochemistry* **76,** 1805-1813.

References

REFERENCES

Abdelhamid E.E., Sultana M., Portoghese P.S., and Takemori A.E. (1991) *J. Pharmacol. Exp. Ther.* **258** (1), 299-303.

Angers S., and Bouvier M. (2000) *Trends Pharmacol. Sci.* **21**, 326-327.

Avidor-Reiss T., Bayewitch M., Levy R., Matus-Leibovitch N., Nevo I., and Vogel Z. (1995) *J. Biol. Chem.* **270**, 29732-29738.

Avidor-Reiss T., Nevo I., Saya D., Bayewitch M., and Vogel Z. (1997) *J. Biol. Chem.* **272**, 5040-5047.

Bahia D.S., Wise A., Fanelli F., Lee M., Rees S., and Milligan G. (1998) *Biochemistry.* **37**, 11555-11562.

Barr A.J., and Manning D.R. (1997) *J. Biol. Chem.* **272**, 32979-32987.

Befort K., Tabbara L., Bausch S., Chavkin C., Evans C., and Kieffer, B. (1996) *Mol. Pharmacol.* **49**, 216-223.

Befort K., Tabbara L., Kling D., Maigret B., and Kieffer B.L. (1996) *J. Biol. Chem.* **271**, 10161-10168.

Befort K., Zilliox C., Filliol D., Yue S.Y., and Kieffer, B.L. (1999) *J. Biol. Chem.* **274**, 18574-18581.

Beindl W., Mitterauer T., Hohenegger M., Ijzerman A.P., Nanoff C., and Freissmuth M. (1996) *Mol. Pharmacol.* **50**, 415-423.

Benovic J.L., DeBlasi A., Stone W.C., Caron M.G., and Lefkowitz R.J. (1989) *Science.* **246**, 235-240.

Bertin B., Friessmuth M., Jockers R., Strosberg A.D., and Marullo S. (1994) *Proc. Natl. Acad. Sci. USA*. **91**, 8827-8831.

Bertin B., Strosberg A.D., and Marullo S. (1997) *Int. J. Cancer*. **71,** 1029-1034.

Berman D.M., and Gilman A.G. (1998) *J. Biol. Chem*. **273**, 1269-1272.

Berman D.M., Wilkie T.M., and Gilman A.G. (1996) *Cell*. **86**, 445-452.

Berstein G., Blank J.L., Jhon D.Y., Exton J.H., Rhee S.G., and Ross E.M. (1992) *Cell*. **70**, 411-418.

Biesen T.V., Hawes B.E., Raymon J.R., Luttrell L.M., Koch W.J., and Lefkowitz R.J. (1996) *J. Biol. Chem*. **271**, 1266-1269.

Birnbaumer L. (1990) *FASEB J*. **4,** 3178-3188.

Bloch B., Dumartin B., and Bernard V. (1999) *Trends Pharmacol. Sci.* **20**, 315-319.

Bot G., Blake A.D., Li S., and Reisine T.(1998) *J. Pharmacol. Exp. Ther*. **284**, 283-290.

Bond C., Laforge K.S., Tian M., Melia D., Zhang S., Borg L., Gong J., Schluger J., Strong J.A., Leal S.M., Tischfield J.A., Kreek M.J., and Yu L. (1998) *Proc. Natl. Acad. Sci. USA*. **95**, 9608-9613.

Bond R.A., Leff P., Johnson T.D., Milano C.A., Rockman H.A., McMinn T.R., Apparsundaram S., Hyek M.F., Kenakin T.P., Allen L.F, *et al* (1995) *Nature.* **374**, 272-276.

Bonatti S., Migliaccio G., and Simons K. (1989) *J. Biol. Chem*. **264**, 12590-12595.

Bourne H.R. (1997) *Curr. Opin. Cell biology.* **9,** 134-142.

Bol G.F., Gros C., Hulster A., Bosel A., and Pfeuffer T. (1997) *Biochem. Biophys. Res. Commun.* **237**(2), 251-256.

Bray P., Carter A., Simons C., Guo V., Puckett C., Kamholz J., Spiegel A., and Nirenberg M. (1986) *Proc. Natl. Acad. Sci. USA.* **83**, 8893-8897.

Brown G.P., and Pasternak G.W. (1998) *J. Pharmacol. Exp. Ther.* **286**, 376-381.

Bryen A.J., and Devi L.A. (1999) *Nature.* **399**, 697-700.

Burt A.R., Sautel M., Wilson M.A., Rees S., Wise A., and Milligan G. (1998) *J. Biol. Chem.* **273**, 10367-10375.

Buss J.E., Mumpy S.M., Casey P.J., Gilman A.G., and Sefton B.M. (1987) *Proc. Natl. Acad. Sci. USA.* **84**, 7493.

Burt A.R., Carr I.C., Mullaney I., Anderson N.G., and Milligan G. (1996) *Biochem J.* **320**, 227-235.

Cavalli A., Babey A.M., and Loh H.H. (1999) *Neuroscience.* **93**, 1025-1031.

Cavalli A., Druey K.M., and Milligan G. (2000) *J. Biol. Chem.* **275**, 23693-23699.

Carr I.C., Burt A.R., Jackson V. N., Wright J., Wise A., Rees S., and Milligan G. (1998) *FEBS Letters.* **428**, 17-22.

Cantiello H.F., Patenaude C.R., and Ausiello D.A. (1989) *J. Biol. Chem.* **264**, 20867-20870.

Cantiello H.F., Patenaude C.R., Codina J., Birnbaumer L., and Ausiello D.A. (1990) *J. Biol. Chem.* **265**, 21624-21628.

Casey P.J., Graziano M.P., and Gilman A.G. (1989) *Biochemistry.* **28**, 611-616.

Casey P.J. (1995) *Science.* **268**, 221-225.

Cassel D., and Selinger Z. (1978) *Proc. Natl. Acad. Sci. USA.* **75**, 2669-2673.

Chuprun J.K., Raymond J.R., and Blackshear P.J. (1997) *J. Biol. Chem.* **272**, 773-781.

Chu P., Murray S., Lissin D., and Von Zastrow M. (1997) *J. Biol. Chem.* **272**, 27124-27130.

Chalecka-Franaszek E., Weems H.B., Crowder A.T., Cox B.M., and Cote T.E. (2000) *J. Neurochem.* **74,** 1068-1078.

Chakrabarti S., Prather P.L., Yu L., Law P.Y., and Loh H.H. (1995) *J. Neurochem.* **64,** 2534-2543.

Chan J.S.C., Chiu T.T., and Wong Y.H. (1995) *J. Neurochem.* **65**, 2682-2689.

Chen G., Way J., Armour S., Watson C., Queen K., Jayawickreme C.K., Chen W.J., and Kenekin T. (2000) *Mol. Pharmacol.* **57**, 125-134.

Chen Y., Harry A., Li J., Smit M.J., Bai X., Magnusson R., Pieroni J.P., Weng G., and Iyengar R. (1997) *Proc. Natl. Acad. Sci. USA.* **94**, 14100-14104.

Cheng P.Y., Wu D., Decena J., Soong Y., McCabe S., and Szeto H.H. (1993) Eur. *J. Pharmacol.* **230**, 85-88.

Christopoulos A. (1998) *Trends Pharmacol. Sci.* **19**, 351-357.

Claude P.A., Wotta D.R., Zhang X.H., Prather P.L., Mcginn T.M., Erickson L.J., Loh H.H., and Law P.Y. (1996) *Proc. Natl. Acad. Sci. USA.* **93**, 5715-5719.

Clarke W.P., and Bond R.A. (1998) *Trends Pharmacol. Sci.* **19**, 270-276.

Clapham D.E., and Neer E.J. (1997) *Annu. Rev. Pharmacol. Toxicol.* **37**, 167-203.

Conklin B.R., Farfel Z., Lustig K.D., Julius D., and Bourne H.R. (1993a) *Nature.* (Lond) **363,** 274-276.

Conklin B.R., and Bourne H.R (1993b) *Cell.* **21**(4), 631-641.

Conklin B.R., Herzmark P., Ishida S., Voyno-Yasenetskaya T.A., Sun Y., Farfel Z., and Bourne H.R. (1996) *Mol. Pharmacol.* **50**(4), 885-890.

Connor M., and Christie M.D. (1999) *Clin. Exp. Pharmacol. Physiol.* **26,** 493-499.

Colquhoun D. (1998) *Br. J. Pharmacol.* **125**, 924-947.

Cotecchia S., Exum S., Caron M.G., and Lefkowitz R.J. (1990) *Proc. Natl. Acad. Sci. USA.* **87**, 2896-2900.

Cowan C.W., Fariss R.N., Sokal I., Palczewski K., and Wensel T.G. (1998) *Proc. Natl. Acad. Sci. USA.* **95,** 5351-5356.

Crain S.M., and Shen K.F. (1998) *Trends Pharmacol. Sci.* **19**, 358-365.

Cvejic S., Trapaidze N., Cyr C., and Devi I.A. (1996) *J. Biol. Chem.* **271**, 4073-4076.

Cvejic S., and Devi L.A. (1997) *J. Biol. Chem.* **272**, 26959-26964.

Danielson P.B., and Dores R.M. (1999) *General and Comparative Endocrinology.* **113**, 169-186.

DeBlasi A., O'Reilly K., and Motulsky H.J. (1989) *Trends Pharmacol. Sci.* **10**, 227-229.

Degtyarev M.Y., Spiegel A.M., and Jones T.L.Z. (1993) *J. Biol. Chem.* **268**, 23769-23772.

Devi L.A. (2000) *Trends Pharmacol. Sci.* **21**, 324-326.

DeVries L., Mousli M., Wurmser A., and Farquhar M.G. (1995) *Proc. Natl. Acad. Sci. USA*. **92**, 11916-11920.

Dixon R.A., Kobilka B.K., Strader D.J., Benovic J.L., Dohlman H.G., Frielle T., Bolanowski M.A., Bennett C.D., Rands E., Diehl R.E., *et al.* (1986) *Nature.* **321**, 75-79.

Dickenson A.H. (1997) *Behav. Brain. Sci.* **20**, 392-404.

Dietzel C., and Kurgan J. (1987) *Cell.* **50**, 1001.

Dohlman H.G., and Thorner J. (1997) *J. Biol. Chem.* **272**, 3871-3874.

Dupuis D.S., Tardif S., Wurch T., Colpaert F.C., and Pauwels P.J. (1999) *Neuropharmacology.* **38,** 1035-1041.

Eason M.G., Jacinto M.T., Theiss C.T., and Liggett S.B. (1994) *Proc. Natl. Acad. Sci. USA*. **91**, 11178-11182.

Evans C.J., Keith D.E.Jr., Morrison H., Magendzo K., and Edwards R.H. (1992) *Science.* **258**, 1952-1955.

Exner T., Jensen O.N., Mahh M., Kleuss C., and Nurnberg B. (1999) *Proc. Natl. Acad. Sci. USA*. **96**, 1327-1332.

Fanelli F., Menzian C., Scheer A., Cotecchia S., and De Benedetti P.G. (1999) *PROTEINS: Structure, Function, and Genetics.* **37**, 145-156.

Farndale R.W., Allan L.M., and Martin B.R. (1991). *In: Signal Transduction A Practical Approach, Oxford University Press, U. K.*, 75-103.

Fong C.W., Bahia D.S., Rees S., and Milligan G. (1998) *Mol. Pharmacol.* **54**, 249-257.

Fong C.W., and Milligan G. (1999) *Biochem J.* **342**, 457-463.

Freissmuth M., Waldhoer M., Bofill-Cardona E., and Nanoff C. (1999) *Trends Pharmacol. Sci.* **20**, 237-245.

Freissmuth M., Boehm S., Beindl W., Nickel P., Ijzerman A.P., Hohenegger M., and Nanoff C. (1996) *Mol. Pharmacol.* **49**, 602-611.

Freissmuth M., and Nanoff C. (1999) *CMLS, Cellular and Molecular Life Sciences.* **55**, 257-270.

Fukuda K., Kato S., Mori K., Nishi M., and Takeshima H. (1993) *FEBS Lett.* **327**(3), 311-314.

Gao B., and Gilman A.G (1991) *Proc. Natl. Acad. Sci. USA.* **88**, 10178.

Georgoussi Z., Milligan G., and Zioudrou C. (1995) *Biochem J.* **306**, 71-75.

Gether U., and Kobilka B.K. (1998) *J. Biol. Chem.* **273**, 17979-17982.

Georgoussi Z., Carr C., and Milligan G. (1993) *Mol. Pharmacol.* **44**, 62-69.

Gierschik P., Bouillon T., and Jakobs K.H. (1994) *Methods. Enzymol.* **237**, 13-26.

Gilman A.G. (1987) *Ann. Rev. Biochem.* **56**, 615-649.

Glass M., and Northup J.K. (1999) *Mol. Pharmacol.* **56**, 1362-1369.

Goldsmith P., Backlund P.S., Rossiter K., Carter A., Milligan G., Unson C.G., and Spiegel A.M. (1988) *Biochemistry.* **27,** 7085-7090.

Grassie M.A., McCallum J.F., Guzzi F., Magee A.I., Milligan G., and Parenti M. (1994) *Biochem J.* **302**, 913-920.

Green A., Johnson J.L., and Milligan G. (1990) *J. Biol. Chem.* **265**, 5206-5210.

Gurevich V.V., Dion S.B., Onorato J.J., Ptasienski J., Kim C.M., Sterne-Marr R., Hosey M.M., and Benovic J.L. (1995) *J. Biol. Chem.* **270**, 720-731.

Hausdorff W.P., Caron M.G., and Lefkowitz R.J. (1990) *FASEB J.* **4**, 2881-2889.

Hart M.J., Jiang X., Kozasa T., Roscoe W., Singer W.D., Gilman A.G., Sternweis P. C., and Bollag G. (1998) *Science.* **280,** 2112-2114.

Hamm H.E. (1998) *J. Biol. Chem.* **273**, 669-672.

Hamm H.E (1991) *Cell. Mol. Neurobiol.* **11,** 563-578.

Hamm H.E., Deretic D., Arendt A., Hargrave P.A., Koenig B., and Hofmann K.P. (1988) *Science.* **241**, 832-835.

Hamm H.E., Deretic D., Mazzoni M.R., Moore C.A., Takahashi J.S., and Rasenick M.M. (1989) *J. Biol. Chem.* **264**, 11475-11482.

Hayashi M. K., and Haga T. (1997) *Arch. Biochem. Biophys.* **340**, 376-382.

Hartman IV, J. L., and Northup J. K. (1996) *J. Biol. Chem.* **271**, 22591-22597.

Hellmich M., Battey J.F., and Northup J.K. (1997) *Proc. Natl. Acad. Sci. USA.* **94**, 751-756.

Hepler J., and Gilman A.G. (1992) *Trends Biochem. Sci.* **17**, 383-387.

Hebert T.E., Moffett S., Morello J.P., Loisel T.P., Bichet D.G., Barret C., and Bouvier M. (1996) *J. Biol. Chem.* **271**, 16384-16392.

Hescheler J., Rosenthal W., Wulfern M., Tang M., Yajima M., Trautwein W., and Schultz G. (1988) *Adv. Second Messenger Phosphoprotein Res.* **21,** 165-14.

Heyman J.S., Vaught J.L., Raffa R.B., and Porreca F. (1988) *Trends Pharmacol. Sci..* **9,** 134-138.

Hiller J.M., Fan L.Q., and Simon E.J. (1996) *Brain Res.* **719**(1-2), 85-95.

Hohenegger M., Waldhoer M., Beindl W., Boing B., Kreimeyer A., Nickel P., Nanoff C., and Freissmuth M. (1998) *Proc. Natl. Acad. Sci. USA.* **95**, 346-351.

Houslay M.D., and Milligan G. (1997) *Trends Pharmacol. Sci.* **22,** 217-224.

Houslay M.D., and Milligan G. (1990) *G- proteins as mediators of cellular signalling processes, WILEY.*

Houslay M.D., Gawler D.J., Milligan G., and Wilson A. (1989) *Cell. Signalling.* **1**, 9-22.

Hurley J.H. (1999) *J. Biol. Chem.* **274,** 7599-7602.

Hurley J.H. (1998) *Curr. Opin. Struct. Biol.* **8**, 770-777.

Hunt T.W., Carroll R.C., and Peralta E.G. (1994) *J. Biol. Chem.* **269**, 29565-29570.

Hunt T. (2000) *Cell.* **100**, 113-127.

Iismaa T.P., Kiefer J., Liu M.L., Baker E., Sutherland G.R., and Shine J. (1994)

Genomics. **24,** 391-394.

Iiri T., Backlund P.S., Jones T.L.Z., Wedegaertner P.B., and Bourne H.R. (1996) *Proc. Natl. Acad. Sci. USA.* **93**, 14592-14597.

Ikeda S.R. (1996*) Nature (London).* **380**, 255-258.

Inoue H., Nojima H., and Okayama H. (1990) *Gene.* **96,** 23-28.

Itoh H., Kozasa T., Nagata S., Nakamura S., Katada T., Ui M., Iwai S., Ohtsuka E., K awasaki H., Suzuki K., *et al* (1986) *Proc. Natl. Acad. Sci. USA.* **83**, 3776-3780.

Iyengar R. (1994) *Methods in Enzymology.* **237.**

Jackson V.N., Bahia D.S., and Milligan G. (1999) *Mol. Pharmacol.* **55**, 195-201.

Jensen A.A., Pederson U.B., Kiemer A., Din N., and Anderson P.H. (1995) *J. Neurochem.* **65**, 1325-1331.

Jian X., Sainz E., Clark W.A., Jensen R.T., Battey J.F., and Northup J.K. (1999) *J. Biol. Chem.* **274**, 11573-11581.

Ji T.H., Murdoch W.J., and Ji I. (1995) *Endocrine.* **3**, 187-194.

Jiang Y., Ma W., Wan Y., Kozasa T., Hattori S., and Huang X.Y. (1998) *Nature.* **395**, 808-813

Ji T.H., Grossmann M., and Ji I. (1998) *J. Biol. Chem.* **273**, 17299-17302.

Johannes Scheuring., Paul J. Berti., and Vern L. Schramm. (1998) *Biochemistry.* **37**, 2748-2758.

Jones K.A., Borowsky B., Tamm J.A., Craig D.A., Durkin M.M., Dai M., Yao W.J., Johnson M., Gunwaldsen C., Huang L.Y., Tang C., Shen Q., Salon J.A., Morse K., Laz T., Smith K.E., Nagarathnam D., Noble S.A., Branchek T.A., and Gerald C. (1998) *Nature.* **396**(6712), 674-679.

Jordan B.A., and Devi L.A (1999) *Nature.* **399** (6737), 697-700.

Katada T., and Ui M. (1982) *Proc. Natl. Acad. Sci. USA.* **79**, 3129-3133.

Katada T., Gilman A.G., Watanabe Y., Bauer S., and Jakobs K.H. (1985) *Eur. J. Biochem.* **151**, 431-437.

Kaupmann K., Malitschek B., Schuler V., Heid J., Froestl W., Beck P., Mosbacher J., Bischoff S., Kulik A., Schigemoto R., Karschin A., and Bettler B. (1998) *Nature.* **396** (6712), 683-687.

Kawate N., and Menon K.M.J. (1994) *J. Biol. Chem.* **269**, 30651-30658.

Kenakin T. (1997) *Trends Pharmacol. Sci.* **18**, 456-464.

Kennedy M.E., and Limbird L.E. (1994) *J. Biol. Chem.* **269**, 31915-31922.

Kest B., Lee C.E., McLemore G.L., and Inturrisi C.E. (1996) *Brain Res. Bull.* **39,** 185-188.

Kellet E., Carr I.C., and Milligan G. (1999) *Mol. Pharmacol.* **56**, 684-692.

Kieffer B.L., Befort K., Gaveriaux-Ruff C., and Hirth C.G. (1992) *Proc. Natl. Acad. Sci. USA.* **89,** 12048-12052.

Kieffer B.L., Befort K., Gaveriaux-Ruff C., and Hirth C.G. (1994) *Proc. Natl. Acad. Sci. USA.* **91,** 1193.

Kieffer B.L. (1999) *Trends Pharmacol. Sci.* **20**, 19-26.

Kjelsberg M.A., Cotecchia S., Ostrowski J., Caron M.G., and Lefkowitz R.J. (1992) *J. Biol. Chem.* **267**, 1430-1433.

Knapp R.J., Malatynska E., Collinss N., Fang L., Wang J.Y., Hruby V.J., Roeske W.R., and Yamamura H.I. (1995b) *FASEB J.* **9**, 516-525.

Knapp R.J., Malatynska E., Fang L., Li X., Babin E., Nguyen M., Santoro G., Varga E. V., Hruby V.J., Roeske W.R., and Yamamura H.I. (1994) *Life Sci.* **54**, PL463-PL469.

Kohno M., Fukushima N., Yoshida A., and Ueda H. (2000) *FEBS Lett.* **473**, 101-105.

Kong H., Raynor K., Yasuda K., Moe S.T., Portoghese P.S., Bell G.I., and Reisine T. (1993) *J. Biol. Chem.* **268**, 23055-23058.

Kong H., Raynor K., Yano H., Takada J., Bell G.I., and Reisine T. (1994) *Proc.Natl. Acad.Sci.USA.* **91**, 8042-8046.

Koelle M.R., and Horvitz H.R. (1996) *Cell.* **84**, 115-125.

Koelle M.R. (1997) *Curr. Opin. Cell Biol.* **9,** 143-147.

Koski G., and Klee W.A. (1981) *Proc. Natl. Acad. Sci. USA.* **78,** 4185-4189.

Kozasa T., Kaziro Y., Ohtsuka T., Grigg J.J., Nakajima S., and Nakajima Y. (1996) *Neurosci. Res.* **26,** 289-297.

Kramer H.K., and Simon E.J. (2000) *Neuropharmacology.* **39**, 1707-1719.

Kramer H.K., Andria M.L., Douglas H.E., and Simon E.J. (2000) *Biochem. Pharmacol.* **60**, 781-792.

Krupinski J., Coussen F., Bakalyar H., Tang W.J., Feinstein P.G., Orth K., Slaughter C., Reed R.R., and Gilman A.G. (1989) *Science.* **244**, 1558-1564.

Kuner R., Kohr G., Grunewald S., Eisenhardt G., Bach A., and Kornau H.C. (1999) *Science.* **283**(5398), 74-77.

Lambright D., Sondek I., Bohm A., Skiba N., Hamm H., and Sigler P. (1996) *Nature.* **379**, 311-319.

Laugwitz K.L., Offermanns S., Spicher K., and Schultz G. (1993) *Neuron.* **10**, 233-242.

Law S.F., and Reisine T. (1997) *J. Pharmacol. Exp. Ther.* **281**, 1476-1486.

Law P.Y., Wong Y.H., and Loh H.H. (2000) *Annu. Rev. Pharmacol. Toxicol.* **40**, 389-430.

Law P.Y., Hom D.S., and Loh H.H. (1985b) *J. Biol. Chem.* **260,** 3561-3569.

Leaney J.L., and Tinker A. (2000) *Proc. Natl. Acad. Sci.USA.* **97**, 5651-5656.

Leaney J.L., Milligan G., and Tinker A. (2000) *J. Biol. Chem.* **275**, 921-929.

Lee J.W., Joshi S., Chan J.S., and Wong Y.H. (1998) *J. Neurochem.* **70**, 2203-2211.

Lee T.W., Cotecchia S., and Milligan G. (1997) *Biochem. J.* **325**, 733-739.

Leff P. (1995) *Trends Pharmacol. Sci.* **16**, 89-97.

Lefkowitz R.J., Cottecchia S., Samama P., and Costa T. (1993) *Trends Pharmacol. Sci.* **14**, 303-307.

Lefkowitz R.J. (1998) *J. Biol. Chem.* **273**, 18677-18680.

Lefkowitz R.J. (1993) *Cell.* **74**, 409-412.

Lefkowitz R.J., Pitcher J., Krueger K., and Daaka Y. (1998) *Adv. Pharmacol.* **42,** 416-420.

Lennarz W. (1983) *Methods. Enzymol.* **98**, 91-97.

Levin L.R., and Reed R.R. (1995) *J. Biol. Chem.* **270**, 7573-7579.

Liu J., Conklin B.R., Blin N., Yun J., and Wess J. (1995) *Proc. Natl. Acad. Sci. USA.* **92**, 11642-11646.

Liu F., Wan Q., Pristupa Z.B., Yu X.M., Wang Y.T., and Niznik H.B. (2000) *Nature.* **403**, 274-280.

Li X., Varga E.V., Stropova D., Zalewska T., Malatynska E., Knapp R.J., Roeske W.R., and Yamamura H.I. (1996) *Eur. J. Pharmacol.* **300**: R1-R2.

Loisel T.P., Ansanay H., Adam L., Marullo S., Seifert R., Lagace M., and Bouvier M. (1999) *J. Biol. Chem.* **274**, 31014-31019.

Loisel T.P., Adam L., Hebert T., and Bouvier M. (1996) *Biochemistry.* **35**, 15923-15932.

Lu W.Y., Xiong Z.G., Lei S., Orser B.A., Dudek E., Browning M.D., and MacDonald J.F. (1999) *Nature.* **2,** 331-338.

Malatynska E., Wang Y., Knapp R.J., Waite S., Calderon S., Rice K., Hruby V.J., Yamamura H.I., and Roeske W.R. (1996) *J. Pharmacol. Exp. Ther.* **278,** 1083-1089.

Martens G. (1992) *Prog. Brain Res.* **92**, 201-214.

Martin S.C., Russek S.J., and Farb D.H. (1999) *Mol. Cell. Neurosci.* **13**(3), 180-191.

Martin E.L., Rens-Domiano S., Schatz P.J., and Hamm H.E. (1996) *J. Biol. Chem.* **271**, 361-366.

MacEwan D.J., and Milligan G. (1996) *FEBS Lett.* **399**(1-2), 108-112.

Matthes H.W.D., Maldonado R., Simonin F., Valverde O., Slowe S., Kitchen I., Befort K., Dierich A., Le Meur M., Dolle P., *et al* (1996) *Nature.* **383**, 819-823.

Maher C.E, Selley D.E., and Childers S.R. (2000) *Biochem. Pharmacol.* **59**(11), 1395-1401.

Mahan L.C., Koachman A.M., and Insel P.A. (1985) *Proc. Natl. Acad. Sci. USA.* **82**(1), 129-133.

Marshall F.H., Jones K.A., Kaupmann K., and Bettler B. (2000) *Trends Pharmacol. Sci.* **20**, 396-399.

Massotte D., Baroche L., Simonin F., Yu L., Kieffer B., and Pattus F. (1997) *J. Biol. Chem.* **272**, 19987-19992.

Mattia A., Farmer S.C., Takemori A.E., Sultana M., Portoghese P.S., Mosberg H.I., Bowen W.D., and Porreca F. (1992) *J. Pharmacol. Exp.* Ther. **260,** 518-525.

Mattia A., Vanderah T., Mosberg H.I., and Porreca F. (1991) *J. Pharmacol. Exp. Ther.* **258**(2), 583-587.

Mao C., Cook W.J., Zhou M., Federov A.A., Almo S.C., and Ealick S.E. (1998) *Biochemistry.* **37**(20), 7135-7146.

Mckenzie F.R., and Milligan G. (1990) *Biochem J.* **267,** 391-398.

McCallum J.F., Wise A., Grassie M.A., Magee A.I., Guzzi F., Parenti M., and Milligan G. (1995) *Biochem J.* **310**, 1021-1027.

Medici R., Bianchi E., Di Segni G., and Tocchini-Valentini G.P (1997) *EMBO Journal.* **16**, 7241-7249.

Merkouris M., Mullaney I., Georgoussi Z., and Milligan G. (1997) *J. Neurochem.* **69,** 2115-2122.

Merkouris M., Dragatsis I., Megaritis G., Konidakis G., Zioudrou C., Milligan G., and Georgoussi Z. (1996) *Mol. Pharmacol.* **50**, 985-993.

Meng F., Wei Q., Hoversten M.T., Taylor L.P., and Akil H. (2000) *J. Biol. Chem.* **275**, 21939-21945.

Meng F., Hoversten M.T., Thompson R.C., Taylor L., Watson S.J., and Akil H. (1995) *J. Biol. Chem.* **270**, 12730-12736.

Meng F., Ueda Y., Hoversten M.T., Thompson R.C., Taylor.L., Watson. S.J., and Akil H. (1996) *Eur. J. Pharmacol.* **311,** 285-292.

Metzger T.G., and Ferguson D.M. (1995) *FEBS Lett.* **375,** 1-4.

Milligan G., Groarke D.A., Mclean A., Ward R., Fong C.W., Cavalli A., and Drmota T. (1998) *Biochemical Society Transactions.* **27,** 149-154.

Milligan G. (1994) *Methods Enzymol.* **237**, 268-283.

Milligan G., Bond R.A., and Lee M. (1995) *Trends.Pharmacol. Sci.* **16**, 10-13.

Milligan G., Parenti M., and Magee A.I. (1995) *Trends.Biochem. Sci.* **20**, 181-186.

Milligan G., Marshall F., and Rees S. (1996) *Trends.Pharmacol. Sci.* **17**, 235-237.

Milligan G., and Bond R.A. (1997) *Trends.Pharmacol. Sci.* **18**, 468-474.

Milligan G., and Mckenzie F.R. (1988) *Biochem. J.* **252**, 369-373.

Milligan G. (1988) *Biochem. J.* **255**, 1-13.

Milligan G. (1998) *Trends.Endocrinol. Metab.* **9**,13-19.

Milligan G., and Klee W.A. (1985) *J. Biol. Chem.* **260**, 2057-2063.

Milligan G., MacEwan D.J., Mercouris M., and Mullaney I. (1997) *Receptors and Channels.* **5**, 209-213.

Milligan G., and Rees S. (1999) *Trends.Pharmacol. Sci.* **20**, 118-124.

Milligan G. (2000) *Trends.Pharmacol. Sci.* **21**, 24-28.

Milligan G. (2000) *Science.* **288**, 65-67.

Minami T., Okuda-Ashitaka E., Mori H., Ito S., and Hayaishi O. (1996) *J. Pharmacol. Exp. Ther.* **278**(3), 1146-1152.

Mixon M.B., Lee E., Coleman D.E., Berghuis A.M., Gilman A.G., and Sprang S.R. (1995) *Science.* **270** (5238), 954-960.

Moffect S., Adam L., Bonin H., Loisel T. P., Bouvier M., and Mouillac B. (1996) *J. Biol. Chem.* **271**, 21490-21497.

Mouillac B., Caron M., Bonin H., Dennis M., and Bouvier M. (1992) *J. Biol. Chem.***267**, 21733-21737.

Morishita R., Nakayama H., Isobe T., Matsuda T., Hashimoto Y., Okano T., Fukada Y., Mizuno K., Ohno S., Kozawa O., Kata K., and Asano T. (1995) *J. Biol. Chem.* **270**, 29469-29475.

Moss J., Yost D.A., and Stanley S.J. (1983) *J. Biol. Chem.* **258**, 6466-6470.

Murphy K.S., and Mahklouf G.M. (1996) *Mol. Pharmacol.* **50**, 870-877.

Mullaney I., Carr I.C., and Milligan G. (1996) *Biochem. J.* **315**, 227-234.

Nathans J., and Hogness D.S. (1983) *Cell.* **34**, 807-814.

Neer E.J., Lok J.M., and Wolf L.G. (1984) *J. Biol. Chem.* **259**, 14222-14229.

Neilan C.L., Akil H., Woods J.H., and Traynor J.R. (1999) *Br. J. Pharmacol.* **128** (3), 556-562.

Ng G.Y., Clark J., Coulombe N., Ethier N., Hebert T.E., Sullivan R., Kargman S., Chateauneuf A., Tsukamoto N., McDonald T., Whiting P., Mezey E., Johnson M.P., Liu Q., Kolakowski L.F.Jr., Evans J.F., Bonner T.I., and O'Neill G.P. (1999) *J. Biol. Chem.* **274**, 7607-7610.

Ng G.Y.K., O'Dowd B.F., Caron M., Dennis M., Brann M.R., and George S.R. (1994) *J. Neurochem.* **63,** 1589-1595.

Northup J.K., Sternweis P.C., Smigel M.D., Schleifer L.S., Ross E.M., and Gilman A. G. (1980) *Proc. Natl. Acad. Sci.USA.* **77**, 6516-6520.

Nukada T., Tanabe T., Takahashi H., Noda M., Haga K., Haga T., Ichiyama A., Kanagawa K., Hiranaga M., Matsuo, *et al* (1986) *FEBS Lett.* **197**, 305-310.

Offermanns S., Schultz G., and Rosenthal W. (1991) *J. Biol. Chem.* **266**, 3365-3368.

Offermanns S., Laugwitz K.L., Spicher K., and Schult, G. (1994) *Proc. Natl. Acad. Sci. USA.* **91**(2), 504-508.

Offermanns S., and Simon M.I. (1995) *J. Biol. Chem.* **270**, 15175-15180.

Okamoto Y., Ninomiya H., Tanioka M., Sakamoto A., Miwa S., and Masaki T. (1997) *J. Biol. Chem.* **272**, 21589-21596.

Omary M.B., and Trowbridge I.S. (1981) *J. Biol. Chem.* **256**, 4715-4718.

Onogi T., Minami M., Katao Y., Nakagawa T., Aoki Y., Toya T., Katsumata S., and Satoh M. (1995) *FEBS Lett.* **357**(1), 93-97.

Osawa S., and Weiss E.R. (1995) *J. Biol. Chem.* **270**(52), 31052-31058.

Pan Y.X., Xu Bolan J.E., Abbadie C., Chang A., Zuckerman A., Rossi G., and Pasternak G.W. (1999) *Mol. Pharmacol.* **56**, 396-403.

Parma J., Duprez L., Van Sande J., Cochaux P., Gervy C., Mockel J., Dumont J., and Vassart G. (1993) *Nature.* **365**, 649-651.

Pei G., Kieffer B.L., Lefkowitz R.J., and Freedman N.J. (1995) *Mol. Pharmacol.* **48**, 173-177.

Pei G., Tiberti M., Caron M.G., and Lefkowitz R.J. (1994) *Proc. Natl. Acad. Sci. USA*. **91**, 2699-2702.

Prather P.L., McGinn T.M., Erickson L.J., Evans C.J., Loh H.H., and Law P.Y. (1994) *J. Biol. Chem.* **269** (33), 21293-21302.

Premont R.T., Inglese J., and Lefkowitz R.J. (1995) *FASEB J.* **9**, 175-182.

Pyne N.J., Murphy G.J., Milligan G., and Houslay M.D. (1989) *FEBS Lett.* **243**, 77-82.

Quock R.M., Burkey T.H., Varga E., Hosohata Y., Hosohata K., Cowell S.M., Slate C.A., Ehlert F.J., Roeske W.R., and Yamamura H.I. (1999) *Pharmacol. Reviews.* **51**, 503- 532.

Reneke J.E., Blumer K.J., Courchesne W.E., and Thorner J. (1988) *Cell.* **55**, 221-234.

Remmers A.E., Engel C., Liu M., and Neubig R.R (1999) *Biochemistry.* **38** (42), 13795-13800.

Roerig S.C., Loh H.H., and Law P.Y. (1992) *Mol. Pharmacol.* **41**(5), 822-831.

Ross E.M., and Gilman A.G. (1977) *J. Biol. Chem.* **252**, 6966-6970.

Ross E.M., Howlett A.C., and Gilman A.G (1979) *Prog. Clin. Biol. Res.* **31,** 735-749.

Rocheville M., Lange D.C., Kumar U., Patel S.C., Patel R.C., and Patel Y.C. (2000) *Science.* **288**(5463), 154-157.

Rovati G.E. (1998) *Trends.Pharmacol. Sci.* **19**, 365- 369.

Rohrer D.K., and Kobilka B.K. (1998) *Physiological reviews.* **78**, 35-78.

Sautel M., and Milligan G. (1998) *FEBS Letters.* **436**, 46-50.

Samama P., Cotecchia S., Costa T., and Lefkowitz R.J. (1993) *J. Biol. Chem.* **268**, 4625-4636.

Salomon Y., Londos C., and Rodbell M. (1979) *Anal. Biochem.* **58,** 541-548.

Schutz W., and Freissmuth M. (1992) *Trends Pharmacol. Sci.* **13**, 376- 380.

Scheuring J., Berti P.J., and Schramm V.L. (1998) *Biochemistry.* **37**, 2748-2758.

Schonerberg T., Schultz G., and Gudermann T. (1999) *Mol. Cell. Endocrinol.* **151**, 181-193.

Scholich K., Barbier A.J., Mullenix J.B., and Patel T B. (1997) *Proc. Natl. Acad. Sci. USA.* **94**, 2915-2920.

Seifert R., Gether U., Wenzel-Seifert K., and Kobilka B.K. (1999) *Mol. Pharmacol.* **56**, 348-358.

Seifert R., Wenzel-Seifert K., and Kobilka B.K. (1999b) *Trends Pharmacol. Sci.* **20**, 383- 389.

Seifert R., Wenzel-Seifert K., Lee T.W., Gether U., Sanders-Bush E., and Kobilka B. K (1998) *J. Biol. Chem.* **273**, 5109-5116.

Seifert R., Lee T.W., Lam V.T., and Kobilka B.K. (1998) *Eur. J. Biochem.* **255**, 369-382.

Seifert R., Wenzel-Seifert K., Gether U., Lam V.T., and Kobilka B.K. (1999) *Eur. J. Biochem.* **255**, 369-382.

Senogles S.E. (1994) *J. Biol. Chem.* **269**, 23120-23127.

Sharma S.K., Klee W.A., and Nirenberg M. (1977) *Proc. Natl. Acad. Sci. USA.* **74**, 3365-3369.

Sheldon R.J., Riviere P.J., Malarchik M.E., Moseberg H.I., Burks T.F., Porreca F. (1990) *J Pharmacol Exp Ther.* **253**(1), 1

Simonin F., Befort K., Gaveriaux-ruff C., Matthes H., Nappey V., Lannes B., Micheletti G., and Kieffer B. (1994) *Mol. Pharmacol.* **46**, 1015-1021.

Simon M.I., Strathmann M.P., Gautam N. (1991) *Science.* **252**(5007), 802-808.

Smit M.J., Leurs R., Alewijnse A.E., Blauw J., Van Nieuw Amerongen G.P., Van De Vrede Y., Roovers E., and Timmerman H. (1996) *Proc. Natl. Acad. Sci. USA.* **93**(13), 6802-6807.

Small K. M., Forbes S. L., Rahman F. F., and Liggett S. B. (2000) *Biochemistry.* **39**, 2815-2821.

Sondek J., Bohm A., Lambright D.G., Hamm H.E., and Sigler P.B. (1996) *Nature.* **379**(6563), 369-374.

Sora I., Takahashi N., Funada M., Ujike H., Revay R.S., Donovan D.M., Miner L.L., and Uhl G.R. (1997a) *Proc. Natl. Acad. Sci. USA.* **94**, 1544-1549.

Sora I., Funada M., and Uhl G.R. (1997b) *Eur J Pharmacol.* **324**(2-3), R1-2.

Sprang S.R. (1997) *Annu. Rev. Biochem.* **66,** 639-678.

Standifer K.M., and Pasternak G.W. (1997) *Cell signal.* **9**(3-4), 237-248.

Stanasila L., Massotte D., Kieffer B.L., and Pattus F. (1999) *Eur. J. Biochem.* **260**, 430-438.

Stein W.D., Cardarelli C., Pastan I., Gottesman M.M. (1994) *Mol Pharmacol.* **45**(4), 763-772.

Sullivan K.A., Miller R.T., Masters S.B., Beiderman B., Heideman W., and Bourne H. R. (1987) *Nature.* **330**, 758-760.

Tang W.J., and Gilman A.G. (1991) *Science.* **254**, 1500.

Taussig R., Tang W.J., and Gilman A.G. (1994) *Methods in enzymology.* **238**, 95-108.

Taylor K.E., and Cahusac P.M. (1994) *Neuropharmacology.* **33**(1), 103-108.

Tesmer J.J.G., Bermann D.M., Gilman A.G., and Sprang S.R. (1997) *Cell.* **89,** 251-261.

Tesmer J.J.G., Sunahara R.K., Gilman A.G., and Sprang S.R. (1997) *Science.* **278,** 1907-1916.

Timothy A.F., and Partick J.C. (1997) *Biochem J.* **321**, 561-571.

Valguette M., Vu H.K., Yue S.Y., Wahlestedt C., and Walker P. (1996) *J. Biol. Chem* **271**, 18789-18796.

Van Ree J.M., Gerrits M.A.F.M., and Vanderschuren J.M.J. (1999) *Pharmacol. Rev.* **51**, 341-396.

Voogd T.E., Vansterkenburg E.L.M., Wilting J., and Janssen L.H.M. (1993) *Pharmacol. Rev.* **45**, 177-203.

Wang J.B., Johnson P.S., Wu J.M., Wang W.F., and Uhl G.R. (1994) *J. Biol. Chem.* **269**, 25966-25969.

Waldhoer M., Wise A., Milligan G., Freissmuth M., and Nanoff C. (1999) *J. Biol. Chem.* **274**, 30571-30579.

Wayman G.A., Wei J., Wong S., and Storm D.R. (1996) *Mol. Cell. Biol.* **16**, 6075-6082.

Wedegaertner P.B., and Bourne H.R. (1994) *Cell.* **77**, 1063-1070.

Wenzel-Seifert K., Arthur J.M., Liu H-Y., and Seifert R. (1999) *J. Biol. Chem.* **274,** 33259-33266.

Wenzel-Seifert K., Lee T.W., Seifert R., and Kobilka B.K. (1998). *Biochem J.* **334,** 519-524.

Wenzel-Seifert K., and Seifert R. (2000) *Mol. Pharmacol.* **58,** 954-966.

West R.E. Jr., Moss J., Vaughan M., Liu T., and Liu T.Y (1985) *J. Biol. Chem.* **260,** 14428-14430.

Wei J., Wayman G., and Storm D.R. (1996) *J. Biol. Chem.* **271**, 24231-24235.

Wei H., Fiskum G., Rosenthal R.E., and Perry D.C. (1996) *Mol. Chem. Neuropathol.* **29** (1), 37-52.

Weiss J.M., Morgan P.H., Lutz M.W., and Kenakin T.P. (1996) *J. theor. Biol.* **178,** 151-167

Weiss J.M., Morgan P.H., Lutz M.W., and Kenakin T.P. (1996) *J. theor. Biol.* **178,** 168-182.

Wess J. (1998) *Pharmacol. Ther.* **80,** 231-264.

Whistler J.L., Chuang H.H., Chu P., Jan L.Y., and Zastrow M.V. (1999) *Neuron.* **23**, 737-746.

White J.H., Wise A., Main M.J., Green A., Fraser N.J., Disney G.H., Barnes A.A., Emson P., Foord S.M., and Marshall F.H. (1998) *Nature.* **396** (6712), 679-682.

Wise A., Watson-Koken M.A., Rees S., Lee M., and Milligan G. (1997a) *Biochem. J.* **321**, 721-728.

Wise A., Carr I.C., and Milligan G. (1997b) *Biochem J.* **325**, 17-21.

Wise A., Carr I.C., Groarke D.A., and Milligan G. (1997) *FEBS Lett.* **419**, 141-146.

Wise A., Sheehan M., Rees S., Lee M., and Milligan G. (1999) *Biochemistry.* **38,** 2272-2278.

Wise A., and Milligan G. (1997) *J. Biol. Chem.* **272,** 24673-24678.

Wilkie T., Scherle P., Strathmann M., Slepak V., and Simon M.I. (1991) *Proc. Natl. Acad. Sci. USA.* **88,** 10049-10053.

Wong Y.G (1994) *Methods Enzymol.* **238,** 81-94.

Wu Z., Wong S.T., and Storm D.R. (1993) *J. Biol. Chem.* **268,** 23766-23768.

Wu D., LaRosa G.J., and Simon M.I. (1993) *Science.* **261,** 101-103.

Xia Z.G., and Storm D.R. (1997) *Curr. Opin. Neurobiol.* **7,** 391-396.

Yaksh T.L. (1999) *Trends Pharmacol. Sci.* **20,** 329-337.

Yatsunami K., and Khorana H.G. (1985) *Proc. Natl. Acad. Sci. USA.* **82** (13), 4316-4320.

Yamaguchi I., Harmon S.K., Todd R.D., and O' Malley K.L. (1997) *J. Biol. Chem.* **272,** 16599-16602.

Yan S.Z., Hahn D., Huang Z.H., and Tang W.J. (1996) *J. Biol. Chem.* **271,** 10941-10945.

Yan S.Z., Huang Z.H., Andrews R.K., and Tang W.J. (1998) *Mol. Pharmacol.* **53,** 182-187.

Yang C.S., Skiba N.P., Mazzoni M.R., and Hamm H.E. (1999) *J. Biol. Chem.* **274,** 2379-2385.

Yoshimura M., and Cooper D.M. (1992) *Proc. Natl. Acad. Sci. USA.* **89**, 6716-6720.

Yung K.K., Bolam J.P., Smith A.D., Hersch S.M., Ciliax B.J., and Levey A.I. (1995) *Neuroscience.* **65** (3), 709-730.

Zhu Y., King M.A., Schuller A.G.P., Nitsche J.F., Reidl M., Elde R.P., Unterwald E., Pasternak G.W., and Pintar J.E. (1999) *Neuron.* **24**, 243-252.

Zhu Y., and Pintar J.E. (1998) *Biol. Reprod.* **59** (4), 925-932.

Zhu Y., Hsu M.S., and Pintar J.E. (1998) *J. Neurosci.* **18** (7), 2538-2549.